DOCTOR OF PHILOSOPHY

Role of Siglec-7 in ganglioside recognition and modulating NK cell biology

Mohan, Bindu

Award date:
2013

DOCTOR OF PHILOSOPHY

Role of Siglec-7 in ganglioside recognition and modulating NK cell biology

Bindu Mohan

2013

University of Dundee

Role of Siglec-7 in ganglioside recognition and modulating NK cell biology

Bindu Mohan

A thesis submitted for the
Degree of Doctor of Philosophy
University of Dundee
October 2013

Table of Contents

Chapter 6 - Discussion

List of Figures

List of Tables

Abbreviations

ADCC	Antibody dependent cellular cytotoxicity
APC	Allophycocynin
BSA	Bovine serum albumin
CTB	Cholera toxin subunit B
CV	Column volume
DAPI	4',6-Diamidino-2-Phenylindole, Dihydrochloride
EDTA	Ethylenediaminetetraacetic acid
ELISA	Enzyme-linked immunosorbent assay
FCS	Fetal calf serum
FITC	Fluorescein isothiocyanate
GD3S	GD3 synthase
GM2S	GM2 synthase
HBSS	Hank's balanced salt solution
HRP	Horse radish peroxide
ICAM-1	Intracellular adhesion molecule-1
IL-2	Interleukin-2
ITAM	Inhibitory tyrosine based activation motif
ITIM	Inhibitory tyrosine based inhibitory motif
LFA-1	Lymphocyte function-associated antigen-1
MAPK	Mitogen-activated protein kinase
MWCO	Molecular weight cut off
NeuAc	N-Acetylneuraminic acid (Sialic acid)
NK	Natural killer
PAA	Polyacrylamide
PBS	Phosphate buffered saline
PPR	Pathogen recognition receptors
PBMC	Peripheral blood mononuclear cells
PBS	Phosphate buffered saline
PCR	Polymerase chain reaction
PDBU	Phorbol 12,13-dibutyrate
PE	R-Phycoerythrin
PFA	Paraformaldehyde
PLL	Poly-L-Lysine

PMSF	Phenylmethanesulfonyl fluoride
PVDF	Polyvinylidene fluoride
PV	Pervanadate
RBC	Red blood cell
SDS	Sodium dodecyl sulphate
SD	Standard deviation
SEM	Standard error of mean
SHP-1	Src homology region 2 domain-containing Phosphatase-1
SNA	Sambucus niagra agglutinin
TBS	Tris-buffered saline
TBST	Tris-buffered saline tween
TMB	3,3′,5,5′-Tetramethylbenzidine
WT	Wild type
7AAD	7Aminoactinomycin D

Acknowledgements

I would first like to thank my supervisor Paul Crocker for providing me with this studentship and for his continuous support, encouragement and kindness over these years. I would like to also thank him immensely for his suggestions and constructive criticisms during the experimental stages of my project and the writing of this thesis.

I would like to thank the past and present members of the Crocker lab in their support and help during the course of this PhD.

I am also thankful to my second supervisor, Hugh Willison, for his invaluable suggestions and ideas. I would also like to thank the members of his lab who have been very kind in helping me set up the ganglioside assays and providing me with antibodies and other valuable reagents.

I would also like to acknowledge the members of my thesis committee, Doreen Cantrell and Andrew Hopkins, who have been extremely supportive and have guided me through my work.

Many other people in the College of Life Science have helped me with reagents and troubleshooting technical problems. I would also like to thank the FACS team, Rosie and Arlene, who have been fantastic with all the cell sorting I needed.

Most importantly, I would like to thank my daughter, Priya, who tolerated my long hours in the lab and was the reason for me to carry on during the tough times. Finally, I would also like to thank my husband, parents, sisters and my dear friends (especially Mariam, Amee and Smita) for their continued love, support, prayers and taking care of Priya in my absence.

Thank you all.
Thank you God.

Abstract

Sialic acid binding Ig-like lectin-7 (Siglec-7), expressed primarily on NK cells, binds preferentially to alpha2,8 linked disialic acids such as present in the ganglioside GD3 that is upregulated in certain cancers. Siglec-7 is classified as an inhibitory receptor as it contains immunoreceptor tyrosine based inhibitory motifs. It has been shown to inhibit NK cytotoxicity in cellular assays thereby implying a role for it in NK cell mediated tumour surveillance.

The aim of this project was to study factors affecting ligand recognition by Siglec-7 and its impact on NK cell functions. An investigation into the mechanism by which Siglec-7 mediates inhibitory signals to regulate NK cell biology was also carried out. Recognition of Siglec-7 for GD3 has been reported to be altered in the presence of complex gangliosides. This project was initiated with an aim to examine the role of such *cis*-interactions between GD3 and other gangliosides such as GM1 in biological systems and thereby its impact on NK cell biology. B16 (78) cell line was genetically modified to over-express both GD3 and GM1.

This model system was then analysed using Siglec-7-Fc precomplexes for the recognition of GD3. Siglec-7-Fc binding of B16 (78) cells with high expression of GD3 and GM1 was significantly lower compared to cells having high expression of GD3 and low expression of GM1. However further investigation of these *cis*-interactions by confocal microscopy revealed that only less than 3% of the cells had patches of co-localization of the two gangliosides. Such lateral segregation of co-expressed GD3 and GM1 was also observed in another cell line model. Next, an investigation into the role of GD3 in modulating NK cell

functions via Siglec-7 was carried out. Primary PBMCs and a Siglec-7 deficient NK cell line, NK92, were used for this purpose. The data obtained showed that Siglec-7 could negatively modulate NK cytotoxicity towards targets expressing disialylated ligands such as GD3. Furthermore Siglec-7 was also able to modulate integrin functions on NK cells. LFA-1 mediated adhesion of effectors to ICAM-1-Fc coated plates and the polarization of perforin granules to ICAM-1-Fc coated beads were negatively affected by the expression of Siglec-7 in the NK92 cell line. Biochemical analysis of LFA-1 mediated signalling in NK92 cells showed negative regulation of Src kinase activation, in an Siglec-7 dependent manner. Overall these findings suggest a role for Siglec-7 in modulating NK cell recognition of tumours with aberrant glycosylation patterns. They also form the basis of further investigation into the mechanisms of inhibitory signalling mediated by Siglec-7 and could therefore be of potential clinical relevance in NK cell mediated tumour clearance.

Chapter 1

Introduction

The role of natural killer (NK) cells in the body's defense against tumours is an area that generates considerable interest. Tumour cell elimination by NK cells is accomplished by a complex interplay of signals received from activating and inhibitory receptors expressed on these cells. Sialic acid binding Ig-like lectin-7 (Siglec-7) is one of the inhibitory receptors present on NK cells. The role of Siglec-7 in modulating NK cell responses to tumours is not well understood. Disialylated gangliosides such as GD3 are one of the well known ligands for this receptor and are found to be over-expressed in certain tumours. The focus of this project is to examine the role of Siglec-7 - ganglioside interactions in modulation of NK cell responses to tumour cells.

This chapter will provide an overview of the immune system with particular emphasis on human NK cells and Siglec-7 as well as the biosynthesis and functions of gangliosides and their role in tumours

1.1 Vertebrate immune system

The immune system is a complex network of cells and secreted molecules whose primary function is to protect the body from external and internal influences that are detrimental to homeostasis. It is made up of two arms – innate immunity and adaptive immunity. The innate system is present in invertebrates, vertebrates and plants and came into existence much earlier than adaptive immunity which is present only in vertebrates (Janeway., 2001, PNAS) (Albert B, Molecular biology of the cell., 2002). While attempting to clear the host of pathogens and toxins, the immune system must also be able to clearly discriminate self from non-self and maintain self-tolerance.

1.2 Innate immune system

The innate immune system is the first line of defense against foreign antigens. It is made of cellular and non-cellular components which include the epithelial barrier, mucus layer covering the epithelial lining, the complement system, membrane bound receptors and intracellular proteins (Chaplin, 2003).

The cellular components of the innate immune system include leukocytes that are derived from common myeloid progenitor cells and natural killer (NK) cells which arise from common lymphoid progenitors. Leukocytes are further divided into neutrophils, monocytes, eosinophils, and basophils. The cells of the innate immune system function by phagocytosis, release of cytokines, chemokines, enzymes and factors such as reactive oxygen species (ROS). They also have an important function in the activation of the adaptive immune system. They do this by processing antigens and presenting them to T-cells and B-cells and by the release of factors such as cytokines. Neutrophils are the first line of defense against bacterial and fungal infections and have a clear role in generating an inflammatory response and shaping adaptive immunity (Mocsai, 2013). Activated neutrophils facilitate recruitment of other cells to the site of inflammation and also engage in cross-talk with dendritic cells (DC), NK cells, T cells and B cells resulting in their maturation, activation, proliferation and functional responses (Mantovani et al., 2011)(Claudio Costantini and Marco A. Cassatella., 2011). Monocytes, macrophages and dendritic cells belong to the group of mononuclear phagocytic cells. They contribute to shaping of the immune system during infections and tumour development by – phagocytosis of dead and infected cells, production of cytokines and presenting antigens to T-cells and B-cells. They express a number of pathogen recognition receptors

(PRRs) which help them with their primary function of phagocytosis of dead and infected cells (Geissmann et al., 2010).

PRRs recognize certain structures conserved between species known collectively as pathogen associated molecular patterns (PAMPs). They can also be from endogenous damaged cells - these are known as damage associated molecular patterns (DAMPs). The four classes of PRR identified to date include – Toll-like receptors (TLR), C-type lectin receptors, Retinoic acid-inducible gene-I-like receptors (RLRs) and Nod-like receptors (NLR) (Takeuchi and Akira, 2010). These receptors are expressed either on the cell surface or are present in the cytoplasm and recognize proteins on bacteria, viruses, fungi and parasites. Sensing of PAMPs and DAMPs results in the release of cytokines, chemokines, type I interferon and other proteins classically associated with inflammatory responses (Takeuchi and Akira, 2010), (Akira, Uematsu and Takeuchi, 2006), (Kawai and Akira, 2010).

1.3 Adaptive immune system

The adaptive immune system is made up of cells belonging to two types – cells that mature in the thymus (T-cells), and cells that mature in the bone marrow, (B-cells). Following their development in the thymus and bone marrow, they move into the secondary lymphoid organs – lymph nodes and spleen. From these organs, they migrate towards site of infection, under the influence of adhesion and chemokine receptors (Bonilla and Oettgen, 2010). Both T-cells and B-cells express an array of activating and inhibitory receptors during different stages of their development and maturation. These receptors are crucial in maintaining homeostasis in the immune system and preventing unwanted responses. T-cells are characterized by the expression of the T cell

receptor (TCR) comprising of the α, β, γ, δ chains, by a process of somatic recombination, known as VDJ recombination. The TCR is associated with a receptor CD3 (ξ, δ, γ, ε), which is required for signaling of the TCR (Santana and Rosenstein, 2003). The TCR receptor recognizes antigenic peptides expressed on MHC class II on APCs and the ubiquitously expressed MHC I. This interaction also requires the recognition of MHC class I by CD8 and MHC class II by CD4 (Smith-Garvin, Koretzky and Jordan, 2009). Antigen recognition results in the clustering of TCR receptors at the immunological synapse and activation of immunoreceptor tyrosine-based activation motifs (ITAM) present on CD3 by the Src family of kinases, which triggers the signaling cascade in the T cells (Kane, Lin and Weiss, 2000). T-cells can be broadly classified as cytokine producing helper T cells (T_H / CD4+) and cytotoxic T cells (CD8+). Cytotoxic action of CD8+ T cells is mediated either by pre-formed cytotoxic granules containing granzymes and perforin or by the expression of FasL. This is parallel to the mechanism adopted by NK cells and has been detailed below. Apart from mounting an immune response against pathogens, T-cells are also very important in activating B-cells, NK cells and DCs. B-cells are responsible for mediating humoral immunity via the production of antibodies (Bonilla and Oettgen, 2010). B-cells express ITAM containing receptors – Igα and Igβ which along with the B-cell co-receptor, CD19 helps in signal transduction following ligand binding or antibody cross-linking (Kurosaki, Shinohara and Baba, 2010).

1.4 Natural killer (NK) cells

NK cells are a unique population of immune cells that fall under the innate immune system as they require no prior sensitization to antigens. However they also share features common to the cells of the adaptive immune system and

hence are thought to be at the interface of these two systems. They represent 2-18% of the total lymphocyte population in human blood (Purdy and Campbell, 2009). They are characterized by numerous germline encoded receptors that unlike T-cell and B-cell receptors do not require somatic recombination. Human NK cells can be broadly divided into two subsets depending on the expression levels of CD56 as $CD56^{dull}$ and $CD56^{bright}$. These two subsets differ in their expression of perforin and therefore cytotoxic potential with the $CD56^{dull}$ being more cytotoxic. 90% of the peripheral blood and splenic NK cells belong to the $CD56^{dull}$ $CD16^{+}$ category and respond better to ligands expressed on target cells (Long et al., 2013a). The smaller subset of the $CD56^{bright}$ $CD16^{+}$ cells, mainly present in tissues, respond stronger to soluble factors such as cytokines (Vivier et al., 2008).

NK cells get recruited to the site of infection via chemokines and recognize tumour targets or virally affected cells by means of a diverse group of activating and inhibitory receptors. They mediate their cytotoxic functions by (i) release of preformed cytotoxic granules containing perforin or granzyme (ii) by the expression of death ligands such as FAS ligand (FASL) and TRAIL (TNF-receptor apoptosis inducing-ligand) and (iii) expression of cytokines such as interferons (IFN-γ), tumour necrosis factor (TNF-α) and granulocyte-macrophage colony-stimulating factor (GM-CSF). Upon ligand binding, the receptors for FASL and TRAIL, expressed on target cells, recruit “death domain” containing proteins which activate the caspase signalling cascade and initiate apoptosis of target cells (Chua, Serov and Brahmi, 2004;Montel et al., 1995). Pore forming perforin and the serine protease granzyme also bring about target cell death by activation of the caspase signaling cascade (Trapani and Smyth, 2002).

In 1986, Karre and colleagues hypothesized that NK cells were able to spare certain tumours expressing major histocompatibility complex (MHC) class I ligands. This mechanism of recognizing potential targets was opposite to that of T cells which relies on ligand presentation by MHC class I and II molecules and came to be known as the “missing self” hypothesis (Karre, 2008;Karre et al., 1986). However with the discovery of the numerous activating and inhibitory receptors expressed by these cells, it has now become clear that sensitivity of target cells to NK effectors does not solely depend on the absence of MHC expression but also on the expression of ligands for the activating receptors. The ligands expressed on target cells can either be non-self ligands expressed on cells infected with pathogens or stress ligands expressed by cells undergoing tumour transformation. NK cell effector responses result from the integration and balance of signals arising from these activatory and inhibitory receptors (Moretta and Moretta, 2004).

Cytotoxicity bought about by NK cells can either be natural cytotoxicity or by antibody dependent cytotoxicity (ADCC). Natural cytotoxicity is bought about activating receptors (discussed below) whereas antibody dependent cellular cytotoxicity (ADCC) is solely under the control of the low affinity Fc receptor, CD16 (FcγRIIIa) (Lanier, 2003).

The function of NK cells can be broadly categorized as follows

1) Defence against tumours and infections - NK cells continuously scan the body for cells that have undergone transformation or have been virally transformed. Cells with increased expression of ligands for activating receptors or having a down-regulation of MHC class I molecules fall prey for these effectors. NK cells act on these cells by mechanisms described above and keep the infection under control till an effective T cell response has been mounted.

2) Maintaining homoeostasis in the organism – An important role for these cells in clearing away immature dendritic cells, antigen presenting cells and activated T cells has been demonstrated, thus proving to be essential in homeostatic mechanisms (Ferlazzo et al., 2004). NK cells are also involved in bidirectional cross-talk with dendritic cells. Cytokines produced by dendritic cells enhance NK effector functions. On the other hand, cell to cell contact between NK cells and dendritic cells is important in DC maturation and activation (Ferlazzo et al., 2004;Gerosa et al., 2005;Morandi et al., 2012;Walzer et al., 2005). Recently, their role in preventing autoimmunity has begun to be recognized for example in multiple sclerosis, rheumatoid arthritis, type-1 diabetes and systemic lupus erythematosis (SLE) (Erkeller-Yuksel, Lydyard and Isenberg, 1997;Rodacki et al., 2007;Schleinitz et al., 2010) (Gur et al., 2013)

3) Reproduction - NK cells are also found in the uterine tissues. Altered NK cell functions have been found in women with recurrent abortions, pre-ecclampsia and infertility (Kwak-Kim and Gilman-Sachs, 2008) (Vacca, Mingari and Moretta, 2013).

NK cells express receptors belonging to two main categories – activating and inhibitory (listed in table 1). These receptors interact with MHC and non-MHC ligands expressed on normal and diseased cells (Lanier 2005). Some of the receptor families consist of members which are only activatory while others are made of both activatory and inhibitory receptors. NK cell response to a target depends on many factors such as surface density of receptors (Sivori et al., 2000), their synergistic activation (as seen in experiments involving multiple activating receptors), activation state of NK cells (Vitale et al., 1998) and strength of the inhibitory signals. In some cases, factors in the tumour

microenvironment such as hypoxia and presence of tumour derived lactate dehydrogenase also negatively affects the expression of activating receptors, (Balsamo et al., 2013) (Husain et al., 2013). Structurally these receptors can also be classified as belonging to either the immunoglobulin (Ig) super family or the C-type lectin receptor family.

1.4.1 Activating receptors

Some of the activatory receptors implicated in tumour cell clearance include – those belonging to the family of natural cytotoxicity receptors (NCR), NKG2D, DNAM-1, 2B4. The NCR family consists of NKp44, NKp30 and NKp46. They are associated with ITAM containing adaptor proteins such as DAP12, via positively charged residues in their transmembrane domains.

Although these receptors have been clearly associated with clearance of tumours of different origins, their ligands remain elusive, especially those of NKp46 and NKp44 (Hudspeth, Silva-Santos and Mavilio, 2013). Using reporter cell lines and recombinant fusion proteins, tumour cell lines and some primary tumours such as melanomas have been shown to express ligands for these receptors (Glasner et al., 2012;Lakshmikanth et al., 2009) (Byrd et al., 2007) . Tumour and non-tumour related ligands identified for NKp30 include - B7-H6, BAT3 and pp65 proteins (Brandt et al., 2009) (Pogge., 2007). The Influenza virus hemagluttinin has been reported to be one of the ligands for NKp46 (Mandelboim et al., 2001). Certain α 2,3 sialic acid containing glycans, heparin and heparan sulfate has also been suggested as putative ligands for the NCRs. These studies used recombinant forms of the receptor and involved invitro techniques such as microarrays and surface plasmon resonance (SPR) (Hecht et al., 2009;Ito et al., 2011;Ito et al., 2012). These receptors have also been

shown to be important in the clearance of some viral infections such as, influenza, human cytomegalovirus (HCMV), and HIV and have also been implicated in certain autoimmune diseases such as diabetes (Gazit et al., 2006) (Magri et al., 2011) (Mendelson et al., 2010) (Fauci, Mavilio and Kottilil, 2005) (Guret al., 2013).

The receptor, NKG2D, recognizes self-proteins that are upregulated by cells under stress. NKG2D is not expressed as a heterodimer and recognizes non MHC class 1 ligands (Zafirova et al., 2011). NKG2D associates with and signals through the YINM motif containing adaptor protein, DAP10. It also associates with DAP12 in some species. The ligands recognized by this receptor in humans include – MHC class-I related proteins A and B (MICA and MICB) and UL-16 binding proteins (ULBP) while in mice it is – GPI anchored group of histocompatibility antigens 60 (H60), the family of retinoic acid early inducible proteins (RAE-1) and the transmembrane UL-16-binding protein-like transcript 1 (MULT1) (Long et al., 2013b) (Raulet et al., 2013). The expression of ligands such as MICA and MICB is low on normal cells and is upregulated upon cellular stress (Gasser et al., 2005). Ligands for NKG2D have been found to be reliable markers for disease progression in cancers of breast (de Kruijf et al., 2012), ovary, (McGilvray et al., 2010), large intestine (McGilvray et al., 2009). They are therefore of potential value in tumour immunotherapy (Cho et al., 2010).

Tumour cells and viruses have adopted different strategies to escape from recognition of these activating receptors. Some notable examples include release of immunomodulatory cytokines such as TGFβ (Sun et al., 2012) (Eisele et al., 2006), shedding of ligands by metalloproteases (Liu et al., 2010;Salih, Rammensee and Steinle, 2002) and downregulation of ligand

expression by microRNA's (Tsukerman et al., 2012) (Bennett et al., 2010) (Jensen et al., 2011) and also by preventing surface expression of activating receptors (Sunet al., 2012)

KIRs are a group of highly polymorphic receptors which can either be activatory or inhibitory (Purdy and Campbell, 2009). These receptors can be divided into different groups depending on (1) their extracellular domain – 2 domains (2D) and 3 domains (3D) or (2) the length of their cytoplasmic domains – Long (L) or Short (S) (Uhrberg et al., 1997). Like other activating NK receptors, activatory KIRs are also associated with adaptor proteins DAP12 and FcεRI-γ which carry ITAM residues in their cytoplasmic domains and facilitate signaling (Kikuchi-Maki, Catina and Campbell, 2005). KIRs recognize distinct subsets of the classical MHC-I molecules - HLA-A, B and C and this recognition is dependent on specific sequences on the HLA molecules. The inhibitory KIRs recognize epitopes on HLA-C (and some subsets of HLA-A and B) and strongly inhibit cytotoxicity of targets expressing this allotype (Moretta et al., 2009). Ligands of many of the activatory KIRs remain unidentified such as KIR2D-S2/S3/S5 and KIR3DS1(Joyce and Sun, 2011). There is extensive homology between the extracellular domains of the activating and inhibitory KIRs but the ligand binding specificities and affinities vary considerably between the different KIRs. A striking example includes the KIR2DS2 whose ligand specificity is not known although it differs from the inhibitory KIR2DL3 and KIR2DL2, with known ligands, by two and four amino acids respectively (Saulquin, Gastinel and Vivier, 2003). However this level of homology also results in some activatory and inhibitory receptors sharing the same HLA ligands but with different binding affinities. The activatory KIR2DS1 and inhibitory KIR2DL1 both bind HLA-C2 KIR expression is clonal and highly diverse between individuals. 14 KIR genes

are present in the leukocyte receptor complex of human chromosome 19 and their segregation is independent of HLA. KIRs have gained much attention in the field of leukemia treatment by haploidentical stem cell transplantation (Decot et al., 2010) (Martner et al., 2013). Donor NK cells possess a set of inhibitory KIRs that recognize missing self class I ligands in the recipient and mediate improved outcome without causing graft-versus-disease.

Figure 1.1 is a schematic representation of some of the activating receptors and their ligands (adapted from Watzl and Urlab, 2012)

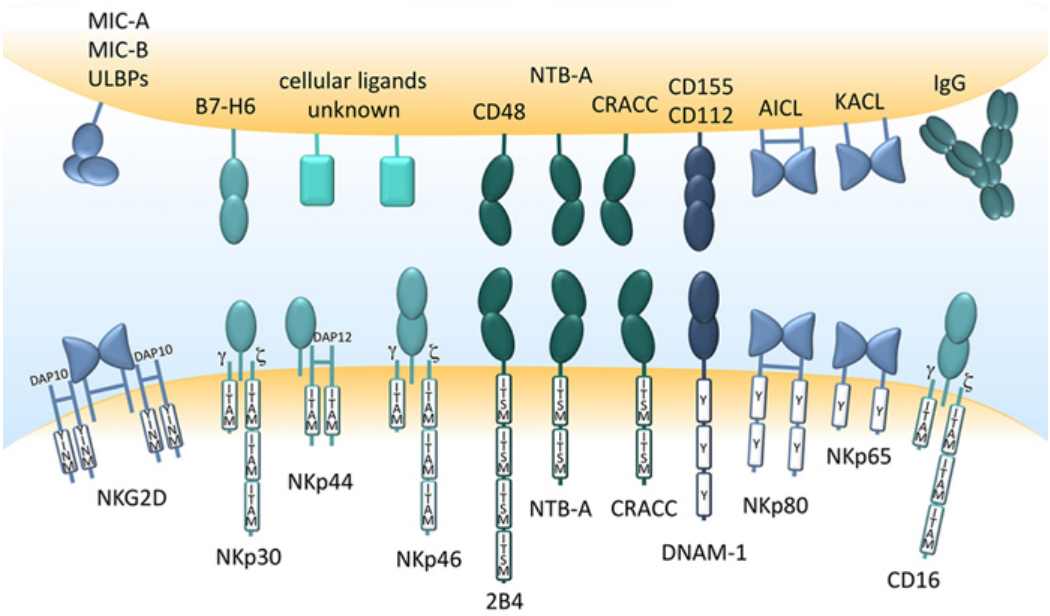

Figure 1.1 : Some of the activating receptors expressed on NK cells (bottom) and their ligands expressed on target cells (top). Receptors belonging to the immunogloubulin super family (Ig) are shown in oval while those belonging to the C-type lectin family are shown as half circles. Tyrosine based signaling motifs ITAM, YINM or ITSM are shown associated with the receptors. Adapted from (Watzl and Urlaub, 2012).

Many other receptors act in concert to support and co-stimulate the above mentioned main activating receptors for example – the lymphocyte function antigen (LFA-1), 2B4, DNAM-1, CD2, NTBA. The role of LFA-1 in NK cell

cytotoxicity and signaling mechanism will be discussed here as a representative of NK activating receptors.

LFA-1, a heterodimer of CD11a and CD18, is one of the many integrin receptors expressed by NK cells (Helander and Timonen, 1998). LFA-1 has been studied extensively in T-cell systems and is known to mediate adhesion, migration and immunological synapse formation. Adhesion of NK cells to their targets is critical to cytotoxicity events. LFA-1 is one of the important co-stimulatory integrin receptors expressed on NK cells. Many early studies have demonstrated that the absence of LFA-1 was associated with defective natural cytotoxicity and antibody dependent cellular cytotoxicity of NK cells (Kohl et al., 1984;Liu et al., 1994) (Shibuya et al., 1999). The role of LFA-1 in mediating NK cell signaling was dissected with the help of a unique model system involving the insect cell line (drosophila Schneider, S2) for the expression of ICAM-1 and ligands for other activating receptors (Barber and Long, 2003). Using primary IL-2 activated NK cells, it was demonstrated that the expression of ICAM-1/2 on S2 cells was enough to bring about perforin polarization and NK cell cytotoxicity in an LFA-1 dependent manner (Barber, Faure and Long, 2004). Freshly isolated resting NK cells however had differential requirements for granule polarization and degranulation. In resting NK cells, LFA-1 was responsible only for adhesion and granule polarization while CD16 for degranulation (Bryceson, Ljunggren and Long, 2009). Synergistic signaling of LFA-1 with CD16 and receptors such as NKG2D and 2B4 was shown to enhance adhesion and cytolytic capacity of resting NK cells (Barber and Long, 2003;Bryceson, Ljunggren and Long, 2009;Bryceson et al., 2005). LFA-1 mediated adhesion, granule polarization and cytotoxicity have been shown to be sensitive to the action of inhibitory receptors such as KIR and CD94/NKG2A (Barber, Faure and

Long, 2004;Bryceson et al., 2005;Burshtyn et al., 2000) suggesting an important role for LFA-1 in NK effector functions. LFA-1 dependent conjugate formation and perforin polarization was also shown to require an intact cytoskeleton (Gross et al., 2010). Following adhesion to target cell, LFA-1 also plays a crucial role in the formation and maturation of the immunological synapse as well as the distribution of receptors at the synapse (Orange, 2008). Although LFA-1 has been intensely studied both in human and mouse NK cells, little is known about the exact signaling mechanisms and downstream effectors involved. The non-receptor protein tyrosine kinase (Pyk2) and the guanine nucleotide exchange factor, Vav-1, were some of the earlier identified signaling molecules implicated in LFA-1 dependent signaling (Gismondi et al., 2000) (Riteau, Barber and Long, 2003). The role of Vav-1 in regulating cytoskeletal changes crucial to NK cytotoxicity is well established (Dong et al., 2009;Galandrini et al., 1999). Using the well known cytotoxic human NK cell line, NK92, synergistic signaling of LFA-1 and CD2 were shown to regulate the activation of the mitogen-activated protein kinase, Erk1/2 (Zheng et al., 2009). Mouse NK cells have been useful in studying the association of LFA-1 with different cytoskeletal proteins such as Talin, to initiate downstream signaling process vital to actin cytoskeletal reorganization and perforin polarization (Mace et al., 2010). In an interesting study, March and Long were able to show that integrin signaling and functions in NK cells is different to that of other systems such as neutrophils and T-cells (March and Long, 2011). Their results demonstrated for the first time the dependence of LFA-1 signaling on ITAM containing adaptor,TCR ζ-chain as well as on the tyrosine kinase Syk and PLC-γ in NK cells. This study also compared the differences in the signaling mechanism between LFA-1 and CD16 (March and Long, 2011).

Table 1.1 gives a list of activating and inhibitory receptors found on human NK cells.

Table 1.1 – List of some of the activating (red) and inhibitory (blue) receptors expressed on human NK cells, their ligands, signalling adaptors/motifs and functions.

Receptor	Ligand	Signalling motif	Type
NKp46	Unknown, viral haemagglutinins?	CD3ξ / FcεRIγ	Activating
NKp30	BAT-3, pp65	CD3ξ / FcεRIγ	Activating
NKp44	Unknown, viral haemagglutinins?	DAP12	Activating
NKG2D	ULBP, MICA, MICB	DAP10/DAP12	Activating
NKG2C/E	HLA-E	DAP12	Activating
CD16	IgG	CD3ξ / FcεRIγ	Activating
KIR-S	HLA-C	DAP12	Activating
DNAM-1	Nectin-2, CD155	Unknown	Activating
LFA-1	ICAM-1		Activating
NKp80	AICL	Hemi-ITAM	Activating
2B4	CD48	ITSM	Activating/Inhibitory
KIR-L	HLA-A, B, C	ITIM	Inhibitory
CD94-NKG2A	HLA-E	ITIM	Inhibitory
Siglec-7	Sialic acid	ITIM	Inhibitory
NKR-P1A	LLT-	ITIM	Inhibitory

ITSM – immunoreceptor tyrosine-based switch motif; ITIM – immunoreceptor tyrosine-based inhibition motif.

1.4.2 Inhibitory receptors

The threshold required for the activating receptors is tightly regulated by the expression of inhibitory receptors. This group includes some members of the

KIR family, CD94:NKG2A, FcγRIIb, Siglec-7. KIRs recognize the classical MHC class I molecules (HLA-A, B and C). The non-classical MHC class I molecules HLA-E (human) and Qa1 (mouse) expressed widely in tissues is recognized by the major inhibitory receptor, NKG2A, which is a C-type lectin, (Braud et al., 1998).

These interactions are key for maintaining tolerance towards normal healthy cells by inhibiting cytotoxicity and cytokine production by these effectors. A feature shared by this group of receptors is the presence of ITIM motifs within their cytoplasmic domains. Phosphorylation of this motif results in the recruitment of Src homology 2 (SH2) domain containing protein tyrosine phosphatases such as SHP-1 and SHP-2 (Kabat et al., 2002). The amino acid sequence characteristic for this motif is V/I/LxYxxL/V (where x is any non-conserved amino acid, Y - tyrosine, V – valine, L – leucine and I - isoleucine). Most inhibitory receptors carry two ITIM motifs, separated by 25 amino acid sequence, which provides the binding site for the tandem SH2 domains of SHP-1 and SHP-2 (Long, 2008). Inhibitory KIRs also carry two ITIM motifs in their cytoplasmic domains, with the exception of KIR2DL4 and KIR2DL5. Mutational studies of the ITIM motifs have helped identify the tyrosine residues required for inhibitory functions. For example using ITIM mutations, Kabat et et al., have shown that like the KIRs, the first ITIM (membrane distal due to the receptor being a type II protein) had a greater effect on the inhibitory functions of NKG2A (Kabatet al., 2002). Because of their ability to block NK cell activation, inibitory receptors negatively regulate NK cell function associated with tumours and viral infections (Al Omar et al., 2011).Thus they provide an avenue for antibody based immunotherapy (Li et al., 2013). For example by blocking NK cell inhibitory KIRs, improved rituximab based NK ADCC response was observed in

a cell line model of anti-lymphoma therapy (Binyamin et al., 2008). The biology of the inhibitory receptor Siglec-7 is detailed in section 1.4.5.

1.4.3 Signaling in NK cells

As discussed above, NK effector responses result from the complex integration of signals derived from activatory and inhibitory receptors. Signaling of activating receptors is possible by their association with ITAM containing adaptors such as FcεRIγ, CD3ζ and DAP12 via positively charged residues (eg., arginine) in the transmembrane domain of the receptor. The ITAM sequence consists of a pair of YxxL/I motifs (where x is any non-conserved amino acid, Y - tyrosine, L – Leucine and I - isoleucine), separated by a 6-8 amino acids (Love and Hayes, 2010) . These receptors include - CD16, NKp30, NKp46, activatory KIRs (Lanier, 2003). The adaptors can exist either as homo or heterodimers. The C-type lectin activating receptor, NKp80, however uses a hemi-ITAM motif for signaling (Dennehy, Klimosch and Steinle, 2011).

Ligand binding has been shown to result in phosphorylation of these ITAM motifs by Src kinase family members and this becomes the docking site for the SH2 domain containing kinases such as Syk and Zap70 (Jiang et al., 2002). This results in the phosphorylation and activation of several other downstream signaling molecules such as SLP-76 (Kim and Long, 2012), phospholipase (PLC) - γ1 / γ2, linker for activation of T cells (LAT), p85 subunit of P13K (Upshaw et al., 2006), guanidine nucleotide exchange factor Vav-1 and Vav-2, extracellular signal-related kinase (Erk1/2) and p38 mitogen activated protein kinase (MAPK) (Vivier, Nunes and Vely, 2004) (Bryceson and Long, 2008) (Riteau et al., 2003)(figure 1.2). Phosphorylation of Vav-1 is required for the actin cytoskeletal changes, clustering of activation receptors, recruitment to the

membrane and formation of the immunological synapse (Graham et al., 2006). These downstream signaling events impact on the NK cell mediated cytotoxicity and cytokine production.

NKG2D is expressed on the membrane as a dimer in association with four units of DAP10, which carries an YXXM signaling motif (Park et al., 2011). Phosphorylation of DAP10 by the Src kinase, Lck, results in the binding of p85 subunit of phosphoinositide 3-kinase (PI3K) or the binding of the small adaptor, Grb2 (Billadeau et al., 2003). However, another isoform of NKG2D (identified first in mice deficient in DAP10), the short “S” isoform is able to associate with DAP12 in cells activated with IL-2 and mediate signaling similar to other DAP12 associated receptors (Gilfillan et al., 2002) (Diefenbach et al., 2002). Segovis and group showed that signaling via NKG2D involved PI3K, which is regulated by the adaptor protein CrkL. This pathways affected NKG2D mediated cellular adhesion, granule polarization and cytotoxicity (Segovis et al., 2009).

Some other activating receptors are able to signal in the absence of ITAM motifs. 2B4 belongs to the SLAM family of receptors that have a switch motif in their cytoplasmic domain, TxYxxV/I. SLAM receptors are physically associated with SLAM-associated adaptor protein (SAP) which facilitates activatory signals (Veillette, 2010). However in the absence of SAP, these receptors propagate strong inhibitory signaling (Donget al., 2009). Integrins such as LFA-1 also belong to this third category of activatory receptors, which are not known to have physical association with ITAM containing adaptors (discussed above). Figure 1.2 is a schematic some of the downstream signaling pathway of different activation receptors (adapted from Waltz and Urlaub, 2012).

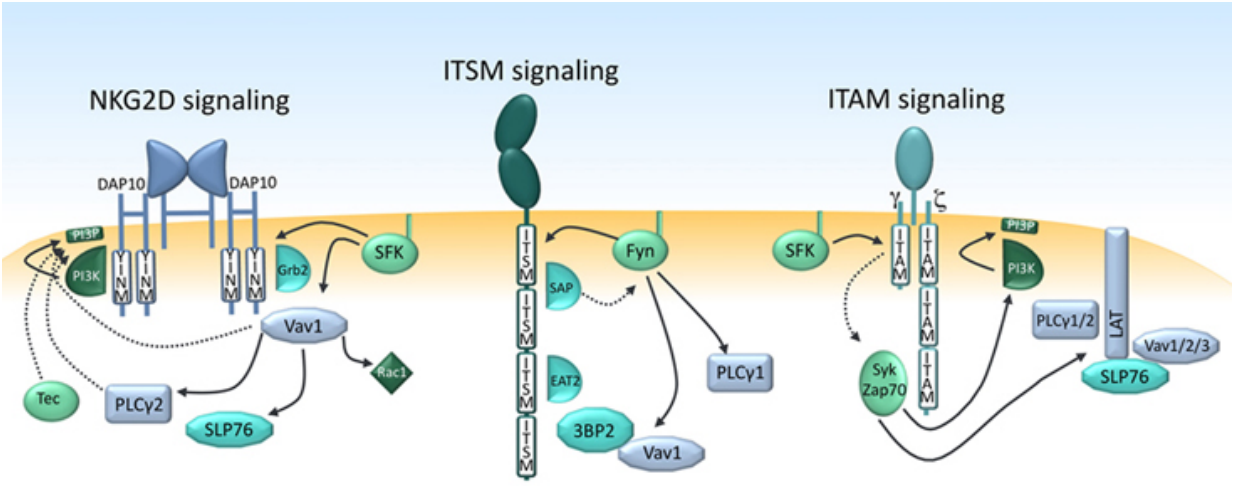

Figure 1.2 Signalling events following ligand recognition by some of the NK activation receptors. Src family of kinases is central to the recruitment of the downstream effectors such as PI3K and Vav-1 to YINM motif of DAP10 (associated with NKG2D), SAP family of adaptors to ITSM and Syk tyrosine kinases to ITAMs . Solid arrows represent activation events while dashed arrows represent recruitment events (Waltz and Urlaub, 2012).

As mentioned above, inhibitory receptors carry between 2 and 4 ITIM motifs. Ligand recognition by these inhibitory receptors results in the recruitment of Src homology 2 domain (SH2) containing phosphatases – SHP-1, SHP-2 and SHIP (in the case of mouse inhibitory Ly49 receptor) (Burshtyn et al., 1997) (Vely et al., 1997). SHP-1 and SHP-2 belong to the class of non-transmembrane associated phosphatases with broad expression patterns. Structurally, they have two SH2 domains on the N-terminus, a central catalytic domain and C-terminus with potential tyrosine phosphorylation sites (Lorenz, 2009). The SH2 domains dock onto the phosphorylated ITIM motifs and are important in regulating the activity of the catalytic domain. The C terminus carries nuclear and lipid raft localization signals. In a resting state, the N-terminal SH2 domain inhibits the activity of the catalytic domain by associating with it. The catalytic domain is released from this inhibitory state when the SH2 domains dock on to phosphorylated ITIM motifs of inhibitory receptors (Lorenz, 2009). SHP-1 null

mice have provided vital information about the role of this phosphatase in negatively modulating signaling by numerous ITIM carrying receptors.

Mutational studies of the ITIMs of KIR, NKG2A and Siglec-7/9 showed that the proximal ITIM motif was sufficient to recruit SHP-1 and result in inhibition of the effector functions (Bruhns et al., 1999) (Avril et al., 2004). However, there is lack of clear evidence as to how these ITIM motifs get phosphorylated. Lck, a member of the Src family of kinases, has been shown to be associated with the dicystine motifs on the cytoplasmic domains of the mouse inhibitory C-type lectin receptor, NKR-P1B, and is responsible for the phosphorylation of its ITIM motifs (Ljutic et al., 2005). However, a similar association has not been shown for any another ITIM bearing receptor. Further, the rapid phosphorylation of these ITIM bearing receptors achieved following pervanadate treatment suggests a possible constitutively phosphorylated state of these motifs (Long, 2008). The substrates targeted by SHP-1 have remained elusive due to the inherently difficult nature of these experiments. However, one particular study made use of a functional “substrate trapping” mutant of KIR2DL1-SHP-1, which picked up only Vav-1(Stebbins et al., 2003). Till recently the dephosphorylation of Vav-1 was thought to result in the termination of the downstream activatory signals. However some other novel mechanisms by which inhibitory signaling could intercept activatory signals has been reported. These include the active phosphorylation of the adaptor Crk by the kinase, Abl (Peterson and Long, 2008) and continuous dephosphorylation of Vav-1 by the E3 ubiquitin ligase c-Cbl (Kim et al., 2010). Figure 1.3 is a schematic representation of some of the inhibitory signaling pathways.

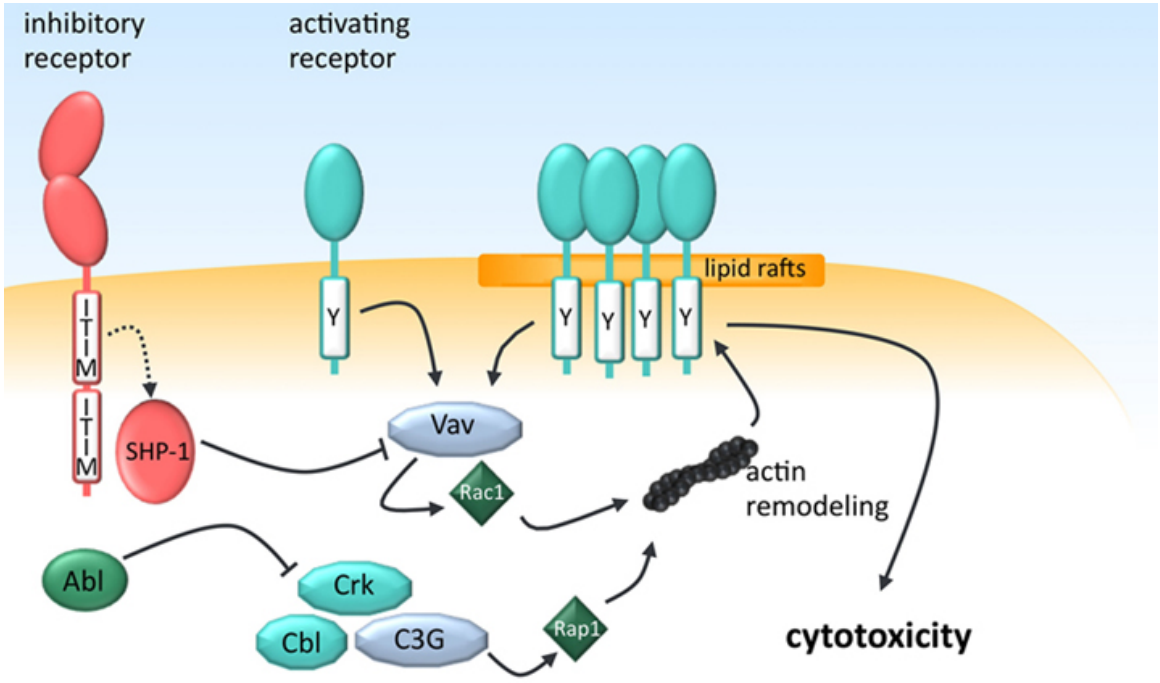

Figure 1.3 Integration of activating and inhibitory signals : Phosphosphorylation of Vav-1 results in clustering of activation receptors and subsequent cytotoxicity. However, activation of SHP-1 by engagement of inhibitory receptors results in the dephosphorylation of Vav-1. Also Abl-dependent phosphorylation of Crk results in the dissocation of the Cbl-Crk-C3G complex. Both these events block actin remodeling and thereby dampen activation signals. Solid arrows represent activation events while blunt arrows represent inhibition (adapted from Waltz and Urlaub, 2012).

Inhibitory receptors such as KIRs affect lipid raft polarization and actin cytoskeletal changes which impact on the formation of the immunological synapse (Lou et al., 2000) (Borhis et al., 2013)(Masilamani et al., 2006)(Faure et al., 2003). KIRs cluster at the immunological synapse in an actin independent manner and is surrounded by a ring of LFA-1 and ICAM-1 (Standeven et al., 2004;Vyas et al., 2001). Using S2 target cell line expressing ligands for CD2, 2B4, ICAM-1 and the inhibitory receptor KIR2DL1, a novel mechanism about how inhibitory receptors function at the immunological synapses was proposed. This study showed that KIR promoted the accumulation of activating receptors

at the inhibitory synapse while excluding LFA-1(Schleinitz, March and Long, 2008). Thus the phosphorylation of activation receptors could be prevented following phosphatase recruitment by KIRs (Dustin, 2010) (Long, 2008).

1.4.4 NK cell licensing

NK cell maturation and development involves a process known as education or licensing. This process enables NK cells to acquire or remain in a fully functional state and respond to loss of MHC on target cells and requires the interaction of the inhibitory receptors with self-MHC I during NK cell maturation and probably thereafter (Cruz-Munoz and Veillette, 2010;Jonsson and Yokoyama, 2009;Raulet and Vance, 2006). Therefore the absence of self MHC molecules results in NK cells being hyporesponsive. Different models have been suggested to explain how this process occurs – (a) the arming model, according to which inhibitory receptor recognition of self-MHC favours functional maturation of NK cells (Yokoyama and Kim, 2006), (b) the disarming model which suggests that NK cells are made hyporesponsive in the absence of a self-MHC receptor, (c) the cis-interaction model which suggests that cis interaction between Ly49 receptor and MHC molecules on the same cell membrane results in functional NK cell responses and (Chalifour et al., 2009) (d) the rheostat model which is based on the quantitative strength of inhibitory signaling (Brodin et al., 2009). NK cells can also be rendered unresponsive by chronic stimulation of their activating receptors. Chronic engagement of NKG2D with its ligands resulted in aberrant NK cell mediated natural and antibody dependent cytotoxicity (Coudert et al., 2008).

The use of MHC deficient mice have led to understanding the importance of inhibitory receptors in the process of NK cell education (Bryceson et al., 2006)

(Johansson et al., 2005). Contrary to the above described, uneducated NK cells from mice deficient in either Ly49 receptor or MHC class molecules responded strongly to infection with mouse cytomegalovirus (Hoglund and Brodin, 2010).

1.4.5 Siglec-7

Siglec-7, an NK cell inhibitory receptor, belongs to the family of sialic acid binding Ig-like lectins. Members of this family are distributed widely in the cells of the hematopoietic system with Siglec-7 being expressed on NK cells and a subset of monocytes and CD8+ T cells (Nicoll et al., 1999). This group showed that red blood cell (RBC) adhesion to COS cells transfected with Siglec-7 was abolished following sialidase treatment of the RBCs implying the role of this receptor in mediating cell – cell interactions (Nicoll et al., 1999). The extracellular domain of this receptor comprises of an N-terminal V-set Ig like domain and two C2-set Ig like domains. It has a unique preference for terminal disialic acids in α 2,8 linkages and to a lesser extend internally branched sialic acids in α 2,6 linkages (Blixt et al., 2003) (Nicoll et al., 2003). Disialic acids in α 2,8 linkages are present on gangliosides belonging to the b-series such as GD3, GT1a and GT1c (discussed below and represented in figure 1.8) and also in serum glycoprotein fetuin, α 2-microglobulin, neural cell adhesion molecule (NCAM)(Attrill et al., 2006). By virtue of an ITIM and ITIM-like motif in its cytoplasmic domain, Siglec-7 has been classified as an inhibitory receptor. Using mutational studies, the ITIM motifs (the proximal one in particular) was shown to recruit SHP-1 and SHP-2 and contribute to the inhibitory properties of this receptor (Falco et al., 1999) (Avrilet al., 2004).

Like other members of the Siglec family, this receptor was also found to be present in a ‘masked’ state on NK cells (discussed below). This was attributed

to the presence of sialylated glycans on NK cells. mRNA analysis of NK cells showed strong expression of ST8Sia VI which facilitates the transfer of sialic acids onto O-linked glycans (Avril et al., 2006a). Treatment of NK cells with an enzyme, sialidase, is needed to remove these *cis*-interactions and facilitate Siglec-7 recognition of probes or ligands in *trans* (Nicollet al., 2003). Therefore these *cis*-interactions could be thought of as a mechanism evolved to modulate thresholds required by activating receptor on NK cells. Using murine targets, Nicoll et al showed that unmasked Siglec-7 is able to modulate NK cell cytotoxicity via recognition of the ganglioside GD3 expressed on target cells (Nicoll et al., 2003). The biological significance of GD3 and its role in tumour progression is discussed in section 1.7 of this chapter.

The functional role of Siglec-7 as an inhibitory receptor was established using adhesion assays, FcεR mediated serotonin release by RBL cells in an over-expression model, myeloid cell proliferation assays and by examining natural or redirected cytotoxicity of human NK cells against murine targets (Nicollet al., 2003) (Avrilet al., 2004). Other studies have also confirmed the inhibitory role of Siglec-7 in different models. By recruiting SHP-1, Siglec-7 was shown to inhibit T cell receptor signaling in the Jurkat cell line and Ca^{2+} influx in a transfected monocytic cell line (Ikehara, Ikehara and Paulson, 2004) (Yamaji et al., 2005). Recombinant or cell surface expressed Siglec-7 bound strongly to lipooligosaccharides (LOS) from HS:19 strains of Campylobacter *jejuni* that either expressed GM1+GD1a+ or GD3+ (either in the purified form or heat inactivated bacteria), in a sialic acid dependent manner(Avril et al., 2006b). Taken together these studies imply that Siglec-7 has a role in modulating tumour responses of NK cells as well as in the modulation of host immune responses to infections. The significance of Siglec-7 in regulating immune

responses was further underscored by the finding of a rare subset of peripheral blood NK cells in patients infected with human immunodeficiency virus (HIV). Examining the various NK cell markers of healthy, acute and chronically infected patients, the authors found that the acutely infected patients had a $CD56^{+}Siglec\text{-}7^{-}$ NK cell phenotype, which changed to a $CD56^{-}Siglec\text{-}7^{-}$ subset in chronic infection (Brunetta et al., 2009). These aberrant subsets were impaired in their ability to degranulate as measured by CD107a release when stimulated by a susceptible target cell line. They were also less efficient in the production of cytokine, IFN-γ, when compared to the CD56+Siglec-7+ subset.

1.5 Siglec family of receptors

The family of sialic acid-binding Ig-like lectin (Siglec) consists of type I membrane proteins with variable number of extracellular domains. This family of lectins came into existence following a study of the sequence similarities and binding properties of CD22, Sialoadhesin and myelin associated protein (Kelm et al., 1994). Many more members of this family were identified in several species eg., human, mouse, primates, over the next few years.

Siglecs are broadly divided into two classes – (1) a highly evolving, closely related CD33-like group and (2) a group consisting of Sialoadhesin, CD22 and myelin-associated glycoprotein. The first group varies considerably between different mammalian species whereas the second group has conserved orthologues between the different species. Figure 1.4 represents some of the members belonging to this family in humans (adapted from Crocker, Paulson and Varki., 2007). To date there are 15 siglecs identified in humans (largest group known so far) and 9 in mouse (Paulson, Macauley and Kawasaki, 2012).

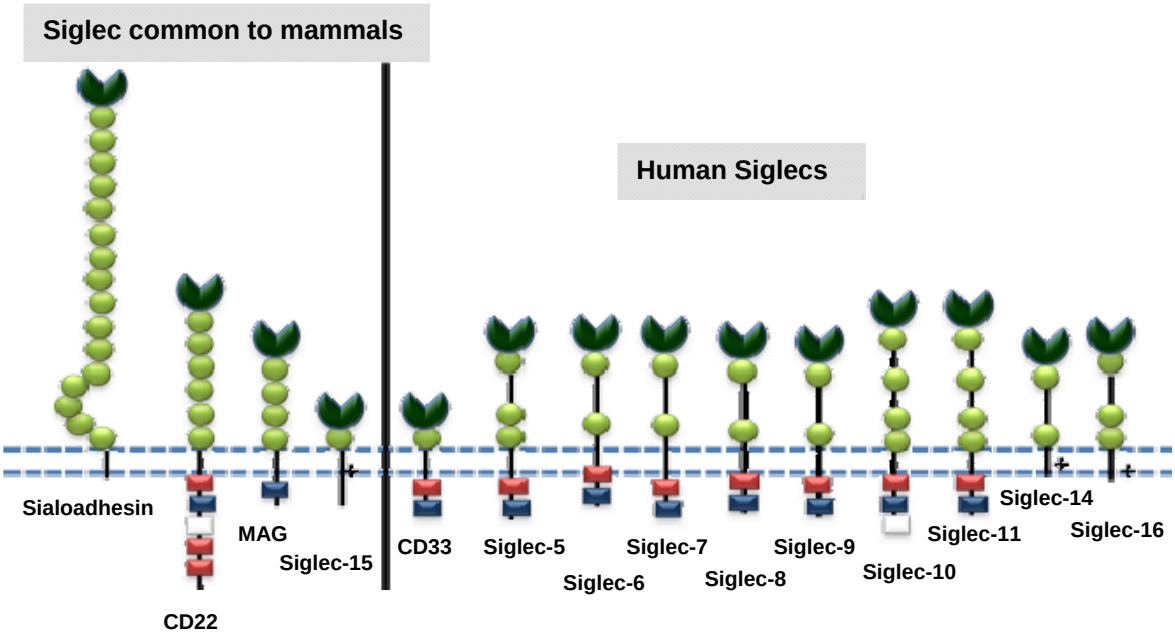

Figure 1.4: Schematic representation of human Siglecs. C2-like domains – light green, V-set domain – dark green; Red square – ITIM motif; Blue square – ITIM-like motif ; "+" – positively charged residue in transmembrane domain (Adapted from Crocker, Paulson and Varki., 2007).

Evolutionarily the family of CD33 related siglecs arose from a small cluster of genes which underwent inverse duplication to form a large gene cluster (Cao and Crocker, 2011). Figure 1.5 shows the phylogenetic relationship between the human and mice siglecs. There is a clear orthologous relationship between Sialoadhesin, CD22 and Siglec-4 (MAG) of human and mice. Although the CD33 related siglecs do not have such a clear orthologus relationship, some of the mouse siglecs fall into the same clade as that of the humans. For eg., human siglec 7, 8 and 9 belong to the same group as the mouse Siglec-E while human Silgec-10 and mouse Siglec-G are closely related (Angata et al., 2001) (Varki and Angata, 2006).

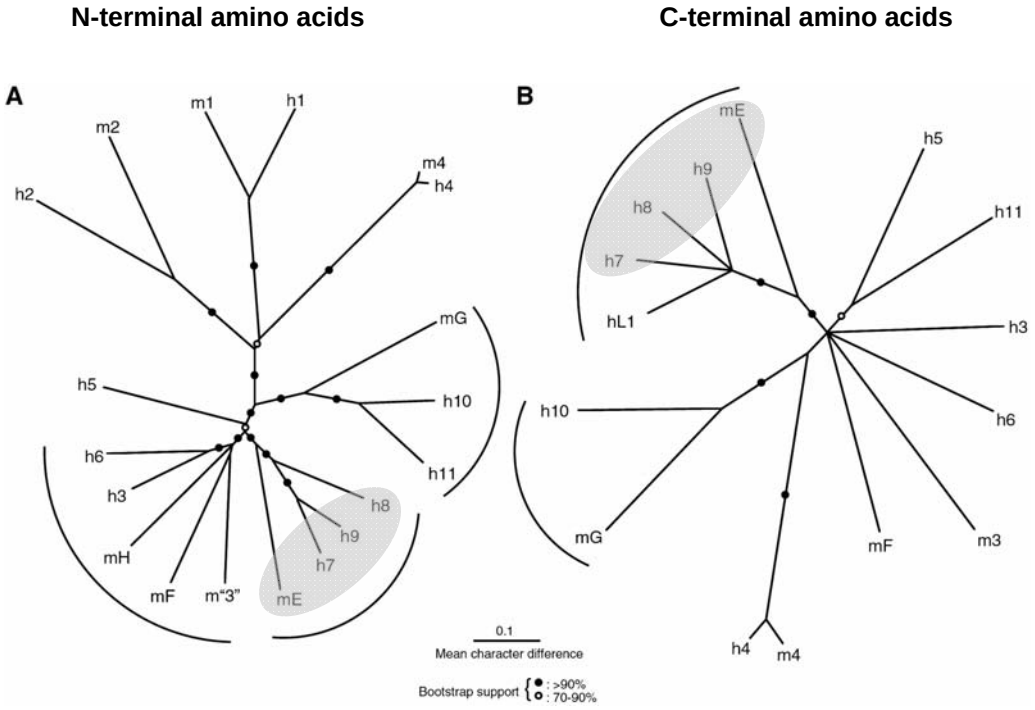

Figure 1.5: Phylogenetic comparison of human and mouse siglecs: Phylogenetic tree derived from N-terminal and C-terminal sequences of human and mouse siglec. Siglecs belonging to the same clade have been shaded in grey. Adapted from (Angataet al., 2001)

The expression of these sialic acid receptors is mostly restricted to hematopoietic cells and cells of the immune system. Structurally, the extracellular domain consists of a V-set immunoglobulin superfamily (Ig) domain and varying number of C2-set domains (as shown in figure 1.4). For example, sialoadhesin has 17 extracellular domains while Siglec-7 has only 3. The V-set domain contains key residues that facilitate binding of sialic acids. In the cytoplasmic domain, most members of this family have ITIM and ITIM-like motifs. The presence of ITIMs fits in with their role as regulators of the immune system. However some members of the human siglec (Siglec-14) and of the mouse (Siglec-H) have no ITIM motifs but instead associate with ITAM bearing adaptors such as DAP12 via their positively charged transmembrane region (Angata et al., 2006;Blasius et al., 2006)

As their name suggest, Siglecs are classically involved in sialic acid recognition. Sialic acids (NeuAc) are a family of 9-carbon sugars found usually as terminal structures of N-linked glycans, O-linked glycans and glycosphingolipids. The second carbon (R2) on the sialic acid forms linkages with other sugars (as described in the figure 1.6) while the R5 can have various modifications such as N-acetyl group (NeuAc), a hydroxyl group (Kdn) or an N-glycolylneuraminic (NeuGc). Sialic acids are highly expressed on cell surfaces and confer the cell with a strong negative charge.

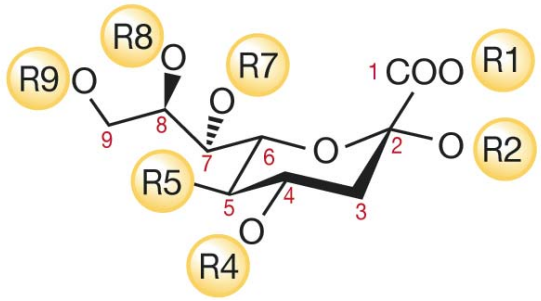

Figure 1.6 Structure of sialic acid – The structure of the 9-carbon sialic acid. The carbon atoms are labelled 1-9. Positions R1-R9 represent the different modifications possible at these positions. For example at position R2 – the carbon can form α linkages Gal(3/4/6), GalNAc (6), GlcNAc(4/6) and another sialic acid (8/9). Adapted from Essentials of glycobiology (2009).

Structural studies of Sialoadhesin and Siglec-7 with sialic acid analogues have revealed the key residues involved in the interactions between siglecs and sialic acids. Some of these interactions are conserved between the different members. The arginine residue (at position 124 in the case of Siglec-7) in the V-set domain forms a salt bridge with the carboxylate group of sialic acids (Alphey et al., 2003;Attrill et al., 2006b) (Attrill et al., 2006a). However, the specificity of each member for different ligands also depends on the underlying glycan linkages. While Siglec-7 has greater preference for disialic acids in α 2,8 linkages, CD22 prefers sialic acids linked to a galactose by α 2,6 linkage.

One of the characteristic features of this family is that most of the members interact with sialylated ligands on the same cell ("*cis*" interactions) and is

therefore masked from binding ligands in *trans* (figure 1.7). This has been attributed to the high concentration of sialic acid containing ligands on the same cells. This phenomenon was first identified for CD33 (Freeman et al., 1995) and CD22 (Razi and Varki, 1998) but then found to be characteristic for most of the members of the Siglec family except for Sialoadhesin (Razi and Varki, 1998). These low affinity *cis* interactions can be abolished by removing cell surface sialic acids either enzymatically by sialidase, chemically by periodate or in some cases by cellular activation, thereby "unmasking" the sialic acid binding site (Collins et al., 2004) (Razi and Varki, 1999). The *cis*-interactions however do not necessarily stop these lectins from interacting with multivalents ligand based probes or high affinity ligands expressed in *trans* or on adjacent cells. The classical example for this is the B cell receptor, CD22, which has been studied extensively. CD22 has been shown to be able to bind to sialylated ligands expressed in *trans* without the need for prior unmasking (Paulson, Macauley and Kawasaki, 2012)

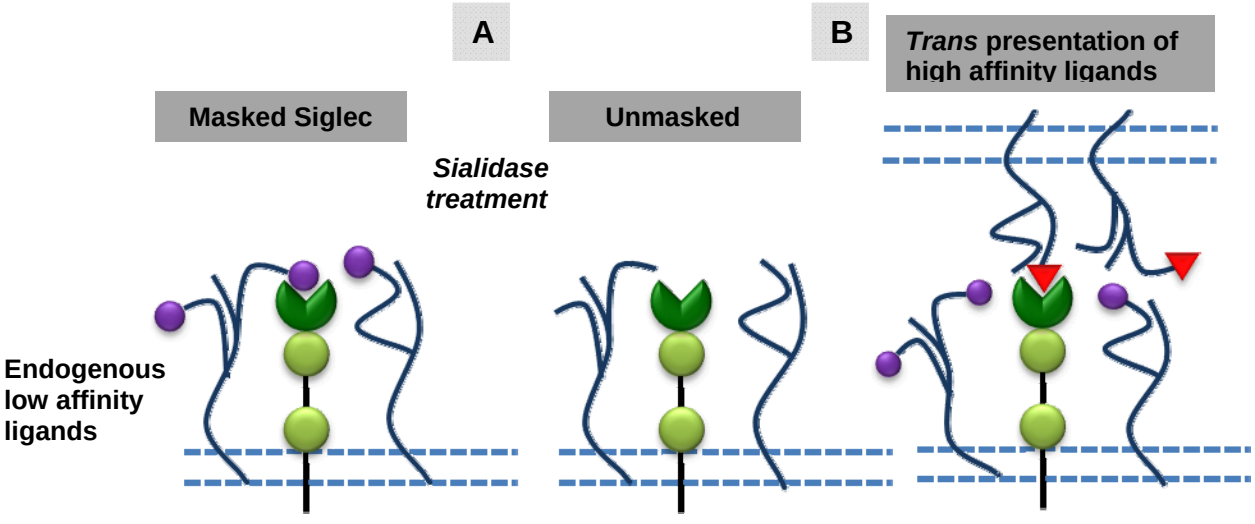

Figure 1.7 – Masked and unmasked state of Siglec receptors on cellular surfaces – (A) Low affinity *cis*-ligands mask the receptor binding site of Siglec receptors. Upon either sialidase treatment or cellular activation, the sialic acid binding site of the receptor is unmasked. (B) Presentation of high affinity ligands in *trans* also unmasks the receptor and facilitates ligand interactions

The functional role of these lectins has been broadly described as sensing “self”, by the recognition of sialic acids. This is similar to role of inhibitory KIR in recognizing MHC expression. Recent investigation of these receptors has shown that they also play important roles in regulating the immune system. Table 1.2 details some of the known functions of these receptors. The presence of the conserved internalization motif, YXXφ, has endowed some of the members of this family with endocytic capabilities (discussed in chapter 5).

CD22, expressed on B cells, is one of the most well studied member of the siglec family especially with regards to its role in B cell receptor (BCR) activation (Poe and Tedder, 2012). Mice B-cells deficient in both CD22 and Siglec-G (mouse orthologue of Siglec-10, with restricted expression on B-cells) showed classic signs of hyperactivation upon BCR ligation, which underscored their role as negative regulators of BCR (Jellusova et al., 2010;Kawasaki, Rademacher and Paulson, 2011;O'Keefe et al., 1996). CD22 and BCR are present in two distinct membrane domains and different models have been proposed to explain how CD22 is able to regulate BCR signalling. The most probable model was proposed by Lanoue et al., whose group used the over-expression of α 2,6-linked sialyl transferase (αST6GalI) to generate CD22 ligands on membrane immobilized hen egg lysozyme (HEL) cells. They showed that the expression of CD22 ligand in *trans* on HEL cells resulted in the dampening of the activation of B-cells (HEL specific) compared to cells, which lacked in the expression of CD22 ligands. The presence of *trans* ligands resulted in the redistribution of CD22 to the site of cell-cell contacts and co-localization with BCR (Lanoue et al., 2002) (Collins et al., 2004).

Mouse models have been useful in providing information about the functions of siglecs *invivo* and in regulating the innate and adaptive immune systems in

infections. Sialoadhesin expressed on macrophages have been shown to facilitate clearance of sialylated pathogens such as *Camplyobacter jejuni* and stimulate proinflammatory responses (Klaas et al., 2012). Siglec-E, expressed on mouse neutrophils, was shown to negatively regulate TLR responses (Boyd et al., 2009) and suppress early neutrophil recruitment in an LPS model of acute lung inflammation (McMillan et al., 2013). The mouse B cell siglec, Siglec-G, has been implicated in preventing sepsis in mice on the one hand and negatively regulating RIG-I signaling during viral infection (Chen et al., 2011;Chen et al., 2013). Recruitment of eosinophils, bought about by parasitic inflammation, is negatively regulated by Siglec-F, expressed on these cells (Kim et al., 2013).

Table 1.2: Expression and some functions of the known human members of the siglec family. Adapted from (Cao and Crocker, 2011)(Varki and Angata, 2006)

Receptor	Cellular expression	Functions
Siglec-1 (Sialoadhesin)	Macrophages	Phagocytosis of sialylated pathogens, production of pro-inflammatory cytokines (Klaaset al., 2012); Regulation of autoimmunity via suppression of regulatory T cells (Wu et al., 2009)
Siglec-2 (CD22)	B cells	Regulation of BCR signaling (Muller et al., 2013) ; and B cell self tolerance to TI-2 antigens (Poe and Tender, 2012)
Siglec-3	Myeloid progenitors, monocytes	Inhibition of $Ca^{2+,}$ cell growth and apoptosis, clearance of amyloid protein by microglia (role in pathophysiology of Alzheimer's disease) (Malpass, 2013)
Siglec-5	Neutrophils, B cells	Increased respiratory burst in neutrophils; down regulation of phagocytic functions in group B streptococcal infections (Carlin et al., 2009a)

Siglec-6	Trophoblasts, B cells	Suppressing invasiveness of trophoblasts (Lam et al., 2011); immunomodulation of B cells in HIV (Kardava et al., 2011)
Siglec-7	NK cells, monocytes and subsets of CD8+T cells	Inhibition of cytotoxicity (Nicollet al., 2003) and T cell signaling (Ikehara, Ikehara and Paulson, 2004); role in pathophysiology of guillain barre syndrome (GBS) (Heikema et al., 2013)
Siglec-9	Neutrophils, monocytes and conventional DC	Suppresion of monocyte and neutrophil activation (Carlin et al., 2009b;Ohta et al., 2010); Downregulation of TLR-mediated proinfammatory cytokines following LPS stimulation (Ando et al., 2008)
Siglec-8	Eosinophils , basophils	Induction of apoptosis
Siglec-10	NK-like cells, B cells, monocytes and eosinophils	Decrease tissue inflammation in case of tissue damage; mediate lymphocyte adhesion (Kivi et al., 2009)
Siglec-11	Macrophages (microglial cells)	Inhibition of production of proinflammatory mediators and phagocytosis
Siglec-16	Macrophages	
Siglec-14	Neutrophils and monocytes	Upregulates inflammatory responses in chronic obstructive pulmonary disease (Angata et al., 2006;Angata et al., 2013) (Yamanaka et al., 2009)
Siglec-15	Macrophages and dendritic cells	Development of functional osteoclasts (Ishida-Kitagawa et al., 2012)

1.6 Gangliosides and tumour associated carbohydrate antigens

Since the main aim of this thesis was to investigate the role of gangliosides in modulating Siglec-7 functions on NK cells, some general background information on these molecules as well as their pathophysiological role in tumorigenesis will be detailed in the sections below.

1.6.1 Gangliosides and biosynthetic pathways

Gangliosides belong to a class of glycosphingolipids, abundantly expressed on the cell membrane, especially in the nervous system. They are a very diverse family of biomolecules, characterized by one or more sialic residues linked to hydrophobic ceramide moiety. While the ceramide moiety is embedded into the plasma membrane, the hydrophilic sugar head group extends out into the extracellular medium (Sonnino et al., 2007). Gangliosides nomenclature is based on the Svennerholm classification for eg., GM1, GD3, GT1a etc. Here the G stands for gangliosides, the second letter (M, D and T) stands for 1,2 or 3 sialic acids respectively and the number (1,2,3) depends on the order of their migration on thin-layer chromatography (Essentials of glycobiology, chapter 10)(Yu et al., 2011). They are divided into 4 classes according to the number of sialic acids attached to the lactosylceramide (shown in figure 1.8) as 0, a, b and c series (Kolter, 2012). Ganglioside expression changes during the process of development. Gangliosides of the “0” and “a” series are expressed on all vertebrate cells. Those of the “b” and “c” series are particularly abundant in the cells of the central nervous system and is critical for normal brain development (Hakomori, 2003). Complex gangliosides are also over-expressed in tumours of neuroectodermal origin such as melanoma, glioblastoma and neruoblastoma and their role in promoting tumorigenesis will be discussed in section 1.6.2 (Birkle et al., 2003). The ganglioside biosynthetic pathway begins with the formation of lactosyl ceramide (LacCer), which is a glucose and galactose residue attached to the ceramide backbone, via β-linkages (Figure 1.8). Then the simplest of gangliosides, GM3, is formed by the enzymatic addition of a sialic acid on to LacCer. The remaining gangliosides are formed by sequential

addition of sialic acid, N-acetylgalactosamine (GalNAc), galactose residues to GM3 from nucleotide sugar donors, by a group of enzymes known collectively as glycosyltransferases (sialyltransferases will be discussed in chapter 3). The synthesis of ceramide and glucosylceramide takes place on the cytoplasmic face of the endoplasmic reticulum (ER) and then turns towards the Golgi lumen where it gets converted to more complex gangliosides. Following trafficking through the Golgi, the final ganglioside product gets incorporated into the cell membrane with the hydrophilic sugar head group extending into the extracellular milieu (Rinaldi, Brennan and Willison, 2010a).

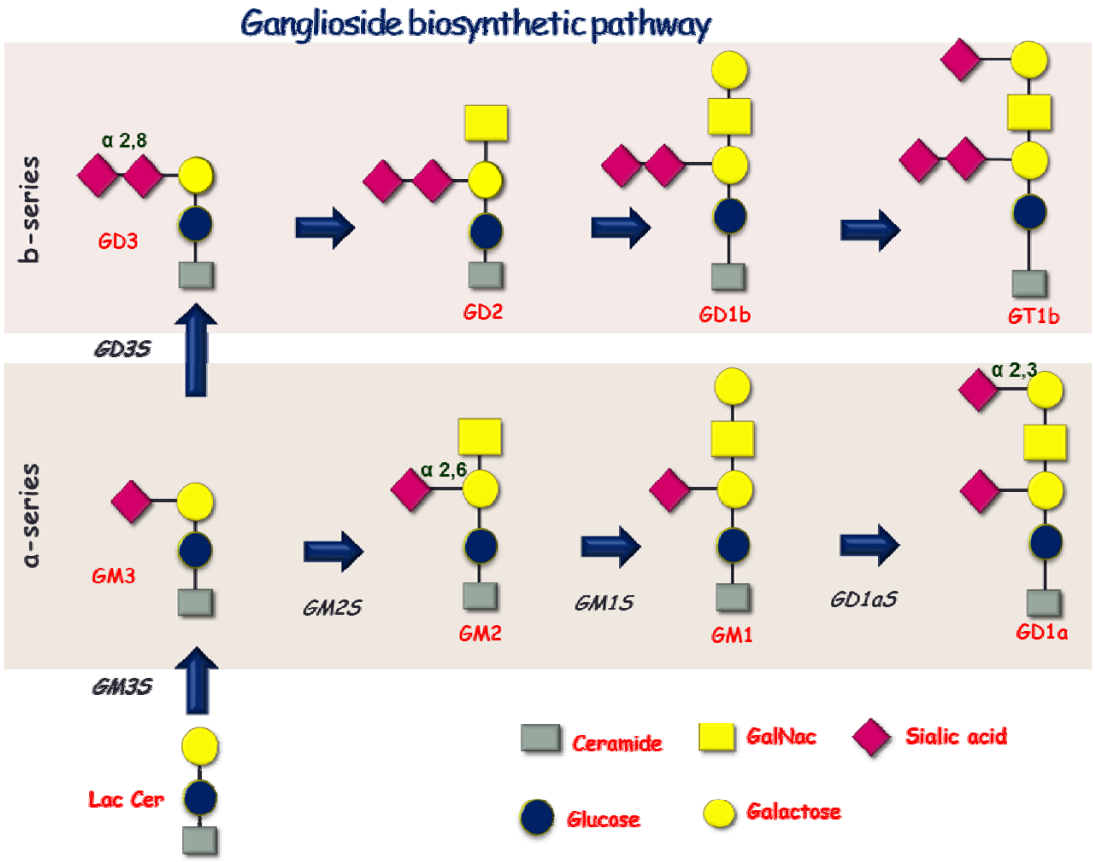

Figure 1.8: Biosynthetic pathway of ganglioside: Beginning with LacCer, the sequential addition of sialic acid, galactose and galnac residues results in the formation of higher and complex gangliosides. The different glycosyltransferases are written out in black and italics and the gangliosides in red.

Along with cholesterol and sphingomyelin, gangliosides are present on the cell membranes in distinct domains known as “lipid rafts”. The presence of lipid

rafts, their organization and isolation has been much debated due to inherent difficulties in isolating and visualizing them (Brown and London, 2000), (Calder and Yaqoob, 2007). The current definition is that rafts are dynamic, ordered, nanoscale, lipid enriched assemblies of proteins which can coalesce by interactions between lipids and proteins (Simons and Sampaio, 2011). The presence of saturated fatty acids in the cholesterol and sphingomyelin components of the rafts favours tight packing of the lipid molecules within these microdomains. Proteins associated with lipid rafts such as receptor and non-receptor tyrosine kinases, integrins and G-protein coupled receptors undergo modifications such as palmitoylation and myristoylation (Kraft, 2013). Lateral interactions between the various components of rafts allows formation of larger platforms capable of taking part in various biological process such a trafficking, endocytosis, signaling and biosynthesis (Sonnino and Prinetti, 2013).

Being expressed on the plasma membrane and present on lipid microdomians gangliosides have important functional roles for example cell-cell interactions, adhesion, proliferation and receptor signaling (Lopez and Schnaar, 2009) (Milani et al., 2010;Wang, Sun and Paller, 2002). The regulation of different growth factors receptors by gangliosides is well studied. GM3 was found to interact directly with epidermal growth factor receptor and inhibit its autophosphorylation (Miljan et al., 2002) while GM1 has been shown to associate with the neural growth factor tyrosine kinase receptor, Trk, and induce its phosphorylation in the PC12 cell line (Mutoh et al., 1995).

The role of gangliosides also expands to pathophysiological conditions such as inflammations (Ohmi et al., 2011), altering immune responses (Monteiro de Castro et al., 2004), autoimmunity (Kaida et al., 2004) and tumorigenesis (explained in section below).

1.6.2 Carbohydrates modulate tumor responses

Glycosylation is important for obtaining functional protein and lipid molecules that are components of cell membranes. However, tumour transformation of cells results in changes of the glycosylation pattern of proteins and lipids. Such changes can be a result of altered/neo expression, incomplete synthesis, over-expression, transcriptional changes and loss of expression. These changes confer the tumour cells with certain advantages such as increased growth and proliferation, metastasis and even immune evasion mechanisms.

Complex gangliosides are overexpressed in many tumours and are usually oncogenic markers for tumour progression. For example - melanomas have over-expression of GD3, neuroblastomas of GD2 and GD3, renal cell carcinoma of GM1, GD1a, GD2 and breast cancers of GD3, 9-o-acetyl GD3/GT3 (Cazet et al., 2010) (Furukawa et al., 2012). Numerous reports have shown that the overexpression of these gangliosides helps tumour cells maintain and expand their tumorigenic properties such as adhesion, proliferation, migration, vascularization and invasion (Birkleet al., 2003). Depletion of GD2 from a neuroblastoma cell line reduced its adhesion to collagen, in a reversible manner, favoring metastasis (Kazarian et al., 2003). The sialyltransferase, GD3 synthase, which is responsible for the formation of the “b” and “c” series complex gangliosides has increased expression in high grade and estrogen receptor (ER) negative breast cancers (Ruckhaberle et al., 2009). Delannoy and group went to dissect the role of GD3 in breast cancer progression by using an ER negative breast cancer cell line, MD-MBA-231. This cell line, transfected with GD3 synthase, showed increased proliferation when cultured in the absence of serum, suggesting non-dependence on growth factors (Cazet et al., 2012;Cazet et al., 2009). GD3 has also been found to enhance the proliferation

and invasion of GD3 expressing melanoma cell line (Hamamura et al., 2008). Furukawa and group have investigated the mechanism underlying this phenotype and found increased phosphorylation of focal adhesion kinases (FAK), p130Cas and paxillin in cells expressing GD3. They further went on to show that there was enhanced activation of integrin signaling in GD3 expressing cells, in the presence of serum. Exposure of GD3 expressing cells to collagen resulted in the clustering of integrins in lipid rafts along with GD3 and FAK with subsequent upregulation of both integrin linked kinase (ILK) and Akt phosphorylation (Ohkawa et al., 2010). Src kinase family (SFK) member, Yes, was also shown to be regulated by GD3 in this model system, impacting on the tumour phenotype (Hamamura et al., 2011). These examples are suggestive of the importance of GD3 in tumour progression. The anti-GD3 antibody, R24, is therefore a promising candidate for antibody based cancer therapy (Torres Demichelis et al., 2013).

Tumour associated gangliosides can also impact on immune responses. Surface expressed gangliosides as well as gangliosides shed from tumours have been shown to affect T-cell antigen presentation, proliferation and cytotoxic responses(Biswas et al., 2009). Gangliosides from renal cell carcinoma cell line were shown to induce activation induced cell death (AICD) of activated T-cells and this was correlated with increased cytochrome-c release and decreased expression of anti-apoptotic factors, Bcl-2 and Bcl-xL (Kudo et al., 2003).

Other tumour associated carbohydrate antigens (TACAs) are also known to be important in tumorigenesis. For example, the blood group related Lewis antigens ($Lewis^X$, $Lewis^Y$, $Sialyl\text{-}Lewis^X$), the carbohydrate structures present in mucins such as Tn antigen, Sialyl Tn, carcino embryonic antigen (CAE) and N-

linked glycans (Adamczyk, Tharmalingam and Rudd, 2012). The enzyme, GnT-V (N-acetyglucosaminyltransferase), is responsible for the synthesis of GlcNAc β1,6 Man (mannose) structure as part of the processing of N-linked glycans. Over-expression of this enzyme in human fibrosarcoma cell line showed increased N-linked glycosylation of α5β1 integrin resulting in a phenotype characterized by decreased adhesion and spreading but increased migration and invasiveness (Guo et al., 2002). Another tumour marker commonly associated with certain tumours is Sialyl-Le^X and Sialyl-Le^A. These tetrasacharide carbohydrate epitopes are ligands for selectins and their over-expression as well as incomplete synthesis has been co-related with the increased metastatic potential of colonic tumour cell lines as well as clinical progression of tumours (Izawa et al., 2000). The disialylated Sialyl-Le^A is expressed on non-malignant colonic epithelial cells and has been shown to be a counter-receptor for Siglec-7 (Miyazaki et al., 2012). This group reported that the expression of the disialylated Sialyl-Le^A is decreased in malignant cells. Using human colon cancer cell line, which expresses only the mono-sialylated Sialyl-Le^A, they showed that genetic manipulation of this cell line resulted in the expression of the disialylated Sialyl-Le^A, decreased binding to E-selectin and increased binding to Siglec-7. Decreased expression of the enzyme ST6GalNAc6, which is responsible for the addition of sialic acid in 2,6 linkage to Sialyl-Le^A, was shown to be responsible for the incomplete transformation of Sialyl-Le^A to Disialyl-Le^A (Miyazaki et al., 2004).

1.6.3 Ganglioside complexes

Gangliosides have been known to be present on cellular surfaces in cryptic states (Nakakuma et al., 1992). Recent research has shown that gangliosides involve in either homo or hetero interactions with each other on cellular surfaces and modulate antibody recognition. This was first brought to light when sera of patients affected with Guillian Barrè syndrome revealed antibodies that recognized complexes of GD1a/GD1b gangliosides and not the individual components (Kaidaet al., 2004). This phenomenon has been investigated recently. Using a novel method of combinatorial glycan array, different combinations of gangliosides were plated in a grid fashion on PVDF membranes in order to study the modulation of binding by lectins (Siglec-7, E and F), antibodies (anti-GM3) and toxins (tetanus toxin (TeNT Hc))(Rinaldi et al., 2009;Rinaldi, Brennan and Willison, 2010b). These experiments revealed different patterns of lectin recognition of the ganglioside complexes which were termed as complex enhanced, attenuated or independent. In the case of Siglec-7, the recognition of the disialylated GD3 was significantly reduced in the presence of complex gangliosides such as GM1, GM2, GD1a, GD1b and GT1a (Rinaldiet al., 2009;Rinaldi, Brennan and Willison, 2010b). A schematic representation of the array with modulation of Siglec-7 recognition of GD3 in complex with other gangliosides is shown in figure 1.9. This data implies that interactions between gangliosides on cellular surfaces could modulate lectin recognition and impact on functional responses.

		GM1	GM2	GM3	GD1a	GD1b	GD3	GT1a	GT1b	GQ1b
	x									
GM1		x								
GM2			x							
GM3				x						
GD1a					x					
GD1b						x				
GD3							x			
GT1a								x		
GT1b									x	
GQ1b										x

Figure 1.9: Schematic representation of the ganglioside PVDF array: Modulation of Siglec-7 recognition of GD3 when in complex with other gangliosides, as shown by Rinaldi et al., 2009. Strong recognition of GD3 is shown as black circle. Lighter shades of circles represent reduced recognition of GD3 (Adapted from Rinaldi et al., 2009).

A biological interpretation of these findings would be that the presence of complex gangliosides such as GM1 on tumours with GD3 overexpression could negatively impact on Siglec-7 recognition of GD3 and favour tumour clearance by NK cells. However tumours such as melanomas and breast cancer tumours selectively overexpress GD3. This upregulation could be thought of as a possible immune evasion mechanism. “Switching off” of the expression of gangliosides such as GM1 and simultaneously enhancing the expression of GD3 in these tumours could strengthen recognition by the inhibitory NK receptor, Siglec-7 and greatly facilitate tumour cell escape from NK cell lysis.

The above observations formed the basis of this project which was to analyse the role of glycans in modulating NK cell tumour cell recognition via the inhibitory receptor, Siglec-7.

1.7 Aims of thesis

The broad aim of this project was to understand the role of Siglec-7 in NK cell biology. Earlier work has shown that this receptor negatively affects NK cell functions, in particular cytotoxicity. However the mechanisms involved and the factors affecting ligand recognition have not been examined.

Therefore, the more specific aims of this project were as follows:

1. Role of GD3 in modulating Siglec-7 recognition: As discussed above, gangliosides such as GD3 are overexpressed on tumours. Therefore, it is of significance to understand how ganglioside expression modulates inhibitory receptor functions and overall NK cell immune responses in tumour clearance.

2. Role of ganglioside complexes in affecting NK cell recognition: Preliminary data (discussed in chapter 3) suggested that complexes of GD3 with structurally more complex gangliosides, for eg., GM1, inhibited Siglec-7 recognition of GD3. An attempt was made to investigate this finding in a biological setting and possible relevance to tumour immunosurveillance by NK cells.

3. Modulation of integrin function by Siglec-7: Based on the recent finding that Siglec-E negatively regulates integrin signalling (discussed in chapter 4) and the fact that integrin signalling is affected in tumour cells, it was thought to be of considerable interest to study integrin regulation by Siglec-7 in the context of NK cell biology.

Chapter 2

Materials and methods

2.1 Reagents

Gangliosides – Monosialoganglioside GM1, Sigma(G7641); Disialoganglioside GD3, Sigma (43683); Dicetylphosphate , Sigma (D2631); Sphingomyelin, Sigma (S7004); Cholesterol, Sigma (C8667); SYBR green, Applied Biosystems (4039155); 3,3',5,5-Tetramethylbenzidine (TMB) substrate reagent, BD OptEia (555214), Albumin, from bovine serum (BSA), Sigma (A2153). Protein A Sepharose 4B, Fastflow, Sigma (P9424) ;TransIT-LTI reagent, Mirus (2300); Carbonate-Bicarbonate buffer, Sigma (C3041); BD OptEIA TMB substrate, BD biosciences (555214); 0.1% Poly-L-Lysine, Sigma (P8920); Paraformaldehyde, Sigma (158127); Triton-X-100, Fisher (BP151-100); Vectashield, Vector labs(H-1200); HindIII, NEB (R0104S); Xbal, NEB (R0145S); Rapid Alkaline Phosphatase, Roche (04 898 133 001); T4 ligase, Roche (10 481 220 001); Agarose; Protein A , Merk (539202); Neuraminidase (sialidase) from *Vibrio Cholerae*, Sigma (N7885); β-mercaptoethanol, Sigma (63689); Protease inhibitor cocktail tablets, Roche (11836170001), 0.5M EDTA (Ethylenediaminetetraacetic acid), Gibco (15575-020); Poly-L-Lysine (PLL) – Sigma (8920); Ficoll-paque, GE (17-1440-02).

Dubelco's Minimal Essential Media (DMEM), Invitrogen (41966). ; RPMI 1640, Invitrogen (11875-093); Ham's F12 Nutrient Media, Invitrogen (21765-029); Glasgow's Modified Eagles Medium (SAFC – 51492C); Ultra-CHO media, Lonza (12724Q) ; Fetal Calf Serum (FCS), PAA (A15-649); Trypsin-EDTA (0.05%), Invitrogen (25300-054) ; Penicillin-Streptomycin (Pen-strep), Invitrogen

(15070-063); L-MSX, Sigma (M5379); GSEM supplement, Sigma (G9785); Dimethyl Sulfoxide (DMSO), Sigma (D2560); Interleukin-2 (IL2) , Peprotech (200-02**);** G418S, Formedium, Hygromycin, Roche (10843555001), Streptavidin Microbeads (Miltenyi, 130-048-101); Ultrapure 0.5M EDTA, Invitrogen (15575-020); PP2 kinase inhibitor, Sigma (P0042); Phorbol 12,13-dibutyrate (PDBU), Sigma(P1269)

2.2 Primary and secondary antibodies

Primary and secondary antibodies used to detect antigens in flow cytometric, western blots, dot blot and (enzyme linked immunosorbent assay) ELISA analysis are listed in the table 2.1 and 2.2 respectively

Table 2.1: List of primary antibodies used

Antibody (Clone)	Antigen	Host species/nature/class	Working concentration	Source/product code
R24 (2.5 mg/ml)	Anti-GD3	Mouse/Monoclonal/IgG3	5 µg/ml	PRC LAB
Anti-ICAM-1 (HA58)	ICAM-1	Mouse/Monoclonal/IgG1κ	0.5 µg/ml	Ebiosciences (13-0549-80)
7.7a	Siglec-7	Mouse/Monoclonal	1/5 dilution	PRC LAB
HI111	CD11a	Mouse/Monoclonal/IgG1κ	10µl/ml	Ebiosciences (11-0119)
GAPDH (14C10)	Carboxy terminus of human GAPDH	Rabbit/Monoclonal/ IgG	1:1000 dilution	Cell signalling (#2118)

Akt	Carboxy terminal sequence of mouse Akt	Rabbit/Polyclonal/IgG	1:1000 dilution	Cell Signalling (#9272)
Phospho-Akt	Serine	Rabbit/Polyclonal/ IgG	1:1000 dilution	Cell Signalling (#9271)
Phospho-Akt	Threonine	Rabbit/Polyclonal/ IgG	1:1000 dilution	Cell Signalling (#9275)
Syk	N-terminus of human Syk (N-19)	Rabbit/Polyclonal/IgG	200 ng/ml	Santa Cruz (#sc-1077)
Phospho-Syk	Tyr525/526 of human Syk	Rabbit/Polyclonal/ IgG	1:1000 dilution	Cell Signalling (#2711)
Phospho-Syk	Tyr323 of human Syk	Rabbit/Polyclonal/IgG	1:1000 dilution	Cell Signalling (#2715)
Src (clone 32G6)	GST-Src fusion protein (residues 1-110 of human Src)	Rabbit/Monoclonal/IgG	1:1000 dilution	Cell Signalling (#2123)
Phospho-Src (D49G4)	Try 416 of human Src	Rabbit/Monoclonal/ IgG	1:1000 dilution	Cell Signalling (#6943)
Phospho-p38 MAPK	Thr180/Tyr182 of human p38 MAPK	Rabbit/Polyclonal/ IgG	1:1000 dilution	Cell Signalling (#9211)
p44/42 MAPK (3A7)	Total p44/p42 MAP Kinase (Erk1/2)	Mouse/Monoclonal/IgG1	1:1000 dilution	Cell Signalling (#9107)
Phospho-p44/42 MAPK (ERK1/2) (clone E10)	Thr202/Tyr204 of human p44/42 MAPK	Mouse/Monoclonal/ IgG1	1:1000 dilution	Cell Signalling (#9106)
p38 MAPK	Total human p38 MAPK	Rabbit/Polyclonal/	1:1000 dilution	Cell Signalling (#9212)

Phospho-p38 MAPK	Thr180/Tyr182 of human p38 MAPK	Rabbit/Monoclonal/IgG	1:1000 dilution	Cell Signalling (#9215)
P13K p85	Human P13 kinase p85	Rabbit/Polyclonal	1:1000 dilution	Cell Signalling (#4292)
∆G9	Anti-human Perforin	Mouse/Monoclonal//IgG2bκ (FITC)	5µg/ml	Ebiosciences (119994)

TBST – 1XTBS (0.1% Tween-20)

Table 2.2: List of secondary and isotype control antibodies

Antibody	Host species	Working Concentration	Supplier
Anti-human HRP	Goat	1 µg/ml	Sigma (A0170)
Anti-rabbit-HRP	Goat	1.3 µg/ml	Sigma (A0545)
Anti-mouse-HRP	Rabbit	2 µg/ml	Sigma (A9044)
Streptavidin-PE		1 µg/ml	Ebiosciences (12-4317)
F(ab')2 Anti-Mouse IgG PE	Goat	1 µg/ml	Ebiosciences (12-4010)
Streptavidin-APC		0.67 µg/ml	Ebiosciences (17-4317)
Anti-mouse IgG FITC	Rat	2.5 ug/ml	E-biosciences (11-4011)
Streptavidin HiLyte Fluor 555		2 µg/ml	Anaspec (#60666)

HRP – Horse radish peroxidase; PE – R-Phycoerythrin; APC - Allophycocyanin

2.3 Molecular biology techniques

Molecular biology techniques were used to clone different constructs into plasmid vectors for expression analysis.

2.3.1 Vectors

pcDNA 3.1(+) is a commonly used mammalian expression vector, carrying a CMV promoter and ampicillin resistance gene. This vector can carry either a neomycin or a hygromycin resistance. In this project, genes for expression of GD3 synthase, ST6Gal1 and ICAM-1 were cloned into this vector carrying hygromycin resistance.

pCB6 – GD2 synthase was cloned into the pCB6 vector with neomycin resistance. This construct was kindly provided by Prof. Hugh Willison (University of Glasgow).

pCDM8 vector – This expression vector, carrying the CMV promoter, is used for high-level transient expression of cloned cDNA in mammalian cells expressing the large T antigen. Human ICAM-Fc, previously cloned into this vector (PRC lab), was re-transformed into MC10616/P3 *E.coli* strain (Invitrogen), sequenced and then used for either transient or stable transfection of CHO cells.

2.3.2 Extraction of messenger RNA

Qaigen RNeasy Mini Kit was used to extract total RNA from cell lines. All steps were carried out at room temperature. 5 -10 X 10E6 cells were harvested and centrifuged for 5 minutes at 300 *x g* and supernatant carefully removed. In case of tissues, a small sample of tissue (frozen in liquid nitrogen) was used. 600 µl of lysis buffer (Buffer RLT supplemented with 1% beta mercaptoethanol) was added to the cell pellet and pipetted well. This lysate was then transferred into

QIAshredder spin columns and homogenized for 20 seconds. 600µl of RNAase free 70% ethanol was then added to the homogenized lysate and mixed well by pipetting up and down. 700 µl of this lysate was then moved into an RNeasy spin column (placed in a 2 ml collection tube) and centrifuged for 15 seconds at 10,000 rpm. After discarding flow through, 700 µl of Buffer RW1 was added to the column and centrifuged at 10,000 rpm for 15 seconds. Then, 500 µl of Buffer RPE was added to the column and centrifuged again at 10,000 rpm for 15 seconds. This step was repeated once more to complete washing the spin column membrane. Finally the column was placed in a new 1.5 ml collection tube and 30-50 µl of RNase-free water was added directly to the centre of the column membrane and centrifuged for 1 minute at 10, 000 rpm to elute the RNA. 2µl of the eluted RNA was used to measure concentration using the Nanodrop 1000, aliquoted and stored at -80^{0}C.

2.3.3 Reverse Transcription of RNA to cDNA

Qiagen QuantiTect Reverse Transcription kit (QAIGEN) was used to reverse transcribe messenger RNA extracted from cells into cDNA for use in downstream cloning and quantitative real-time polymerase chain reaction (PCR) analysis. genomic DNA Wipeout Buffer, Quantiscript Reverse Transcriptase (QRT), RT primer mix, and RNase-free water were thawed at room temperature whilst the template RNA was thawed on ice. The protocol was divided into two steps – 1) eliminating genomic DNA and 2) converting mRNA to cDNA. The following reactions were set up.

4 µl of gDNA Wipeout Buffer (7x), template RNA (upto 1µg) and RNAase free water to a total volume of 28µl were mixed together. This mix was then incubated for 2 minutes at 42^{0}C and then immediately placed on ice and

transferred to a tube containing 12µl of Reverse-transcription reaction components (2 µl of QRT, 8µl of QRTB (5x) and 2µl of primer mix). After mixing all components in the tube well, the mix was incubated at 42^0C for 15 minutes and finally 3 minutes at 95^0C to inactivate the enzyme. cDNA was then aliquoted and stored at -20^0C.

2.3.4 PCR amplification of cDNA

KOD Hot start DNA polymerase (Novagen) was used to amplify prepared cDNA using primers carrying restriction enzyme sequences which would enable cloning of the amplified DNA into respective plasmid vectors. 50µl of the following mix was prepared for each PCR amplification - 10x Buffer KOD Hot Start DNA polymerase – 5µl; 25mM MgSO4 – 5 µl; dNTPs (2 mM) – 5 µl; PCR grade water; 1 µl of sense primer (10 µM); 1 µl of anti-sense primer (10 µM); 1 µl of template DNA; 1 µl of KOD Hot Start DNA polymerase and 5 µl of DMSO.

The following cycling conditions were used to carry out the PCR reaction – Polymerase activation – 95^0C for 2 min; Denature – 95^0C for 20 seconds; Anneal – Lowest primer Tm^{0}C for 10 seconds; Extension – 70^0C (1 minute per Kb) and total number of cycles – 20-30.

2.3.5 Agarose electrophoresis

100 ml of 0.8-1% agarose gels were prepared using agarose added to 100ml of 1xTAE buffer and then bought to boiling temperature in the microwave. The solution was then cooled, 5µl of Ethidium Bromide (stock @100 mg/ml) was added to the solution prior to pouring it out onto prepared electrophoresis trays.

Once set, gels were transferred to electrophoresis tanks carrying 1xTAE buffer, combs removed and DNA samples (mixed with 6x loading dye) loaded onto

wells. Gels were then run at 100V for 40 – 60 minutes and DNA analysed using a UV transilluminator. Pictures were taken using an LCD camera.

2.3.6 Gel extraction of DNA and purification

Following agarose electrophoresis to resolve DNA samples, the DNA band at the right molecular weight was extracted from the gel using the QIAquick gel extraction kit. 100% ethanol was added to the Buffer PE prior to the purification protocol and all centrifugation steps were carried out at room temperature at 13000 rpm. The DNA band was sliced from the gel under UV light. 3 volumes of Buffer QG was added to the gel (100µl for 100mg of gel) and incubated at 50^0C until the gel slice had completely dissolved, with occasional vortexing. The sample was then applied to a QIAquick spin column and centrifuged for 1 minute. The column was then washed using 750 µl of Buffer PE and centrifuged for 1 minute. The flow through was discarded and the column spun again for 1 minute to remove residual Buffer PE. The spin column was then placed in a clean 1.5 ml microfuge tube and DNA eluted using 50µl of water (RNAase-free).

2.3.7 Measuring concentration of DNA/ RNA/purified protein

The concentration of DNA/ RNA/purified protein was measured using the Nanodrop 1000. 2 µl of buffer TE (pH 8.0)/water/sample buffer was used to calibrate the instrument. 1.5 - 2µl of sample was then measured at absorbance 260 and 280 nm. DNA samples with an absorbance ratio (A260/A280) of 1.8 – 2.0 were used for downstream cloning and transfection of cell lines.

2.3.8 Restriction enzyme digestion

In this project, several DNA constructs were cloned into plasmid vectors for the purpose of cell transfections. The cloning process involved the use of different

restriction digest enzymes for DNA and vector backbone digestions, dephophatase treatments and ligations. Enzyme digestions were done either simultaneously or sequentially. Table 2.3 lists the item used in the digest mix.

Table 2.3 : Restriction digestion enzyme mix

DNA	**X (2 µg for insert and 1 µg for vector backbone)**
BSA (X10)	5 µl
NE Buffer (x10)	5 µl
Enzyme 1	2 µl
Enzyme 2	2 µl
H_20	upto 50 µl

The digest mixture was left to incubate for 2 hours in a 37^0C water bath. At the end of the digest, 3µl of Rapid Alkaline Phosphatase buffer (10x) and 3 µl of phosphatase enzyme were added to the vector backbone digest mix and incubated for 15 minutes at 37^0C. The enzyme was inactivated by incubating the digest mix for 2 minutes at 75^0C. Following enzyme digestion, 6x loading dye was added to the mix and loaded on to wells of a 0.8-1% agarose gel and ran as described above.

2.3.9 DNA ligations

Ligation of enzyme digested vector backbone and insert DNA is set up according to the concentration and size of the insert. 100ng of the vector backbone is mixed with 3 or 5 times more of plasmid insert DNA, 1.5 µl of T4 ligation buffer (Roche) and 1µl of T4 ligation enzyme and made upto 15 µl with water. The ligation reaction was left to incubate for 1 hour at room temperature.

2.3.10 Bacterial transformation of ligation reactions or plasmid DNA

DH5α competent cells are used for the purpose of transforming plasmid DNA and ligation products into bacteria. 5µl of ligation mix (or 1 µl of purified plasmid DNA) was taken and added to 50 µl of thawed DH5α bacterial cells (DSTT, University of Dundee) and incubated on ice for 30 minutes. This mixture was then heat-shocked at 42^0C (in a water bath) for 45 seconds and incubated again on ice for 10 minutes. 200 µl of warm Super Optimal Broth (SOB or SOC) media was added to the cells and allowed to recover for one hour in an 37^0C, shaking incubator. 50 – 100 µl of the transfection mix was then plated on to LB agar plate (with suitable antibiotic selection) and left to incubate at 37^0C, overnight.

2.3.11 Bacterial culture

Single bacterial colony were then selected and put into 3ml of LB media and cultured overnight at 37^0C. Bacterial culture was then spun down at 3000 rpm for 5 minutes, supernatant removed and plasmid DNA extracted using Wizard® *Plus* SV Minipreps DNA Purification kit (Promega).

For large scale DNA extraction, Qiagen Plasmid Prep Maxi kits were used. A single colony of transformed bacteria was grown in 10 ml of selection media, overnight at 37^0C. This culture was then used to inoculate 200ml of selection media and incubated at 37^0C for 16 hours. Culture was then spun down for 10 minutes at 10,000 rpm and extraction of plasmid DNA carried out according to manufacturer's instructions

2.4 Cell culture techniques

2.4.1 Culture conditions for cell lines used in this project

B16 (78) – This mouse melanoma cell line was kindly provided by Dr. Hugh Willison (University of Glasgow). This cell line is a subline derived from a melanoma clone (Cloudman S91) obtained from a male mouse of the DBA strain (Yasamura et al., 1966). Cells were cultured in completed DMEM +7.5% FCS + 1% Pen-Strep, at 37^0C in 5% CO_2 in a tissue culture incubator. Cells grew as adherent culture and were split 1 in 5 dilution when 80-90% confluent. Cells were harvested with 2-3 ml of Trypsin/EDTA for purposes of splitting. Cell stocks were frozen down in 10% DMSO in FCS.

NK92 - This NK leukemic cell line of human origin was a kind gift by Dr. Eric Vivier (CIML, Marsille, France). The origin of this cell line was from malignant non-Hodgkin's lymphoma of a 50 year old male Caucasian. Cells were cultured in completed RPMI 1640 media (10% FCS and 1% Pen-Strep) + 100 IU/ml IL2. Lyophilized IL2 was diluted in 100 mM acetic acid to 5 µg/ml and aliquots frozen and stored at -80^0C. Cells were maintained at 1-2 x 10E5 cells per ml and split every 3-4 days. Cells grew in suspension as clusters of 8-10 cells at 37^0C in 6% CO_2 in tissue culture incubator. They were frozen the on the second day following a split in 10% DMSO in FCS.

CHO cells – Chinese hamster ovary cells, were cultured in complete Ham's F12 nutrient media with 10% FCS and 0.1% Pen-Strep and grew at 37^0C in 5% CO_2 in a tissue culture incubator. Cells are adherent and were maintained by splitting them 1 in 5 dilution when 80-90% confluent. Cells were harvested with 2-3ml of trypsin/EDTA for splitting.

MBA-MD-231 cells (A human breast cancer cell line) – This cell line originated from epithelial cells of an adenocarcinoma from a 51 year old caucassian female. Cells were cultured in completed DMEM +10% FCS + 1% Pen-Strep, at 37^0C in 5% CO_2 in a tissue culture incubator. Cells grew as adherent cultures and were split 1 in 5 dilution when 80-90% confluent. Cells were harvested with 2-3 ml of Trypsin/EDTA for purposes of splitting. Cell stocks were frozen down in 10%DMSO in FCS.

K562 – This cell line originated from the bone marrow tissue of a chronic myelogenous leukemia patient**.** The K562 was cultured in complete RPMI 1640 (10%FCS+1% PS). They grew in suspension and were split for culture by diluting out 1:10 in complete media.

2.4.2 Cellular transfection methods

Transfection of nucleic acid (DNA) into cell lines can be achieved by different methods. In this project different approaches were tested with different cell lines and conditions optimized for individual cell lines.

1) Calcium transfection of B16 cells

Cells were plated onto to 15cm dishes 18-24 hours prior to transfection. On the day of the transfection, the culture media was replaced with fresh media. 30 µg of DNA, 62 µl of 2M CaCl2 were made up to a final volume of 1.5 ml with water in a 15ml falcon tube and mixed well. Another tube containing 1.5 ml of 2xHBS was gently vortexed and prepared DNA solution was added dropwise while vortexing. This mixture was then incubated at room temperature for 30 minutes and then added on to the cells. Media was replaced 24 hours after transfection.

For stable transfections, the culture media of the cells was replaced with media containing selection after 48 hours of transfection.

2) Nucleofection of NK92 cells

Amaxa Cell Line Nucleofector Kit R (Lonza) was used to transfect NK92 cells with cDNA of interest. 5 x 10E6 NK92 cells, cultured at 0.2 X10E6 cells per ml, were spun down and resuspended in 100µl of transfection reagent mixture (82µl of Nucleofector solution and 18µl of supplement). 5 µg of DNA was added to cell suspension and transferred to cuvettes provided in the kit. Cells were then nucleofected using A-024 program on the nucleofector device and transferred to warm media with IL-2 in 6-well dish. 24 hours post-transfection, growth media was replaced with media containing selection (0.5 mg/ml G418).

3) Transfection of cells using TransIT

18-24 hours prior to transfection, 3 x 10E6 cells were plated out onto 10 cm dishes in about 15 ml of complete growth media. To 1.5 ml of Opti-MEMI Reduced Serum media, 15 µg of DNA and 45 µl of TransIT-LTI reagent were added and mixed gently. This mixture was incubated at room temperature for 15-30 minutes and then evenly distributed on to cells. Cells were left to incubate for 24-78 hours and then analysed by flow cytometry for antigen expression.

2.4.3 Enrichment of transfected cells

The different methods that have been used in this project to enhance the percentage of transfected population of cells include FACS or MACS sorting to obtain a polyclonal population of high antigen expressers and limiting dilution to obtain a stably transfected single cell clone.

1) Fluorescence activated cell sorting (FACS) – This method involves the separation of transfected cells from the wild type population by antibody staining and isolation by flow cytometry. FACS was carried out by Flow Cytometry Services, College of Life Sciences, University of Dundee.

Transfected cells were cultured in complete media with selection for 7 days. Around 20x10E6 cells, B16 (78) or NK92, were harvested, stained with biotinylated cholera toxin subunit B (1µg/ml)(Sigma – C9972), R24 antibody (5 µg/ml) or anti-Siglec-7 antibody (clone 7.7a) respectively. Streptavidin – PE or Fab anti-mouse PE were used as secondary antibodies respectively. High expressers were analysed and collected using a flow cytometric sorter. This positive fraction of cells were then washed and put back into culture. Once semi-confluent, cells were analysed for antigen expression by FACS staining and aliquots frozen at 2x10E6 per ml in FCS + 10% DMSO.

2) Magnetic Activated cell sorting (MACS) - This method involves the use of the magnetic streptavidin beads to select for transfected cells stained with biotinylated antibody, followed by using MACS sorter to enrich them.

Around 10XE6 B16 cells transfected with ICAM-1, were harvested and resuspended in labeling buffer (1x PBS + 2mM EDTA + 0.5% FCS) stained with 0.5 µg of biotinyated anti-ICAM antibody. Following the manufacturer's protocol, cells were resuspended in 90µl of labelling buffer and then incubated with 10 µl of Streptavidin Microbeads for 15 minutes at 4^0C. Cells were washed in labeling buffer and resuspended in 500 µl of labelling buffer. Labelled cells were then passed throµlh prepared and primed automacs separator, using appropriate program. Enriched cells were collected, washed and put back into culture.

3) Single cell cloning - Single cell cloning was carried out by the limiting dilution method. Transfected cells were plated at 10 cells, 2 cells and 1 cell per well in 96-well tissue culture U plates, in 200 µl of complete media. Half of the media was replaced every 3-4 days. Once confluent, 5-10 clones from the plate containing < 10% of expanding clones were transferred to a 6 well plate and cultured further in selection media. Clones were screened by flow cytometry and positive clones (>70% expression) were frozen down.

2.4.4 Culturing of CHO cells for production of Siglec-7-Fc

1 litre of GMEM culture media was prepared with 100 ml of dialysed and filter sterilized FCS, 10 ml of PenStrep, 20ml of sterile glutamine synthase supplement (GSEM)(x50 stock) and 1ml of L-methionine sulfoxinime (L-MSX) (200mM stock). Frozen stock of CHO cell clone, stably transfected with Siglec-7-Fc, was thawed and put into culture with the above prepared media.

Once cells were established in culture, media was changed for either complete GMEM media (with 0.5% FCS) or serum free UltraCHO media (with 1% PenStrep). When cells became 100% confluent, the supernatants were collected and centrifuged at 2000 rpm for 10 minutes to remove debris. Finally 10mM sodium azide was added to the supernatant and stored either at 4^0C or 1ml aliquots were snap frozen in liquid nitrogen.

2.4.5 Culturing of CHO cells for production of ICAM-1-Fc and ST6GalI

24 hours following transfection of CHO cells with vectors carrying ICAM-1-Fc or ST6GalI, cell culture media was replaced with media containing selection, either hygromycin (0.2 mg/ml) or G418S (0.5 mg/ml). In case of a double

transfection, cells were cultured in media containing both hygromycin and G418S. Cells were allowed to be in selection for one week. As control, wild type CHO cells were grown in selection for the same duration of time. Cells were counted and plated in 96 well flat TC plates at 10 cells per well, 2 cells per well and 1 cell per well with 200ul of complete media. 24 hours later, 100 ul of media was changed for 100ul of selection media. Clones were allowed to grow in selection media. Stable transfected CHO cells expressing ICAM-1-Fc and ICAM-1-Fc + ST6Gal1 were expanded in T175cm2 flask till 100% confluent. Cells were harvested and transferred to roller bottles in 250 ml of complete F12 media (10% FCS) and kept rolling at 10 rpm at 37^0C. Cells were allowed to adhere and adapt to the new culture conditions for 2 days before the media was exchanged for F12 media + 0.5% FCS. Cells were maintained in these conditions for 1 week, media collected (harvest 1) and fresh F12 + 0.5% FCS were added to the roller bottles. This was repeated another 3-4 times till <50% of the cells started sloughing off the surface of the bottle before terminating the cultures. Each harvest was spun down at 10, 000 rpm for 10 minutes, supernatant passed through a 0.2 μm filter and stored at 4^0C with 2 mM sodium azide.

2.5 Extraction of PBMC and culture of cells

PBMCs were extracted using Ficoll-paque extraction method from healthy volunteers. 15-20 ml blood was taken from donors and mixed with 10% of sodium citrate. This mixture was centrifuged for 30 minutes at 1300 rpm, no brake. Buffy coat was gently removed, added to tubes containing PBS and washed at 1000 rpm for 10 minutes (x3). Cells were then resuspended in RPMI

media, counted and 1-2 x10E6 cells added to 6 well TC plate. IL-2 was added to the wells at 200 IU/ml. After 4 days in culture, activated cells were used in assays.

2.6 ICAM-1-Fc protein purification

2.6.1 Preparation of protein A / G column for purification

The following buffers were prepared a day or two prior to purification process. pH of all buffers were adjusted with concentrated HCl. All buffers were then sterilized using 0.22 µM filters, degassed and chilled.

Elution buffer - 0.1M Glycine pH 3

Column stripping buffer - 0.1M Glycine pH 2.5

Neutralization buffer - 1M Tris pH 8 (Tris base)

Binding buffer - PBS with 0.02% Sodium Azide

2.6.2 Purification of ICAM-1-Fc

Cell culture supernatant from roller bottle culture was collected and centifuged at 10,000 rpm for 20 minutes. Supernatant was then filtered using a 0.22 µM vacuum filter, 5mM sodium azide added and stored at 4^0C. A new protein G column was prepared by first rinsing a chromatography column (731-1550, Biorad) with MilliQ deionized water. The column was then half filled with binding buffer and any air bubbles from below the support disc were dislodged by gently tapping the column. The column was then emptied of any liquid and preventing any air bubble from entering. 20% ethanol from protein A sepharose 4B slurry was replaced with binding buffer. Resin slurry was swirled to obtain a homogenous suspension and added to column without introducing any air bubbles. Resin was then allowed to settle in the column for 30 minutes and topped up with 1-2 cm of binding buffer. Purification was carried out at 4^0C,

using chilled, degassed buffers. The column was then connected to the inlet cap and column was allowed to equilibrate with 10 column volume (CV) of binding buffer. Filtered and degassed cell culture supernatant was passed over the column at 0.2-0.8 ml min^{-1} and eluate collected in a new bottle.

Column was then washed with 10 CV of binding buffer. 1-3 CV of elution buffer was passed throμlh the column and 1ml elutions were collected into microfuge tubes containing 100 μl of neutralization buffer and mixed well. Protein is expected to come off in 1-3 CV. Column was again washed with 10 CV of binding buffer.

To store columns, it was first cleaned off residual protein by passing 10 CV of stripping buffer followed by 10 CV of binding buffer. Column was then washed in 10 CV of 20% ethanol and sealed and stored at 4^0C

Protein concentration of the eluate was checked using Nanodrop 1000 readings. Positive fractions were then serially concentrated and buffer exchanged (>95%) with binding buffer using Vivaspin concentrators (10,000 rpm molecular weight cut off) (spun at 4000 rpm, 10 minutes).

2.7 ELISA for testing Fc chimera

96 well Immulon 4BX plates were coated with 1/200 dilution of Anti-human IgG (Fc specific) (Sigma, 12136) in 0.05M, pH 9.6 carbonate-bicarbonate buffer (Sigma, C3041), overnight. Plates were washed in PBS+0.25%BSA (wash buffer), 3 times and blocked with 200 μl of 5% milk in PBA. After washes, 100μl of dilutions of standards and Fc chimera supernatant were added to the wells,

incubated at room temperature for 2 hours and washed in wash buffer. Wells were incubated with 100µl of 5 µg ml-1 of biotinylated anti-ICAM antibody (13-0549, Ebiosciences) or 10µg ml-1 of Biotinylated Sambucus niagra (SNA) lectin (B1305, Vector labs), incubated for 1 hour at room temperature and washed again. 100 µl of either 1:2500 dilution of alkaline phosphatase conjµlated anti-human IgG (A9544, Sigma) or 1:1000 dilution of streptavidin-alkaline Phosphatase, made in 1 x TBS (0.25% BSA) were added to the plates and incubated for an hour. After washing plates in TBA, 100 µl of PNPP substrate (N1891, Sigma) was added to the wells. Plates were read every 5-10 minutes at 405nm. In some assays, for detection of Fc, an Anti-Human IgG (Fc specific) Peroxidase (Sigma, A0170) was used followed by TMB substrate.

2.8 Preparation of red blood cells (RBCs)

1-2 ml of blood was collected from healthy volunteers and diluted in 40 ml of 1xPBS. No anti-coagulant was used in the process. Cells were washed three times in PBS by centrifµling at 1300 rpm for 5 minutes at room temperature and removing the supernatant. After the final wash, 20 ml of Alsevers reagent was added to the cells and the RBCs were allowed to settle at 4^0C.

2.9 Sialidase treatment of cells

Cells were harvested and washed twice in DMEM without FCS. Cells were resuspended in DMEM at 1 x 10E6 cells per ml and sialidase added at 0.17 IU/ml. Treated cells were then incubated for 1 hour at 37^0C, 8 % CO_2, with occasional agitation. Following incubation, cells were washed twice in DMEM

containing 10% FCS. For sialidase treatment of RBCs, 25 µl of packed RBCs were resuspended in 5 ml of DMEM media and treated with sialidase.

2.10 Red blood cell solid phase adhesion assay

96 well 4HBX Immunolon plate was coated with 100 µl of goat anti-human IgG AT 1:200 dilution in carbonate-bicarbonate buffer (pH 9.6). Plate was incubated overnight at 4^0C. The plate was then washed three times with 200 µl of wash buffer (1xPBS + 0.25% BSA; PBA) and then blocked with 200 µl of 5% milk in PBA. After washing off the block, 100 µl of Siglec-7-Fc chimera at varying dilutions were added to the plate and incubated at 37^0C for an hour. Plate was washed 3 times in wash buffer and 100 µl of RBC suspension was added per well and incubated at room temperature for 1 hour. The wells were washed as follows to remove unbound RBCs. 150 µl of wash buffer was added to each well of the plate and placed on the orbital shaker for 3 seconds (moderate speed). Wash buffer was then removed from wells using one strong flick of the plate. This wash process was repeated 2 additional times. The plate was then dried and cells fixed with 50 µl of methanol. The plate was then allowed to dry in a tissue culture hood for 15 minutes. TMB substrate was prepared according to manufactures instruction and 100 µl added to the wells of the plate and incubated for 30 minutes at room temperature. The reaction was stopped by adding 50 µl of sulphuric acid and the plate was read at 450nm.

2.11 Antibody staining of cells for flow cytometry analysis

Cells were harvested using 5-10 ml of 1X PBS + 1mM EDTA and resuspended in FACS wash buffer (1xPBS + 2mM EDTA + 0.25% BSA + 2mM sodium azide) at 10 x10E6 cells per ml. 100 µl of cells were then plated per well in a 96-well

U-bottom non-tissue culture (TC) plate and spun down at 1300 rpm for 3 minutes at 4^0C. Cells were then resuspended in 100 µl of the respective antibody at the titrated concentration of 5-10 µg/ml in FACS buffer and left to incubate for 30 minutes on ice. Antibody stained cells were then washed three times in 200 µl of FACS wash buffer and incubated with 100 µl of the secondary antibody (at a pre-determined concentration), for half hour on ice. Following 3 washes with FACS buffer, cells were either stained with 1/300 dilution of 7AAD or fixed with 100µl of 1% PFA in FACS wash buffer. Cells were analysed by flow cytotmetry.

2.12 Preparation of Fc-chimera complexes

Siglec-7-Fc was precomplexed to anti-human Fc specific-HRP or anti-human Fc specific Dylight 647 fluorescent probe to be used in ELISA or flow cytometric analysis respectively. Siglec-7-Fc and secondary antibodies were diluted to different concentrations in 1X PBS +1% BSA, in separate tubes. Siglec-7-Fc was then mixed with the secondary antibody in a 1:3 ratio (volume/volume) and left to incubate for an hour at room temperature (for anti-Fc-HRP conjµlate) and on ice (for anti-Fc-Dylight conjµlate). 100µl of this pre-complex was then used either for ELISA or to stain 1x10E6 cells for flow cytometry/ confocal microscopy staining.

2.13 Confocal Microscopy for detection of GD3 and GM1

B16 cells were harvested with 1mM EDTA. 1X10E6 cells were spun down and washed once with FACS wash buffer. Cells were then resuspended in 100 µl of facs buffer, in 96 well (U bottom plate), and then stained with 5 µg/ml of R24 antibody and 1µl/ml of biotinylated cholera toxin subunit B. Following 30

minutes incubation on ice, the cells were washed twice and stained with 2 µl/ml of anti-mouse IgG (FITC conjugate) and Streptavidin (HiLyte Fluor 555 conjugate). Following the washes, cells were fixed with 1% PFA for 30 minutes on ice. Cells were washed once with PBS and resuspended in 30-50 µl of Vectashield (with DAPI). Resuspended cells were then mounted onto glass slide using hydramount mounting media and sealed with varnish.

Images were collected using the LSM 710 Confocal laser scanning microscope using the x40 or x100 oil immersion objectives. Differential interference images were collected along with the fluorescence images. Images were then analysed using the LSM image software and quantified using Volocity software.

2.14 Dot blots for sialic acid dependent recognition of ICAM-1-Fc

1cm grids were drawn on nitrocellulose membranes strips (Protran, Whatman). Different concentrations of 2 µl of ICAM-Fc (5 µg to 0.1 µg of total protein) were spotted onto the center of the grid and allowed to dry for 10-15 minutes at room temperature. Dried blots strips are then blocked in 5% milk in TBST (1x TBS + 0.1% Tween-20). For sialidase treatment of ICAM-1-Fc, blots were incubated in acetate buffer (sodium acetate + 1mM calcium chloride) with sialidase at 0.17 IU/ml dilution for one hour at room temperature. Sialidase was quenched using 10% FCS in PBS, for 10 minutes. During this incubation period, Fc pre-complex was prepared by mixing 1 volume of Siglec-7-Fc (at 5 µg/ml) and 3 volumes of anti-Fc HRP (1/1000 dilution) in 1%PBA (1xPBS and 1% BSA) and incubating for an hour at room temperature. Blots were incubated with Siglec-7-Fc pre-complexes, biotinylated anti-human ICAM antibody (clone HA58, ebiosciences) or biotinylated Sambucus Niagra Lectin (SNA, Vector labs, B-1305), for one hour at room temperature (or overnight at 4^0C). Blots were then

washed thrice in TBST. SNA and anti-ICAM blots were then incubated with Avidin-HRP (1/1000) in TBST for one hour at room temperature. Blots were incubated using ECL reagent for 1 minute, excess removed and exposed to X-ray film.

2.15 Biochemistry assay and western blotting

6 well tissue culture plates were coated with 10 µg/ml of protein A, overnight. Plates were washed with PBS+0.25%BSA (wash buffer) and blocked with PBS + 5%BSA for 1 hour at room temperature. Plates were coated with 5 µg ml-1 of ICAM-Fc (clone 54), overnight. Plates were washed with wash buffer and then blocked again with 10%FCS in PBS and left in cold PBS till cells were ready to be plated.

NK92 cells were harvested and resuspended in RPMI 1640 + 10%FCS at 0.2 x 10E6 cells per ml. Cells were IL2 starved for 2 hours at 37^0C. Cells were then harvested and resuspended in ice-cold adhesion buffer (HBSS (-Ca^{2+}+ 2mM Mg^{2+})). Cells were then plated onto cold ICAM-Fc coated plates and centifuged at 900 rpm for 30 sec. Plates were then incubated at 37^0C for different time points. Unbound cells were removed from wells into microfuge tubes and 200 ul of lysis buffer (Tris.HCl, 150mm NaCl, 0.1%Triton-X-100, pH 8, 1 tablet of protease inhibitor, phenylmethanesulfonyl fluoride (PMSF), 2mM sodium orthovanadate and 0.1% beta-mercaptoethanol) was added to the wells. The unbound cells were spun for 10 minutes at 13,000 rpm, supernatant removed and 100 µl lysis buffer added. Both unbound and bound cells from the respective cells were mixed. Src inhibitor, PP2, was added at 1250 dilution to control cells and incubated for 10 minutes at room temperature before plating onto wells.

Lysed cells were centifuged at 14,000 rpm for 10 minutes to remove cellular debris. Protein concentrations of lysates were estimated using BCA protein assay kit (Pierce), as described in section 2.15. Lysates were then mixed with NuPage sample loading buffer and NuPage sample reducing agent and boiled for 10 minutes at 70^0C. 15µg of protein were loaded onto 12 well NuPage 4-12% Bis-tris gels and run at 200 V in NuPage MOPS SDS Running Buffer (x20). Gels were then transferred to nitrocellulose membrane (Protran, Whatman) in cold 1x Transfer buffer (NuPage Transfer Buffer (x20) and 10% methanol), at 30V for 90 minutes. Membranes were blocked with 5% marvel in TBST (1X TBS + 0.1% tween-20) for one hour. Blots were stained with the respective primary antibodies, overnight. Blots were washed well in TBST (3 times, 10 minutes each). A 1:3000 dilution of secondary antibody in 2% milk or BSA were added to the blots and incubated for 2 hours at room temperature. Blots were washed in TBST and developed using Immobilon Western Chemiluminescent HRP susbtrate (Millipore).

2.16 BCA assay

BCA assay is the standard method employed to quantify the concentration of total protein in cellular lysates. BCA assay kit (Thermo scientific) is used for this purpose. The detection range of the kit is between 2 mg/ml and 125 ng/ml (when 25 µl of the standard/sample is used). BSA (2mg/ml) is used as the standard for the estimation of protein concentration in lysates.

Both standard and lysate samples were diluted in water. 25 µl of each standard and samples (diluted 1:50) were added to 96 well plate in triplicate. Reagent A and 1:50 dilution of Reagent B were mixed and 200 µl of this is applied to the samples. The plate was then covered in foil and left to incubate for 30 minutes

at 37^0C. The plate was then read at 570nm using a plate reader. Standard curve for the samples are plotted as absorbance vs. concentration. Protein concentrations of the lysates are extrapolated from the slope of the standard curve (Graphpad prism).

2.17 Adhesion assay

96 well tissue culture grade plate were coated with 1:10 dilution of poly-l-lysine (in water), PBS (for blanks) or 10µg ml-1 Protein A and incubated overnight at 4 ^{0}C. Plates were washed with wash buffer (1 X PBS + 0.25% BSA) and blocked with 5% BSA in PBS for 1 hour at room temperature. Wells were then coated with 5 µg ml-1 of ICAM-Fc in 0.25% BSA in 1xPBS, for 1 hour at room temperature. Plates were washed again with wash buffer and blocked with 10% FCS in 1xPBS for 2 hours at room temperature and washed with PBS. NK92 cells were harvested and resuspended at 10E6 per ml in cold binding buffer (HBSS +/- $MgCl_2$) and 200µl added to wells. For controls, cells were treated with either 10 mM EDTA or PDBU at 20 ng ml^{-1} in binding buffer, for 15 minutes on ice before adding them onto prepared plates. Cells were settled on to wells by a pulse spin (30 seconds, 800 rpm). Plates were then incubated for 15 minutes at 37 ^{0}C. Unbound cells were washed off by inverting plates into a container with 4 litre of 1X PBS, supplemented with 0.25mM $MgCl_2$ for 30 -60 minutes at room temperature. Bound cells were fixed by adding 100 µl of methanol and aspirating off after 1 minute. 50 µl of 0.5% Crystal Violet (dissolved in 25% methanol) was added to each well, incubated for 10 minutes at room temperature and wells were thoroughly washed with PBS. 100 µl of methanol was added to each well and plates were read at 570 nm.

2.18 Cytotoxicity assay

Cytotox 96 Non-radioactive assay kit was used to analyze the cytotoxicity of effector cells on target cells. Both effector and target cells were split 48 hours prior to the assay. Cells were harvested and resuspended in cytotoxicity buffer (RPMI 1640 + 1%FCS) at different cell concentrations. Effectors and targets were plated out in 200µl of cytotox buffer in 96 well (U-shaped) tissue culture plates, centifuged at 250g for 4 minutes and incubated for upto 5 hours. 45 minutes prior to the termination of the assay, 20µl of lysis buffer (0.1% Triton-X) was added to the wells with targets alone. At the end of the assay, plates were centifuged again and 50µl of supernatant from each well was transferred to a 96 well 4 HB Immulon ELISA plate. Assay buffer was prepared according to manufacturer's instructions and 50 µl added to each well. Plates were incubated for 30 minutes at room temperature and absorbance was measured at 492 nm on plate reader. Background absorbance was subtracted from each sample and percentage cytotoxicity was calculated as follows:

$$\frac{\textbf{(Sample OD – Effector spontaneous release – Target spontaneous release)}}{\textbf{(Target maximal release – Target spontaneous release)}}$$

2.19 Granule polarization assay

2 x 10E6 Protein A polystyrene particles (6-8 µm) were gently vortexed and washed in 1 X PBS twice by centrifuging at 6000 rpm for 5 minutes. Beads were then coated with 5µg of ICAM-Fc in 1 X PBS, kept on a vortex at 4^0C for 1 hour. Beads were then washed twice in 1 X PBS and resuspended in 100 µl of HBSS (-Ca^{2+}, 2mM Mg^{2+}).

18 mm cover slips were coated with Poly-L-Lysine (1/10 dilution in water), over night, in 6 well tissue culture plates. Coverslips were then washed off PLL with PBS. 0.5X10E6 cells were spun down, resuspended in 100µl of HBSS (-Ca, -Mg) and spotted on to Poly-L-Lysine coated 18mm cover slip. Cells were left to settle on the coverslips by incubating at 37^0C, 5%CO_2, for 1 hour. Following the incubation, the buffer on the cover slip was replaced with 100 µl of ICAM-Fc coated beads. Coverslips were again left to incubate for one hour at 37^0C, 5%CO_2. Following this, unbound cells and beads were washed off in 2 ml of PBS in a 6 well TC plate. Bound cells were then fixed with 4% paraformaldehyde (PFA) for 10 minutes at room temperature. PFA was washed off twice in PBS and bound cells were permeabilized with 1xPBS + 0.1% Triton-X-100 (permeabilization buffer), for 10 minutes at room temperature. Cells were then blocked with 10% mouse serum in permeabilization buffer. Cells were then stained with 5µg/ml of anti-human perforin (FITC conjugated) in block buffer, overnight, in a humidified chamber. Next day, cells were washed twice in permeabilization buffer and mounted onto slides using 5 µl of Vectashield mounting media (with DAPI). Mounted coverslips were sealed and left to dry. Images were collected using the LSM 710 Confocal laser scanning microscope using the x40 or x100 oil immersion objectives. Differential interference images were collected along with the fluorescence images.

2.20 Ganglioside assay

Lysophilized ganlioside stocks were reconstituted at 1 mg/ml using choloroform : methanol (1:1) and stored at -20^0C. The working dilutions were made by sonicating ganglioside stocks for 3 minutes in a water bath. The required amount was then dissolved in methanol in a glass vial to a concentration of 2

µg/ml and was stored at 4^0C for upto 2 weeks. Ganglioside complexes were prepared by sonicating individual gangliosides in the stock vials and then mixing them at a 1:1 ratio in a new glass vial. This mixture was then again sonicated for 3 minutes. When using liposomes reconstituted with gangliosides (prepared as described in section 2.21), gently vortex, add 100µl /well to an ELISA plate and incubate at 4ºC overnight to coat. 4HBX Immulon HB ELISA plate was coated with 100µl of 2 µg/ml of the respective ganglioside. 100µl of methanol was first coated to reduce background contamination. The plate was then dried in a hood overnight and transferred to 4^0C for an hour. Plates were then washed with 0.1% PBA (1X PBS + 0.1% BSA) and dried. Siglec-7-Fc antibody pre-complex was prepared by diluting the Fc chimera to 1 µg/ml and goat anti-human IgG-Fc-HRP TO 1:1000 in 1%PBA (1X PBS + 1%BSA). The two dilutions were mixed in 1:3 ratio and incubated for an hour at room temperature. 100 µl of this pre-complex was then added to the plate and incubated for 2 hours at 4^0C. Plate was then washed 3 times with 300 µl of 0.1% PBA. 100 µl of TMB substrate was added to the plates and reaction stopped with 50 µl of stop solution (3.6% (v/v) of phosphoric acid) and the plate was read at 450nm.

2.21 Preparation of ganglioside reconstituted liposomes

Liposomes incorporating ganglioside and ganglioside complexes were prepared using cholesterol : sphingomyelin : dicetylphosphate : ganglioside 1 (: ganglioside 2) in a 5:4:1:1(:1) molar ratio. Blank liposomes (not containing ganglioside but containing the other components) were prepared to use in negative control wells. The above component lipids were dissolved to 10mg/ml in 1:1 chloroform : methanol in a 15ml falcon to give the required molar ratio. Dicetylphosphate was kept at a lower concentration (2.5mg/ml) to avoid

precipitation. This mixture was then dried under a steady stream of N_2 in the fume hood, leaving a thin film in the tube which was then resuspended in 5-10 ml of PBS, pH 7.4 (3-5x final target volume). This mixture was alternatively vortexed and sonicated for 15min, releasing the lipid from the walls of the tube and producing a uniformly milky solution. It was then alternatively freeze-thawed x5 by plunging into liquid N_2 and then placing in a water bath at 37^{o}C (to produce multi-lamellar vesicles). This was then clarified by centrifulation for 20min@600g, 1800rpm and pellet discarded. The solution was extruded 9-11x throμlh a 0.4μm, using a hand driven extruder, to produce unilamellar vesicles. Finally the solution was ultracentifuged for 1 hour @ 110000g, resuspended in final required volume of PBS and stored in glass vial.

2.22 Quantitative real-time PCR (qRT-PCR)

Real time- PCR was used in this project to measure the amount of messenger RNA levels of a particular gene in non-transfected cells relative to cells transfected with that particular gene.

Power SYBR green PCR master mix (Applied Biosystems) was used for the RT-PCR of the various cDNA samples. The following mix consisting of 12.5 of SYBR green, 1 μl each of sense and anti-sense primers, 5 μl of cDNA and 5.5 μl of RNAase free water was prepared and plated out. Both primer concentration and dilutions of cDNA were optimized for each gene.

The PCR reaction mixture was prepared using 5 μl of cDNA, 12.5 μl of SYBR Green Master mix, 1 μl each of forward and reverse primers and made up to a total volume of 25 μl. No Reverse Transcriptase samples were also prepared and tested during the PCR run. A StepOne instrument (Applied Biosystems) was used to carry out real-time PCR. A total of 40 cycles was run with each

cycle set as follows – 15 seconds at 95 ^{0}C and 1 minute at 60 ^{0}C. Each sample was run in triplicate.

Relative fold change in gene expression in each unknown sample was quantified by the comparative $\Delta\Delta C_T$ method, normalized to GAPDH (reference gene). C_T (cycle threshold) values obtained from the PCR runs were averaged and analysis conducted as follows. C_T of the reference gene was deducted from the C_T of the target gene to obtain ΔC_T, in each sample. The ΔC_T of the reference gene was then deducted from ΔC_T value of the target gene from each sample to obtain $\Delta\Delta C_T$ value. This represents the fold change in gene expression of the target gene in the sample relative to the calibrator tissue, kidney in this case.

2.23 Primers used in generation of clones and qRT-PCR

Primers used in the cloning of DNA and qRT-PCR are listed in tables 2.4 and 2.5 respectively.

Table 2.4 : Primers used in the cloning of DNA into pcDNA 3.1 vector

Primer	Sense sequence (5' – 3')	Antisense sequence (5'-3')
GD3S	CCCAAGCTTGCGATGAGCCCCTGC	GCTCTAGACTAGGAAGTGGGCTGTGGTG
Human ICAM-1	CCCAAGCTTGCGATGGCTCCCAGCAGCC	GCTCTAGATCAGGGAGGCGTGGCTTGTGTGTTC

Shaded region within primer represents gene specific regions, underlined regions represents enzyme restriction sites

Table 2.5 : Primers used in qPCR for the analysis of levels of messenger RNA

Primer	Sense sequence (5'-3')	Anti-Sense sequence (5'-3')
GM3S	GCTTCAAGCAATGGTAAAAAATGA	TTCTGCCACTTGCTTCCAAA
GM2S	AACCGGGTGGCACATCTGGAATTC	CAGAGCAGGAGCCAACACGAAGGA
GM1S	GTCAGCAGCACACAGGGATA	CTGGGACGTTGACATACACG
GD1a	CAGCATGGCTACCTTGCCCTACCT	GCCGAGGCGCTGTAGTCCTGAATA
CMAH	GGTGGTCAGGATGATTGAAACAGATG	TCACCCGGCTATGGATTTCTTC

2.24 Cloning of GD3s into pcDNA 3.1 vector

mRNA, extracted from mouse brain lysates, was used in the generation of GD3s cDNA. Then using the primers for GD3s (table 2.4) cDNA was amplified by PCR (figure 2.1, A). Resulting product and vector backbone (pcDNA3.1 hygromycin) were digested with HindIII and XbaI, ligated, transformed, colonies screened and sequenced. Plasmid prep of the resulting clone was analysed by restriction enzyme digests as shown in figure (2.1,B).

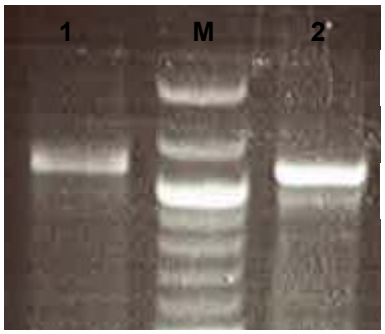

1 – PCR product
M – 100 bp ladder
2 – PCR product after genomic DNA digestion

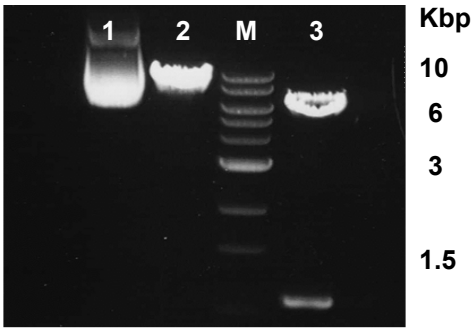

1 – Undigested
2 – HindIII digest
M – 1Kbp ladder
3 – HindIII – Sal1 digest

Figure 2.1: PCR amplification and cloning of mouse GD3s: 2 µl of cDNA was amplified by PCR using 1 µM of primers (annealing temperature of 66.7^{0}C). (A) 5 µl of samples before

and after digestion of genomic DNA, were run on 1% agarose gel. (B) Plasmid prep of GD3 synthase cloned into pcDNA 3.1 was run on 0.8% agarose gel either undigested, single digestion with HindIII or double digested with HindIII and Sal1.

2.25 Cloning of ICAM-1 into pcDNA 3.1

ICAM-1 was overexpressed in these cells by extracting mRNA from K562 cells. This was used to generate cDNA which was then amplified using primers to the human ICAM-1 sequence (table 1; figure 2.4, A). Amplified cDNA and vector backbone (pcDNA 3.1) were subject to restriction enzyme digests (figure 2.2, B) and ligated. Ligation product was transformed into DH5α cells and resulting clones screened by restriction digest analysis and DNA sequencing. Plasmid DNA maxi prep was prepared using the clone with the right size insert

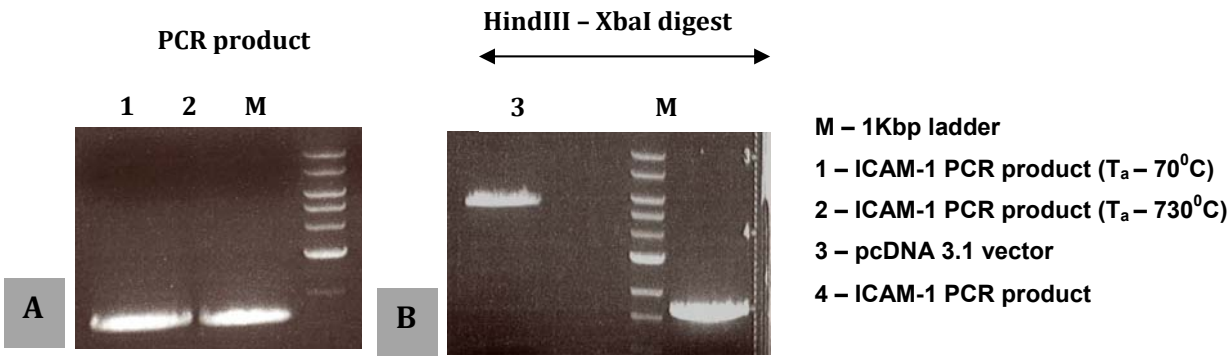

Figure 2.2: PCR and cloning of full length human ICAM-1: (A) PCR reaction mix was set up using cDNA, 1 µM sense and antisense primers, KOD buffer and dNTPs. PCR reaction was set up as follows- :- Activation – 2 min @ 95^{0}C, denaturation – 20 sec @ 95^{0}C, annealing – 10 sec @ 70^{0}C and 73^{0}C, extention – 32 sec @ 70^{0}C for a total of 35 cycles. PCR product was run on a 1.3% agarose gel and purified using Qaigen gel extraction kit. (B) 2 µg of PCR product and 2 µg of p CDNA 3.1 plasmid vector were digested with HindIII and Xbal for 2 hours at 37^{0}C. Digestion products were run on a 1% agarose gel and gel extracted.

2.26 Cloning of ICAM-1-Fc and ST6Gal1

Previously cloned ICAM-1-Fc and ST6Gal1 were retransformed into bacterial cells (as described in chapter 4, section 4.1.1). Figure 2.3 shows restriction enzyme digestion of selected clones of ICAM-1-Fc and ST6Gal1.

CHO cell were transfected with purified DNA for ICAM-1-Fc and ST6Gal1. Selection of stable ICAM-1 producers was achieved by transfecting an empty pcDNA 3.1 vector carrying a selection marker for hygromycin resistance. Plasmid DNA for the empty vector, ICAM-1-Fc and ST6Gal1 were transfected in a ratio of 1:2:2 as described in the methods section. As a control, a separate transfection with only plasmid DNA for ICAM-1-Fc was also carried out.

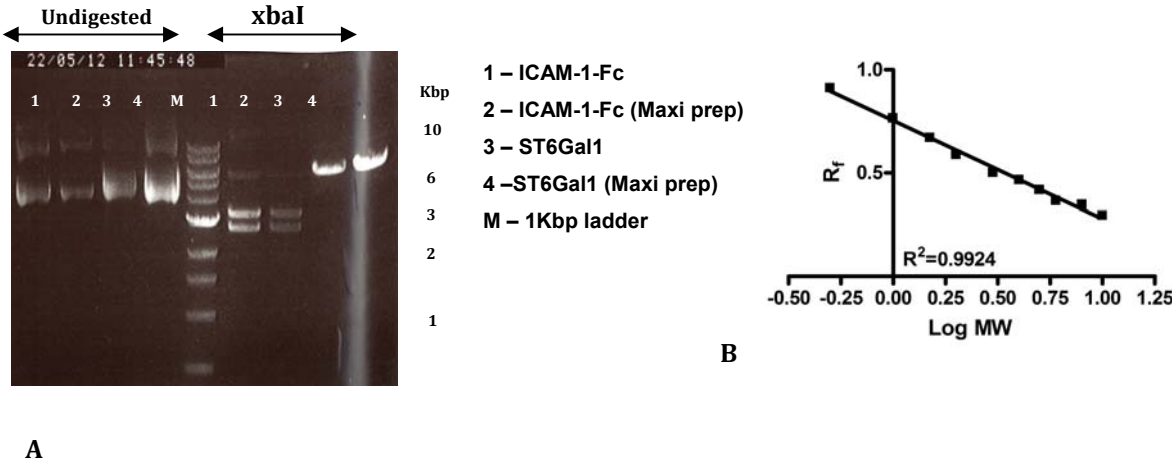

Figure 2.3: Restriction digest analysis of ICAM-1-Fc and α 2,6 sialyltransferase : 1µg of ICAM-1-Fc cloned into pCDM8 and ST6Gal1 cDNA cloned into pCDNA 3.1 vector were digested with XbaI for 1 hour at 37^0C. DNA with no enzyme (undigested) was kept as control. After incubation, digests were mixed with 6x loading dye and loaded on to 1% agarose gel. Gel was run at 100V for 50 minutes. (B) Linear regression curve analysis for molecular weight ladder. Log of molecular weight marker is plotted against distance travelled by the marker (R_f)

2.27 Cloning of Siglec-7 mutants

Cloning of mutants for Siglec-7 was carried out using PCR based site directed mutagenesis (SDM) technique. pcDNA3.1 Siglec-7 was used as the DNA template. 50µl of the following mix was prepared for each PCR amplification - 10x Buffer KOD Hot Start DNA polymerase – 5µl; 25mM MgSO4 – 5 µl; dNTPs (2 mM) – 5 µl; PCR grade water; 1 µl of sense primer (10 µM); 1 µl of anti-sense primer (10 µM); 1 µl of template DNA; 1 µl of KOD Hot Start DNA polymerase and 5 µl of DMSO. Primers used are shown in below in table 2.6. Reaction was set up as follows: Activation – 2 min @ 95^0C, denaturation – 20 sec @ 95^0C, annealing – 30 sec @ 65^0C, extension – 10 sec @ 70^0C for a total of 35 cycles. Following PCR, the product was treated with 1 µl of Dpn1 enzyme and 1 µl of buffer, in a total volume of 30 µl for 1 hour at 37^0C. PCR products were run on 0.7% agarose gel in 1XTAE (Figure 2.4A) and then purified. Purified DNA was then transformed into DH5 α cells. Mutant clones were analysed by restriction digest (Figure 2.4, B) to confirm product size and putative clones were sequenced.

Table 2.6 Primers used in the SDM of mutants of Siglec-7

Primer	Sense sequence (5'-3')	Anti-sense sequence (5'-3')
R124A	GGAGATACTTCTTTGCTATGGAGAAAG	CTTTCTCCATAGCAAAGAAGTATCTCC
YIF (Y437F)	AAAGAGAGATCCAGTTTGCACCCCTCAGCTTTC	GAAAGCTGAGGGGTGCAAACTGGATCTCTCTTT
Y2F (Y460F)	AAGCCACCAACAATGAGTTCTCAGAGATCAAGATCC	GGATCTTGATCTCTGAGAACTCATTGTTGGTGGCTT

Sequence in red represents the mutated sites

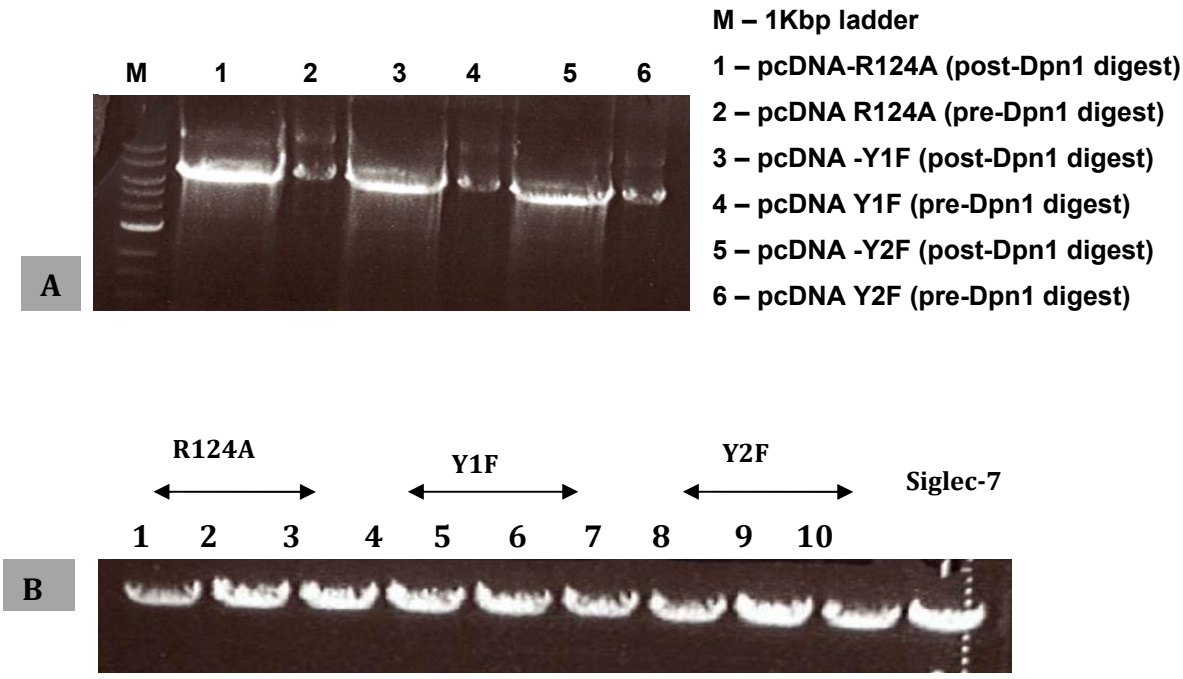

Figure 2.4: Cloning of Siglec-7 mutants (A) Plasmid DNA of Siglec-7 in pcDNA3.1 vector was used as template to generate the mutant clones using site directed mutagenesis. (B) Clones grown in ampicillin resistant plate was then analysed by restriction digest and compared to the template Siglec-7 DNA.

Chapter 3

Role of ganglioside complexes in modulating Siglec-7 recognition of GD3

3.1 Introduction

There is accumulating evidence that glycolipids do not exist on the cell membrane as individual entities but interact with other glycolipids and glycoproteins to form new structures that affect recognition by antibodies and lectins.

The basis of this project originated from an interesting study that demonstrated how various glycolipid-glycolipid interactions affected the recognition of proteins, antibodies and lectins (Rinaldi et al., 2009). This study utilized the technique of glycoarrays to spot 20 different glycolipids either individually or in combinations creating a grid pattern on PVDF membrane. The membrane was then probed with Tetanus Hc-HRP (Tet-Hc-HRP), Cholera toxin subunit B (CTB) and recombinant Siglec7-Fc protein. The authors observed complex mediated increase and decrease of ligand binding for these different proteins. Although Tet-Hc-HRP did not bind individual gangliosides, it showed an increased binding to some of the heterodimers. CTB, that binds GM1 with high affinity, was unaffected when in complex with other gangliosides. The binding of Siglec-7-Fc to its natural ligand GD3 was attenuated in the presence of complex sugars such as GM1, GD2, GD1a, GD1b, GT1a, GT1b and GQ1b (Rinaldi et al., 2009). The inhibition of Siglec-7-Fc binding to GD3 was independent of

whether PVDF membrane or polystyrene ELISA plate was used as the assay platform.

Tumours adopt different mechanisms to evade the recognition and attack by immune cells. The classical example of tumour escape mechanism is the down regulation of MHC-I to avoid recognition by T cells. Tumours also adopt other techniques such as secretion of certain proteins to promote the recruitment of regulatory T cells (Tregs), modifying their stromal micro-environment etc (Zindl and Chaplin., 2010) (Birkle et al., 2003). Gangliosides shed by tumours also have an important role in affecting anti-tumour responses. GD3, a tumour associated antigen in melanomas, has long been known for its role in promoting the tumourigenic properties of melanomas (reviewed by Furukawa et al., 2008). GD3 and GD2 have been shown to interact with integrins and focal adhesion kinases (FAK) in melanomas and certain lung cancer cell lines (Cheresh et al., 1987). Therefore, it is possible that one of the mechanisms adopted by tumours like melanomas to escape NK mediated cytotoxicity is the overexpression of gangliosides like GD3.

The glycoarray findings by Rinaldi et al., and the knowledge that tumours overexpress various ganglioside species provide interesting grounds for investigating how tumour associated gangliosides could possibly modulate NK cytotoxicity. A tumour recognition model could be hypothesized as follows. Tumours with overexpression of GD3 such as melanomas would be recognized by Siglec-7 on NK cells. Strong ligand recognition by this receptor would trigger inhibitory signals, which would override signals from potential activating receptors, and decrease NK cell mediated natural cytotoxicity (Figure 3.1, target

A). However, if a target cell was to expresses sufficient density of complex gangliosides such as GM1, then *cis*-interactions between the two gangliosides could occur. This could result in the masking of Siglec-7 epitopes on GD3 (Figure 3.1, target B). This would affect Siglec-7 recognition of its natural ligand, thereby modulating the inhibition mediated by this receptor. Thus increased cytotoxicity by the effector cells on this genre of targets could be expected.

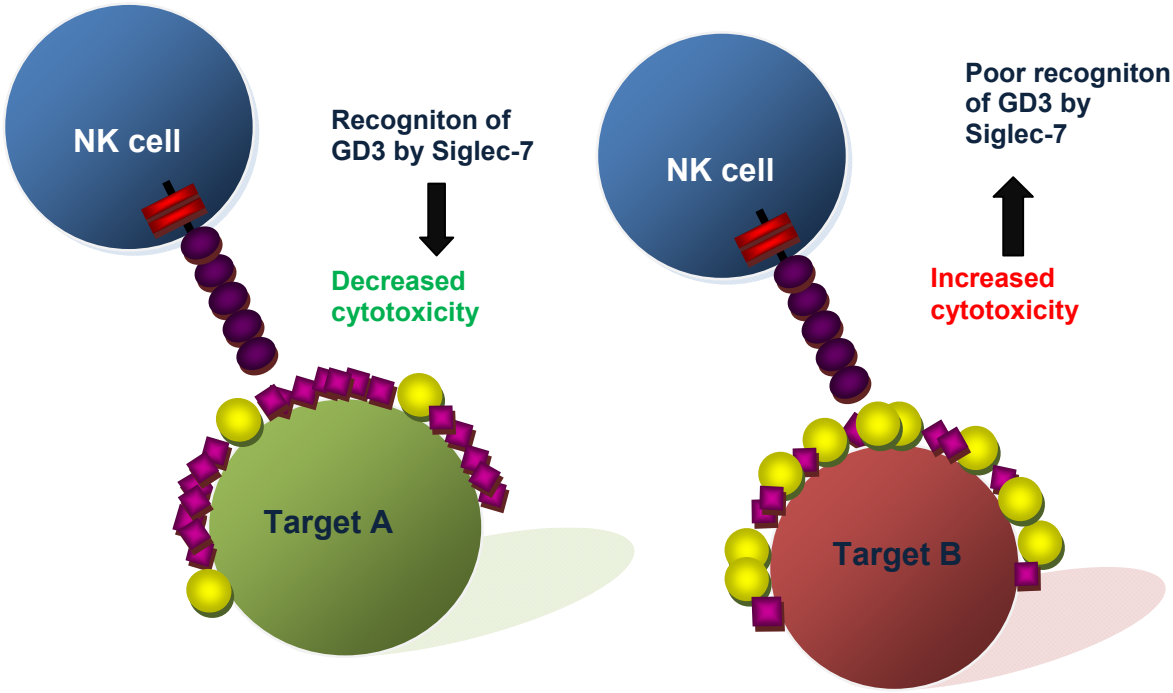

Figure 3.1: Proposed model for the project: Target A, with high expression of GD3, is recognized by Siglec-7 on NK cell and leads to decreased killing. GD3 on Target B is masked by the expression of GM1 and hence not efficiently recognized by the inhibitory receptor, increasing its susceptibility to NK cytotoxicity. GM1 , GD3

Project aims:

The focus of this project was to investigate if this complex mediated attenuation of Siglec-7, seen on glycoarrays using lectin Fc-chimeras, is of significance at a cellular level. The broader aim of this project was to investigate the role played by such glycolipid *cis*-interactions in affecting tumour recognition by NK cells.

Biochemical and cellular approaches were undertaken towards this goal. Using tools like Fc-chimeras and a cellular overexpression model, Siglec-7 recognition of GD3 overexpressed in complex with GM1 would be investigated. Depending on results obtained from initial studies, primary human NK cells would be used to examine the significance of these findings in biological assays.

3.2 Characterization of Siglec-7-Fc

Unlike protein-protein interactions, protein-glycan interactions are often avidity based and multivalent due to the low affinity of protein glycan interactions (Varki et al, Essentials of Glycobiology, 1999). In some cases these interactions therefore depend on factors such as density of ligands and number of ligand recognition sites on the receptor.

For this project, it was decided to use Siglec-7-Fc chimeras for cellular assays. The chimera consists of the entire extracellular domain of the receptor linked by disulfide bonds to the Fc and hinge regions of human IgG as shown in the figure 3.2. Stable CHO cell clones generated previously in the lab were used for the purpose of large scale generation of the Fc-chimera. The Glutamine Synthetase (GS) expression system was used in the expression of the Siglec-7-Fc chimera. This system utilizes the fact that in the absence of external glutamine, cell survival depends on the transfected GS gene to produce glutamine from glutamate and ammonia. L-MSX was used as a selection agent for this purpose. It is commonly used in the production of recombinant proteins especially antibodies in CHO cells and others cell lines. It is an inhibitor of the GS enzyme and increasing doses of L-MSX results in the efficient amplification

of the gene of interest linked to the GS gene. Moreover very high levels of protein expression (up to 10 mg/L) can be obtained with this system.

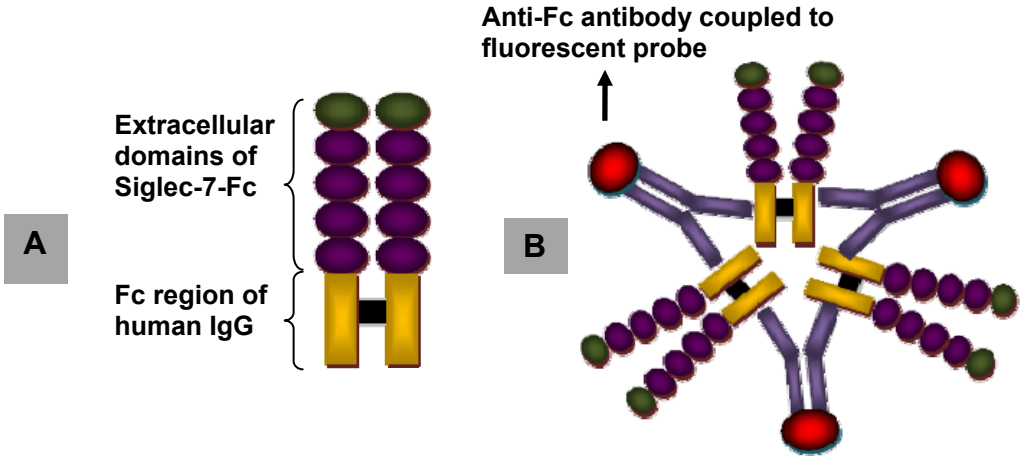

Figure 3.2: Schematic representation of (A) Siglec-7-Fc chimera (B) Pre-complex of Siglec-7-Fc with a secondary anti-Fc antibody coupled to a fluorescent probe.

3.2.1 Preparation of Siglec-7-Fc

A stable CHO-K1 cell clone was cultured in GMEM media with 0.5% FCS, 2% GSEM and 200 µM of L-MSX. It was also decided to compare the activity of Siglec-7-Fc prepared in the presence or absence of serum. For that reason cells were also cultured in serum free UCHO media.

The chimeras were quantified by using an anti-Fc antibody ELISA. Purified Sialoadhesin-Fc (Sn-Fc) was used as the protein standard in this ELISA. Figure 3.3 shows the standard curve used to calculate concentration of Siglec-7-Fc. Siglec-7-Fc expressed in GMEM media was calculated to be 16 µg/ml and that in UCHO media was 20 µg/ml.

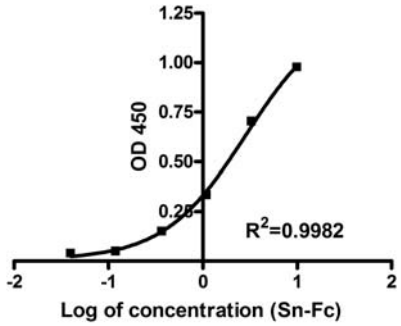

Figure 3.3 Standard curve for estimation of Siglec-7-Fc concentration: A 96 well plate was coated with 200 µl of 12 µg/ml of anti-human IgG, diluted in carbonate bicarbonate buffer. After overnight incubation, the plate was washed x3 with PBA (PBS + 0.25% BSA). The plate was blocked with 5% marvel in PBA. After 1 hour blocking at room temperature, the plate was washed again and 100 µl of dilutions of standard and unknown samples was added. After incubation, the plate was washed again in PBA and then 50 µl of alkaline phosphatase conjugated goat anti human IgG in TBA (TBS+0.25%BSA). Following 1 hour incubation, the plate was washed with TBA, then incubated with 100 µl of PNPP and the coloured product read on an ELISA plate reader after 5-10 minutes.

3.2.2 Testing Siglec-7-Fc by RBC solid phase adhesion assay

Siglec-7-Fc expressed in either GMEM or serum free UCHO media were tested for binding of RBCs in an adhesion assay. RBCs express glycoproteins carrying sialic acids for example glycophorins. Dilutions of the Siglec-7-Fc chimera were coated onto a microtitre plate. RBCs were added to these wells, incubated and then unbound cells washed off. Figure 3.4 (A) shows quantification of the adhesion of RBCs to Siglec-7-Fc supernatants. To ensure no loss in protein functionality after long term storage of chimera at - 80^0C, the assay was also carried out using frozen and thawed proteins (Figure 3.4, B).

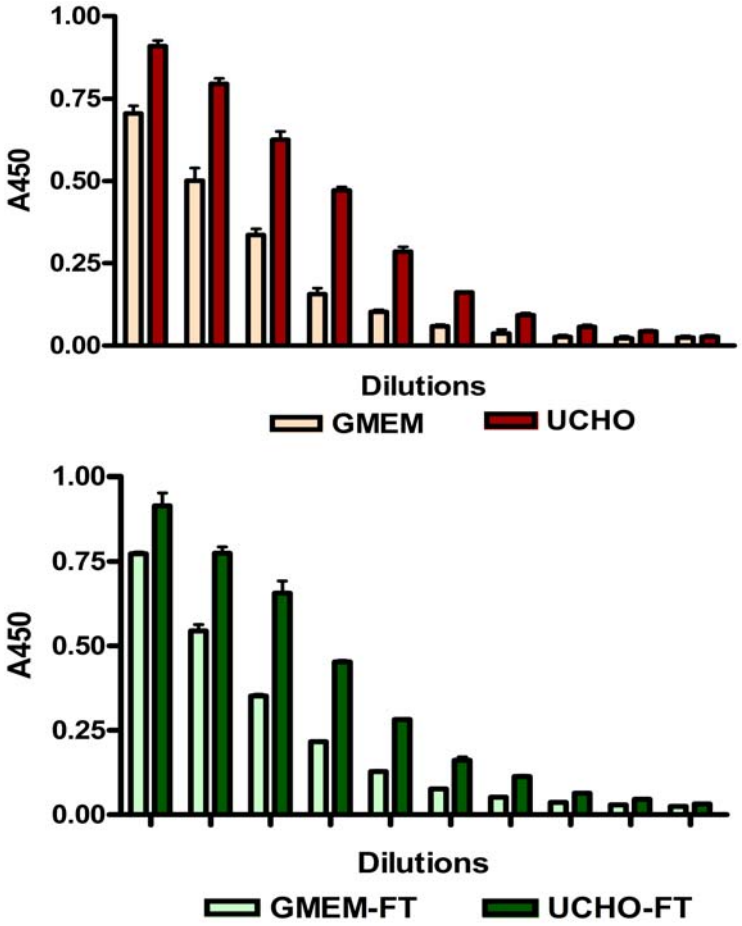

Figure 3.4: Adhesion of RBCs to Siglec-7-Fc chimera: Dilutions of Siglec-7-Fc were incubated on a plate coated with goat anti-human IgG. Following 1 hour incubation and washing with 1X PBS (0.25% BSA), 0.5% (v/v) of RBCs were added to the plate and incubated for 1 hour at room temperature. Wells were then washed and bound cells fixed with methanol before adding TMB substrate for detection. Error bars represent standard deviation between samples (n=3). FT – freeze-thawed

3.3 Siglec-7-Fc recognition of GD3 is inhibited in the presence of GM1 – plate based ELISA

To test the inhibition of Siglec-7 recognition of GD3 by GM1, ganglioside ELISAs were carried out using Fc-chimeras, based on the protocol developed by Rinaldi et al., 2009. The protocol was further optimized for the best signal to noise ratio. GD3 and GM1 gangliosides were diluted in methanol to a working

concentration and coated directly onto 96 well microplates. Methanol alone was used as the blank in each case. RBC binding to Siglec-Fc-Fc prepared in UCHO was higher compared to that prepared in GMEM (Figure 3.4). Hence Siglec-7-Fc expressed in UCHO cells was used in these assays.

3.3.1 Titrating Siglec-7-Fc pre-complex on GD3

Siglec-7-Fc at 3 µg/ml and anti-human Fc-HRP (horse radish peroxidase) conjugate at 1 µg/ml were mixed together in different ratios (volume / volume). These were used to detect GD3 coated onto plates as shown in figure 3.5. The best signal to noise ratio was obtained for the 3:1 ratio.

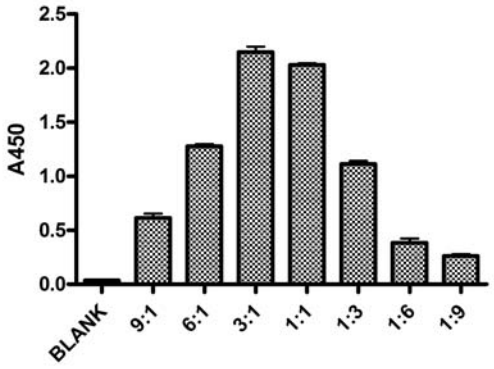

Figure 3.5: Titration of Siglec-7-Fc precomplexes for the detection of GD3 - Stock of GD3 was diluted to 2 µg/ml in methanol and plated onto 96-well microtitre plate. After overnight incubation, plates were blocked, and then incubated with different concentrations of the pre-complexes. After 1 hour incubation, plates were washed and detected with TMB substrate. Error bars represent standard deviation between samples (n=3).

3.3.2 Ganglioside ELISA to test recognition of GD3 by Siglec-7-Fc

Next, sensitivity of the Siglec-7-Fc precomplexes in the detection of GD3 was examined. GD3 at concentrations ranging from 20 µg to 30 ng were plated and

detected using Siglec-7-Fc pre-complexes at the optimized ratio of 3:1 (Figure 3.6).

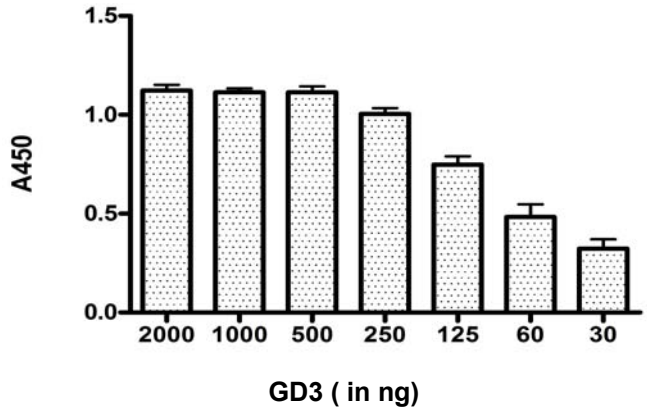

Figure 3.6: Titrations of GD3 on ganglioside binding assay. Stocks of GD3 were sonicated and dilutions prepared in methanol. Microtitre plates were coated with 100 µl of GD3 and left to dry overnight. Following blocking with 2% PBA, pre-complex of Siglec-7-Fc and anti-human IgG HRP conjugate was added to wells and incubated for 4 hours at 4^0C. TMB was added as detection substrate and plates read at 450 nm. Error bars represent +SEM from two independent experiments. X-axis represents total input ganglioside in 100 µL.

3.3.3 Siglec-7-Fc recognition of GD3 in GD3:GM1 complexes

Siglec-7 inhibition of GD3 recognition by an equal amount of GM1 was first analysed. As shown in figure 3.7, GD3 recognition was reduced by more than 50% when mixed with GM1.

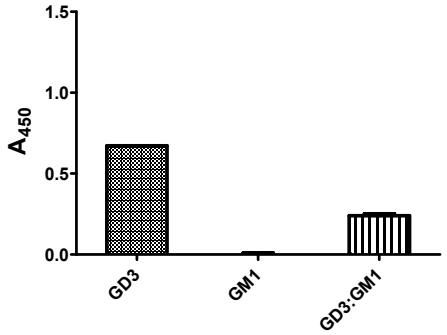

Figure 3.7: GM1 inhibits Siglec-7-Fc recognition of GD3. 100 µl of 200 ng each of GD3 and GM1 were coated on a microtitre plate, diluted in methanol. Assay was carried out as described in figure 3.6.

3.3.4 Increasing amounts of GM1 affects recognition of GD3 by Siglec-7-Fc

Next, the inhibition of GD3 over a range of GM1 concentrations was tested. Different amounts of GM1 (60 to 2000 ng) were mixed with 500 ng of GD3 and were plated out for detection by Siglec-7-Fc as shown in figure 3.8. GM1 was able to significantly inhibit Siglec-7-Fc recognition of GD3 when used at x0.5, x1, x2 or x4 increased amounts of GM1. The ganglioside GT1b was used as a positive control while GM1 as negative control in this assay.

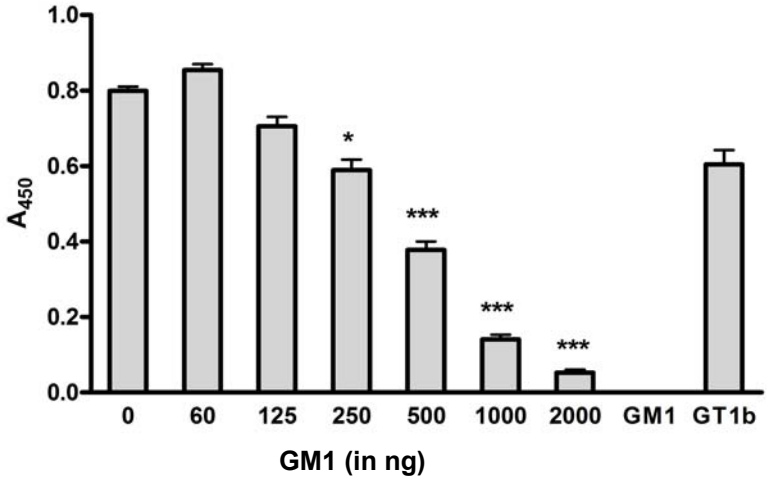

Figure 3.8: Titration of GM1 for the inhibition of GD3 : To 500 ng of GD3, varying amounts of GM1 was added and 100 µl of these complexes were plated out. 500 ng of GM1 was used as the negative control and 500 ng of GT1b was used as the positive control for detection by Siglec-7-Fc in the assay. Experiments were carried out as detailed in the legend of figure 3.6. Statistical test – One-way ANOVA using Dunnet's post test, comparing control group (no-GM1) to all other groups. Error bars represent SEM from 3 individual experiments. ** - P < 0.5; * - P < 0.001***

3.3.5 GM1 specifically inhibits Siglec-7-Fc recognition of GD3

Specificity of the inhibition by GM1 was demonstrated by pre-complexing GD3 with other non-disialylated sugars such as GM3 and lactosyl ceramide (LacCer).

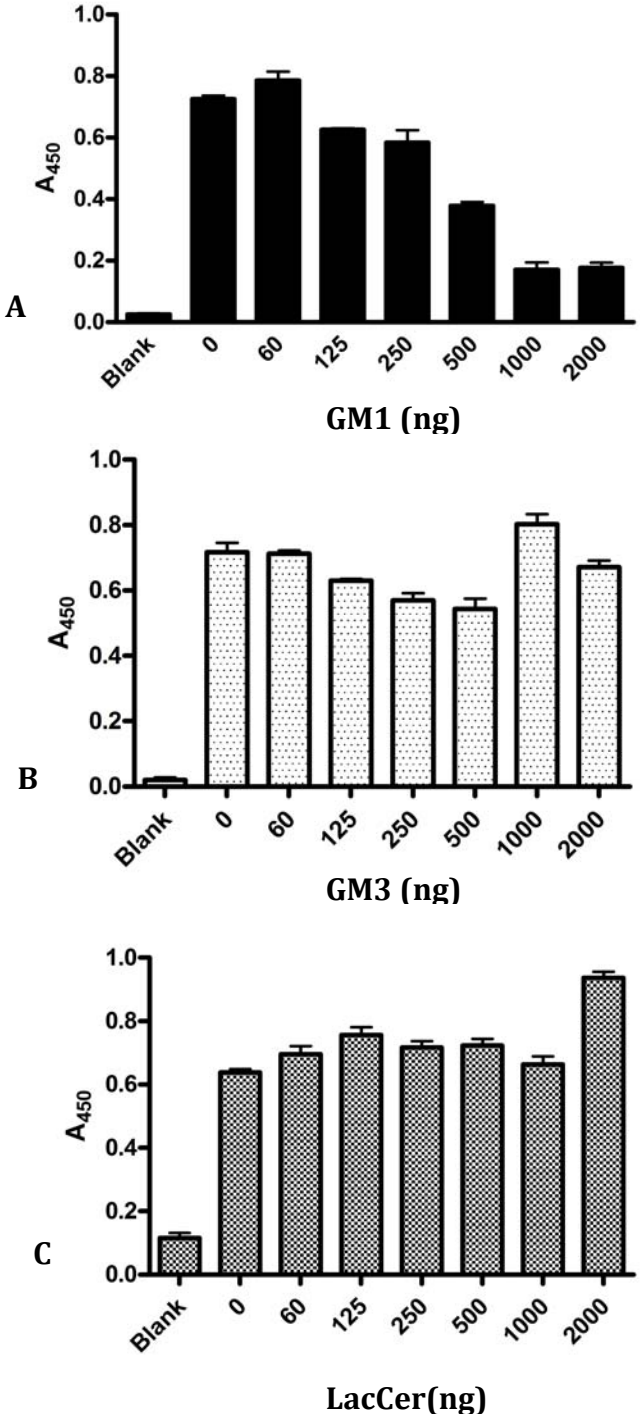

Figure 3.9: GM1 specifically inhibits Siglec-7-Fc recognition of GD3 : 500 ng of GD3 was complexed with varying amounts of GM1 (A), GM3(B) and lactosyl ceramide (LacCer)(C). 100 µl of each complex was plated out and recognition of GD3 by Siglec-7-Fc examined. Experiment carried out as detailed in the legend of figure 3.8. Error bars represent SEM. Data is representative of 1 of 3 experiments conducted. X-axis represents total input of ganglioside complexes in 100 µl volume.

Figure 3.9 (A) shows that Siglec-7-Fc binding of GD3 is affected by increasing amounts of GM1. However, recognition of GD3 when in complex with GM3, figure 3.9 (B), or with LacCer, figure 3.9 (C), by Siglec-7-Fc remained unaffected.

3.4 Siglec-7-Fc recognition of GD3 is inhibited in the presence of GM1 – liposome ELISA

The lipid layers of liposomes mimic cell membranes. Hence to confirm the above findings of the inhibitory effect of GM1 on GD3, the gangliosides were reconstituted into liposomes. These were coated out onto microtitre plates and detected using Siglec-7-Fc.

3.4.1 Testing of GD3 or GM1 reconstituted liposomes

Liposomes were prepared using cholesterol, sphingomylein and dicetylphosphate. These were then left either blank or reconstituted with 500 ng of GD3 or GM1. These liposomes were then plated out and incorporated gangliosides detected using Siglec-7-Fc precomplexes. As shown in figure 3.10, the lectin specifically recognizes GD3. Blank liposomes were used as a negative control.

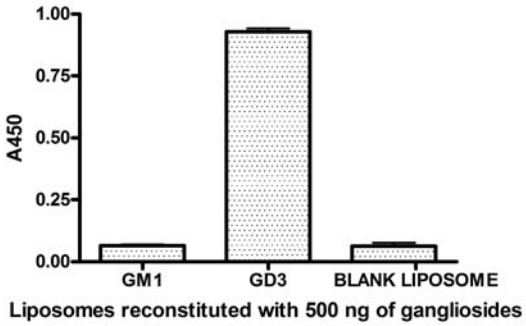

Figure 3.10: Siglec-7-Fc specific recognition of GD3 in liposomes - Liposomes with gangliosides were prepared by using cholesterol, sphingomylein, dicetylphosphate and the respective gangliosides (described in materials and methods) Liposomes ,resuspended in PBS, were plated out onto 96-well mictrotitre plates and the assay carried out as described in the legend of figure 3.6. Error bars represent standard deviation (n=3) and experiment is representative of n=3.

3.4.2 Siglec-7 recognition of GD3 is inhibited by GM1, in liposomes

Binding of Siglec-7-Fc to GD3 was inhibited in the presence of equal amounts of GM1 in liposomes (1:1 molar ratio).

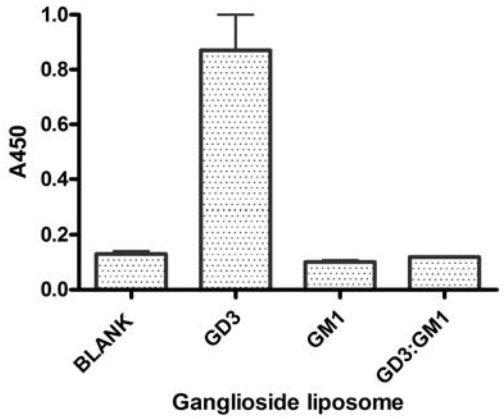

Figure 3.11: GM1 inhibits Siglec-7 mediated binding of GD3 following reconstitution in liposomes – Liposomes were prepared with either GD3 or GM1 or a 1:1 molar ratio of GD3 and GM1. Assay was carried out as described in legend of figure 3.10. Assay represents experiment from n=2.

3.4.3 Siglec-7-Fc and antibody recognition of GD3 is inhibited by GM1

GD3 was reconstituted into liposomes with increasing molar concentrations of GM1. The liposomes were then detected either using Siglec-7-Fc precomplexes (Figure 3.12, A), R24 antibody (Figure 3.12, B) and cholera toxin B subunit (Figure 3.12, C). R24 detection of GD3 and CTB detection of GM1 was optimized using liposomes reconstituted with GD3 or GM1 respectively (data in Appendix, A1)

As shown in plate based ELISA, Siglec-7 recognition of GD3 was significantly decreased at all concentrations of GM1 (Figure 3.12, A). CTB detection of GM1 was unaffected by the presence of GD3 (Figure 3.12, C). However, antibody R24 detection of GD3 was reduced by the increasing concentrations of GM1 (Figure 3.12, B).

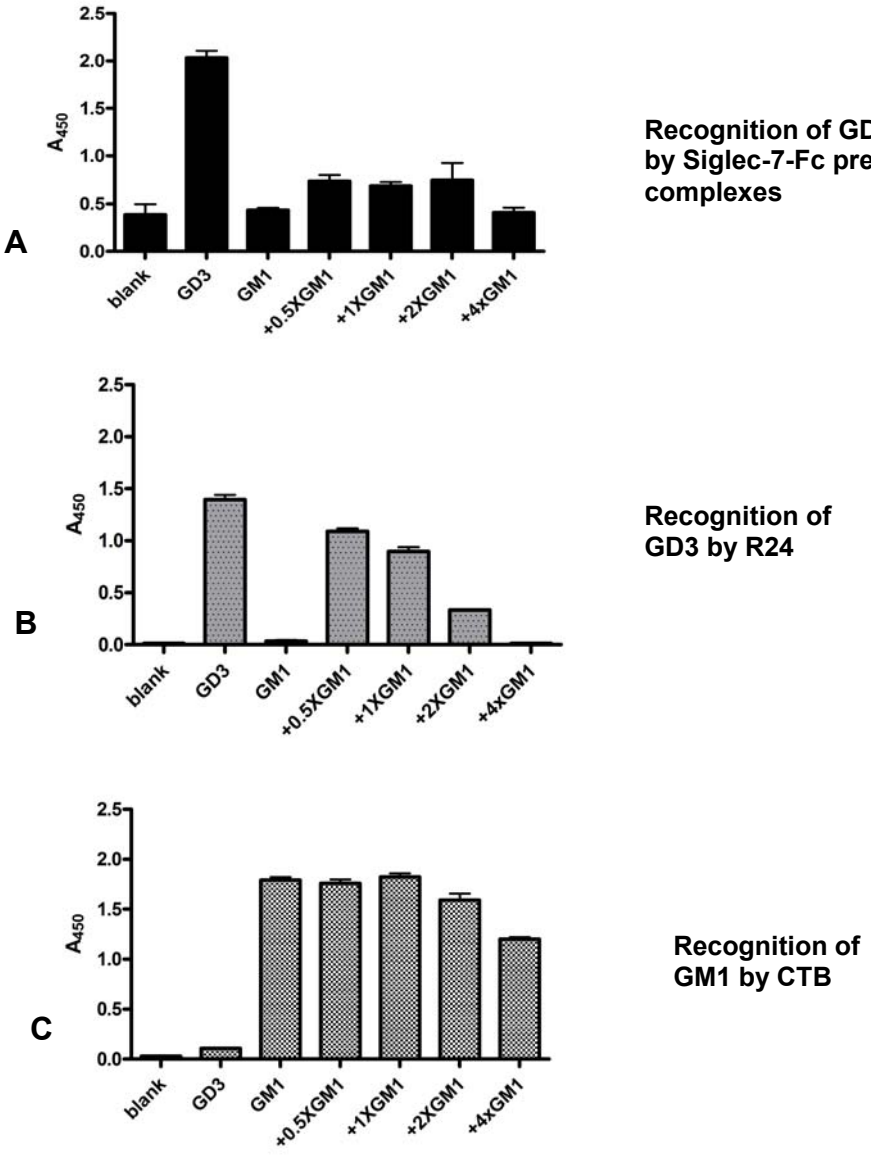

Figure 3.12: Siglec-7-Fc and R24 antibody recognition of GD3 is inhibited by GM1 in liposomes. Assay was carried out as described in legends of figure 3.10 and 3.12. GM1 was added in increasing molar ratios compared to GD3 ie at 0.5 , 1, 2 and 4 times more than GD3 (A) Siglec-7-Fc recognition of GD3 is inhibited by increasing concentrations of GM1 (B) Recognition of GD3 by the R24 antibody is also reduced by increasing concentrations of GM1. (C) Recognition of GM1 by CTB was unaffected by the presence of GD3. Error bars represents SDM (n=3). Experiments using R24 and CTB on the recognition of liposomes carrying GD3 and GM1 were carried out only once.

3.5 Expression of GM1 on B16 (78) cells

Having established in both ELISA based and liposome based assays that GM1 could *cis*-inhibit GD3 recognition by Siglec-7, I next moved to a biological system using a model cell line. For this purpose, the B16 (78) cell line was chosen as a model system as it expresses only GM3, the precursor of all gangliosides belonging to the a, b and c series in the ganglioside biosynthetic pathway (as described in the introduction – figure 1.8) (Hirabayashi et al., 1985).

The B16 (78) cell line lacks in expression of GD2 synthase (GD2S) (β 1,4 galactosyltransferase) which converts GM3 to GM2, and GD3S (α 2,8 sialyltransferase) which coverts GM3 to GD3 (figure 3.13). However, it expresses the GM1 synthase (GM1S) (β 1,3 galactosyl transferase) which converts GM2 to GM1. Therefore this cell line was transfected with GM2S and GD3S to achieve surface expression of GM1 and GD3.

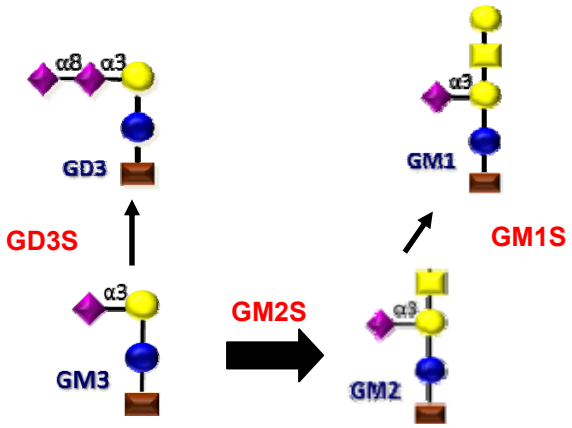

Figure 3.13 – Ganglioside profile of the B16 (78) cell line when transfected with GM2S and GD3S

3.5.1 Stable transfection of GD2 synthase

In order to bring about the expression of GM1, GM2 synthase was transfected in this cell line. Expression of GM2 will in turn lead to the expression of GM1.

The plasmid vector CB6-GM2S-FLAG was a kind gift from Dr. Hugh Willison (Glasgow) and was transfected into B16 (78) cells by calcium phosphate transfection. Stable clones were generated by limiting dilution (as described in materials and methods) and cultured in selection medium with 0.5 mg/ml of G418. Transfectants were stained for expression of GM1 using CTB. The dilution of CTB to be used was optimized using the HL-60 cell line which expresses GM1. Figure 3.14 (A and B) represents a few clones stained with biotinylated CTB and Streptavidin-A488 as secondary. Most of the clones had similar expression of GM1, with ~50% of the cells showing relatively high expression. In a separate experiment, transfectants were also sorted for positive and negative fractions by FACS. These fractions were also analysed for GM1 expression as shown in figure 3.14, B.

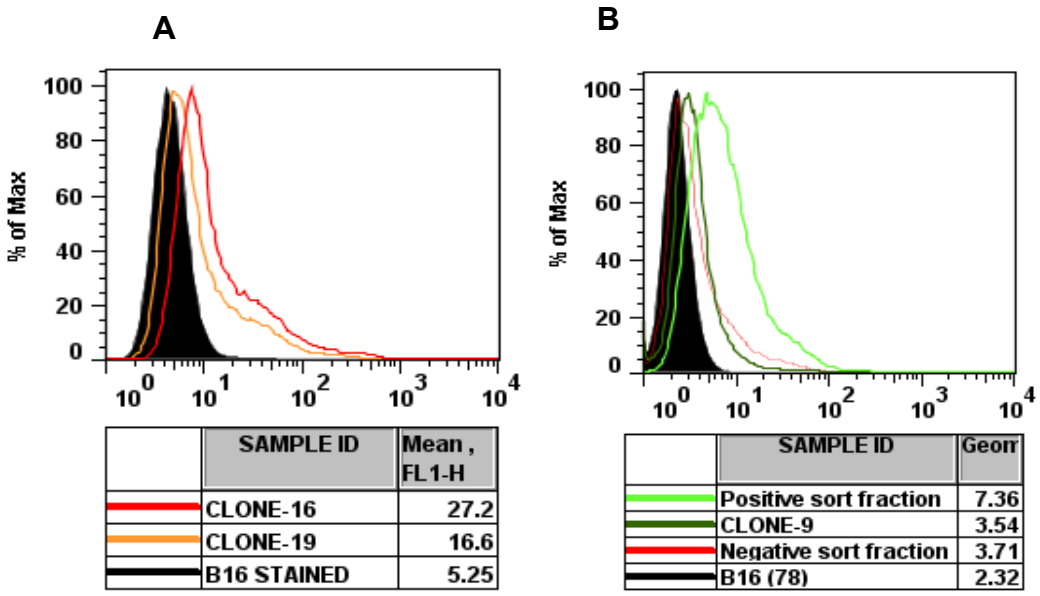

Figure 3.14: Expression of GM1 on B16 (78) GM2 synthase transfectants: 1x 10E6 cells were harvested and incubated with 1 µg/ml of CTB for one hour on ice. Cells were then washed with 1XPBA (PBS + 0.25% BSA) and incubated with 1/1000 dilution of Streptavidin-A488 conjugate for 30 minutes on ice. Cells were washed again in 1X PBA

and analysed by flow cytometry. (A) Expression of GM1 on clonal population of B16(78) GM2 synthase transfected cells. (B) Transfectants were subject to sorting by flow cytometry. The positive and negative fractions were stained with CTB for expression of GM1.

3.5.2 Confirming the presence of GM2S-FLAG in B16 (78) cells

In order to confirm the presence of the plasmid GM2S-FLAG in the B16 (78) cells transfectants, GM1 positive clones were analysed by western blotting and confocal microscopy.

Figure 3.15 (A), shows western blotting carried out on whole cell lysates from three of the GM1 positive clones using anti-FLAG antibody. Also included are lysates from positive and negative fractions following a FACS sort of polyclonal B16 (78) GM1 cells. The intensity of anti-FLAG staining in each sample corresponded with the respective GM1 expression levels as analysed by flow cytometry. Wild type cells (lane 1) and negative fraction from FACS sorting (lane 4) did not stain positive for anti-FLAG antibody. However enriched fraction from the FACS sorting (lane 3) , clones 16 and 19 were positive for anti-FLAG. This confirmed the expression of the GM2S-FLAG gene within the transfectants.

Figure 3.15,B is a representative image of confocal microscopy staining conducted on B16 (78) GM1 cells with either anti-FLAG (A) or CTB (B). Staining of HL-60 (positive control) and B16 (78) (negative control) were also done. Anti-FLAG antibody showed specific punctate staining within the cell while CTB stains GM1 present on the cell surface. It was interesting to note that FLAG tagged glycosyltransferase and GM1 expression on the cells were expressed independent of each other. This could possibly be related to cell cycle

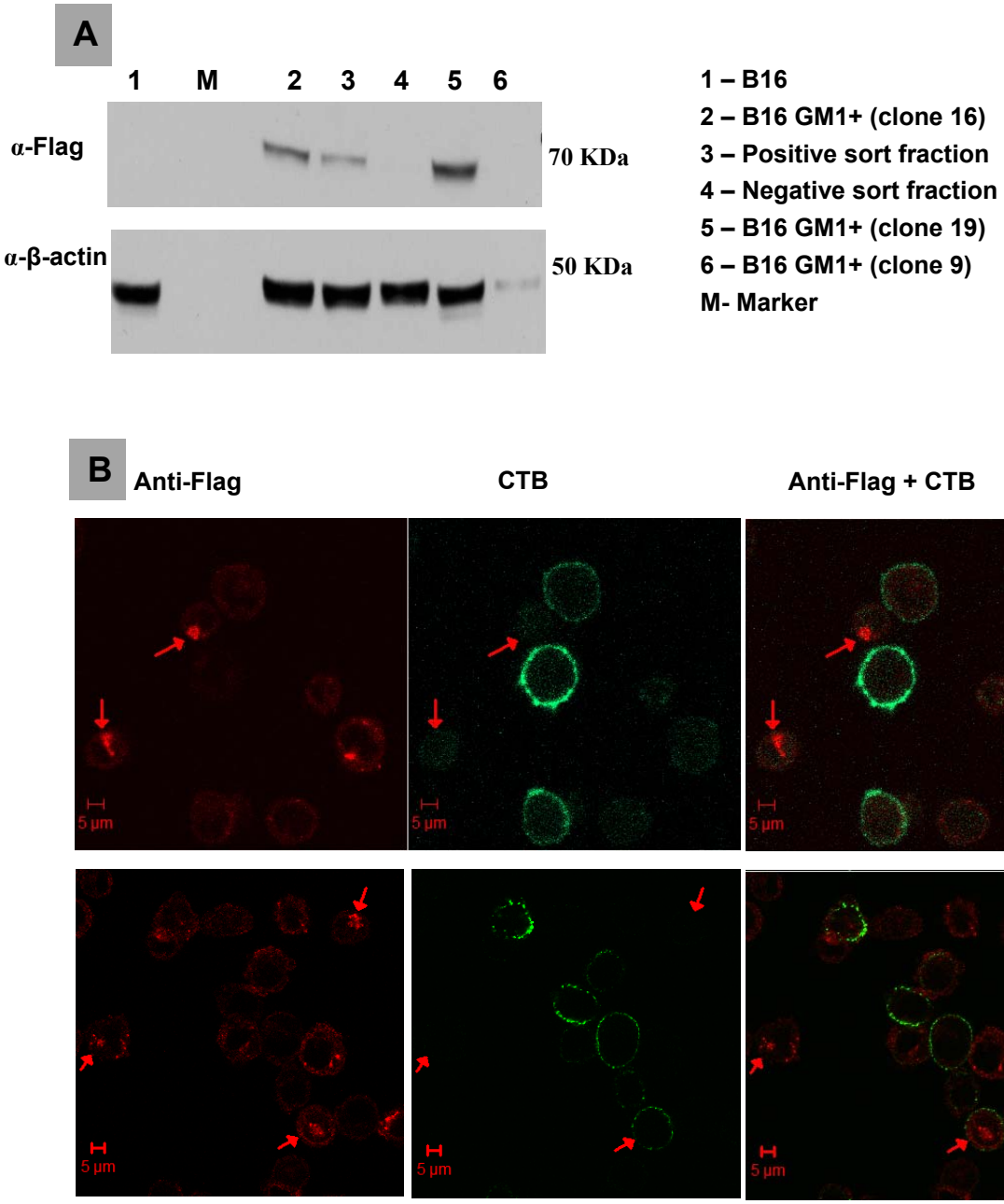

Figure 3.15: GM2S-FLAG is expressed in B16 (78) transfectants: (A) 0.5 X 10E6 cells from each sample was used to prepare lysates (described in materials and methods). 20µl of each lysate was run on a 4-12% bis-tris gel, in MES buffer. Gels were then transferred to nitrocellulose membrane, blocked and incubated with 1:1000 dilution of anti-FLAG or β actin antibody. Following overnight incubation, blots were washed and incubated with suitable secondary HRP antibody and detected using ECL substrate, following one hour incubation at room temperature. (B) 1 x 10E6 cells were fixed with 2% PFA for 10 minutes at room temperature (RT), washed and then permeabilized with 0.5% saponin for 10

minutes at RT. Cells were then washed with wash solution (1XPBS + 0.2% Tween-20), blocked for 30 minutes at RT and then incubated with anti-FLAG (5 ug/ml) or CTB (2 ug/ml) for 30 minutes at RT. Cells were then washed and stained with suitable secondary antibodies, washed and mounted onto coverslips. Cells were imaged using the LSM 700 at x 100 magnification and images were analysed using LSM image analysis software. The red arrows point to the expression of GM2S-FLAG in the transfectants.

regulation or post-translational modification of this glycosylatransferase. However no further experiments were carried to investigate this phenomenon.

3.5.3 Messenger RNA levels of glycosylltransferases

mRNA expression levels of the different synthases such as GM3S, GM1S, GM2S and GD1aS were all analysed by real-time quantitative PCR. Primers used are described in the Materials and Methods (table 2.5). Mouse tissues (brain, kidney, bone marrow, liver and lung) were used as positive or negative controls according to the reported expression levels of these enzymes. B16 (78) wild type cells were positive for the transcripts of GM3aS (Figure 3.16, A), corresponding to the reported expression of GM3 in these cells (Hirabayashi et al., 1985). They were also positive for the expression of GM1S and GD1AS but completely lacked mRNA expression of GM2S (Figure 3.16 – B, C, D). The GM2S transfected clones 16 and 19 showed differential expression of GM2S and GM1S which corresponded with the expression levels of GM1 on these cells as analysed by CTB staining (Figure 3.13). Both wild type and GM1 transfectants also showed weak expression levels of GD1aS mRNA (Figure 3.16, C) compared to the positive controls. This corresponded to the expression

of GD1a on B16 (78) GM1 cells by flow cytometry staining (shown in Appendix, A3).

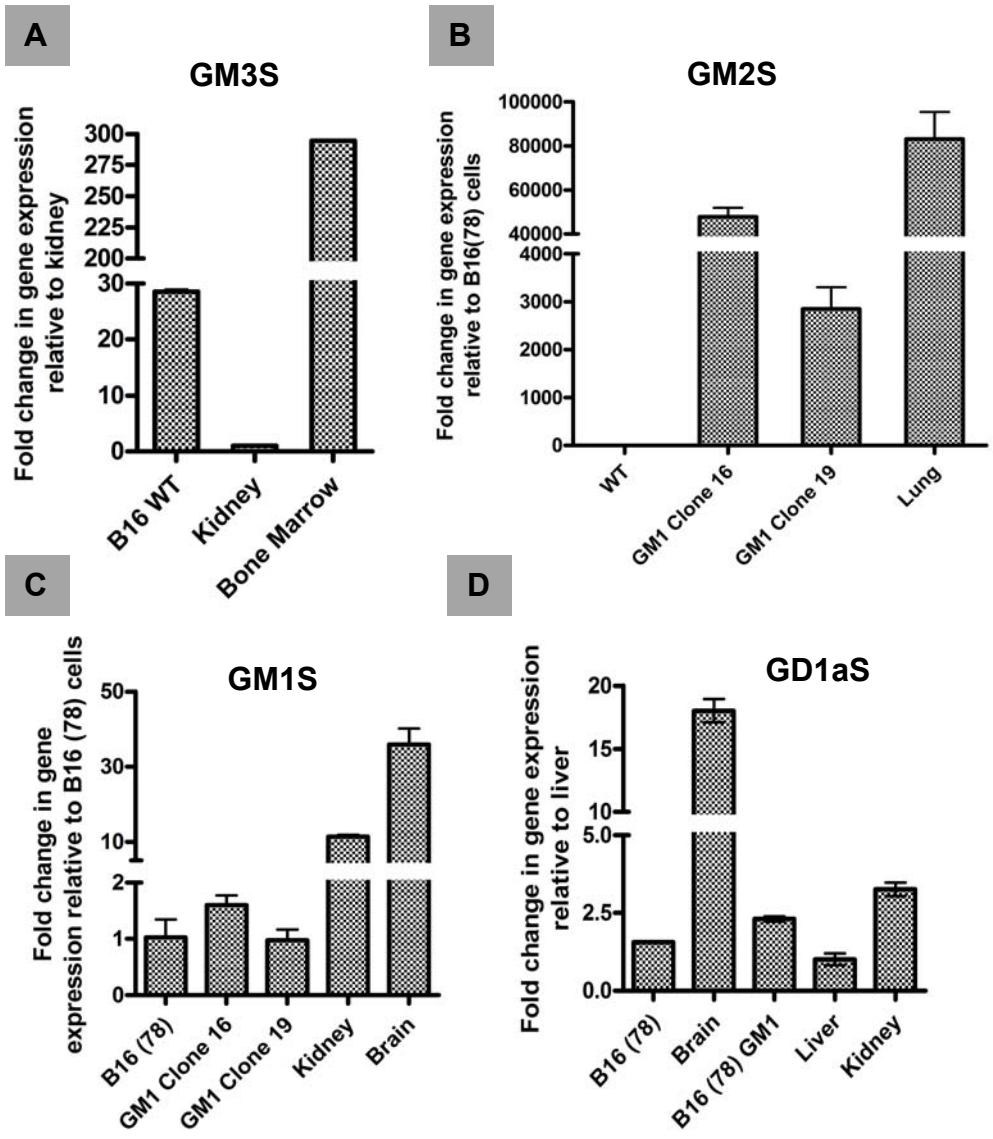

Figure 3.16: Relative fold change in mRNA expression of GM3s, GM2S, GM1s and GD1as in B16 (78) cells, plotted with SD values. mRNA was extracted from B16 cells and various mouse tissue samples. cDNA was prepared from 1 µg of mRNA and then RT-PCR conducted on these samples using optimized primers for the gene of interest. Relative fold change in gene expression was quantified by the Comparative ΔΔCT method, using GAPDH as normalizer and mouse tissue as the calibrator (taken as 1). Y-axis represents the fold change in gene expression, relative to kidney

3.6 Cloning and expression of GD3S in B16 (78) cells

B16 (78) cells lack in the expression of ST8SIA1/GD3 synthase (GD3S). Expression of GD3 on these cells was achieved by transfecting both wild type and B16 (78) GM1 transfectants with GD3 synthase.

3.6.1 Stable transfection of GD3 synthase into B16 (78) WT and B16 (78) GM1 cells

mRNA, extracted from mouse brain lysates, was used in the generation of GD3S cDNA (as detailed in Materials and Methods, figure 2.1). In order to express GD3 on B16 (78) wild type and B16 (78) GM1 transfectants, two methods were tried – Ca^{2+}phosphate and polyethylamine transfection reagent (PEI). While Ca^{2+} phosphate transfection gave greater transfection efficiency (20%) for the wild type cells, similar transfection efficiencies were seen for B16 (78) GM1 cells with both methods (Figure 3.17). Transfectants were cultured in selection medium for 2 weeks to obtain a polyclonal population of cells expressing GD3. Cells were then stained with a mouse monoclonal anti-GD3 antibody (R24) (as described in materials and methods), followed by anti-mouse PE antibody.

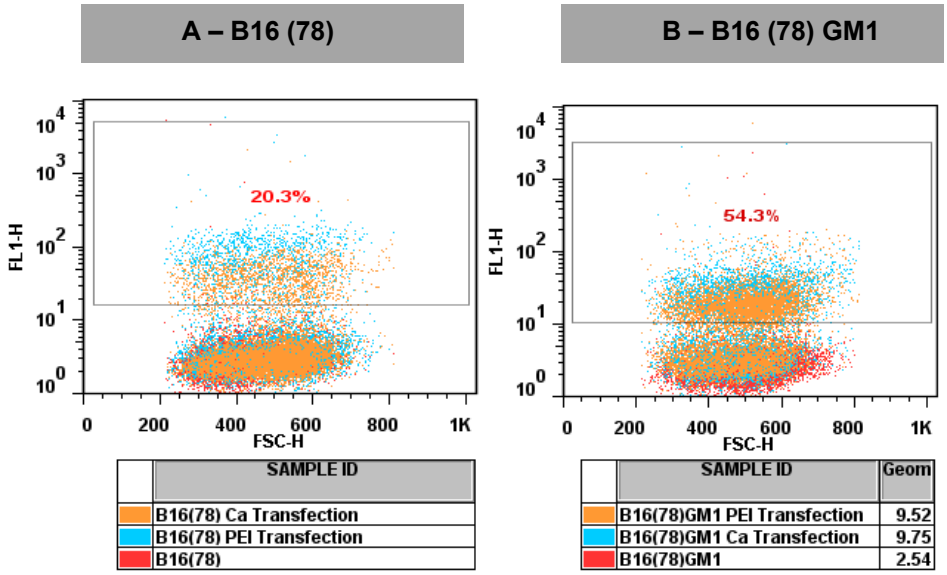

Figure 3.17: Transfection efficiency of GD3S into (A) B16 (78) cells and (B) B16 (78) GM1 cells: Cells were transfected with 30 µg of GD3S plasmid DNA by Ca2+ transfection and PEI (as described in Materials and methods). Numbers in the dot blots refer to percentage cells transfected by Ca^{2+} phosphate transfection in the wild type cells and by PEI transfection in B16 (78) GM1 cells. For antibody staining, 1x10XE6 cells were harvested, stained with 10 µg/ml of R24 antibody, followed by anti-mouse FITC and washed and analysed by flow cytometry.

3.7 mRNA expressions of Cytidine monophosphate N-acetyl neuraminic acid hydroxylases (CMAH) gene

The enzyme CMAH is responsible for the conversion of the N-acetyl form of sialic acid (NeuAc) into the N-glycolyl form (NeuGc). The expression of the glycolyl form of sialic acids could affect recognition of sialylated ligands by Siglec-7 and GD3 by the monoclonal antibody, R24.

Previous studies have shown that the B16 (78) cell line is negative for CMAH. To confirm this, messenger RNA levels of the CMAH gene were analysed by RT-PCR as described above. Figure 3.18 shows negligible levels of CMAH gene expression in this cell line compared to adult mouse liver tissue which

corresponds well with previous studies conducted on this enzyme (Gabri *et al*., 2009).

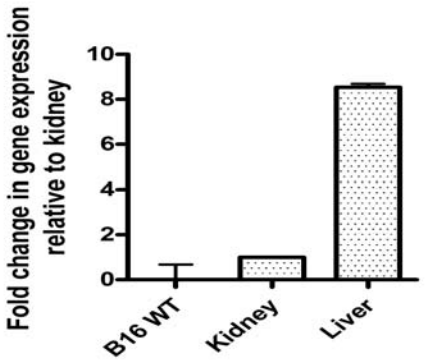

Figure 3.18: B16 (78) cells lack the expression of CMAH gene: Using primers for CMAH (described in appendix), B16 (78) wild type cells, mouse kidney and liver tissues samples were quantified for the expression of this gene by RT-PCR, as described in figure 3.16.

3.8 Sialic acid dependent binding of Siglec-7-Fc to B16 GD3 cells

As discussed in section 3.2, precomplexing the Siglec-7-Fc-chimeras with anti-Fc antibody increases avidity of the lectin for its glycan ligand and enhances binding. Using this method, the recognition of Siglec-7-Fc to GD3 expressed on B16 (78) cells was analysed.

3.8.1 Optimization of Siglec-7-Fc pre-complexes –RBC adhesion assay

Formation of pre-complexes of Siglec-7-Fc with goat anti-human Fc fluorescent conjugate was optimized using RBCs. Different concentrations of Siglec-7-Fc ranging from 0.1-3 µg/ml of Siglec-7-Fc were mixed with varying concentrations of anti-Fc antibody (conjugated to Dylight 649) (0.1 – 3 µg/ml). Binding of the different combinations of these precomplexes to RBCs was then analysed by

flow cytometry. Based on the initial findings (data not shown), Siglec-7-Fc at 1 µg/ml and anti-Fc antibody at 3 µg/ml were chosen as the concentrations with the best signal : noise ratio. To further optimize the total amount of precomplexes added to each sample, the assay was repeated with different dilutions of the precomplexes formed at this 1:3 (µg/ml) ratio, as shown in figure 3.19.

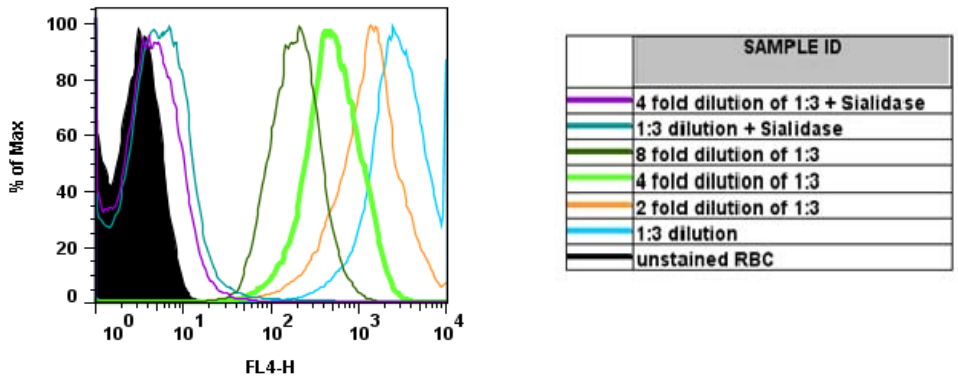

Figure 3.19: Optimization of the concentration of Siglec-7-Fc precomplex dilutions: Precomplexes were made using 1 µg/ml of Siglec-7-Fc and 3 µg/ml of goat anti-human Fc DyLight 649 and left to incubate on ice for one hour. 0.5% (v/v) of RBCs were treated with 0.17 IU / ml of sialidase for 1 hour at 37^0C, 8% CO_2 in DMEM media. Sialidase was quenched and removed by washing cells twice with DMEM + 10% FCS. 100 µl of different dilutions of Siglec-7-Fc precomplexes were added onto non-treated and treated RBCs. RBCs were incubated for one hour on ice with pre-complexes before washing in facs wash buffer and analysing by flow cytometry.

Sialidase treated RBC were used as a negative control in each case. Four fold dilution of the 1:3 ratio of Siglec-7-Fc precomplexes was within the dynamic range of the flow cytometer. Therefore, it was decided to use this dilution of Siglec-7-Fc precomplexes for further cell based assays.

3.8.2 Siglec-7-Fc pre-complexes recognize B16 (78) cells in a sialic acid dependent manner

Next, the recognition of GD3 expressed on B16 (78) cells by Siglec-7-Fc precomplexes and the R24 antibody was analysed. Figure 3.20 shows binding of R24 (A) and Siglec-7-Fc precomplex (B) to wild type and B16 (78) GD3 cells, with (+ sialidase) and without sialidase (- sialidase) treatment.

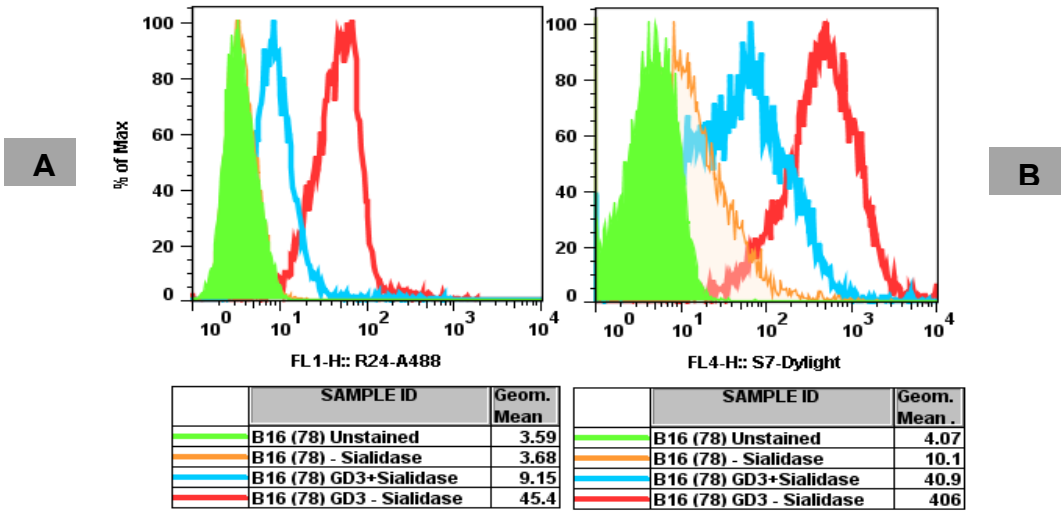

	SAMPLE ID	Geom. Mean
	B16 (78) Unstained	3.59
	B16 (78) - Sialidase	3.68
	B16 (78) GD3+Sialidase	9.15
	B16 (78) GD3 - Sialidase	45.4

	SAMPLE ID	Geom. Mean .
	B16 (78) Unstained	4.07
	B16 (78) - Sialidase	10.1
	B16 (78) GD3+Sialidase	40.9
	B16 (78) GD3 - Sialidase	406

Figure 3.20: Recognition of GD3 on B16 (78) cells by Siglec-7-Fc and R24 antibody: B16 (78) GD3 cells were harvested and sialidase treated as described in section 3.19. Siglec-7-Fc precomplexes were prepared as described in section 3.19. Sialidase treated (+sialidase) and untreated (-sialidase) cells were incubated with either (A) 10 µg/ml of R24 antibody or (B) 100 µl of Siglec-7-Fc precomplexes (as described above). Cells were stained with anti-mouse FITC antibody, washed and then analysed by flow cytometry.

R24 bound specifically to GD3 expressing B16 (78) cells, with 80% reduction in the intensity following sialidase treatment. Siglec-7-Fc bound GD3 in a sialidase dependent manner as there is 90% reduction in binding to sialidase treated cells. Siglec-7-Fc also gave a small shift with wild type B16 (78) cells suggesting the presence of unknown sialylated ligands on these cells.

3.8.3 R24 recognition of GD3 is not inhibited by S7-Fc pre-complexes

GM1 modulation of Siglec-7 recognition of GD3 would be examined by incubating B16 (78) GD3 cells with Siglec-7-Fc precomplexes, R24 antibody and CTB. It is possible that binding of Siglec-7 precomplexes to the cells could block R24 recognition of GD3. To confirm this, B16 (78) GD3 cells were incubated with equal concentrations of R24 and increasing concentrations of Siglec-7-Fc pre-complexes. Staining of wild type cells with R24 and Siglec-7-Fc precomplexes was used as the negative control. Figure 3.21 represents mean fluorescence intensity (MFI) values obtained for the antibody and precomplexes staining of each sample. Increasing amounts of Siglec-7-Fc did not block recognition of GD3 by R24 antibody. The column in the figure (B) describes the concentrations of Siglec-7-Fc and anti-Fc antibody used to make the precomplexes.

A

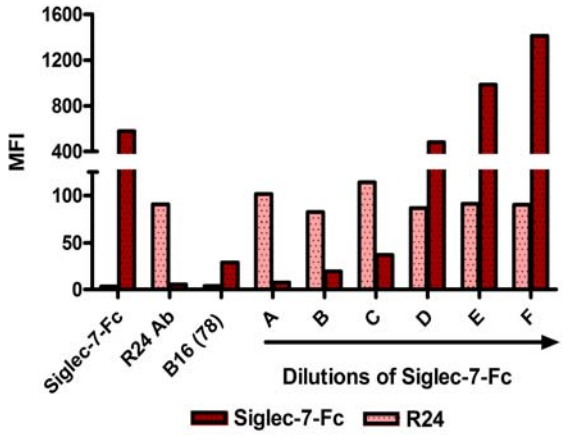

B

	Siglec - 7 – Fc (µg /ml)	Anti-Fc DyLight (µg /ml)
A	0.1	0.3
B	0.2	0.6
C	0.3	0.9
D	1	3
E	2	6
F	3	9

Figure 3.21 R24 recognition of GD3 is not blocked by Siglec-7-Fc precomplexes: B16(78) GD3 expressing cells were incubated with increasing concentrations of Siglec-7-Fc precomplexes prepared as shown in the column (B) and 10µg/ml of R24 antibody. Following incubations and washes cells were stained with anti-mouse FITC and analysed by flow cytometry. (A) Graph represents MFI values obtained for Siglec-7-Fc and R24 antibody in the different samples.

3.9 Modulation of Siglec-7 recognition of GD3 by GM1

A main aim of the project was to analyse the inhibition of GD3 by GM1 on cell surfaces and the potential modulation of Siglec-7 recognition of GD3. To achieve this, GD3 and GM1 gangliosides were expressed on B16 (78) cells.

3.9.1 Expression of GD3 and GM1 on B16 (78) transfectants

Figure 3.22 shows expression of GD3 and GM1 on B16 (78) cells, transfected with either GD3S (A) or GM2S (B) and cells transfected with both (D). Wild type cells were used as a negative control as they lack in expression of both GM1 and GD3 (C). Staining procedure is detailed in materials and methods.

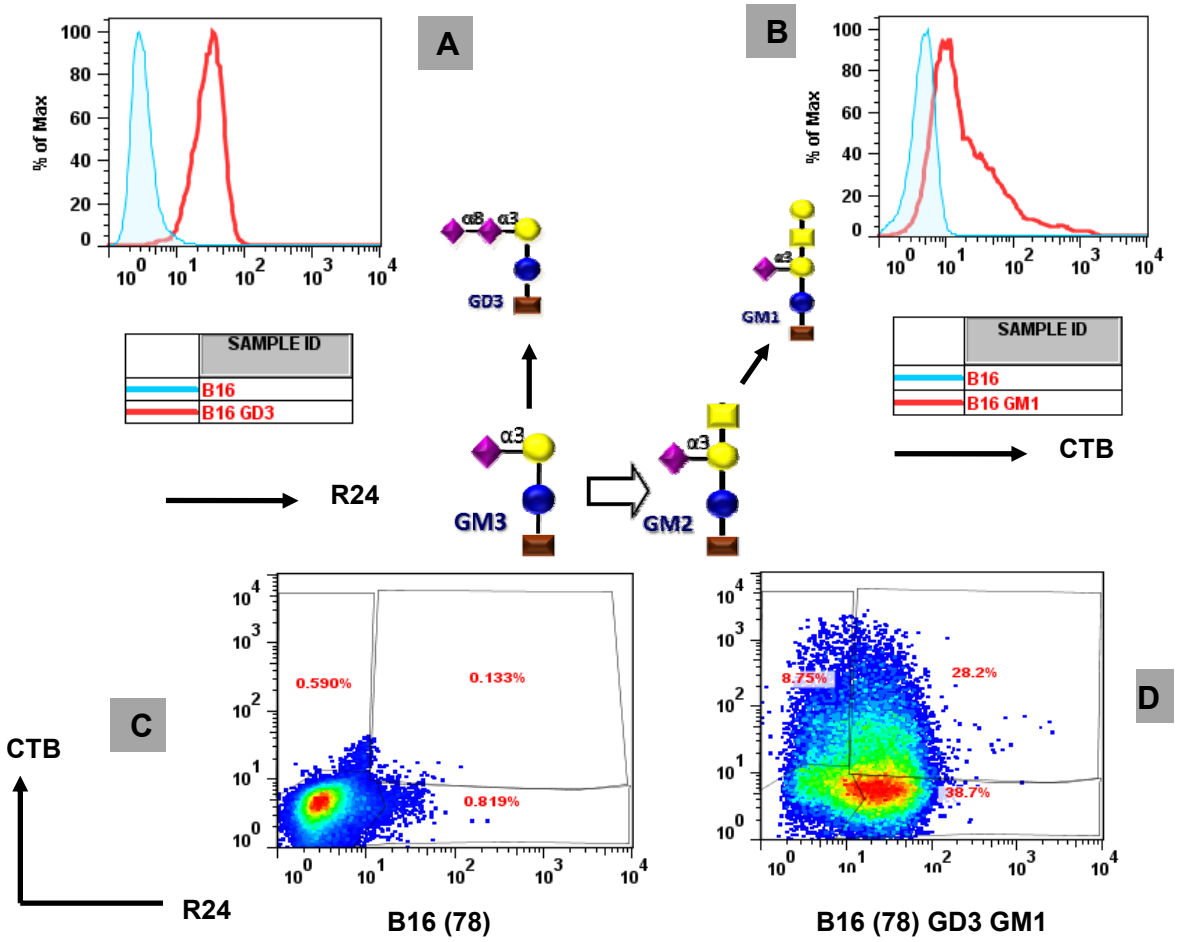

Figure 3.22 – Overexpression of GD3 and GM1 on B16 (78) cells: B16 (78) wild type cells (WT) were transfected with either GD3S or/and GM2S. Transfectants were stained with 10 µg/ml of R24 antibody or/and 1 µg/ml of biotinylated CTB. Following incubations with either anti-mouse FITC or/and streptavidin PE conjugate, cells were stained with 1/300 dilution of 7AAD (stock at 0.1 µg/ml) for 10 minutes on ice to identify dead cells before analysing them by flow cytometry. (A) WT cells and GD3S transfected cells stained with R24 antibody for detection of GD3. (B) WT cells and GM2S transfected cells were stained with biotinylated CTB for detection of GM1. WT cells stained with both R24 antibody and biotinylated CTB, showing lack in expression of GD3 and GM1 (C) B16(78) cells transfected with both GD3S and GM2S, for detection of GD3 and GM1 (D). Numbers in the gated population represents percentage of the different subsets of cells.

3.9.2 Siglec-7-Fc precomplex binding of B16 GD3 GM1 cells

The B16 (78) GD3 GM1 cells were used to analyse the inhibition of Siglec-7-Fc recognition of GD3 in the presence of GM1. GD3 and GM1 expressing subsets were identified using R24 antibody and CTB. In figure 3.23, the dot plot represents B16 (78) cells expressing GD3 and GM1 as defined by R24 antibody and CTB. The different subsets of cells with high (H) and low (L) expressions of GD3 and GM1 have been boxed out as $GD3_LGM1_L$, $GD3_HGM1_L$, $GD3_HGM1_H$, $GD3_LGM1_H$. MFI values of GD3 and GM1 are shown in red, next to the dot plot. The subsets have been marked, keeping the MFI values for GD3 expression constant. The histograms on the right and left side of the dot plot represent Siglec-7-Fc staining of each of these subsets of cells.

In the experiment represented in figure 3.23, Siglec-7-Fc recognition of GD3 on $GD3_HGM1_L$ cells is 1.42 fold higher than $GD3_HGM1_H$ cells. Similarly, the intensity of Siglec-7-Fc staining of $GD3_LGM1_L$ is 2.45 times higher than the staining of $GD3_LGM1_H$ cells. This data suggests that the presence of high density of GM1 and GD3 negatively regulates the recognition of GD3 by Siglec-7 in a GM1 dependent manner. Analysis of 3 repeats of this experiment showed that Siglec-7-Fc binding of $GD3_HGM1_L$ cells is 1.6 ± 0.08 times higher than binding to $GD3_HGM1_H$ cells.

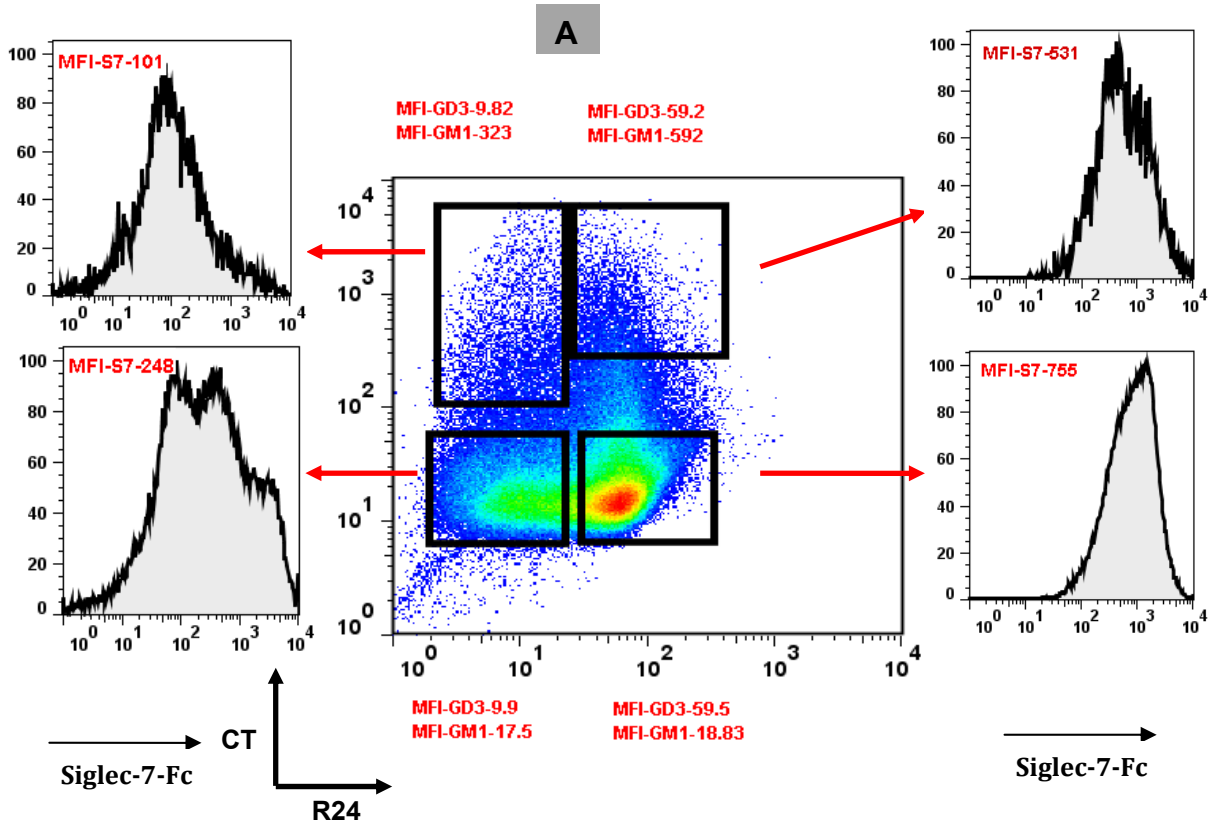
A
MFI-S7-101
MFI-S7-248
MFI-S7-531
MFI-S7-755
MFI-GD3-9.82
MFI-GM1-323
MFI-GD3-59.2
MFI-GM1-592
MFI-GD3-9.9
MFI-GM1-17.5
MFI-GD3-59.5
MFI-GM1-18.83
CT
Siglec-7-Fc
R24
Siglec-7-Fc

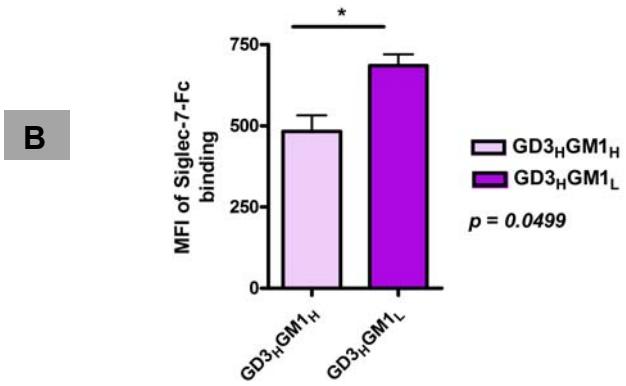
B
*
MFI of Siglec-7-Fc binding
750
500
250
0
GD3HGM1H
GD3HGM1L
p = 0.0499
GD3HGM1H
GD3HGM1L

C

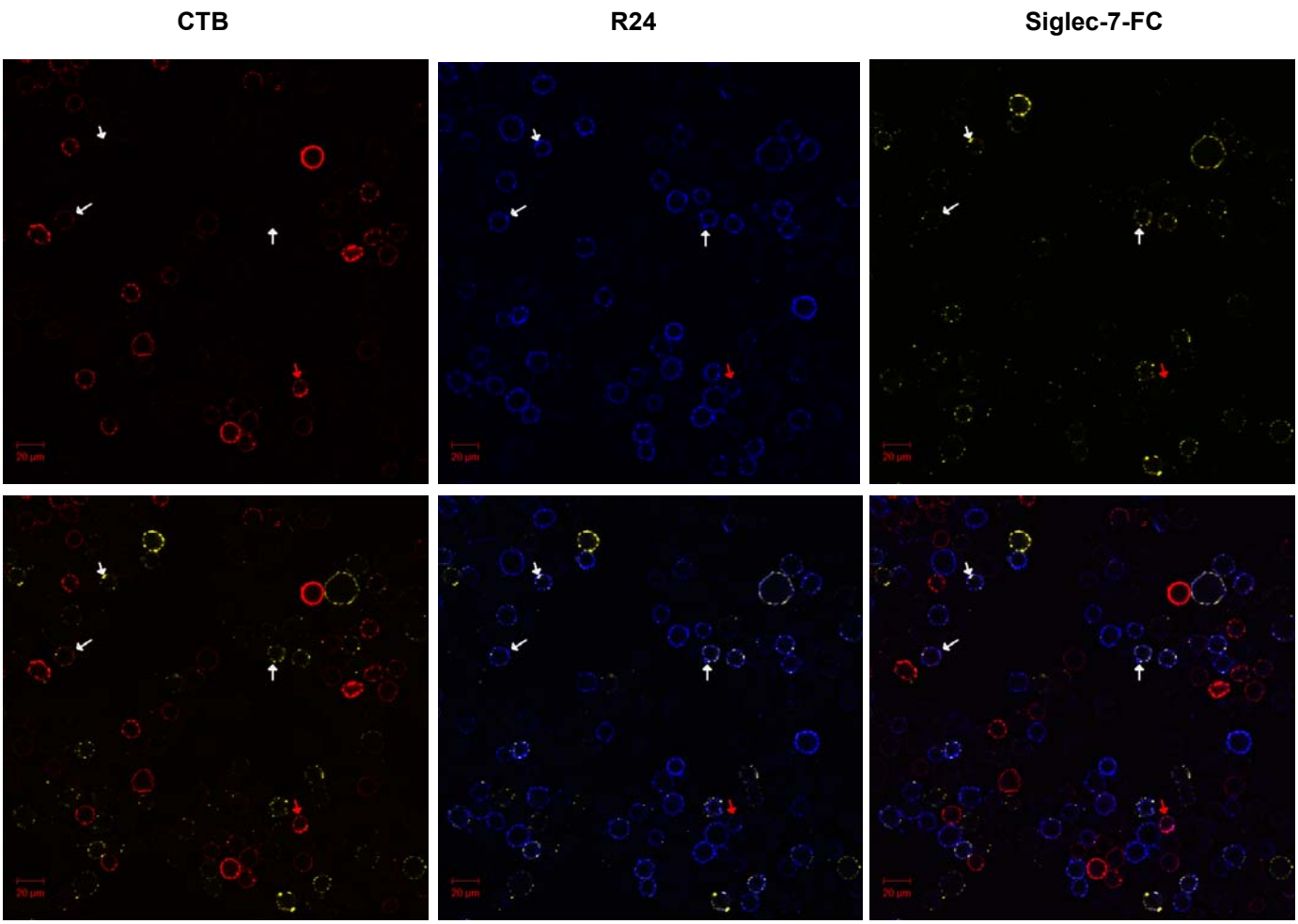

Figure 3.23 – Siglec-7 recognition of GD3 is inhibited by GM1, on B16 (78) cells: (A) Flow cytometric analysis of B16(78) GD3 GM1 cells using R24 antibody, biotinylated CTB and precomplexes of Siglec-7-Fc with anti-Fc DyLight 649 (carried out as described in 3.19). Following staining with anti-mouse FITC and streptavidin PE, cells were washed with FACS wash buffer, stained with 7AAD (as described in figure 3.22) and analysed by flow cytometry. Histograms represent Siglec-7-Fc staining of the different subsets (marked out boxes) of double transfectants identified using R24 antibody and CTB namely $GD3_LGM1_L$, $GD3_HGM1_L$, $GD3_HGM1_H$, $GD3_LGM1_H$. Numbers within histogram represent MFI values of Siglec-7-Fc precomplex staining (B) MFI values of Siglec-7 staining comparing $GD3_HGM1_H$ and $GD3_HGM1_L$ subsets of cells. Error bars represent standard error of mean between 3 experiments. (C) B16 (78) GD3 GM1 cells were stained with biotinylated CTB,

R24 mAb and precomplexes of Siglec-7-Fc and anti-Fc DyLight 649 (as described in above). Cells were washed, incubated with suitable concentration streptavidin-555 and anti-mouse FITC respectivley washed, fixed with 2% PFA before mounting onto cover slips. Images were taken on the LSM 700, at x40 magnification and analysed using the LSM image analysis software. White arrows in the images point to the binding of Siglec-7-Fc to $GD3_HGM1_L$ cells; Red arrows represent R24 and CTB binding to $GD3_HGM1_H$ cells.

3.10 Minimal GD3 GM1 co-localization on double transfectants

From the above described flow cytometry data, it was evident that only a small percentage of the B16 (78) cells have high expression of both GM1 and GD3. To confer masking of the GD3 epitope, both GM1 and GD3 would have to be co-localized on the same micro-domains. Therefore the percentage of cells showing GD3 and GM1 co-localization was quantitatively assessed using confocal microscopy staining.

R24 and CTB stained wild type and GD3, GM1 B16 (78) expressing cells were fixed and imaged using the LSM 700. Imaged cells were quantified using the Volocity software and cells were divided in two groups - (**A**) number of cells expressing both GD3 and GM1 and (**B)** number of GD3 GM1 positive cells having patches of GD3 GM1 co-localization. Table 3.3 represents percentage of each group calculated from a total of 739 cells from 18 images analysed. Only 3% of the total number of cells had patches of GD3 GM1 co-localization. Bar chart (Figure 3.24) represents the distribution of cells from each group for the individual images.

Total number of cells analysed	Cells expressing both GD3 and GM1	Cells having patches of co-localization of GD3 and GM1
739	56	25
% of the total number of cells analysed	7%	3%

Table 3.1: Quantification of B16 (78) cells expressing both GD3 and GM1 and cells carrying patches of GD3 GM1 co-localization

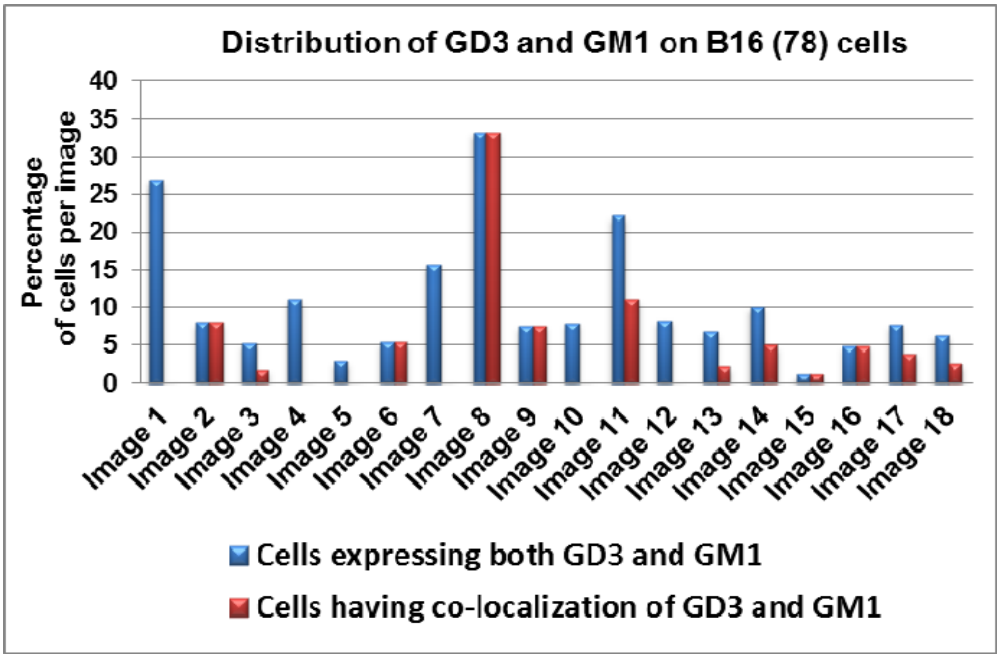

Figure 3.24: Distribution of GD3 and GM1 on B16 (78) cells : Histogram represents the number of cells from each image of double transfected B16 (78) cells expressing GD3 and GM1 and the number of cells showing patches of co-localization of the two gangliosides.

Figure 3.25 shows representative images of wild type (A) and double transfectants (B, C and D). Figure 3.25, D is a 3D projection of the cell shown in figure 3.25 (C). The images clearly demonstrate that the majority of GD3 and GM1 exist independent of each other, in separate spatial microdomains on the cell membrane.

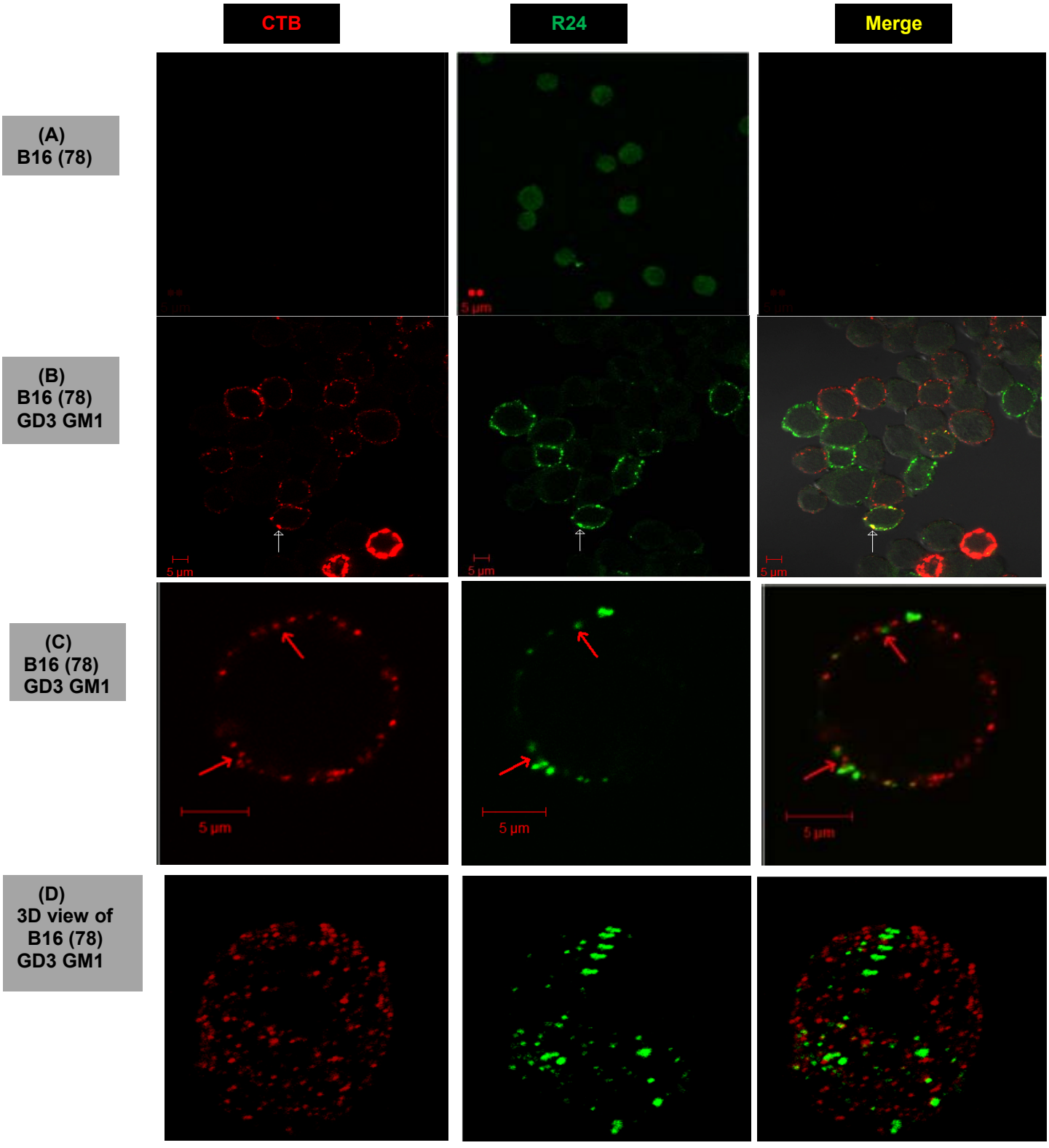

Figure 3.25: GM1 and GD3 are expressed laterally segregated of each other on B16(78) cells - Confocal microscopy analysis of GD3 and GM1 on B16 (78) transfectant cells: B16 (78) wild type and transfectant cells were harvested, stained with CTB and R24 antibody, followed by their secondary antibodies – Streptavidin-555 and anti-mouse FITC as

described in figure 3.23. Cells were then fixed with 4% PFA and mounted onto cover slips. Images were collected at 100x magnification using the LSM 700. Image analysis was carried out using Zeiss LSM Image browser. White arrows represent patches of co-localization of GD3 and GM1. Red arrows represent non-co-localized GD3 and GM1. Images are from experiment representative of n=3.

3.11 Cholesterol depletion of lipid rafts

The complex nature of gangliosides and their expression patterns can make them “invisible” to certain methods of detection. Extraction of gangliosides from cells has been reported not to correlate with their immuno staining (Nakakuma et al., 1992). This is because the epitopes are not exposed for optimal binding by the antibody being used. In such cases, the ganglioside is known to be “cryptic”. This is a well reported phenomenon and organization of these gangliosides in lipid rafts is attributed to be responsible for their cryptic nature (Lloyd et al., 1992; Greenshields et al., 2009).

To confirm that GD3 and GM1 were not forming complexes on the B16 (78) cell line, it was decided to disrupt lipid rafts by depleting the cells of cholesterol. Methyl beta cyclodextrin (MβCD) is a cholesterol sequestering reagent that is routinely used in disrupting lipid rafts (Greenshields et al., 2009). Depleting cholesterol from cell membranes would be expected to dissociate any potential GD3 GM1 ganglioside complexes and release cryptic GD3. The efficiency of MβCD treatment can be analyzed by measuring the cholesterol released following the treatment (Greenshields et al., 2009).

3.11.1 Titration of effective concentration of MβCD

Firstly, the effect of lipid raft disruption by MβCD on ligand recognition of Siglec-7-Fc was analyzed using B16 (78) GD3 cell line. As shown in figure 3.26, increasing concentrations of MβCD reduced the binding of Siglec-7-Fc precomplexes to these cells. Therefore this technique was used as a quantitative measure of raft disruption in the experiments conducted here.

From the histogram of Geo Mean Intensities (Figure 3.26, B), it can be seen that, a concentration of 10 µM resulted in a reduction of > 90% of Siglec-7-Fc binding. There was also a decrease in the percentage of live cells at higher concentrations of MβCD, as measured by 7AAD staining (Figure 3.26, C). Based on these findings, it was decided to use 1 µM of MβCD for further experiments.

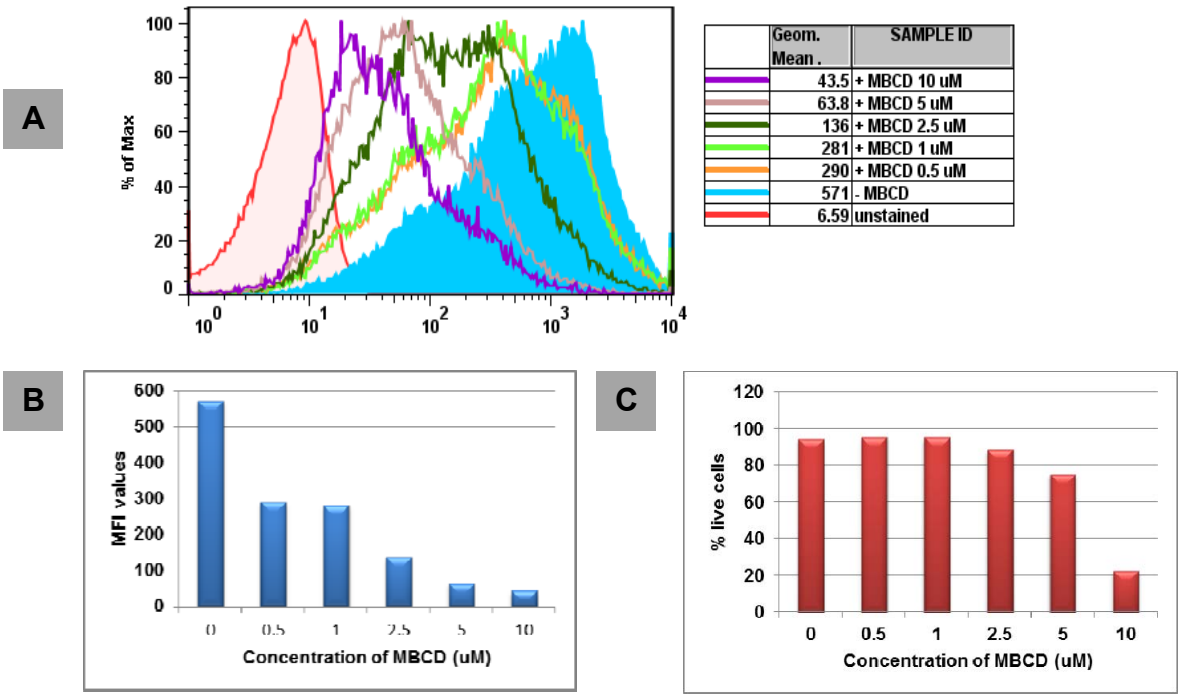

Figure 3.26 Optimizing MβCD concentration for lipid raft dissociation: 1 x10E6 B16 (78) cells were harvested and treated with different concentrations of MβCD for 30 minutes at 37^0C, in serum-free media. Cells were washed with ice-cold serum-free media and

incubated with (A) and (B) Siglec-7-Fc precomplexes as described earlier (B) with 7AAD as described in figure 3.22. Washed cells were analysed using flow cytometry

3.11.2 Effect of MBCD on R24 and CTB binding to B16 cells

MβCD treated cells were analysed for binding of Siglec-7-Fc, R24 and CTB to double transfected B16 (78) cells. While Siglec-7-Fc binding of B16 (78) GD3 cells was significantly reduced following treatment with MβCD, there was no effect on B16 (78) GD3 GM1 cells (Figure 3.27, A). Similarly the binding of R24 was not affected in the double transfectants following cholesterol treatment (Figure 3.27,B). These results suggest an absence of cryptic GD3 on B16 (78) GD3 GM1 cells. Hence disruption of lipid rafts had no effect on either Siglec-7-Fc or antibody R24 binding. CTB binding to these three populations of cells are shown in Figure 3.27 (C).

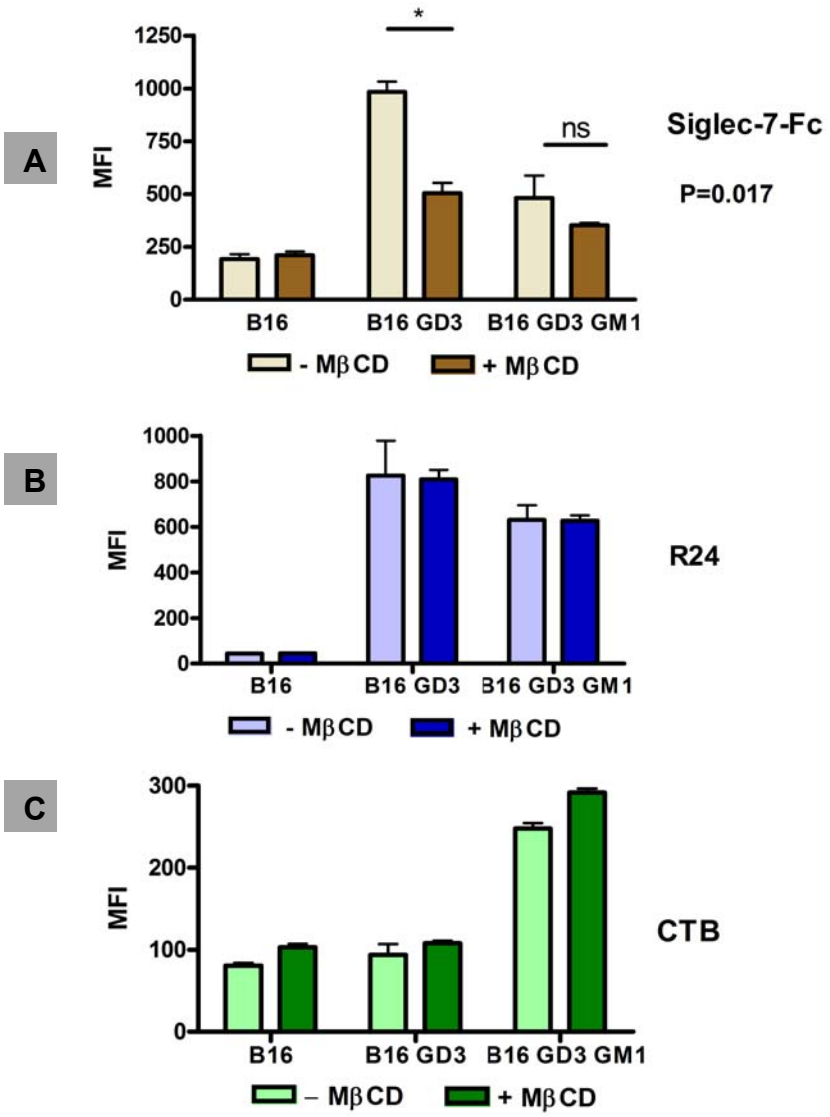

Figure 3.27: Absence of cryptic GD3 on B16 (78) GD3 GM1 cells: B16 (78) cells were harvested and treated with or without 1 μM MβCD as described in figure 3.26. Cells were washed and incubated with R24 antibody, CTB or Siglec-7-Fc precomplexes. Following incubation with either anti-mouse PE or Streptavidin conjugate, cells were washed with facs wash buffer, stained with 7AAD and analysed by flow cytometry. Error bars represent standard deviation between samples (n=3). Experiment shown is representative of n=2.

3.12 Discussion

Rinaldi et al., 2009 showed that on PVDF arrays, Siglec-7-Fc recognition of GD3 was significantly inhibited when this disialic acid containing ganglioside was in complex with structurally more complex gangliosides such as GM1. The aim of this project was to evaluate the biological significance of these findings in a biological system and to examine the role of such glycolipid complexes in immune cell receptor modulation.

Initial assays conducted here were aimed at re-confirming findings of the glycoarray data (Rinaldi et al., 2009). Recombinant Siglec-7-Fc, generated by CHO cells in UCHO media, was precomplexed to anti-Fc antibody to enable avidity based binding of the lectin to its glycol ligand (Figure 3.2). Precomplexes were specifically able to recognize GD3 coated on microtitre plates, over a range of concentrations (20 µg to 30 ng) (Figure 3.6). Siglec-7-Fc was also able to recognize GD3 incorporated into liposomes (Figure 3.10). The masking effect of GD3 by GM1 was seen when the gangliosides were either coated directly onto plates or when they were incorporated into liposomes (Figure 3.9 and 3.11).

These findings suggested that irrespective of the assay format, a structurally more complex ganglioside is able to inhibit Siglec-7 recognition of GD3. This has been named as “complex attenuated” effect (Rinaldi et al., 2009). This could be attributed to either steric hindrance by a structurally more complex ganglioside such as GM1 or formation of a neo structure when the two sugars are in close proximity. Both these mechanisms could potentially block Siglec-7 recognition of its natural ligand.

Gangliosides are overexpressed in many cancers and play important roles in cell adhesion, motility, etc. Overexpression of gangliosides on tumour surfaces may lead to their clustering in microdomains such as rafts. Structural determinants and underlying glycosidic linkages affect lectin recognition of their carbohydrate ligand. Hence in tumours, overexpression and clustering could affect lectin and antibody recognition of these tumour associated antigens (TAA) and impact tumour associated immunity.

The monoclonal antibody, R24 and toxin CTB were used in parallel wth Siglec-7-Fc precomplexes to confirm the presence of GD3 and GM1 incorporated into liposomes. Interestingly, increasing concentrations of GM1 also inhibited R24 antibody recognition of GD3 (Figure 3.12). At 4 times higher amounts of GM1, there was complete inhibition of R24 binding. It is possible that the terminal NeuAcα2-8NeuAc structure on GD3 is masked by GM1, which blocks recognition by the R24 antibody. However, no experiments were undertaken to investigate this finding further.

R24 antibody is known to have strong preference for the disialic acid epitope NeuAcα2-8NeuAcα2-3Gal, found on GD3, GD1b, GQ1b (Tai et al., 1998)(Avril et al., 2006). In a study by Greenshields et al., (2009), antibody recognition was shown to be affected by ganglioside complexes. GM2, GD1a and GD1b were found to negatively affect the recognition of an anti-GM1 antibody for GM1 by masking the non-reducing galactose and internal sialic acid epitope on GM1 (Greenshields et al., 2009). In their study, similar results were also obtained when PC12 rat neuroendocrine cells were overexpressed with GD1a and GM1. However in these experiments, GM1 binding by CTB or another clonally

different GM1 antibody was unaffected. These results were explained by the low affinity of the antibody for its epitope compared to CTB.

For examining the biological significance of the inhibition imposed by GM1, a mouse melanoma cell line, B16 (78), was genetically modified to over express both GM1 and GD3. The expression of GM1 and GD3 was confirmed using cholera toxin subunit B (CTB) and R24 antibody in flow cytometry analysis (Figure 3.22). Transfection of GM2S in these cells resulted in clonally restricted expression of GM1 (Figure 3.14) whereas >98% of cells stained positive for GD3 when transfected with GD3S. R24 mAb binding to these cells was GD3 mediated as no binding of wild type cells was seen (Figure 3.20, A). Similar findings have been reported for the P815 GD3 transfected cells (Nicoll et al., 2003).

Glycosyltransferases are responsible for the biosynthesis of gangliosides. These enzymes are transcriptionally regulated and their expression determines ganglioside repertoires at the cell surface (Ruan et al., 1992). Abnormal glycosylation patterns on tumour cells can be directly related to the relative levels of these glycosyltransferases. Ganglioside composition of cells is not only regulated by the levels of the different glycosyltransferases but also depends on the relative ratio between them. Some neuroblastoma cell lines express high levels of GD2 but low levels of GD3. This has been related to low levels of GD3S and comparatively higher levels of GM2S (Ruan et al., 1999).

In the B16 (78) cells double transfected with GM2S and GD3S, only between 5 and 20% of the cells co-expressed GD3 and GM1. The percentage of these double positive cells decreased while cells were maintained in culture. The remaining subsets within this population of cells were predominantly GD3

positive or negative for both GD3 and GM1. Only 10% of the cells were positive for GM1.

Transcript levels of the enzymes involved in the biosynthesis of GD3 and GM1 were analysed by quantitative real-time PCR and correlated to ganglioside profiles in B16 (78) cells. The wild type cells were positive for expression of transcripts for GM3s, GM1s and GD1as (Figure 3.16). mRNA levels of GM2s in B16 (78) GM1 clones 16 and 19 corresponded to the expression of GM1 on these cells. A possible role of cell cycle regulation of this glycosyltransferase (GM2S) was suspected. Further experiments in this direction are required. Another possible explanation for this phenomenon is the rapid conversion of GM1 into the next ganglioside in the biosynthetic pathway, GD1a. However, when GM2S transfected cells were stained with anti-GD1a antibody (MOG35), < 1% cells stained positive (shown in Appendix, Figure A3). The mRNA level of GD1as was examined by RT-PCR (Figure 3.16,D) and found to be comparable to mouse liver cells which are reported to have low transcript levels of this enzyme.

The limited expression of GM1 might also be regulated by other factors such as the level of GM1s which catalyses the conversion of GM2 to GM1. The mRNA levels of GM1s in the transfectants were compared to expression levels in mouse brain tissue. Transcript levels were found to be 20 fold less in the clone with the maximal expression of GM1 (Clone 16) and 38 fold less in the clone with weak expression of GM1 (clone 19) (Figure 3.16, C). Based on these data, it is possible to infer that low levels of GM1s in these cells limit the conversion of all of the cellular pool of GM2 into GM1. Expression of GM2 would have to be analysed by means of antibody staining.

In the double transfectants, both GM2S and GD3S would be expected to compete for the substrate GM3 and convert it to either GM2 or GD3 respectively. While GD3 expression depended only on GD3S, GM1 expression depended on both recombinant GM2S and endogenous GM1s. Weak expression of GM1s could therefore limit the expression of GM1 in these cells. Moreover ganglioside composition of melanoma cells are known to be typically GM3=GD3 and less commonly GM3=GD3=GM2=GM1 (Ruan et al., 1999). The pattern of ganglioside expression in this mouse melanoma double transfectant cells is in line with these previous studies and may explain the higher percentage of double transfected cells only expressing GD3. Co-expression of both GD3 and GM1 is present in only a very small subset in the double transfectant population.

Siglec-7-Fc bound the wild type cells weakly and gave a strong shift in fluorescence intensity with B16 (78) GD3 cells (Figure 3.20, B). At least 80% of increased binding of Siglec-7-Fc to B16 (78) GD3 cells compared to wild type cells can be attributed to GD3 expression.

Pre-complexing of an Fc chimera can lead to the formation of large complexes (Figure 3.2). Therefore the possible blocking of R24 recognition of GD3 by the Siglec-7-Fc precomplexes was examined (Figure 3.21). Interestingly, the R24 antibody recognition of its disialic acid epitope on GD3 was not affected by increasing amounts of Siglec-7-Fc precomplexes. High affinity of R24 mAb for its ligand could overcome the avidity based binding of the lectin precomplexes to GD3. The main aim of the project was to examine the blocking effect of GM1 on the recognition of GD3 by Siglec-7-Fc. Therefore experiment to analyse the

effect of Siglec-7-Fc recognition of GD3, in the presence of saturating amounts of R24 antibody was not carried out.

The biological significance of the masking effect of GD3 by GM1 (as seen in the plate based assays) was analysed by Siglec-7-Fc staining of the double transfectant population (Figure 3.23). The presence of four subsets within this transfectant population made the assay internally well controlled. Siglec-7-Fc precomplexes binding of $GD3_HGM1_H$ expressing cells was significantly weaker than $GD3_HGM1_L$ cells. These results correlate with the ELISA based assays using ganglioside complexes directly coated onto plates or incorporated into liposomes. Confocal microscopy staining using Siglec-7-Fc precomplexes also showed a similar bias for Siglec-7-Fc recognition of GD3 not co-localized with GM1.

Confocal microscopy staining also showed that in cells with expression of both GD3 and GM1, the gangliosides were laterally segregated. Only 7% of the double transfectants had dual expression of both GD3 and GM1 on their cell surface and only 3% of the total cells had patches of co-localization of the two gangliosides (Figure 3.24). For GM1 masking of the sialic acid epitope on GD3, co-localization of the two gangliosides on the same lipid raft would be a pre-requisite. The lack of co-existence of these gangliosides on the same microdomain could have implications on the interaction of these two species of gangliosides and thereby hinder *cis*-interactions. Thus it would be difficult to assess the biological significance of this finding using primary NK cells.

To confirm the absence of masked/cryptic GD3 on these transfectants, cholesterol depletion studies using MβCD were undertaken. Although Siglec-7-Fc binding to B16 GD3 cells was significantly affected following MβCD

treatment, there was no change seen in the binding of Siglec-7-Fc to double transfectants which implies that possibly only a very small percentage of GD3 and GM1 exist within the same microdomains (Figure 3.27). Cholesterol depletion had also no effect on R24 binding to the double transfected cells. This reconfirms the absence of any cryptic GD3 when over expressed on these cells.

In parallel with the work on the B16 (78) melanoma cell line, co-expression of GD3 and GM1 was also attempted on another cell, the MDA-MB-231. These human breast cancer cells are negative for GD3 expression but expresses gangliosides belonging to the a-series of the ganglioside biosynthetic pathway ie GM2 and GM1. This cell line was therefore transfected with pCDNA 3.1-GD3S plasmid and clones expressing different levels of GD3 and GM1 were obtained. However on examining these transfectants by confocal microscopy, a similar pattern of lateral segregation of GD3 and GM1 was observed (data not shown).

Lateral segregation of gangliosides on cell surface depends on various factors. While my studies were underway, Dong et al., (2010) reported that GD3 and GM1 have distinct distribution patterns when co-expressed on human breast cancer cell lines. Using multiple reaction monitoring (MRM) analysis, GD3 was proposed to distribute onto glycolipid enriched microdomains (GEM/lipid rafts) and non-GEM domains based on the fatty acid composition of these molecules and degree of saturation of the fatty acid chains. The ability of GM1 and GD3 to cluster independently of each other in membrane rafts with minimal co-localization has also been previously demonstrated. However these experiments were conducted on artificial monolayers and healthy rat neuronal

cells (Vyas et al., 2001). Therefore their findings cannot be extrapolated to ganglioside expression on tumours.

Gangliosides are complex molecules. While their large hydrophilic oligosaccharide head groups protrude out into the extracellular milieu, their hydrophobic ceramide backbone is embedded within the lipid layers of the cell membrane. Their expression, distribution and organization in lipid domains on the cell surface are dependent on various factors (Sonnino et al., 2007).

It is possible that on the B16 (78) cell line too, differences in structure and composition of the over-expressed gangliosides favours their lateral segregation into separate membrane microdomains. Interactions of these molecules with other protein and lipid components of the cell membrane might be another factor affecting their distribution on the cell membrane. The *cis*-interactions between GD3 and GM1 was hypothesized to alter NK cell cytotoxicity. It would be therefore interesting to analyze if such interactions occur on non-transformed cells as well as primary tumours.

The role of GD3 in modulating the role of Siglec-7 in NK cells is discussed in chapters 4 and 5.

Chapter 4

Role of Siglec-7 in modulating LFA-1 recognition on NK cells

4.1 Introduction

Siglec-7 is evolutionarily related to the mouse neutrophil siglec, Siglec-E (as described in the introduction, page 26). Recent findings from our lab suggested a regulatory role for Siglec-E in integrin (CD11b) signalling (McMillan et al., 2013). Their results also showed a constitutive association of Siglec-E with SHP-1 and its role in regulating β_2 integrin activation of Syk tyrosine kinase and p38. These findings would imply an evolutionarily conserved function of Siglec-7 in negatively regulating integrin functions.

The aim of this project was to investigate the role of the NK cell inhibitory receptor, Siglec-7 in regulating β_2 integrin mediated functions. A brief overview on intergrin biology in leukocytes will be detailed here before explaining the specific aims of this part of the project.

Integrins are heterodimeric cell – surface adhesion proteins expressed on all leukocytes and are important in aiding leukocyte migration both in normal physiology and during inflammation (Hogg et al., 2002),(Harburger and Calderwood, 2009). Leukocytes commonly express the following β2 integrins – Leukocyte Function Associate Antigen-1 (αLβ2), Mac-1(αMβ2) and the Very Late Antigen-4 (α4β1) belonging to the β1 family. ICAM-1, a cell surface adhesion molecule, is the preferred ligand for adhesion receptors such as LFA-1 and Mac-1 (Marlin and Springer., 1987)(Lawson and Wolf.,2009). Integrin activation results in cellular responses such as survival, respiratory burst, cytokine production, complement mediated phagocytosis, cellular polarization and degranulation (Abram and Lowell, 2009). These heterodimeric

transmembrane proteins consist of an α and a β subunit. Integrins are tightly regulated under normal physiological conditions and therefore do not mediate cell-cell or cell – extracellular matrix interactions. Upon receiving signals from chemokines and other cellular receptors, integrins go from a completely inactive, bent conformation through an intermediate affinity state to a high affinity, open conformation. This is known as the “inside-out” signalling. (Abram and Lowell, 2009;Hogg, Patzak and Willenbrock, 2011). Along with the above mentioned conformational changes, integrins also undergo clustering in lipid rafts for enhancing their avidity for ligands.

“Outside in” signalling follows clustering of integrins and conversion of the intermediate form of LFA-1 to the high affinity form and tightening adhesion with ligands. The cellular responses that follow outside-in signalling are varied in different cell types of leukocytes. Outside in signalling of integrins can also be bought about by the addition of divalent cations and by antibody crosslinking (Yan, Fumagalli and Berton, 1995). (Hogg et al., 2003). Figure 4.1 (A) is a schematic representation of some of the key molecules involved in the integrin signalling cascade in leukocytes (Adapted from Hogg, Patzak and Willenbrock., 2011).

Similar to its role on T-cells and B-cells, LFA-1 plays an important role in adhesion and co-activation of NK cells (Kurzinger et al., 1981). Its role in NK cells has been detailed in chapter 1 (pages 12-13). Functions and downstream signalling of LFA-1 in NK cells have been studied using NK cell lines and primary NK cells (Barber et al., 2004)(Perez et al., 2004). Depending on the experimental strategy involved, these studies have used either ICAM-1 expressed as Fc-chimeras and coated on beads, plates etc or target cells that express ICAM-1.

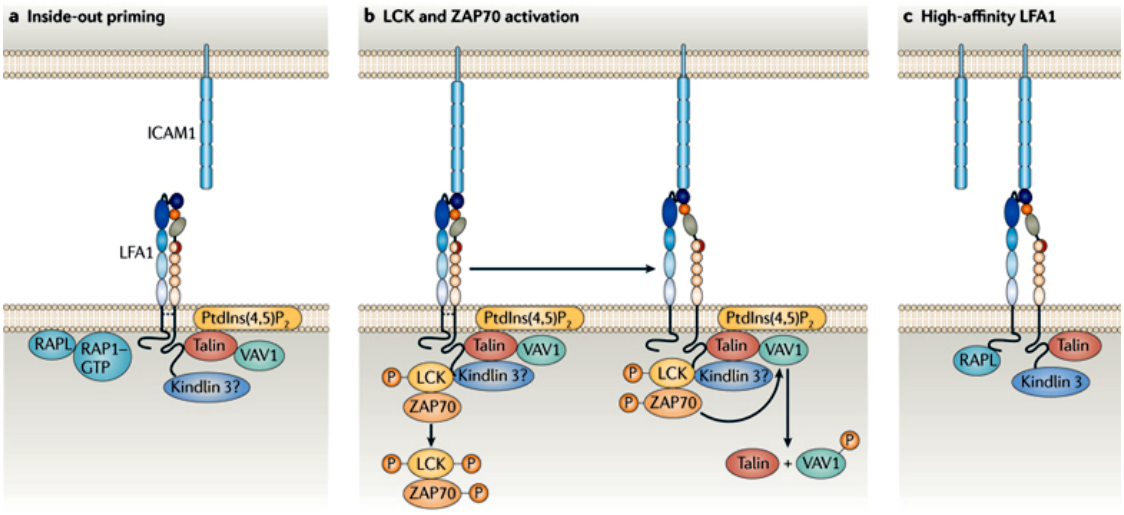

Figure 4.1 (A): Outside-in signalling of LFA-1 : (a) Following inside out signalling Vav-1, talin, possibly kindlin3, RAP1 and RAPL associate with LFA-1 at the cell membrane (b) Src and Syk family members associate with LFA-1 and get phosphorylated following binding of LFA-1 to ICAM-1. Phosphorylated ZAP70 then phosphorylates Vav1 causing talin release from the Vav1-talin complex. (c) Binding of talin to the β-subunit of LFA-1 and RAPL to the α-subunit results in the final conversion of LFA-1 into the high-affinity conformation. PtdIns(4,5)P_2, phosphatidylinositol-4,5-bisphosphate; RAPL - regulator of adhesion and cell polarization enriched in lymphoid tissue. Adapted from Hogg, Patzak and Willenbrock., 2011)

Based on the findings of Siglec-E in the negative regulation of CD11b in neutrophils, the following two models were proposed for the possible role of Siglec-7 in NK cells. Model A (Figure 4.1, B) suggests that Siglec-7 recognizes glycosylated ICAM-1 (or other sialylated molecules in the vicinity) and dampens signalling triggered by activated LFA-1. According to model B (Figure 4.1,B), constitutive association of Siglec-7 with receptors like LFA-1 is sufficient to dampen the downstream signalling generated by LFA-1 following ligand recognition.

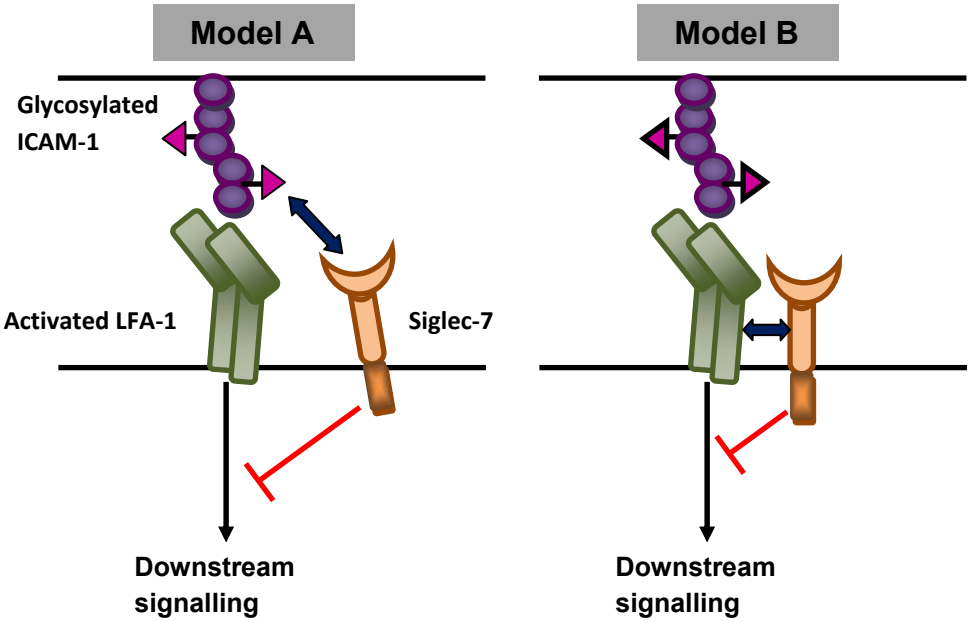

Figure 4.1 (B): Proposed model of Siglec-7 inhibition of LFA-1 signalling. In model A, Siglec-7 recognition of the glycosylated ICAM-1 results in negative regulation of LFA-1 mediated signalling. In model B, Siglec-7 is constitutively cis-associated with LFA-1. Activation of LFA-1 following ligand binding is sufficent for Siglec-7 to exert its inhibitory functions on LFA-1 signalling.

Project Aims:

The aims of this project were to investigate the potential role of Siglec-7 in modulating integrin functions in the context of NK cell biology by:

1) Examining LFA-1 mediated functions such as adhesion and perforin polarization in the presence and absence of siglec-7 expression.

2) Investigating downstream signalling events mediated by LFA-1 following ligand binding in the presence and absence of siglec-7 expression

Towards these goals an NK cell line and purified recombinant ICAM-1-Fc was used in this project. Preliminary cytotoxicity assays involving LFA-1 and ICAM-1 are presented in Chapter 5.

ICAM-1 consists of 5 Ig-like domains (D1-D5), a transmembrane domain and a short cytoplasmic tail. ICAM-1 is heavily glycosylated in its D2, D3 and D4 domains carrying 4, 2 and 2 predicted sites of N-linked glycosylation respectively as shown in Figure 4.2, A. LFA-1 interacts with the D1 of ICAM-1 via its insertion (I) domain (Jun et al., 2001;Landis et al., 1994). Under physiological conditions, ICAM-1 is expressed at low levels on endothelial cells and lymphocytes but its expression is upregulated in various pathological conditions by inflammatory cytokines for eg: asthma, atherosclerosis and tumours (Hubbard and Rothlein., 2000)(Roland et al., 2007).

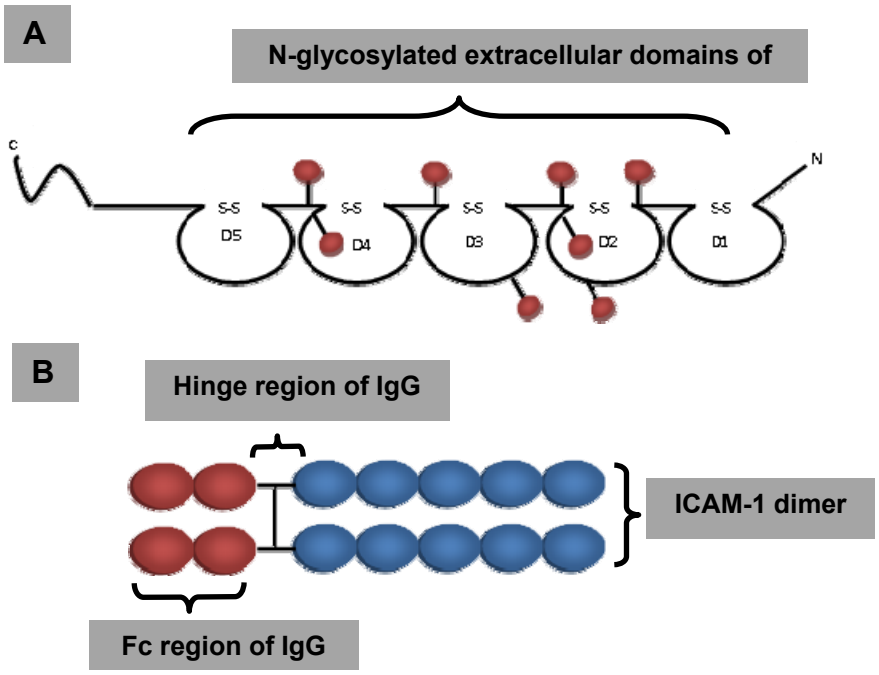

Figure 4.2: Schematic representation of (A) ICAM-1 with N-glycosylation sites (shown as red spheres) (B) Recombinant dimeric ICAM-1 linked to the Fc region of IgG

ICAM-1-Fc chimeras are useful tools in aiding the study of receptor-ligand function. Structurally, they consist of dimers of the five extracellular Ig domains of ICAM-1 linked to the hinge region and Fc fragment of human IgG (Figure 4.2,B).

The functional role of receptors is studied by over-expressing or blocking the receptor of interest (blocking antibodies or gene silencing) in either primary cells

or cell lines. Here, over-expression of Siglec-7 in an NK cell line was the chosen method.

NK cell lines are routinely used as model systems in studying the biological functions of NK cell receptors, screening drug candidates that will modulate NK functions etc (Yusa and Campell., 2003)(Wang et al., 2012). Some examples of human NK cell lines include NK92, NKL, KHGY-1, NK3.3. While most of these cell lines have excellent cytotoxicity towards NK target cells, their receptor profiles vary considerably (Gong et al., 1994)(Yagita et al., 2000) (Kornbluth et al., 1982).

Having almost no expression of any of the inhibitory KIR receptors, the NK92 cell line exhibits potent cellular cytotoxicity mediated by perforin and granzymes (Gong, Maki and Klingemann, 1994) (Lutz and Kurago, 1999). This is an IL-2 dependent cell line and hence requires an external supply of IL-2 for survival, proliferation and effector functions (Tam et al., 1999). NK92 are known to express adhesion molecules other than CD11a such as CD2, CD11c and CD28 (Zheng et al., 2009).

4.2 Generation and characterization of ICAM-1-Fc

Chinese hamster ovary (CHO) cells are the most commonly used cell line for the large scale production of antibodies and recombinant proteins due to the stable, long term and mammalian glycosylation patterns which can be attained (Hossler, Khattak and Li, 2009). Here, CHO cells were chosen for the expression of the ICAM-1-Fc chimera. Wild type CHO cells are not known to express the α 2,6 sialyltransferase, ST6Gal1, since they only produce N-glycan sugar chains carrying the NeuAc α 2,3 Galβ1,4GlcNA-R (Lee, Roth and Paulson, 1989). Therefore to increase the probability of the ICAM-1-Fc having

N-linked glycosylation with NeuAc α 2,6 Galβ1 pattern, thereby also favouring recognition by Siglec-7, it was decided to co-transfect these cells with the enzyme ST6Gal1.

4.2.1 Cloning of ICAM-1-Fc and ST6Gal1

Previously constructed ICAM-1-Fc and ST6Gal1 clones, kindly provided by Dr D. Simmons and Dr S. Kelm respectively were used. ICAM-Fc cloned into pCDM8 vector was retransformed into K12 MC1061/P3 strain of ultracompetent *E.coli* cells while the ST6Gal1 cloned into pCDNA 3.1 (neomycin resistance) was retransformed into DH5α cells (detailed in the Materials and Methods section – Section 2.26).

4.2.2 Transfection of ICAM-Fc and α 2,6 sialyltransferase plasmids into CHO cells

Supernatants were collected after one week and an ELISA conducted on them to confirm the presence of ICAM-1-Fc and α 2,6 linkages using anti-ICAM-1 antibody and Sambucus niagra agglutinin (SNA) respectively (Figure 4.3). The lectin SNA has a strong preference for Neu5Ac α 2,6 Gal sequences (Naoto Shibuya et al., 1996). Single cell cloning of transfected CHO cells was performed by limiting dilution as described in the methods section. Cloning by limiting dilution follows the Poisson probability distribution, according to which a clonal frequency of 33% would have > 90% chance of being clonal (Kojima et al., 1988).

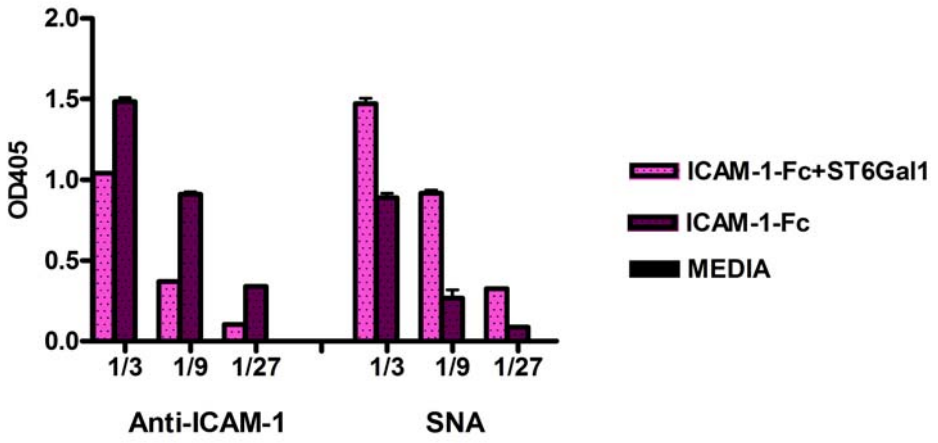

Figure 4.3: ELISA to confirm the transfection of ICAM-1-Fc and ST6Gal1 in non-clonal CHO cells. 96 well plates were coated with anti-Fc IgG, blocked and plated with different dilutions of supernatant of transfected CHO cells. Plates were then incubated with biotinylated anti-ICAM antibody or SNA and detected with streptavidin alkaline phosphatase and pNPP substrate. Bars represent the different preparations of ICAM-1-Fc with and without ST6Gall and media alone which was used as blank in the assay.

On this basis, an anti-Fc ELISA was conducted to test for selected clones (Figure 4.4,A). Only 2 clones from the ICAM-1-Fc transfection and 6 clones from the ICAM-1-Fc + ST6Gal1 double transfection tested positive for anti-Fc antibody. These clones were then subjected to anti-ICAM-1 and SNA ELISAs (Figure 4.4, B and C). Clone 17 from the ICAM-1-Fc transfection alone was positive for ICAM-1 and negative for SNA binding while clones 54 and 58 from the double transfection were strongly positive for both ICAM-1and SNA binding.

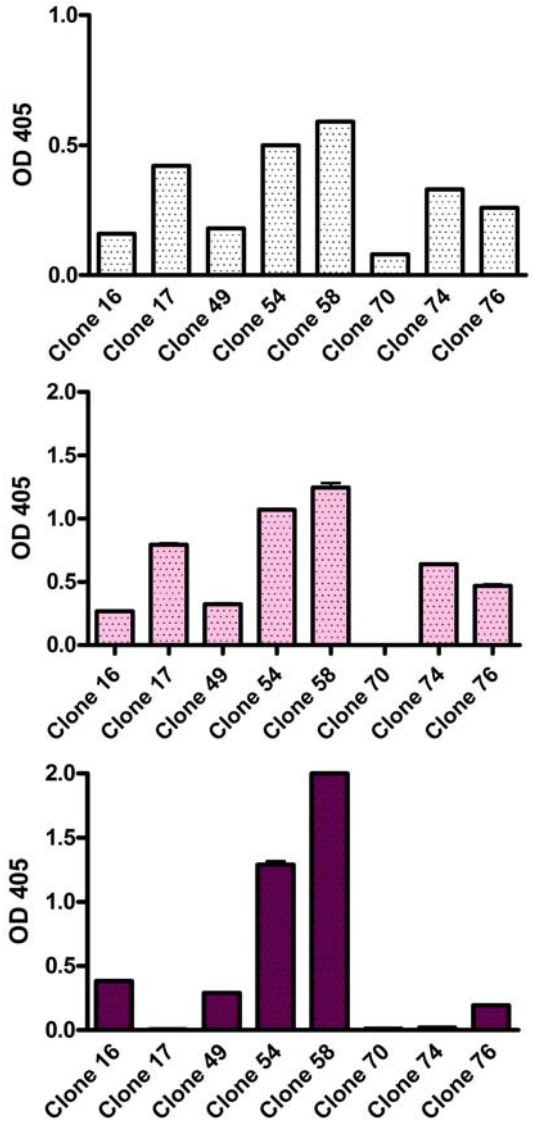

Figure 4.4: CHO cells transfectants express ICAM-1-Fc - ELISA was carried out to characterize supernatant from CHO cell clones expressing ICAM-1-Fc and ST6Gal1. ELISA was carried out on supernatants from different clones to detect (A) Fc (B) ICAM-1 (C) α 2,6 linkages. 96 well plates were coated with anti-Fc IgG, blocked and 1/15 dilution of supernants of clones that grew in selection media were added and incubated for 1 hour at room temperature. Plates were then incubated with biotinylated anti-ICAM-1 antibody or biotinylated SNA for one hour at room temperature. Washed plates were incubated with Streptavidin alkaline phosphatase (1:1000) and 100 µl of pNPP substrate was added and plates read at 405nm. For Fc detection, plates were incubated with 100 µl of anti-human Fc-alkaline conjugate (n=2). Error bars represents standard deviation (n=3).

4.2.3 Purification of ICAM-Fc supernatants

Both Protein A and G bind most human IgG subclasses with high affinity and are therefore routinely used in the purification of Fc chimeras, antibodies and other recombinant proteins. The purification of ICAM-1-Fc was initially undertaken using protein G Sepharose column. However the yields were low and the flow through contained substantial levels of unbound Fc chimera as determined by ELISA (data not shown).

Hence it was decided to re-run the supernatants through a protein A Sepharose column. Elutions were measured using the Nanodrop (readings given in table 1). Table 4.1, A, shows details of ICAM-1-Fc supernatant quantified using ELISA from the different CHO cell harvests and table 4.1, B, gives protein concentrations as determined by Nanodrop readings before and after buffer exchange.

	Clone 17		**Clone 54**		**Clone 58**	
	Concentration (mg/ml)	**Total protein (µg)**	**Concentration (mg/ml)**	**Total protein (µg)**	**Concentration (mg/ml)**	**Total protein (µg)**
Harvest 1	1.22	612.43	1.59	792.53	1.02	507.86
Harvest 2	1.26	628.31	1.53	765.96	1.03	512.80
Harvest 3	1.59	794.94	1.35	675.64	1.29	647.25
Harvest 4	1.72	858.21	1.65	826.26	1.41	704.60
Harvest 5	0.97	487.33	1.53	764.24		
	1.35	**3381.22**	**1.53**	**3824.63**	**1.19**	**2372.50**
Volume of supernatant		**2.5 L**		**2.5L**		**2L**

Table 4.1 A: ELISA Quantification of ICAM-1-Fc supernatant from CHO cell harvest

ICAM-Fc clones	**Elution 1 (mg per ml)**	**Elution 2 (mg per ml)**	**Total Protein mg/2ml**	**After spin concentration (mg/ml)**	**Total protein (µg)**
Clone 17	0.95	0.04	0.99	1.35	1200
Clone 54	1.09	0.13	1.22	1.30	1300
Clone 58	0.67	0.09	0.76	0.90	900

Table 4.1 B: Protein quantified by Nanodrop after ICAM-1-Fc purfication using Protein A column

4.2.4 SDS page analysis of purified proteins

Sodium dodecyl sulfate polyacrylamide gel electrophoresis (SDS-PAGE) is the most convenient method of separating proteins according to the molecular weight and analyzing their purity. The use of a reducing agent in the samples breaks down intramolecular disulfide bonds.

3 µg of each ICAM-1-Fc protein, non-reduced and reduced, were run on a gradient polyacrylamide gel under constant voltage (Figure 4.5, A). Figure 4.5 (B) shows linear regression analysis curve plotted using relative migration distance (R_f) vs the known molecular weights (MW) of the ladder.

The calculated molecular weights (MW) of the ICAM-1-Fc under reducing conditions are as follows – clones 17 and 54 – 109.58 KDa and clone 58 – 105.3 KDa. The molecular weight of the non-reduced Fc proteins could not be extrapolated from the standard curve as the proteins migrated outside the range of the molecular weights of the marker but was approximately 200 KDa, the expected size. The gel also confirmed a purity of > 95%.

An ELISA using the lectin SNA to confirm the presence of α 2,6 sialic acid linkages of the ICAM-1-Fc (clone 54) was carried out (Figure 4.6). The results confirmed that the two clones (54 and 58) which were transfected with ICAM-1--Fc and ST6Gal1 were strongly positive for SNA binding in a concentration dependent fashion while clone 17 which was not transfected with ST6Gal1 did not bind the lectin.

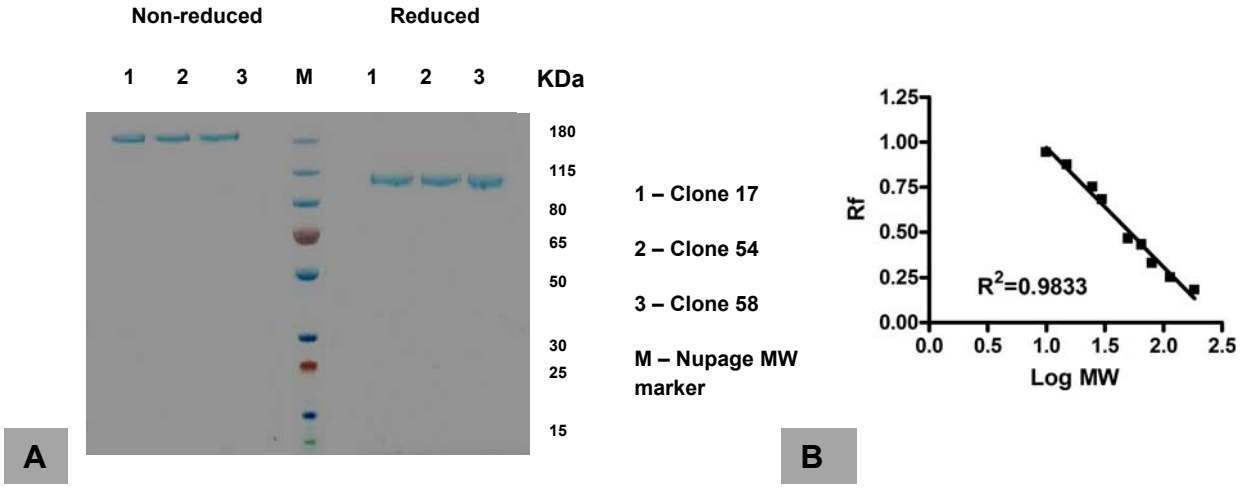

Figure 4.5: SDS-PAGE analysis of purified ICAM-1-Fc supernatant purified using protein A column. 3 µg of each of the purified supernatants from clones 17, 54 and 58 were prepared in loading dye, without or with reducing agent. Samples were boiled for 5 minutes at 100 ^{0}C and then ran on 4-12% Bis-Tris gel at 200V for 35 minutes. Gel was washed with water and stained with Nupage Simply Blue Safe stain for 1 hour at room temperature. Gel was then destained with water and imaged. (B) Linear regression curve for molecular weight marker used in SDS-PAGE analysis.

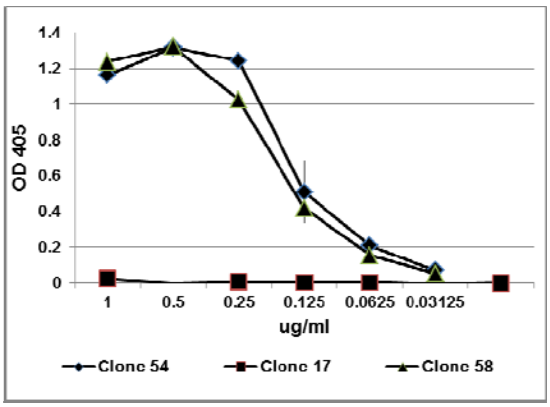

Figure 4.6: ELISA for the detection of α 2, 6 sialylation using biotinylated SNA. 96 well plates were coated with anti-Fc IgG, blocked and different concentrations of purified ICAM-Fc proteins were added and incubated for 1 hour at room temperature. Plates were washed 3 times with PBA (0.25% BSA) and then incubated with biotinylated SNA (10 µg/ml) for 1 hour at room temperature. Washes were repeated after incubation and plates were coated with Streptavidin alkaline phosphatase (1:1000) in TBA (0.25% BSA). After washes in TBA (0.25% BSA), 100 µl of pNPP substrate was added and plates read at 405nm.

4.3 Sialic acid dependent binding of S7-Fc to ICAM-Fc – Dot Blots

Binding of Siglec-7-Fc-precomplexes to ICAM-1-Fc chimeras was attempted in an ELISA format. However, the precomplexes failed to detect any ligands. This was thought to be due to the relatively low coating density of the Fc chimeras on a 96-well plate that do not provide sufficent multivalency for pre-complexed Siglec-7-Fc binding. Hence the chimeras were analysed for Siglec-7-Fc binding using dot blots in which high protein density can be achieved. This technique is a convenient method to identify and analyse proteins and study protein-ligand interactions. In parallel, the anti-ICAM-1 antibody and SNA lectin would also be used to confirm the presence of ICAM-1 and α 2,6 linkages on ICAM-1.

4.3.1 Recognition of GD3 by Siglec-7-Fc precomplexes

Siglec-7-Fc recognition of sialylated ligands on dot blots was optimized using ganglioside GD3 spotted onto PVDF membranes. Figure 4.7 (A –D) shows the optimization data using different concentrations of Siglec-7-Fc and Anti-Fc-HRP (Table 2). 5 µg/ml of Siglec-7-Fc and 1:1000 dilution of the anti-human Fc-HRP gave the best signal to noise ratio.

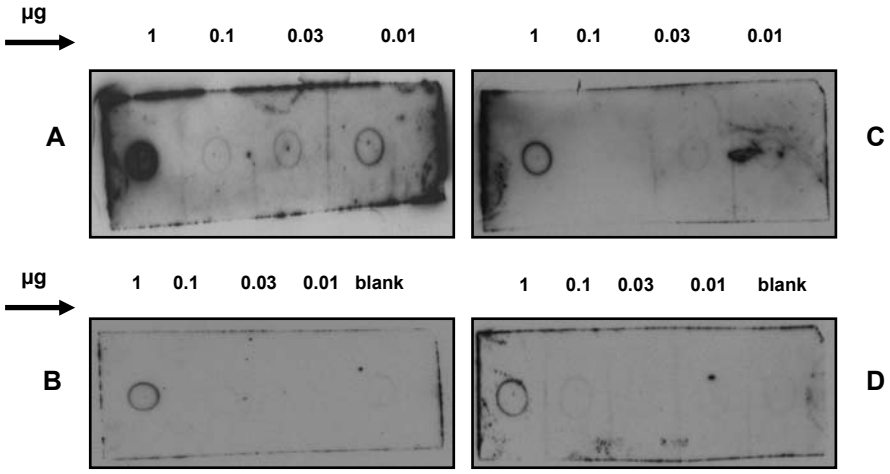

	Siglec-7-Fc	Anti-Fc-HRP
A	5 µg/ml	1:1000
B	5 µg/ml	1:3000
C	1 µg/ml	1:1000
D	1 µg/ml	1:3000

Table 4.2

Figure 4.7: Dot blots for the optimization of Siglec-7-Fc precomplexes: 1 µg, 0.1 µg , 0.03 µg and 0.01 µg of GD3 (diluted in methanol) were spotted onto PVDF strips, dried for one

hour and then blocked with 5% milk. Blots were then quenched with 10% FCS. Titrations of Siglec-7-Fc and anti-Fc-HRP were used (as shown in column) to prepare precomplexes by mixing them in 1:3 (volume/volume). Precomplexes were added onto blocked membrane and then left to incubate overnight at 4^0C. Blots were then washed thoroughly in 1XTBS + 0.1% Tween-20 and then detected using ECL substrate. Methanol only was spotted on as negative control (blank).

4.3.2 Sialic acid dependent recogntion of ICAM-Fc by Siglec-7-Fc and antibodies

Titrations of ICAM-1-Fc (clone 17 and 54) were spotted in duplicates on nitrocellulose membranes and treated with or without sialidase. Blots were then incubated with either Sigec-7-Fc precomplexed to anti-Fc antibody, anti-ICAM-1 antibody or SNA lectin (Figure 4.8, B). Titrations of GD3 spotted onto PVDF membranes were used as a positive control for Siglec-7-Fc binding (Figure 4.8, A).

Siglec-7-Fc precomplexes bound strongly to ICAM-1-Fc from both clones and this was partially reduced following sialidase treatment (Figure 4.8, C). The anti-ICAM-1 antibody

also recognized both clones but also showed some reduction following sialidase treatment (Figure 4.8, D). SNA binding to both clones was significantly reduced following sialidase treatment (Figure 4.8, E). The bar charts in Figure 4.8 represents the average signal obtained from duplicate samples in each case.

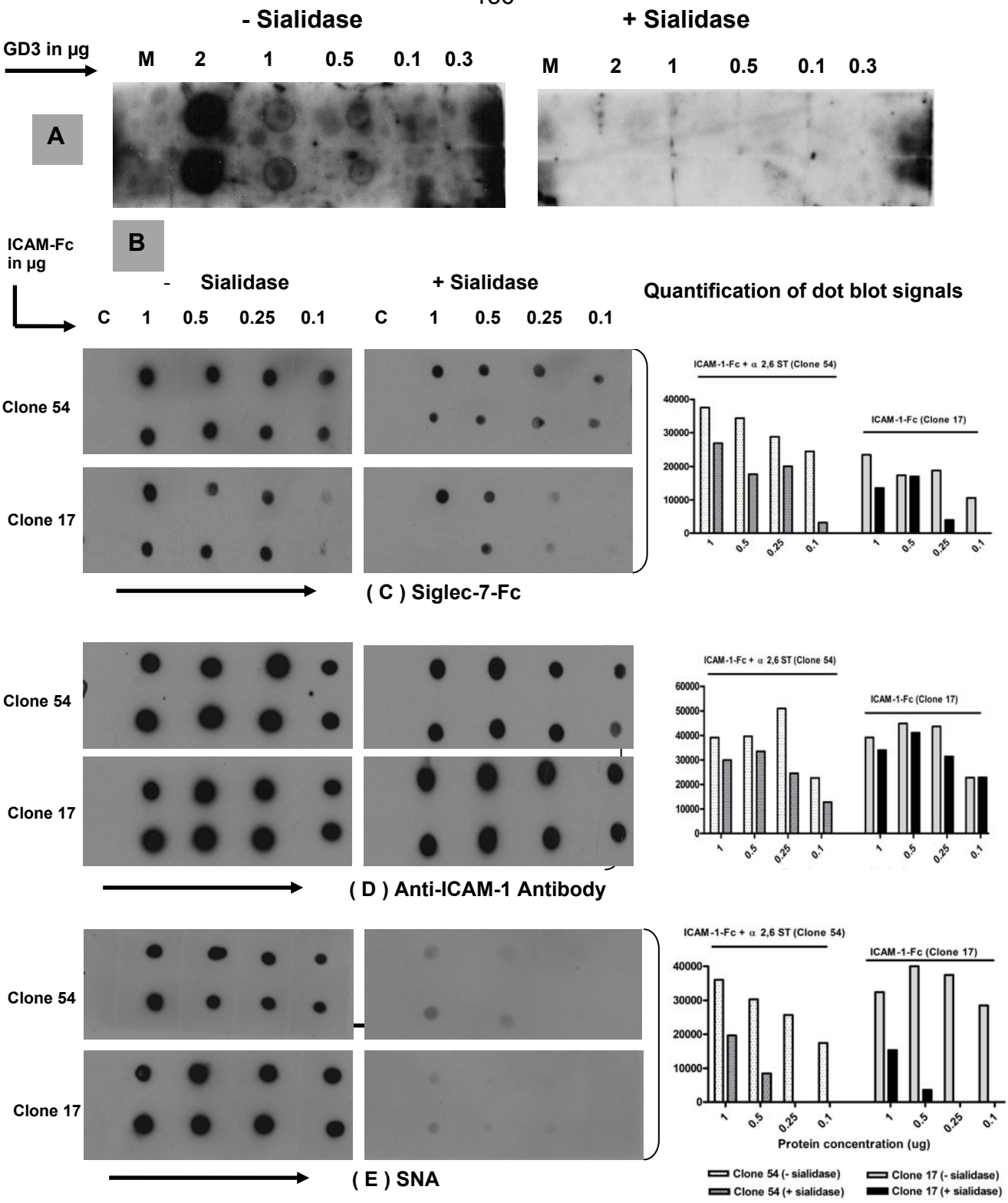

Figure 4.8: Detection of ICAM-Fc by Siglec7, Anti-ICAM-1 antibody and SNA using dot blots: (A) Different concentrations of GD3 were spotted onto PVDF membrane and incubated with Siglec-7-Fc precomplexes as described in figure 4.7. (B) Different concentrations of ICAM-1-Fc (with and without α 2,6 sialylation) were spotted onto nitrocellulose membrane in duplicates, dried for one hour and then blocked with 5% milk. Sialidase treatments of blots were carried out by incubating blots in 0.17 IU/ml of

sialidase in sodium acetate buffer for one hour at 37^{0}C. Blots were then quenched with 10% FCS and then incubated with (C) Siglec-7-Fc precomplexes (as described in figure 4.6), (D) Anti-ICAM-1 antibody and (E) SNA, overnight at 4^{0}C. Blots were then washed in TBST and incubated for an hour with Avidin-HRP (1:5000). Blots were washed again and detection carried out using ECL substrate. Experiment is representative of n=2.

4.4 Characterization of NK92 cell line and PBMC

NK92 cell line was a kind gift from Dr. Eric Vivier (CIML, Marsielle). Culture conditions were optimized as to the media, IL-2 requirements and cell concentrations (detailed in the Materials and Methods sections).

4.4.1 Expression of CD56, Siglec-7 and LFA-1 on NK92 cell line

NK92 cells are known to be positive for CD56 ^{bright}, CD2, CD11a, CD54 and negative for CD3, CD16, Mac-1 and for KIRs (Gong et al., 1994; Komatsu F and Kajiwara M., 1998).

Using suitable antibodies and isotype controls, expression levels of CD56, Siglec-7 and LFA-1 on NK92 cells were compared to those of IL-2 activated human peripheral blood mononuclear cells (PBMCs). Cells were stained with suitable antibodies or isotype controls and analysed by flow cytometry. As shown in figure 4.9, both NK92 and IL-2 activated PBMC were positive for CD56 (A). While PBMC have CD56 ^{dim} and CD56 ^{bright} populations, NK92 cells are only positive CD56 ^{bright}. CD56+CD3- PBMCs were also positive for Siglec-7 (B) while NK92 was negative for this receptor. Finally as reported, NK92 also stained positive for LFA-1(C) (Zheng et al., 2009).

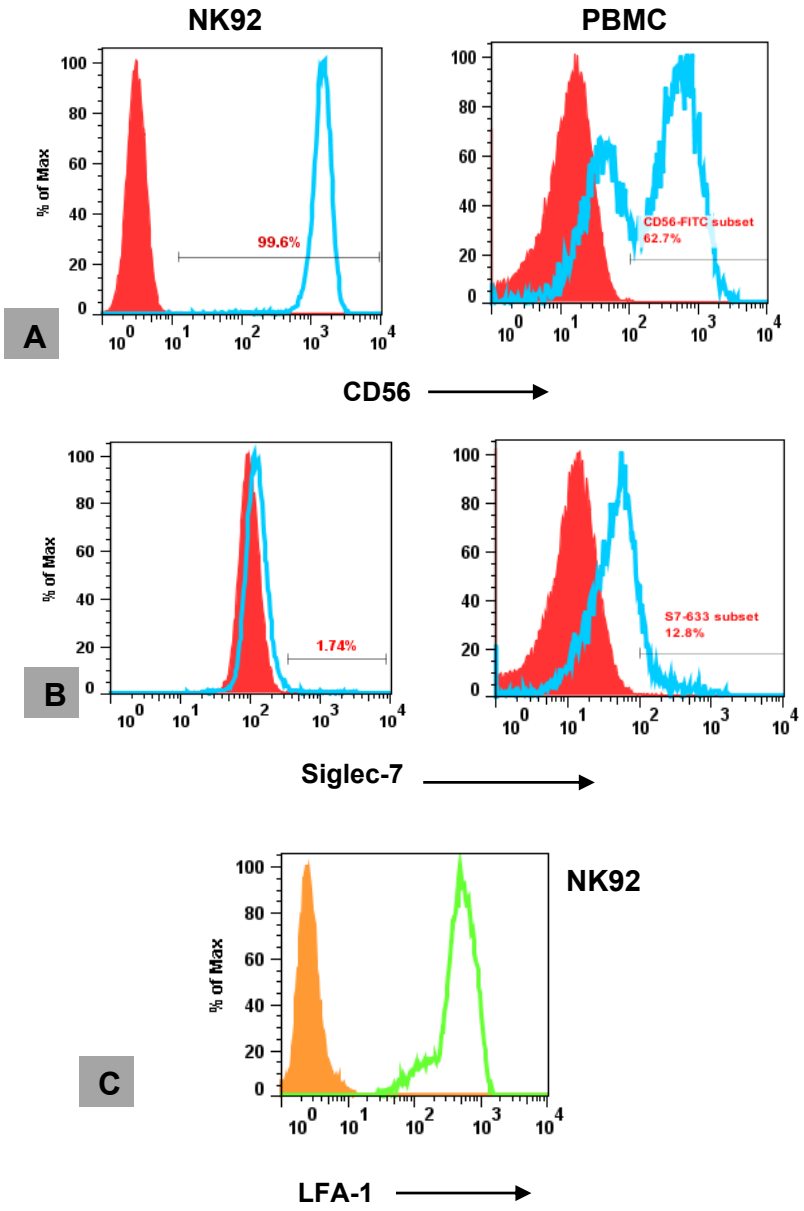

Figure 4.9 : Flow cytometry characterization of NK92 cell line - IL-2 cultured PBMCs (gated on CD3 negative population) for the detection of CD56-FITC , Siglec-7 expression or relevant isotype controls. 1X10E6 cells were stained with anti-CD56 antibody (A) or sheep polyclonal anti-Siglec-7 antibody (B), diluted in wash buffer (blue histograms). Relevant isotype control for CD56 and pre-immune sheep sera were used (red filled histograms) Samples were incubated for 30 minutes on ice. Cells were then washed x3 with wash buffer and then stained with anti-sheep secondary antibody for 30 minutes on ice. (C) NK92 cells were also stained with anti-LFA-1-FITC (green line) and relevant isotype control (orange filled histogram). Following washes in wash buffer, cells were fixed with 1% PFA and then analysed by flow cytometry.

4.4.2 Siglec-7 mRNA levels in NK92 cell line

In order to confirm the absence of Siglec-7 expression in this cell line, mRNA levels were quantified using RT-PCR. Primers used for this are shown in Table 2.5, in the Materials and Methods. The method used for quantification was the ΔΔCt method in which the mRNA level of the target gene of interest is normalized to levels of GAPDH in the cell. Figure 4.10 shows fold change in Siglec-7 mRNA expression levels in NK92 cells compared to PBMCs. These results confirmed that NK92 cells have no transcripts for Siglec-7. Hence these tally with what was observed by flow cytometry.

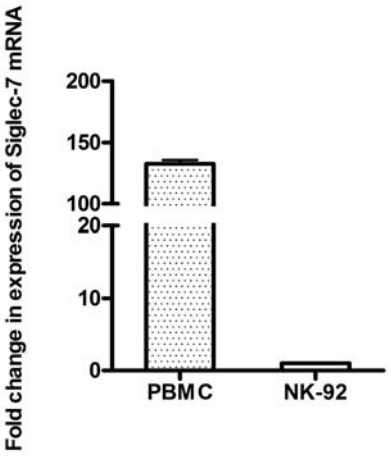

Figure 4.10 SIglec-7 messenger RNA expression levels in NK92 cells: cDNA prepared from 1 µg of PBMC and NK92 m RNA. RT-PCR was conducted on these samples using optimized primers for Siglec-7 and GAPDH. Relative fold change in gene expression was quantified by the Comparative $\Delta\Delta C_T$ method, using GAPDH as normalizer and NK92 as the calibrator (taken as 1). cDNA from PBMCs were used as the positive control. Y-axis represents the fold change in gene expression, relative to PBMC.

4.4.3 Generation of Siglec-7 expression vector and mutants

Based on the above findings, it was decided to transfect these cells with vectors carrying full length cDNA for Siglec-7 and its mutant forms. A previously cloned Siglec-7 cDNA in the pcDNA 3.1 vector (neomycin selection) (clone 14) was used for this purpose. The vector sequence was confirmed by plasmid DNA sequencing using the T7 forward and reverse primers. This plasmid vector was then re-transformed into DH5 α cells and a single clone was used in the preparation of purified DNA.

This DNA prep was also then used to make Siglec-7 mutants by site directed mutagenesis using primers described in Table 2.4 (Materials and Methods). Siglec-7 mutants included:

a) Sugar binding mutant, R124A in which the Arginine at position 124 is mutated to an Alanine (A). The mutation of this residue to an Alanine (A) is known to reduce sialic acid dependent binding of Siglec-7(Angata and Varki, 2000). b) Tyrosine mutations in the ITIM and ITIM-like motifs in the cytoplasmic domains, Y1F(YY437F) and Y2F(Y460F) respectively. The membrane proximal ITIM has been shown to be important in inhibitory signalling mediated by Siglec-7 (Avril et al., 2004).

The cloning of these mutants has been detailed in the Materials and Methods section (Section 2.27). Mutant clones were sequenced to confirm the presence of the desired mutations (data not shown).

4.4.4 Over-expression of Siglec-7 and mutants in NK92 cell line

In previous studies NK92 cells have been transfected with success in different ways. For this project, a number of methods were attempted for transfecting this cell line such as the transfection reagent Lipofectamine (Zhang et al., 2004) and use of retroviral and lentiviral systems (Savan et al., 2009). While these methods gave very minimal levels of transfection, as assessed by flow cytometry staining of Siglec-7, nucleofection with a commercially available kit had better efficiency. Following nucleofection, transfected cells were cultured in selection media for two weeks before cloning plates were set up using the limiting dilution method as discussed in Materials and Methods, 2.4.3. Clones were allowed to grow in selection media for a month before they were analysed by flow cytometry using anti-Siglec-7 mAb (supernatant 7.7a) as shown in

Figure 4.11, A. Clones with low, medium and high expression of Siglec-7 were cultured in flasks before freezing 2-3 vials of each clone.

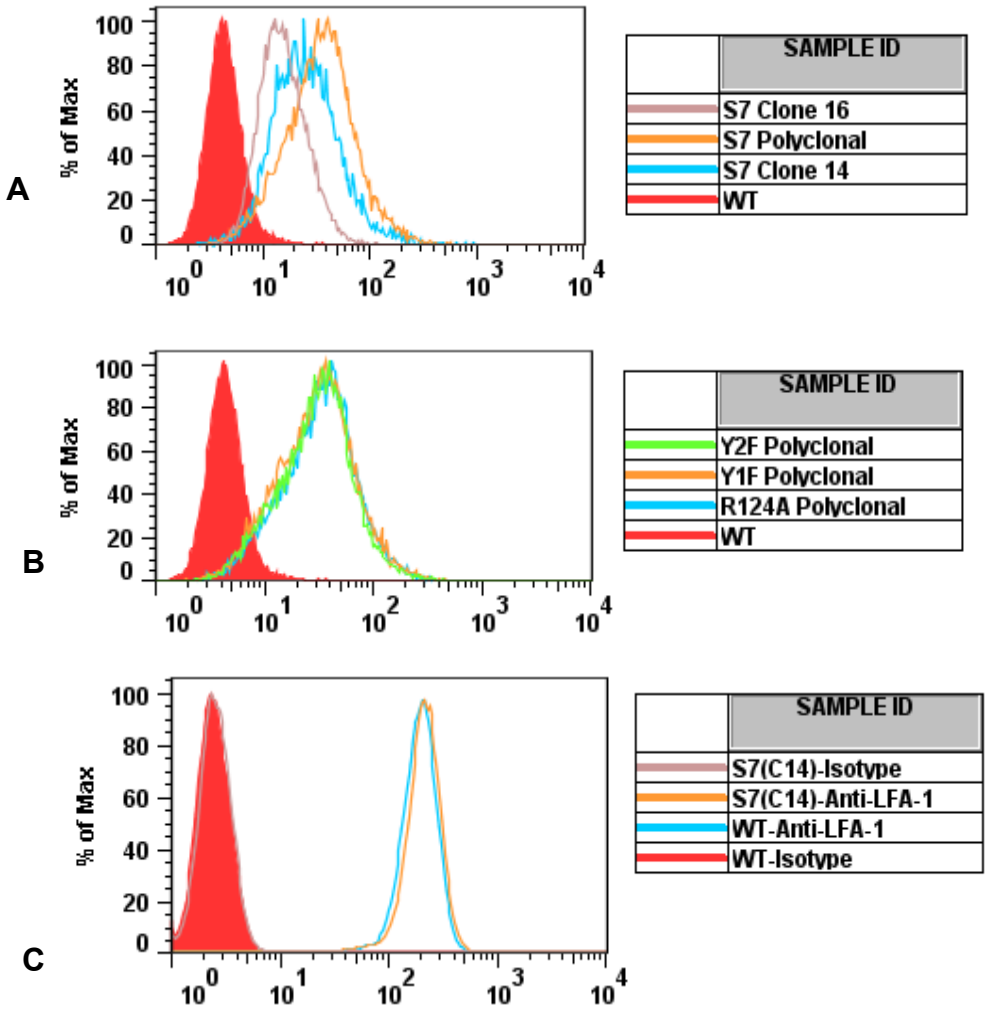

Figure 4.11: Overexpression of Siglec-7 in NK92 cell lines : WT NK92 cell line was electroporated with 4 µg of Siglec-7/ R124A/ Y1F or Y2F plasmid DNA. (A) WT and Siglec-7 cells (polyclonal or clonal) were stained with 1/5 dilution of mouse monoclonal anti-Siglec-7 antibody (7.7a) in wash buffer and incubated for 30 minutes on ice. Cells were then washed x3 in wash buffer and stained with 1/200 of anti-mouse PE. Cells were washed again in wash buffer, fixed with 1% PFA and then analysed by flow cytometry. (B) Same was repeated for the Siglec-7-R124A/Y1F/Y2F mutant polyclonal population. (C) WT and Siglec-7 (Clone 14) was also stained with anti-LFA-1 antibody and isotype control.

Siglec-7 mutants (R124A, Y1F and Y2F) were also nucleofected into NK92 wild type cells and cultured in selection media. Both polyclonal populations and clones derived from limiting dilution of the NK92 expressing mutants were analysed by flow cytometry staining and aliquots frozen (Figure 4.11, B).

One constant problem that was faced in maintaining Siglec-7 (or mutants) expressing NK92 cells was the loss of expression over a period of time in culture. This made it difficult to have uniform and high expression of the receptor prior to biological assays. Hence FACS sorting was used to select for high expressers.

Since the core of this project involved studying the biological effects of integrin signalling, expression of LFA-1 on Siglec-7 expressing NK92 cells was also examined (Figure 4.11, C). Staining of the wild type and transfected cells with an anti-LFA-1 antibody and suitable isotype control showed that the expression of Siglec-7 in the NK92 cells did not affect LFA-1 levels.

4.4.5 Expression of Siglec-5 and 9 on NK92 cell line

Primary NK cells are known to express Siglec-7 and to a lesser extent, Siglec-9 while neutrophils express Siglec-5 and -9. In order to rule out the possible expression of other Siglecs on NK92 cells, antibody staining and flow cytometric analysis was carried out. While human neutrophils stained positive for Siglecs-5 and -9 (Figure 4.12, A), NK92 cells were devoid of these members of the Siglec family (Figure 4.12, B).

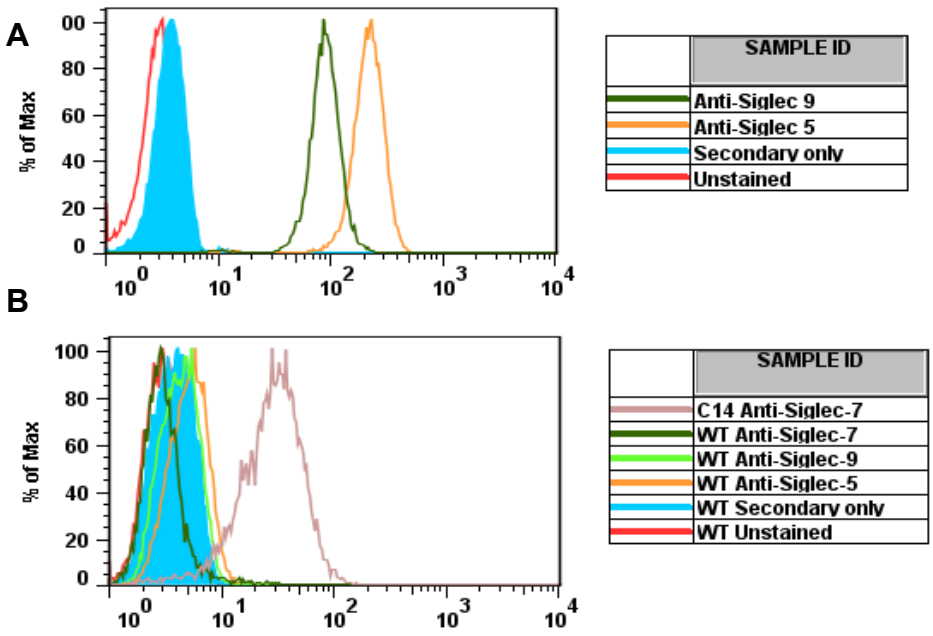

Figure 4.12: NK92 cells do not express Siglec-5 or Siglec-9 : Human neutrophils (A) and NK92 cells (B) were stained with anti-Siglec 5, 9(Kalli) and 7(7.7a) mouse monoclonal antibodies for 30 minutes on ice, diluted 2.5x in wash buffer. Cells were washed in wash buffer and then stained with 1/200 dilution of anti-mouse PE for 30 minutes on ice. Following x3 washing with wash buffer, cells were fixed with 1%PFA and analysed by flow cytometry. Cells stained with secondary alone was used as negative control

4.5 Adhesion of wild type and Siglec-7 expressing NK92 cells to ICAM-Fc

Adhesion assay have been used for studying the role of LFA-1 in neutrophils, macrophages, platelets and lymphocytes. The use of ICAM-1-Fc chimeras coated onto plates is a commonly used method of assessing LFA-1 mediated adhesion (Dransfield et al., 1992).

4.5.1 Siglec-7 negatively affects adhesion of NK92 cells to ICAM-1-Fc

Purified ICAM-1-Fc (clone 54 – carrying α 2,6 sialic acid linkages) was coated on plates to which NK92 cells (± Siglec-7) were added and incubated. Unbound cells were washed off and the bound cells were analysed using crystal violet (as

detailed in Materials and Methods). Divalent cations such as Mg2+ are known to activate integrins and help them attain their fully active confirmation. In the adhesion assay described here, varying concentrations of Mg2+ has been used to activate integrins. Figure 4.13 represents OD values obtained for wild type and Siglec-7 expressing NK92 cells when activated with or without Mg^{2+} and added on to wells coated with ICAM-1-Fc. Integrin mediated adhesion to ICAM-1-Fc was absent when the cation was chelated using EDTA or when human IgG was used instead of ICAM-1-Fc. Phorbol esters such as Phorbol 12,13 dibutyrate (PDBU) are known to cause inside out activation of integrins. Hence cells treated with PDBU were used as positive control. Cells added to wells coated with poly-L-lysine (PLL) were used as another internal control to obtain maximal adhesion of cells.

In all cases, the binding of wild type NK92 cells to ICAM-1-Fc in the presence of Mg^{2+} was significantly higher than that of Siglec-7 expressing NK92 cells. In order to keep within the physiological levels of Mg^{2+}, concentrations between 0.1 and 5 mM were chosen. Cells added onto PLL coated wells were also resuspended in 1mM Mg^{2+}.

Adhesion of WT and Siglec-7 cells to different preparations of ICAM-1-Fc was also compared (shown in appendix).

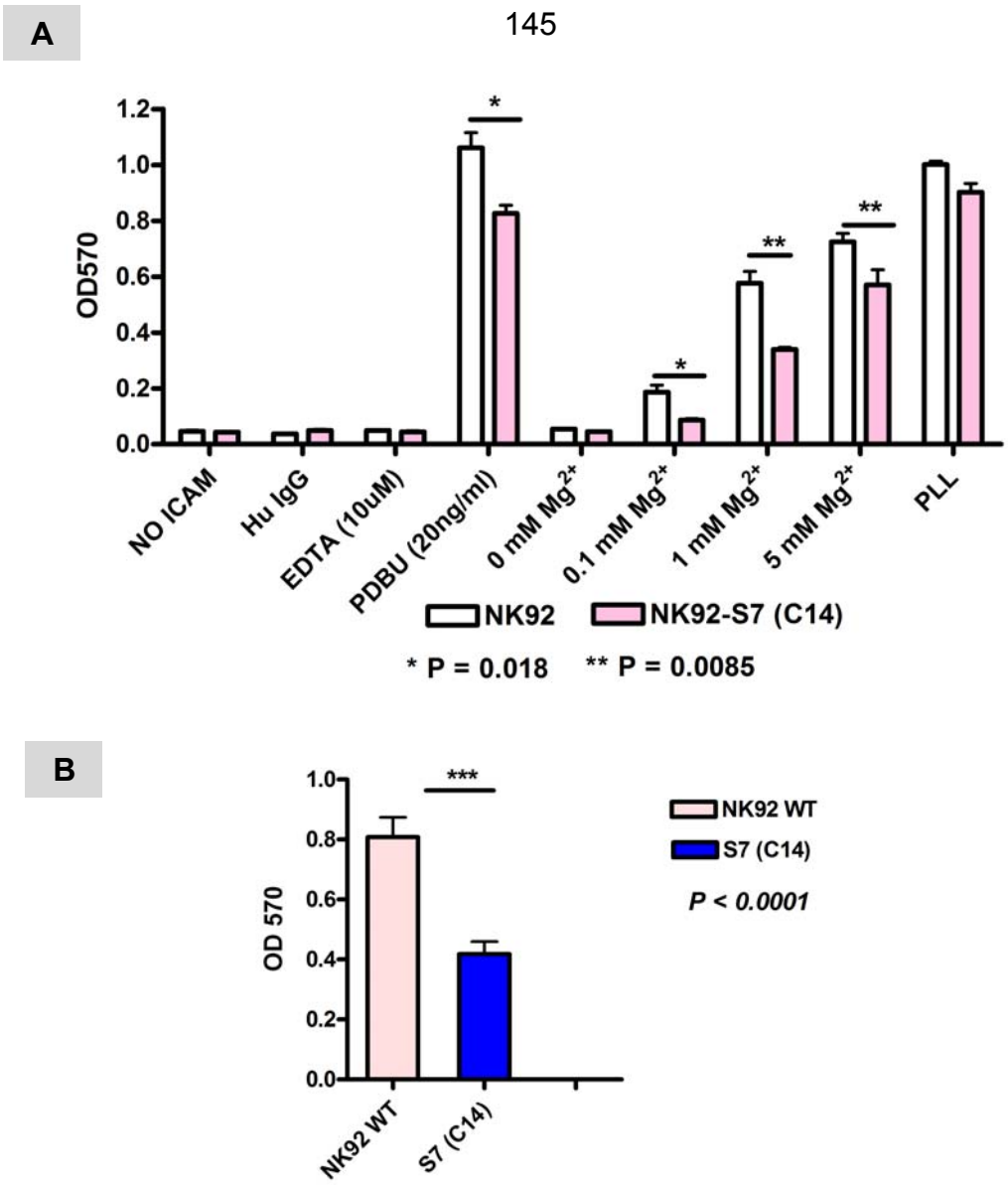

Figure 4.13: Siglec-7 reduces adhesion of NK92 cells to ICAM-1-Fc coated wells : (A) 96 well tissue culture plates were coated with 10 µg/ml of protein A or 0.01% of poly-L-Lysine (PLL), overnight. Plates were coated with 5 µg/ml of ICAM-Fc or human IgG in PBS. 2 x 10E5 NK92 WT or NK92 Siglec-7 (C14) were resuspended in 1XHBSS (-Ca^{2+}) with different concentrations of +Mg^{2+}. For control groups, cells were either treated with 10 µM of EDTA or 20 ng/ml of PDBU for 10 minutes on ice. Cells were added to wells, spun down and incubated for 30 minutes at 37^0C. Unbound cells were then removed from the plate by gravity wash and bound cells were fixed, stained and plates read at 570 nm. Cells added to PLL coated plate was used as control to obtain maximal binding of cells. (B) Adhesion of NK92 WT and Siglec-7 (C14) cells onto ICAM-1-Fc coated wells from 3 different experiments (conducted on 3 different days), in the presence of 1 mM Mg2+, is compared. Error bars represent standard error of mean.

4.5.2 Sialic acid independent adhesion of NK92 Siglec-7 cells to ICAM-1-Fc

The adhesion assays conducted (Figure 4.13) using wild type and Siglec-7 expressing NK92 cells suggests a negative regulatory role of this receptor in modulating LFA-1 mediated adhesion of the cells to ICAM-1-Fc coated on plates. In order to understand the role of sialic acid linkages present on ICAM-1-Fc in influencing the binding of Siglec-7, ICAM-1-Fc coated plates were treated either with or without sialidase (in acetate buffer). The conditions used for the treatment of the coated plates were optimized previously in this lab.

NK92 cells (+/- Siglec-7) were added to the sialidase treated plates, unbound cells removed and adhesion measured. In this assay, along with Siglec-7 expressing clone 14 (S7(C14)) that was used in the previous assay, another independent clone that had > 90% receptor expression was also used, clone A (CA).

At 1 mM concentration of Mg^{2+}, both Siglec-7 clones had significantly reduced adhesion to ICAM-1-Fc compared to wild type cells (Figure 4.14, A). Interestingly, this was not reversed following sialidase treatment of the LFA-1 ligand. The adhesion of wild type cells, was, however increased following sialidase treatment. This could be due to the removal of negatively charged sialic acids from the ligand, increasing adhesion of cells (Figure 4.14, B)

A sugar binding Siglec-7 mutant, R124A, was also used in these experiments to investigate the role of sialic acids recognition in this assay. The R124A mutation did not reverse the binding of the transfectants to that of wild type cells (Figure 4.14, A). The above data suggests that Siglec-7 is able to regulate LFA-1 mediated adhesion in the absence of sialylated ligands.

Two further experiments reconfirming the sialidase independent effect on the adhesion of wild type, Siglec-7 and R124A mutants was carried out using two

different ICAM-1-Fc preparations. Results obtained are similar to that shown in Figure 4.14 and is shown in appendix.

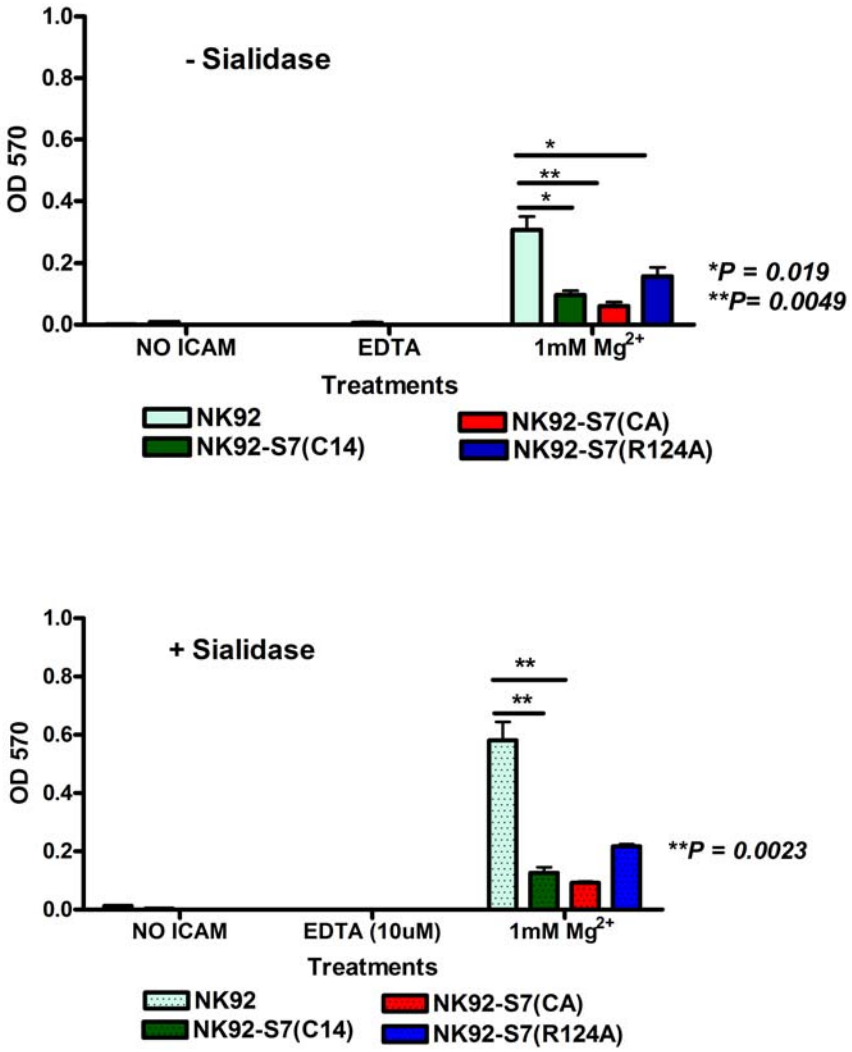

Figure 4.14: Sialic acid independent adhesion of NK92 WT or NK92 Siglec-7 (C14 and CA) cells to ICAM-1-Fc : Procedure was carried out as described in figure 4.13. ICAM-1-Fc coated plates were treated with 0.17 IU/ml of sialidase for 1 hour at 37 ^{0}C. Sialidase treatment was quenched using 10%FCS. Cells were then washed with RPMI with 10% FCS and resuspended in 1XHBSS (-Ca^{2+}, +Mg^{2+}). EDTA treated cells were used as negative control. NK92 cells expressing the mutant R124A were only plated in duplicates on the sialidase treated plate and hence level of significance was not analysed.

4.6 Siglec-7 modulates Src kinase phosphorylation following LFA-1 binding of ICAM-1-Fc

In NK cells, LFA-1 has been shown to affect activation of kinases and factors such as Vav-1 resulting in the actin cytoskeletal reorganization and polarization of perforin granules (Riteau et al., 2003; EM Mace et al., 2010).

In an attempt to study signalling pathways triggered in the NK92 cell line downstream of LFA-1, pan and phospho antibodies were used to examine the phosphorylation status of different down stream molecules in whole cell lysates.

4.6.1 Optimization of divalent cation concentration

As discussed earlier, divalent cations are needed to change conformations of integrins such as LFA-1 from a closed low affinity to an open high affinity state. Because different cations have varied effects on integrin conformations, divalent cation concentrations were optimized using wild type NK92 cells. Assay buffers containing either Mg^{2+} or Mn^{2+} were tested. Clone 54, ICAM-1-Fc fusion (+ α 2,6 sialic acid linkages) was used for all biochemistry assays. Cells resuspended in the assay buffer but not plated onto ICAM-1 were used as negative controls. Cells treated with pervanadate (PV), a protein tyrosine phosphatase inhibitor, were used as positive controls in these experiments (McMillan et al., 2013). Whole cell lysates were measured for protein concentration and used for western blotting. Blots were then analysed using pan and phospho antibodies for different downstream molecules. Figure 4.15 shows the phosphorylation status of some of the key molecules known to be important in LFA-1 mediated signalling in NK cells such as Src, Syk, Akt, Erk1/2 and p38 MAPK. A time dependent increase in phosphorylation was only seen in the case of pY416 Src and pS473 Akt. The phospho Src antibody recognizes

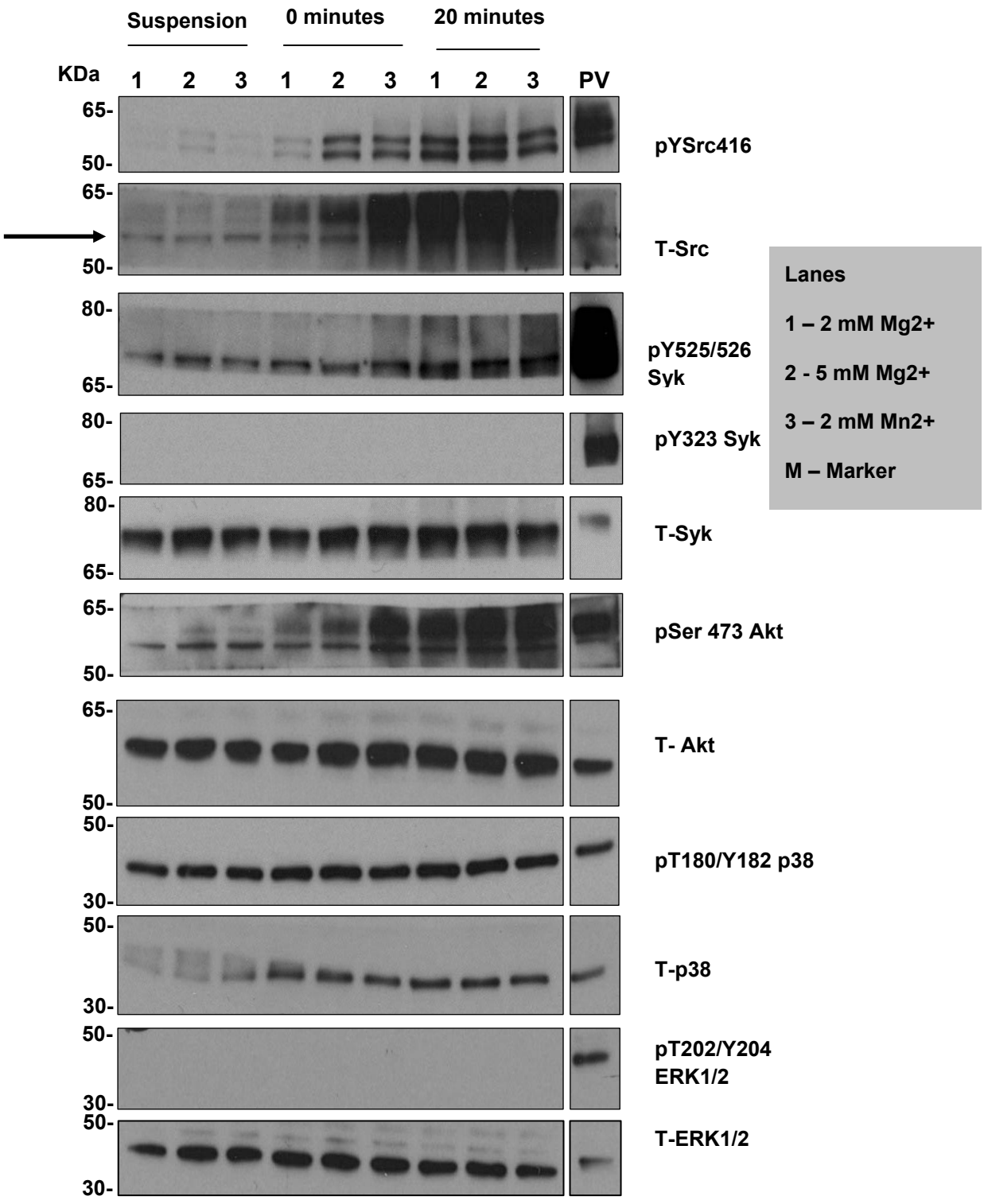

Figure 4.15: Optimizing divalent cation concentration for LFA-1 mediated activation of intracellular signalling molecules: 6 well tissue culture plates were coated with 10 µg/ml of Protein A, blocked with 5% BSA and then coated with 5 µg/ml of ICAM-1. Plates were again blocked with 10% FCS and stored in PBS at 4^0C. NK92 cells were harvested and incubated in complete media without IL-2 for 4 hours at 37^0C. Cells were then spun down, resuspended in 1xHBSS with different concentrations of Mn^{2+} or Mg^{2+}. Cells were added

to plates, spun down at 900 rpm for 30 seconds and incubated for 0 and 20 minutes. Both bound and unbound cells were then lysed in lysis buffer, lysate cleared by centrifµgation and 15 µg ran on 4-12% bis-tris SDS PAGE gel. Gels were then transferred to nitrocellulose membrane , blots blocked and stained with rabbit or mouse primary antibodies with overnight incubation. Following washes in TBST, blots were incubated in sheep anti-rabbit-HRP antibodies. Blots were washed and developed using ECL chemiluniscent substrate. T=Total; p = Phospho; PV – Pervanadate

phosphorylated Src and cross reacts with other members of the Src family such as Lck, Lyn, Fyn, Yes, Hck when phosphorylated at tyrosine 416. Src phosphorylation at Tyr 416 and Akt at Ser 473 showed minimal basal levels of phosphorylation both in suspension and at the 0 minute time point. This then increased by 20 minutes in both cases. There was no phosphorylation observed for pY323 on Syk and pT202/Y204 on Erk1/2. Syk tryrosine 525/526 and pT180/Y182 p38 MAPK showed very minimal increase in phosphorylation in an integrin dependent manner over the time course.

4.6.2 Role of Siglec-7 in modulating LFA-1 mediated signalling via Src kinase in NK92 cells

2x10E6 wild type and Siglec-7 expressing NK92 cells (clone 14) were resuspended in assay buffer and plated onto wells coated with ICAM-1-Fc (clone 54). A time course experiment was carried at 0, 5 and 20 minutes. Wells coated with no ICAM-1-Fc was used as negative control (for 20 minutes). Western blotting was conducted using whole cell lysates. Figure 4.16 (A and B) shows whole cell lysates probed for pY416 Src from two different experiments. Since the total Src antibody gave multiple bands (Figure 4.15), GAPDH was used in these experiments to probe for total amount of protein in each of the whole cell lysates. Cells treated with PP2, a Src kinase inhibitor, were used as

negative control in these experiments. Suspension cells and cells treated with PP2, showed low levels of pY416-Src phosphorylation (Figure 4.16,A). Panel A and B represents two independent experiments showing an increase in pY416-Src phosphorylation in wild type NK92 cells which was reduced by 2 fold in Siglec-7 expressing NK92 cells by 20 minutes.

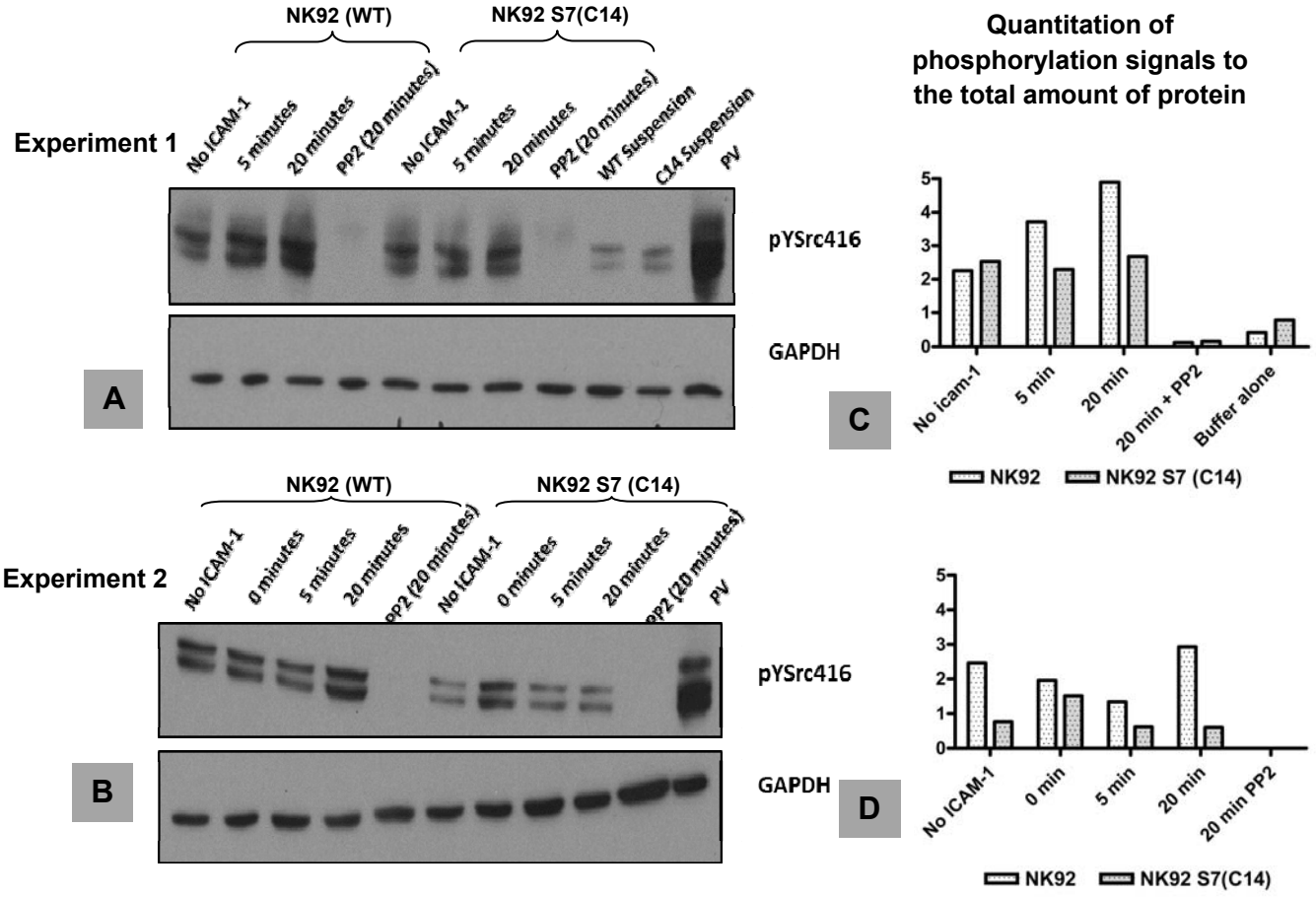

Figure 4.16: Siglec-7 negatively modulates LFA-1 mediated Src kinase signaling in NK92 cells: (A) and (B) are results from two experiments comparing LFA-1 mediated Src kinase phosphorylation between wild type NK92 and Siglec-7 expressing NK92 (C14) cells. Whole cell lysates were blotted for pYSrc416 and GAPDH. Experiments were conducted as described in figure 4.15. Cells treated with PP2, a Src kinase inhibitor, were used as the negative control while PV treated cells served as the positive control. (C) and (D) Bar charts represent densitometry of Src phosphorylation signals from each experiment shown in (A) and (B). PV – Pervanadate

Although a time dependent increase in phosphorylation of Src is seen in panel A, this is less evident in panel B. Figure 4.16, C and D represents densitometry conducted on the signals obtained and is represented as the ratio intensity of phosphorylation of Src to total protein as measured by GAPDH.

Data on pSer473Akt from one experiment also showed an increase in the phosphorylation levels in wild type NK92 cells, devoid of Siglec-7 (figure shown in Appendix, figure A5). However, in a repeat experiment conducted, there was no difference between the two cell types.

4.7 Role of Siglec-7 in modulating integrin mediated polarization of perforin in NK92 cells

Another functional readout for LFA-1 is the polarization of perforin granules (March et al., 2011). ICAM-1-Fc coated to Protein A beads was used for this purpose. The coating of ICAM-1-Fc to the beads was optimized by flow cytometry staining using anti-ICAM-1 antibodies as shown in figure 4.17.

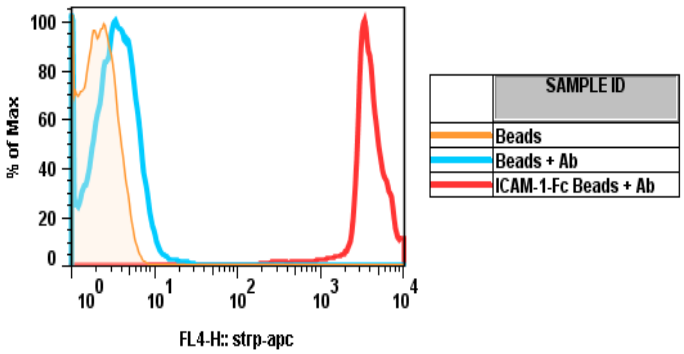

Figure 4.17: Coating of Protein A beads with ICAM-1-Fc: Protein A beads were sonicated for 6 cycles, each cycle lasting 30 seconds. 1x10E6 beads were then pipetted out and washed in 200 µl of 1XPBS (twice). Beads were then incubated with or without 5 ug of ICAM-1-Fc protein (clone 54), on a spin rotor at 4^0C for 30 minutes. Unbound protein was washed off in PBS. Beads were then blocked with 10% mouse serum for 30 minutes on ice and then stained with 0.5 µg of anti-ICAM-1 antibody (30 minutes on ice) followed by 1/500 dilution of streptavidin-APC. The beads were then analysed by flow cytometry.

NK92 wild type (WT) cells and NK92 Siglec-7 expressing clone (C14) were incubated with ICAM-1-Fc coated beads, stained for perforin and examined by confocal microscopy as shown in figure 4.18, A. Protein A beads coated with human IgG and cells treated with PP2 inhibitor were used as negative controls in the experiment.

For distinguishing polarized cells from unpolarized cells, each cell in contact with a bead was arbitrarily divided in half. If the cell had perforin staining localized in that half of the cell which was in contact with the bead, it was considered to be polarized (Figure 4.18, A). Based on this classification, z-stack images (100x magnification and zoom 1) from all samples were analysed using the image analysis software, Volocity. Figure 4.18 B, are representative images from the different samples. White arrows point to polarized cells while red arrows point to non-polarized cells. Fisher's exact test, comparing WT cells to the remaining treatment groups (Figure 4.18, C) shows that the proportion of polarized cells to non-polarized cells in the WT sample group is significantly higher compared to PP2 treated or the NK92 Siglec-7(C14) cells. Figure 4.18, D, represents the percentage of polarized conjugates in the different groups.

A

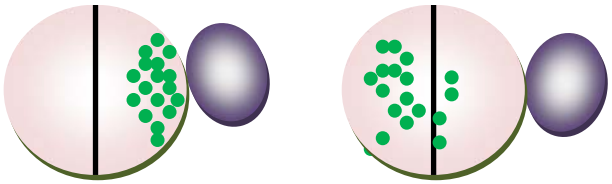

B

WT + ICAM-1 BEADS

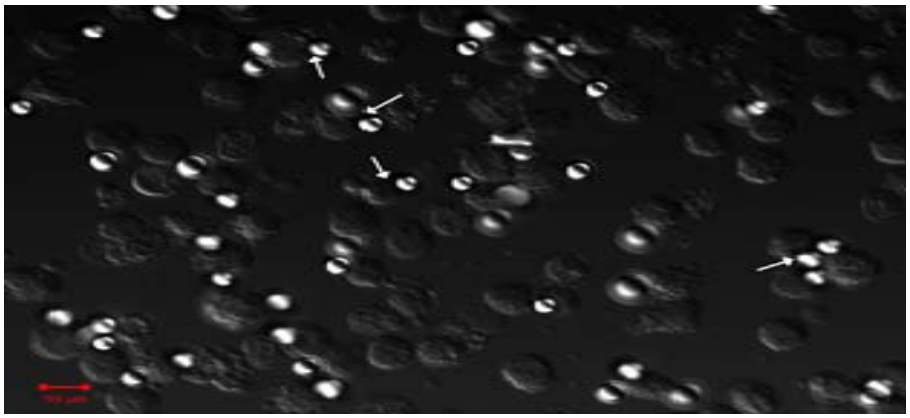

MERGE

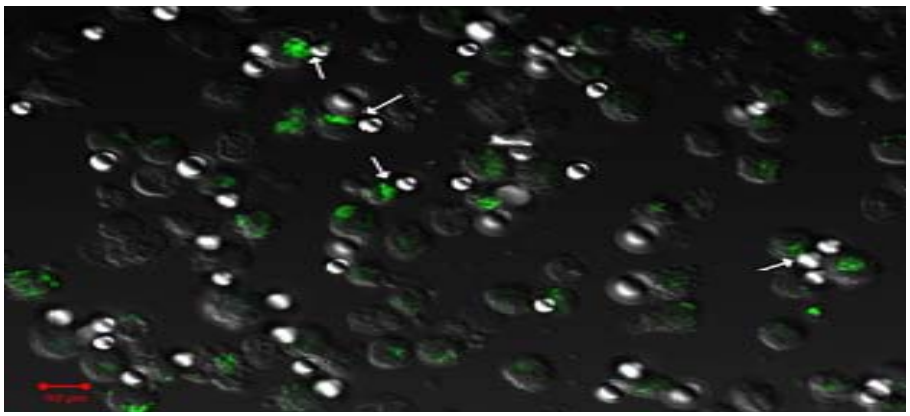

S7(C14) + ICAM-1 BEADS

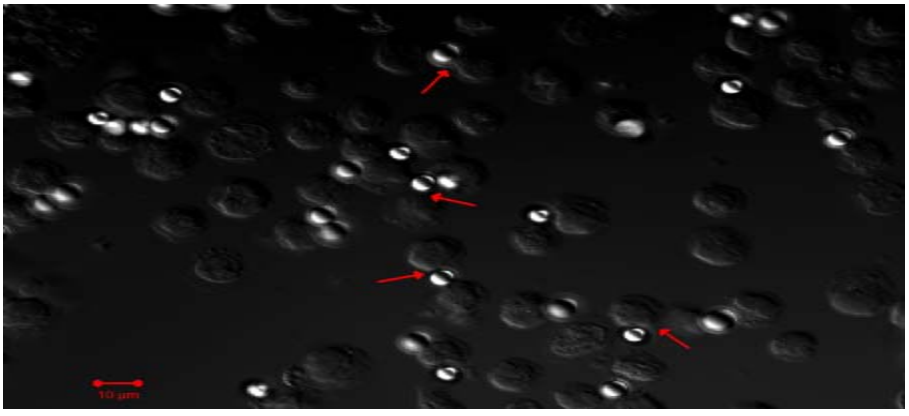

MERGE

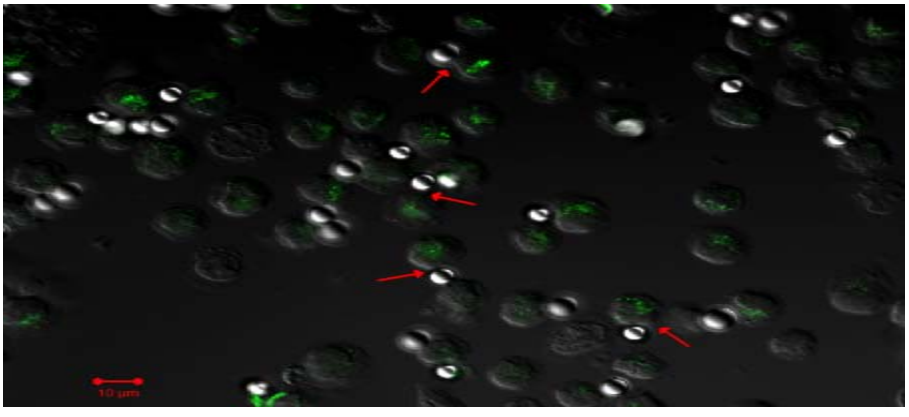

WT + ISOTYPE CONTROL

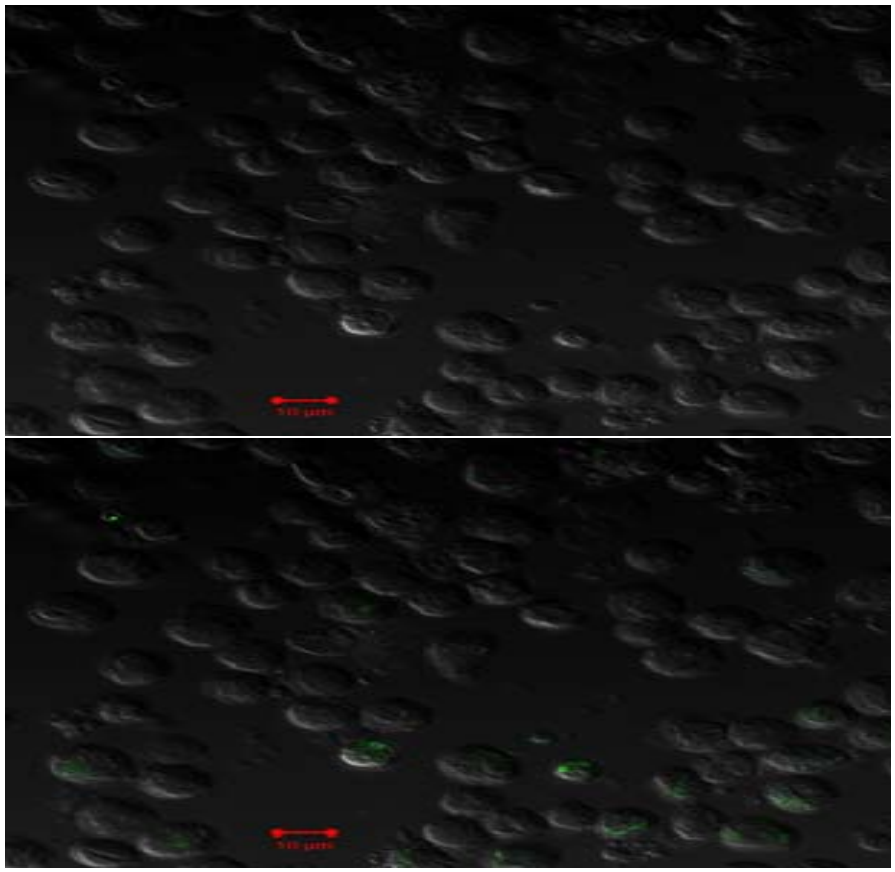

MERGE

S7(C14) + ICAM-1 BEADS + PP2

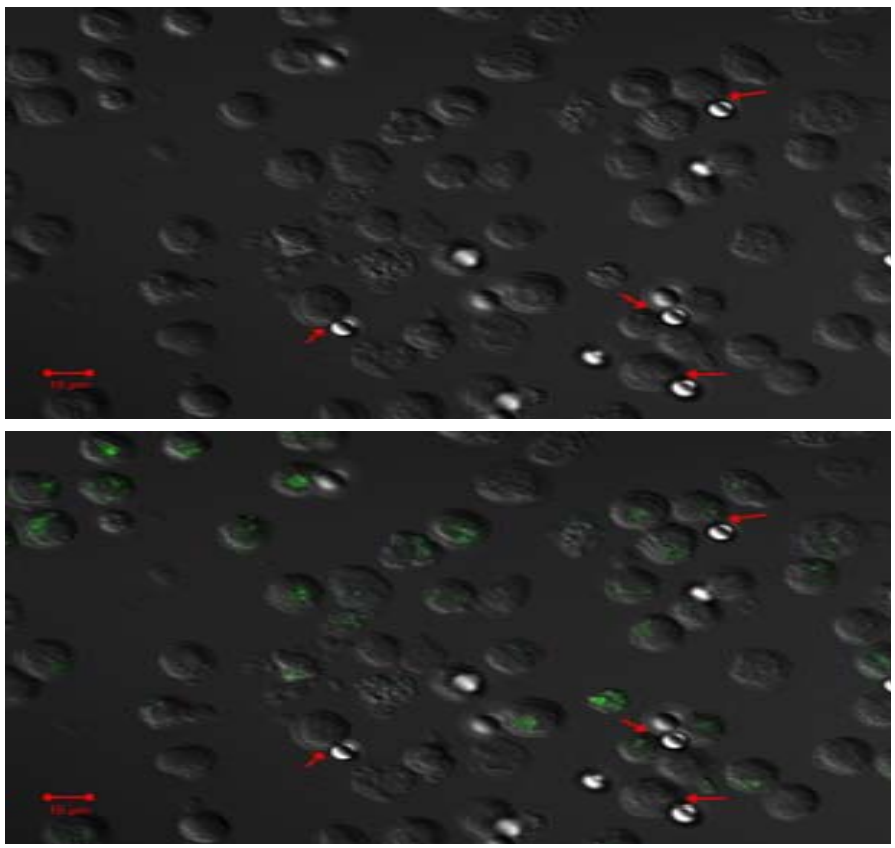

MERGE

C

	Polarized cells	Non-polarized cells	Fisher's test (P value)
WT	91	74	
WT + PP2	21	44	0.0021
S7 (C14)	40	83	0.0002
S7 (C14) + PP1	19	29	0.0121

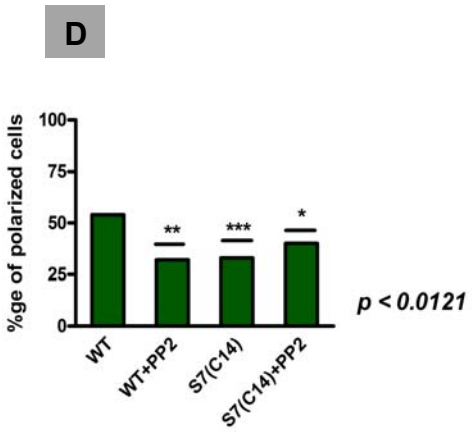

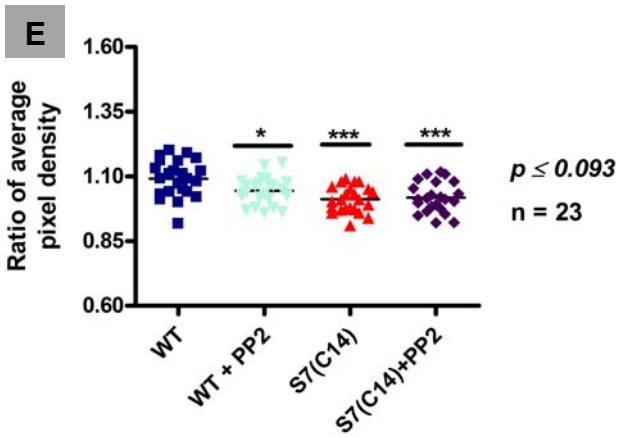

Figure 4.18: Siglec-7 expression on NK92 cells negatively affects LFA-1 mediated perforin polarization – (A) Schematic diagram of bead : cell conjugate, with polarized (*above*) and non-polarized (*below*) perforin granules. (B) Protein A beads were conjugated with ICAM-1-Fc as described in figure 4.18. 0.5 X 10E6 WT and Siglec-7 expressing clone (C14) were treated with or without PP2 inhibitor. The cells were resuspended in 1X HBSS and plated onto poly-L-Lysine coated 18mm coverslips and left to settle for 1 hour at 37^{0}C. Buffer on the cells were replaced with 1 X 10E6 beads coated with either ICAM-1-Fc or human IgG and resuspended in 5 mM Mg^{2+}, were added on to the cells and left to incubate for 1 hour at 37^{0}C. Coverslips were washed in PBS + 1% BSA, fixed with 4% paraformaldehyde for 15 minutes at room temperature (RT) and permeabilized with PBS + 0.1% triton for 15 minutes at RT. Cells were then blocked with 10% mouse serum for 30 minutes at RT and incubated with 20 µg/ml of anti-perforin (FITC conjugated) in block buffer, overnight at 4^{0}C. Coverslips were washed and mounted using Vectashield (with DAPI). Images were acquired using the LSM 700, X100 magnification and zoom 1. For z-stacks, slices of 1 µm thickness were collected for each image. White arrows – polarized cells; Red arrows – non-polarized cells. (C) Table 4.3 -

showing the number of polarized and non-polarized conjugates in each sample group and statistical analysis using the Fisher's exact test. (D) Bar chart representing the percentage of polarized conjugates formed in each sample group (E) Mean intensity of perforin in the polarized half of the bead : cell conjugates were normalized to the mean intensity of staining in the whole cell. N represents the number of bead : cell conjugates examined for this analysis. Experiment represents n=1.

Further analysis was also carried out comparing the perforin staining intensities of the cells conjugated to beads in the different groups. For this purpose, mean intensity value of perforin staining in the polarized half of the cell was normalized to the mean intensity value in the whole of the cell. Normalized ratios for the different groups are shown in figure 4.18, E. The intensity measurement also shows a significant decrease in intensity in the PP2 treated cells and the C14 cells compared to the WT cells. Taken together, these data suggests a role for Siglec-7 in negatively regulating LFA-1 mediated perforin polarization in NK92 cells.

The isotype control for the anti-perforin antibody used gave high background (data not shown). This could be either because the dynamic range of the anti-perforin antibody is small or could be the result of high autofluoresence. Hence further optimization using another fluorescent conjugated antibody which will give an improved signal to noise ratio will be needed.

4.8 Discussion

This part of the project was based on the recent findings from our lab that highly related murine Siglec-E could modulate β_2 integrin signalling in neutrophils. Therefore the main aim was to investigate whether Siglec-7 shared similar functions in regulating integrin functions in NK cells. Indeed the data presented here shows a role for Siglec-7 in modulating integrin signalling and functions.

Since the ICAM-1-Fc chimeras, used as LFA-1 ligands, were generated in wild type CHO cells, a predominantly α-2,3 sialylation of the expressed recombinant protein was expected. In order to bias the linkages on the glycosylated ICAM-1-Fc to NeuAc α-2,6 βGal1, CHO cells were transfected with plasmid DNA for the sialyltransferase, ST6Gal1. Overexpressed ST6Gal1 in these cells would be expected to compete with the endogenous ST3Gal1 and bias the sialic acid linkages on the expressed protein.

In characterization of the ICAM-1-Fc protein, ELISAs conducted on the ICAM-1-Fc chimera's (Figure 4.4) showed that while supernatant from clone 17 (transfected with only ICAM-1-Fc) was negative for SNA binding, supernatants from clones 54 and 58 (transfected with ICAM-1-Fc and ST6Gal1) bound SNA. However, the lectin based ELISA is only qualitative and hence does not confirm the absence of α-2,3 linkages on the clones 54 and 58. Further invitro assays using purified sialyltransferase ST6Gal1 would be needed to quantitatively assess the α-2, 6 linkages on these chimeras. The lectin MAL I is known for its specificity for NeuAc α-2,3 Galβ 1,4 GlcNAc linkages (Knibbs et al., 1991). Binding of this lectin to RBCs in a sialic acid dependent manner using a flow cytometry based assay confirmed that the lectin was functional (data not shown). However, it failed to recognize the ICAM-1-Fc chimeras on ELISA

based assays (data not shown). This could be due to unfavourable ligand density or presentation on polystyrene ELISA plates, for MAL I recognition.

Dot blots carried out to determine recognition of these chimeras by Siglec-7-Fc precomplexes showed an increased avidity of this lectin precomplex for both clones 17 and 54 of ICAM-1-Fc (Figure 4.8, A). This fits well with the known fact that Siglec-7 can weakly bind sialic acids that are present not only in α-2,6 but also α-2,3 glycosidic linkages (McMillan and Crocker, 2008). However, the binding to the clone 54 was 1.5 - 2.3 fold higher compared to clone 17. Although sialidase treatment reduced the recognition of Siglec-7-Fc, it was not completely abolished suggesting the ability of the receptor to bind ligands independent of sialic acids.

The lectin SNA bound clone 54 on dot blots in a sialic acid dependent manner, but it also bound clone 17 (Figure 4.8, E). This finding is interesting and is contradictory to the ELISA data. A possible explanation for this could be high ligand density and assay format, favouring lectin recognition of sialic acids in α-2,3 linkages when spotted onto nitrocellulose membrane. However the signal intensity was independent of ligand concentration which could also indicate possible non-specific binding by the pre-complexes.

In the case of the antibody however, following sialidase treatment, there was some reduction in binding to the ICAM-1-Fc clones (Figure 4.8, D). This could be either from loss of protein or underlying linkages needed for antibody recognition. Therefore, these experiments would need to be optimized further to make firm conclusions on Siglec-7 recognition of the ICAM-1-Fc clones, in a sialic acid dependent manner.

NK92, an NK cell line was used in this project as a model system to investigate the role of Siglec-7 in modulating integrin functions by the two models proposed

in figure 4.1 B. This cell line lacks the expression of Siglec-7 as shown by antibody staining (Figure 4.9) and mRNA expression levels (Figures 4.10). Therefore Siglec-7 and its mutants were over-expressed in this cell line (Figure 4.11). LFA-1 expression levels remained unaffected in both the wild type and transfectant cells (4.11, C).

Adhesion assays carried out using wild type and Siglec-7 expressing NK92 cells on ICAM-1-Fc coated plates demonstrated the possible regulatory role of Siglec-7 in modulating outside-in signalling of integrins. At all concentrations of Mg^{2+}, there was a significant difference in adhesion between wild type NK92 cells and Siglec-7 transfectants, S7(C14)(Figure 4.13). The role of divalent cations in strengthening outside in signalling of integrins has been extensively studied with respect to T cells (Labadia et al., 1998) (Cabanas and Hogg, 1993) (Dransfieldet al., 1992). Mg2+ has been shown to bind the extracellular domain of LFA-1, change its confirmation to high affinity, upregulate expression of the m24 antibody epitope on LFA-1 and increase adhesion of T cells to immobilized ICAM-1 (Porter et al., 2002). Outside-in signalling leads to clustering of LFA-1 and cytoskeletal rearrangements via proteins such as Talin that are associated with it (Smith et al., 2005) (Cairo, Mirchev and Golan, 2006) (Bakker et al., 2012). In NK cells, Siglec-7 could be modulating LFA-1 by regulating either the conversion of inactive LFA-1 into the high affinity confirmation induced by Mg^{2+} or affecting other events downstream of outside-in signalling such as LFA-1 clustering. Further experiments such as antibody staining of the high affinity confirmation state of LFA-1, use of inhibitors to cytoskeletal rearrangement such as Cytochalasin D and blocking antibodies to LFA-1 would be needed to clearly identify the mechanism involved.

Interestingly both sialidase treatment of the ICAM-1-Fc and sugar binding mutant (R124A) were not able to reverse the Siglec-7 inhibition of adhesion (Figure 4.14). It is therefore tempting to consider a sialic acid independent binding of Siglec-7 to the glycosylated ICAM-1. These results are contrary to the known requirement of sialic acid in ligand recognition by Siglec-7. However due to time constraints these experiments could not be repeated. Confirming effective sialidase treatment of ICAM-1-Fc coated onto the wells would require a positive control such as the sialidase-sensitive Siglec-7 RBC adhesion assay or direct biochemical analysis of the ICAM-1-Fc protein. The data obtained to date, however, would support model B (Figure 4.1 B) wherein a constitutive association of Siglec-7 with β2 integrins is hypothesized, which could negatively regulate integrin activation and signalling independently of sialic acid-dependent binding. This could occur through co-localization of Siglec-7 with activated LFA-1 into so called 'lipid rafts' on NK cells.

"Outside-in" integrin signalling results in the strengthening of integrin mediated adhesion by bringing about cytoskeletal changes and assembly of a number of signalling molecules to the point of adhesion (Totani et al., 2006, Hogg et al., 2011). In an attempt to define LFA-1 mediated downstream signalling events that could be affected by Siglec-7, a biochemical approach was adopted. LFA-1 on NK92 cells were stimulated via "outside-in" signalling using ICAM-1-Fc coated onto plates. Using western blotting of whole cell lysates of wild type NK92 cells bound to the ICAM-1-Fc plates, time dependent increase in phosphorylation of Src kinase, Syk, Akt, p38 MAPK and Erk1/2 MAPK was examined.

Binding of ICAM-1-Fc to NK cells triggered activation of only Src kinases and Akt in a time dependent manner (Figure 4.15). No time dependent integrin mediated activation of Syk, p38, MAPK and ERK1/2 MAPK was observed.

Src-family protein tyrosine kinases (SFK) consists of nine structurally related nonreceptor tyrosine kinases with ubiquitous cell expression – B cells (Blk, Fgr, Lyn), T cells (Lck), NK cells (Lck), Myeloid cells (Fgr, Hck,Lyn), ubiquitous (Fyn, Src, Yes, Yrk) (Parsons and Parsons., 2004). Figure 4.19, A, represents the domain structure common to members of this family. SFKs like many other receptor tyrosine kinases (RTKs) are in a state of auto-inhibtion with the SH2 domain interacting with a phosphorylated tyrosine residue of the kinase region and the SH3 domain interacting with the linker region (Blume-Jensen and Hunter., 2001). Ligand binding to the SH2 or the SH3 domains or the dephosphorylation of the C-terminal tyrosine (by CD45 or SHP-2) releases these kinases from its inhibitory state. This results in the auto-phosphorylation of a key tyrosine residue in the activation loop of its kinase domain leading to a highly active enzymatic state (Figure 4.19) (Ingley., 2012). The main role of this family of kinases is the regulation of cell signalling of membrane receptors. Hence they have been implicated in numerous fundamental cellular processes such as growth, survival, migration etc. Many detailed reviews of this family of kinases with regards to their roles in B-cells and T-cells can be found – Lowell., 2011, Gauld and Cambier., 2004, Palacios and Weiss., 2004.

In NK cells, Src kinase activation is one of the proximal steps in both integrin mediated signalling as well as signalling mediated by other activation receptors (Mocsai et al., 2002)(Totani et al., 2006). The SFK are responsible for the phosphorylation of various downstream kinases and adaptor molecules (Vivier, Nunes and Vely, 2004). The use of specific pharmacological inhibitors such as

PP1 demonstrated the importance of Src kinases in the early activation of Vav-1 following LFA-1 recognition of ICAM-1 expressed on insect target cells (Riteau, Barber and Long., 2003). Src kinases such as Fyn and Lck, have been clearly implicated in activation of several downstream signalling molecules, NK natural cytotoxicity as well as ADCC mediated by activating receptors (Augugliaro P et al., 2003)(Cone et al., 1993), (Pignata et al., 1993) (Adrian T Ting et al., 1995)(Claudia CS Chini et al., 2000). Ligand induced phosphorylation of CRACC (CD2-like receptor-activating cytotoxic cell), an NK activating receptor, by the adaptor EAT-2 has been shown to be negatively affected by pharmocological inhibitors, such as PP2 (Tassi and Colonna., 2005).

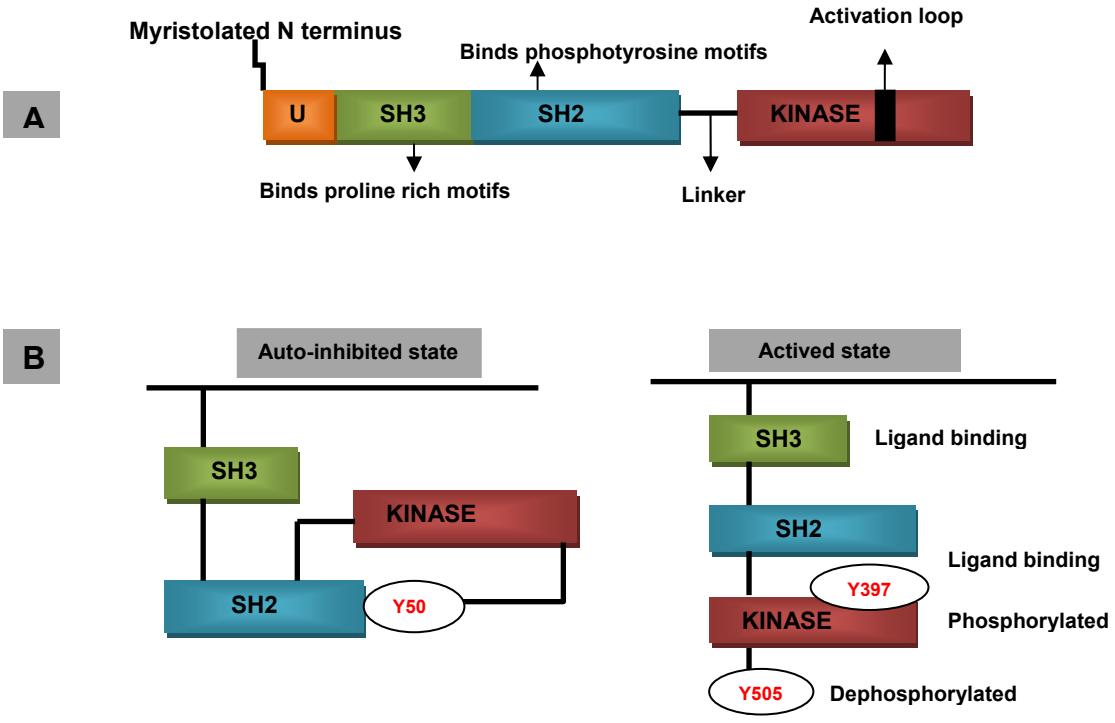

Figure 4.19: (A) Diagrammatic representation of the modular structure common to the members of the Src-protein family kinases (SFKs). (B) Auto-inhibited and active confirmations of SFK. Tyrosine sites shown with respect to Lyn (adapted from Steve Martin., 2001).

Although there is no direct evidence on the nature of the SFK member present in the NK92 cell line, there are reports where blocking these tyrosine kinases by using inhibitors like PP2 affects cytoxicity and downstream signalling (Ruckrich and Steinle., 2013) (Choi and Mitchison., 2013)(Bambard et al., 2009). Recently the phosphorylation of the hemi-ITAM of the NK activating receptor NKp80 was found to be affected by blocking Src kinases using PP2, in the NK92 cell line (Ruckrich and Steinle., 2013).

Syk kinase plays an important role in integrin signalling in neutrophils, and macrophages via ITAM containing adaptors DAP12 and FcRγ (Mocsai, Ruland and Tybulewicz, 2010). Using primary NK cells and immunoprecipitation studies with relevant antibodies one report demonstrated that LFA-1 signalling in human NK cells activates TCR-ζ, Syk kinase and PLC-γ, induced granule polarization and cause accumulation of the microtubule organization centre (MTOC) at the target effector immunological centre (March and Long, 2011).

In the experiments conducted here using NK92 cells, there was no phosphorylation of Syk at Y323 observed and while phosphorylation of pY525/526 Syk was present, there was only a minimal increase over time (Figure 4.15). The absence of pY323 Syk was unexpected since this residue is the equivalent of the mouse Y317 Syk that has been shown to be activated by CD11b binding of fibrinogen in mouse neutrophils (McMillan et al., 2013). The phosphorylation observed at Y525/526 could be basal as there was only minimal over time. So, it is possible that in this cell line, signalling via LFA-1 could either involve phosphorylation of another tyrosine site on Syk or bypass Syk kinase completely.

p38 MAPK is activated in an integrin dependent manner in different cell types such as primary NK cells and neutrophils (Mocsai et al., 2002) (Mainiero et al., 2000). Here, the NK92 cells showed a constitutively high basal level of phosphorylation of p38 (Figure 4.15). There was no increase in phosphorylation over time. One explanation for the high basal phosphorylation status of p38 could be the IL-2 mediated signalling in this cell line. However, IL-2 has been shown not to activate p38 in primary human NK cells (Yu et al., 2000). Moreover the NK92 cells used in these assays were cultured in IL-2 cytokine but were rested for four hours prior to plating out on ICAM-1 coated plates.

The absence of phosphorylation of ERK1/2 (as examined using 2 different antibodies) following integrin engagement in these experiments was also unexpected. Zhen et al., 2009 demonstrated that blocking of NK92 adhesion to target K562 cells by using anti-CD11a antibodies, greatly reduced Erk1/2 phosphorylation at Thr202/Tyr204 (Zhenget al., 2009).

Our lab has demonstrated a negative role for Siglec-E in outside-in signalling, leading to Src kinase dependent Syk kinase activation. This increase in phosphorylation of Syk kinase (Y317) and p38 MAPK when Siglec-E knock-out mouse bone marrow cells were plated onto CD11b ligand, fibrinogen, was sialic acid dependent suggesting that Siglec-E recognition of sialic acids present on fibrinogen negatively regulated CD11b signalling (McMillan et al., 2013).

Here, comparing integrin mediated Src kinase phosphorylation between wild type NK92 cells and NK92 expressing Siglec-7, a 2-fold reduction in the signal intensity was observed at the 5 and 20 minute time points (Figure 4.16). The Src inhibitor PP2 completely abolished LFA-1 mediated activation of Src kinase

in both cell types. These results suggest that Siglec-7 is capable of negatively regulating the recruitment and/or activation of Src kinases and thereby dampen LFA-1 signalling following ICAM-1 recognition.

In one experiment, there was a significant reduction in phosphorylation of Akt Serine473 in Siglec-7 transfectants at 5 and 20 minute time points (Figure A5, Appendix). But this was not observed in a repeat experiment. This could be due to experimental factors and possibly protein degradation. Akt has been linked to Syk via a Syk-P13K-Rac1 pathway in IL-2 activated NK92 cells. The authors utilized both kinase assays as well biochemical validation of the relevant Akt phosphorylation sites in NK92 cells and NK92 transfected with kinase deficient Syk (Jian et al., 2003).

LFA-1 has been shown to affect perforin polarization in NK cells when in contact with targets expressing ICAM-1 (March and Long., 2011). Here, using ICAM-Fc coated beads, Siglec-7 was shown to inhibit LFA-1 mediated perforin polarization in NK92 cells (Figure 4.18). These results parallel studies which show that inhibitory receptors (CD94-NKG2A and LLT1) are capable of blocking LFA-1/ICAM-1 induced perforin polarization in primary human NK cells (Das and Long., 2010).

Recombinant ICAM-1-Fc (clone 54) used in the biochemical and perforin polarization assays was co-expressed with ST6GalI in order to favour N-linked glycosylation terminating with α-2,6 rather than α-2,3 sialic acid linkages, the former being preferred by Siglec-7. This chimera therefore serves as a ligand for LFA-1 and a potential counter receptor for Siglec-7. However data from dot blot assays (Figure 4.8) and adhesion assays (Figure 4.14) are suggestive of sialic acid independent recognition of ligands by Siglec-7

Recently, Siglec-G, an inhibitory receptor of macrophages, was shown to negatively regulate RIG-I dependent induction of type 1 IFN in response to RNA viral infection. This was however independent of sialic acid binding. Expression of Siglec-G allowed recruitment of SHP-2, RIG-1 and the ubiquitin ligase, Cbl. This promoted the ubiquitination of RIG-I and therefore degradation (Chen et al., 2013).

Collectively, the data shown here imply a strong role for the inhibitory receptor, Siglec-7, in regulating LFA-1 functions in NK cells. One possibility is that Siglec-7 is able to modulate LFA-1 receptor functions by means of constitutive cis-association with LFA-1 in microdomains, as shown in model B (Figure 4.1 B). Based on the results obtained, a proposed model of Sigec-7 regulation of LFA-1, in a sialic acid independent manner, is shown in figure 4.20.

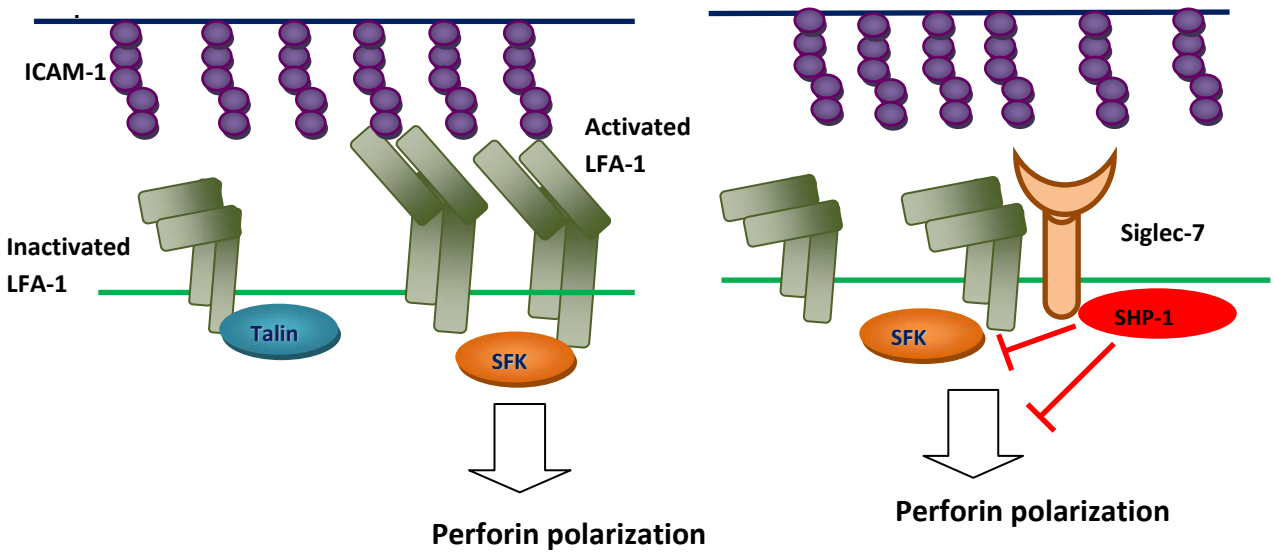

Figure 4.20: Siglec-7 modulates LFA-1 signalling, in a sialic acid independent manner: (A) Outside-in signalling of LFA-1 results in receptor clustering, recruitment of kinases such as Src and polarization of perforin in NK cells. (B) *Cis*-interactions between LFA-1 and Siglec-7 results in inhibition of these LFA-1 mediated events, possibly by the recruitment of SHP-1.

Siglec-5 and Siglec-E, have been shown to signal independent of their ITIM motif's and are weakly associated with SHP-1 (Avril et al., 2005; McMillan et al., 2013). Therefore experiments examining the recruitment of or constitutive association of SHP-1 phosphatase with the ITIMs of Siglec-7 in these cells would also be needed to determine the exact mechanism by which Siglec-7 is able to modulate LFA-1. Also, a definitive role of sialic acid recognition in these assays has not been established. Further experiments using ICAM-1-Fc lacking in α-2,6 sialylation (clone 17) to investigate *trans* sialic acid interactions of Siglec-7 would be needed. The use of targets expressing ligands for LFA-1 would also strengthen the data obtained here. Towards this goal, genetically modified B16 mouse melanoma cells expressing human ICAM-1 could be used.

Chapter 5

Evaluating Siglec-7 functions in regulating NK cell cytotoxicity

5.1 Introduction

NK effector functions are tightly regulated by many activatory, inhibitory and co-stimulatory receptors (E.O.Long et al., 2013). They recognize targets by a complex system of numerous, but well integrated receptor-ligand interactions. To evaluate the role of individual NK cell receptors, a standard approach adopted is the expression of its ligands on defined target cells or overexpression of the receptor on NK cell lines. Xenogenic species are sometimes better suited as targets because of the mismatch in KIR-MHC recognition, which removes inhibitory signals that could be triggered upon target cell recognition. A good example of a well established xenogeneic target used in the study of many of the NK receptors, especially LFA-1, is the Drosophila Schneider 2 (SC2) cell line (Barber et al., 2004. Cyril Fauriat., 2009; Schleinitz et al., 2008).

Siglec-7 has been shown to be in a “masked” state at the cell surface by interacting with the numerous sialylated glycans in *cis* (Avril et al., 2006). These *cis*-interactions between sialylated glycoproteins/glycolipids and Siglec-7 are thought to be important in the maintaining the receptor in quiescent state. Sialidase treatment of cells removes the sialic acids from the cell surface thereby “unmasking” Siglec-7. This helps promote *trans* interaction between Siglec-7 on NK cells and sialic acid ligands expressed on target cells to increase the potency of siglec-dependent inhibitory functions (Nicoll et al., 2003). Figure 5.1 is a schematic representation of this process.

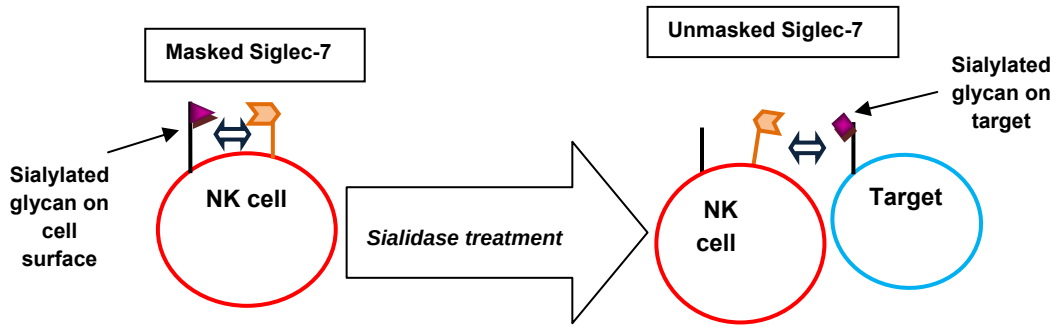

Figure 5.1: *Cis* and *trans* interactions of Siglec-7: Siglec-7 expressed on NK cells are masked by *cis*-interactions between numerous sialic acid containing counter-receptors on the cell surface. On sialidase treatment, these *cis*-interactions are lost and the receptor is free to mediate *trans* interactions with targets expressing sialylated ligands. This is known as the unmasking of the receptor.

Nicoll et al transfected the P815 mouse mastocytoma cell line with GD3S and used the GD3 expressing cells as a model to demonstrate the inhibitory role of Siglec-7. IL-2 activated PBMC were either sialidase treated or not treated and used in cytotoxicity assays against P815 GD3 targets. They were able to show that the P815 target cells became more sensitive to killing by NK cells when the effectors were treated with sialidase (Nicoll et al., 2003). An interesting finding from these experiments was that in the absence of sialidase treatment of PBMCs, P815 GD3 cells were more sensitive to cytotoxicity than P815 wild type cells. This phenomenon was explained by the possible presence of an activating receptor on NK cells that recognize GD3 as a ligand.

For this project however the B16 (78) cell line was chosen as a model system. The initial aim was to reconfirm the inhibitory role of Siglec-7 using B16 (78) cells as targets and then investigate the effect of overexpressing gangliosides GD3 and GM1 on killing susceptibility as discussed in Chapter 3.

Aims:

Although the initial goal of this project was to assess the biological significance of ganglioside complexes in modulating Siglec-7-dependent NK cytotoxicity, results from chapter 3 showed that over-expression of GD3 and GM1 in the B16 (78) cell line did not lead to efficient formation of ganglioside complexes. Hence measuring modulation of NK cell function in this context was not considered a worthwhile aim.

Instead, it was decided to investigate the role of Siglec-7 in regulating NK cell biology as follows:

1. Role of GD3 in modulating Siglec-7 recognition – This was studied using IL-2 activated PBMCs and a genetically modified NK cell line.

2. Regulating integrin functions - Data shown in chapter 4 are strongly suggestive of a role of this inhibitory receptor in affecting integrin mediated adhesion and polarization of perforin granules. A biological outcome of this finding was then investigated and preliminary experiments by means of cytotoxicity assays carried out on targets expressing ICAM-1.

5.2 Role of Siglec-7 in regulating effector functions of CD56+ primary NK cells via GD3 expression on target cells

PBMC isolated by ficoll gradient of blood from different donors were used in these assays. PBMCs were cultured for 4 days in IL-2.

5.2.1 Modulation of NK cell mediated cytotoxicity in a sialic acid dependent manner

Cytotoxicity of human PBMCs against target cells was measured using an ELISA based assay, which measures lactate dehydrogenase (LDH) release from target cells. The number of targets required for detection of LDH was optimized for each cell line. Targets cells included B16 (78) wild type cells, B16 (78) cells overexpressing GD3 and the K562 cell line which served as the positive control as it is known to be highly susceptible to killing by NK cells.

Figure 5.2 (A) represents the percentage cytotoxicity of IL-2 activated PBMC (±) sialidase treatment on B16 (78) ± GD3 and K562 control cells. Cytotoxicity of the B16 (78) GD3 cells was reduced compared to wild type control cells. Sialidase treatment of the effector cells reduced lysis of both B16 (78) ± GD3 cells to effector cytotoxicity (Figure 5.2, B).

One of the methods that have facilitated investigation of ligand binding specificity of the various Siglecs is the use of sialoside-polyacrylamide (PAA) probes. These multivalent platforms can have sialic acid in different linkages, covalently attached to the PAA polymer and is biotinylated to enable easy detection.

The efficiency of sialidase treatment in the cytotoxicity assays conducted here was confirmed by examining binding of sialidase treated CD3-CD56+ PBMCs to

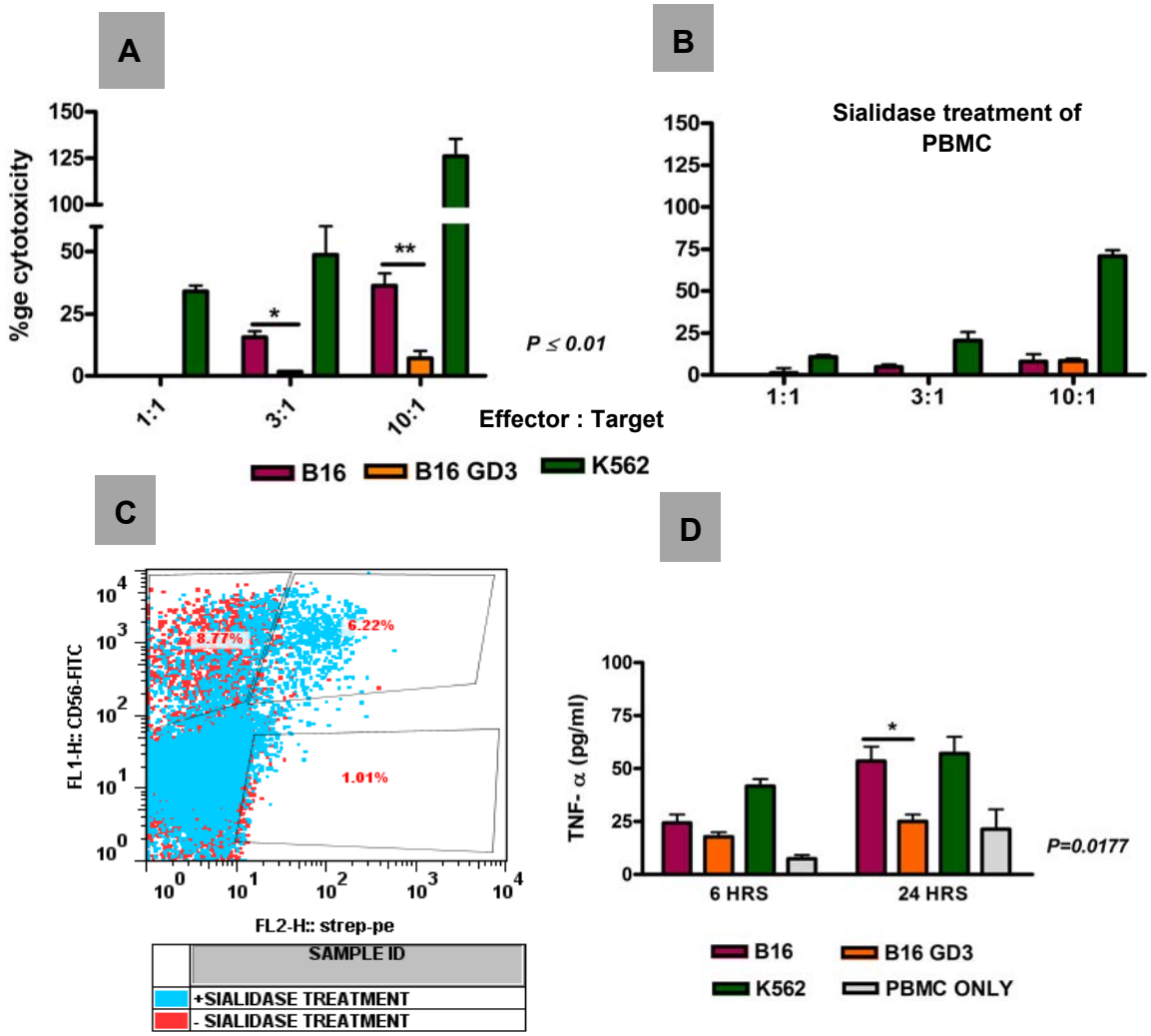

Figure 5.2: Increased sensitivity of B16 ± GD3 cells to cytotoxicity by human PBMCs: Human PBMCs, cultured in IL-2 for 4 days, were treated without (A) or with sialidase (B) (0.17 IU/ml) for 1 hour at 37^0C in DMEM and quenched with 10% FCS. $1x10^4$ B16 and B16 GD3 expressing targerts were added to the PBMCs at different cell concentrations and incubated for 4 hours at 37^0C. Following the incubation period, 50 µl of the supernatant was used to measure LDH release using assay substrate. Data was normalized to effector and target spontaneous release and percentage cytotoxicity calculated according to equation given in materials and methods. Error bars represent standard deviation between samples (n=3) and experiment is representative of n=5 (C) Siglec-7 is masked on PBMCs – Sialidase treatment of PBMC was used to unmask Siglec-7 and promote binding to sialylated ligands. Following sialidase treatment (or not) PBMCs were incubated with biotinylated α 2,8 - PAA probes. Cells were then stained with anti-CD3 and anti-CD56 antibodies and analysed by flow cytometry. The dot blot represents

greater binding of salidase treated (blue dots) human PBMCs to biotinylated disialylated probes compared to non-sialidase treated PBMCs (red dots). Experiment is representative of n=5 (D) Siglec-7 recognition of GD3 down regulates TNF-α response of PBMCs to B16 GD3 cells. Targets and effectors were incubated for 24 hours and 100 µl of supernatant was collected at 6 hour and 24 hour time point. TNF-α ELISA kit was used to detect TNF-α in the culture supernatants. Error bars represent standard deviation between samples (n=4).

biotinylated PAA probe carrying sialic acids in α 2,8 linkages (shown in figure 5.2, C). 49% of the sialidase treated CD56+ PBMCs bound the sugar probes. Binding of these cells to lactosyl-ceramide PAA probes was found to be negative (data not shown).

The cytokine response of IL-2 activated PBMCs to B16 (78) ± GD3 target was also analysed by measuring TNF-α release by ELISA, in a separate experiment. There was a 2-fold reduction in the amount of TNF- α released at 24 hours when effectors were in contact with B16 (78) GD3 targets as compared to wild type B16 (78) cells (shown in figure 5.2, D).

5.2.2 Clonal expression of GD3 modulates NK cell mediated cytotoxicity

The data shown above suggests that GD3 expression on target cells affects NK cell cytotoxicity. To explore the possible role of Siglec-7 in these assays, cytotoxicity assays were performed using B16 clones expressing different levels of GD3 and cytotoxicity correlated to the expression levels of GD3.

For this purpose, GD3 expressing B16 (78) clones were generated by limiting dilution as described previously. Clones were analyzed by flow cytometry (Figure 5.3, A). Clones with high, medium and low expression levels of GD3 were subject to cytotoxicity using IL-2 cultured non-sialidase treated PBMCs as

described above. Figure 5.3, B shows the %ge lysis of B16 (78) cells expressing different levels of GD3, compared to the wild type B16 (78) cells. Clones 3 and 6 with the highest expression of GD3 had significantly reduced cytotoxicity compared to clone 7, which had 5 fold less expression of GD3. The cytotoxicity of clone 7 was comparable to the wild type B16 (78) cells, which lacked in GD3 expression.

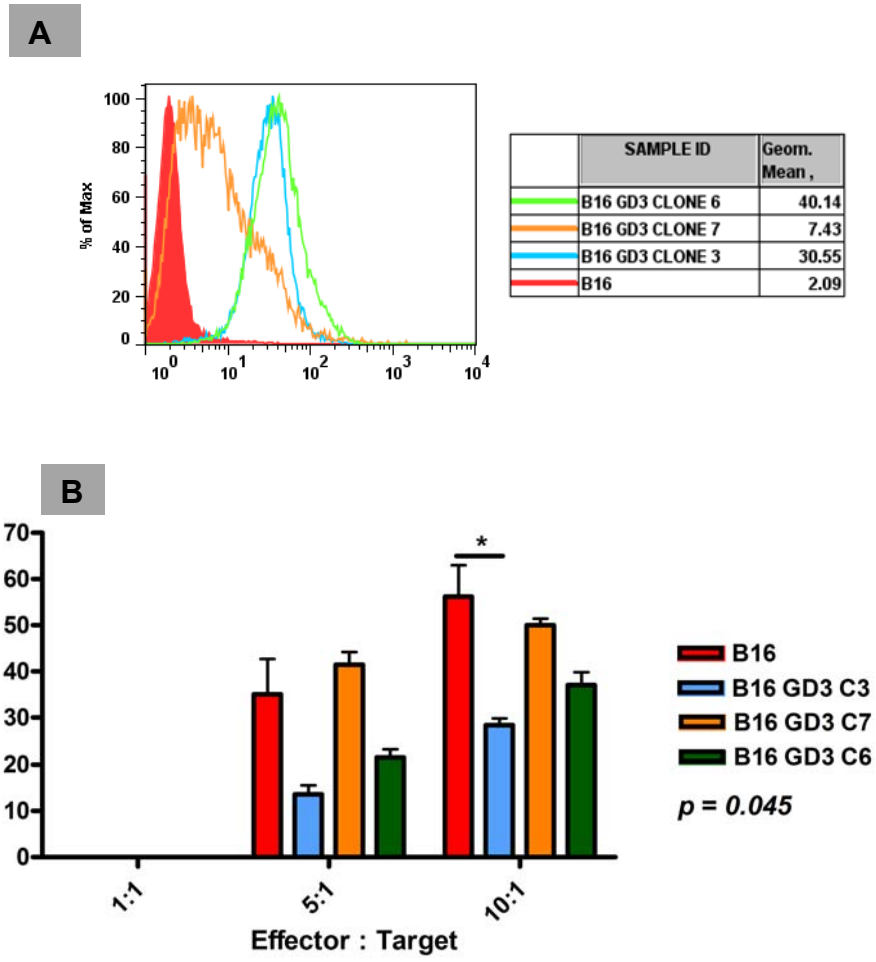

Figure 5.3: Susceptibility of B16(78) clones expressing different levels of GD3 to cytotoxicity of PBMC: B16 (78) cells, transfected with GD3S were cloned by limiting dilution. (A) B16 (78) wild type cells and GD3 expressing clones were stained with anti-GD3 antibody (R24) for 30 minutes on ice. Cells were then washed and stained with anti-mouse FITC antibody for 30 minutes on ice. Washed cells were then analyzed by flow cytometry. (B) B16 (78) cells were also subjected to cytotoxicity by IL-2 activated PBMC as explained in figure 5.2. Error bars represent standard deviation between samples (n=3).

5.2.3 Blocking of RBC adhesion by Siglec-7 antibodies

The aim of these experiments was to investigate if anti-siglec-7 antibody could reverse GD3-dependent suppression of killing. Sheep polyclonal anti Siglec-7 serum, mouse monoclonal antibody (clone 7.7A) and sheep polyclonal Fab fragments to Siglec-7 were used in the cytotoxicity assays. In chapter 4, both sheep polyclonal anti-Siglec-7 serum and the mouse monoclonal antibody (clone 7.7a) have been used to specifically identify Siglec-7 positive cells. RBCs adhere to Siglec-7-Fc coated on to anti-Fc coated plates (as described in chapter 3). The binding of RBCs to Siglec-7-Fc coated plates was blocked by the incubating the plate with dilutions of sheep antisera, mouse monoclonal antibody tissue culture supernatant (clone 7.7a) or different concentrations of Fab fragments. The polyclonal sheep antiserum efficiently blocked RBC adhesion over a range of dilutions (Figure 5.4, A). Pre-immune sheep serum was used as a negative control and did not inhibit RBC adhesion. Monoclonal antibody, clone 7.7a, only reduced adhesion when used as neat supernatant (Figure 5.4, B).

At concentrations ranging between 20 µg/ml and 1 µg/ml, Siglec-7 Fab antibody fragment also significantly blocked the adhesion of RBCs to Siglec-7-Fc (Figure 5.4, C). Adhesion was sialic acid dependent as sialidase treated RBCs failed to bind to Siglec-7-Fc (Figure 5.4, C).

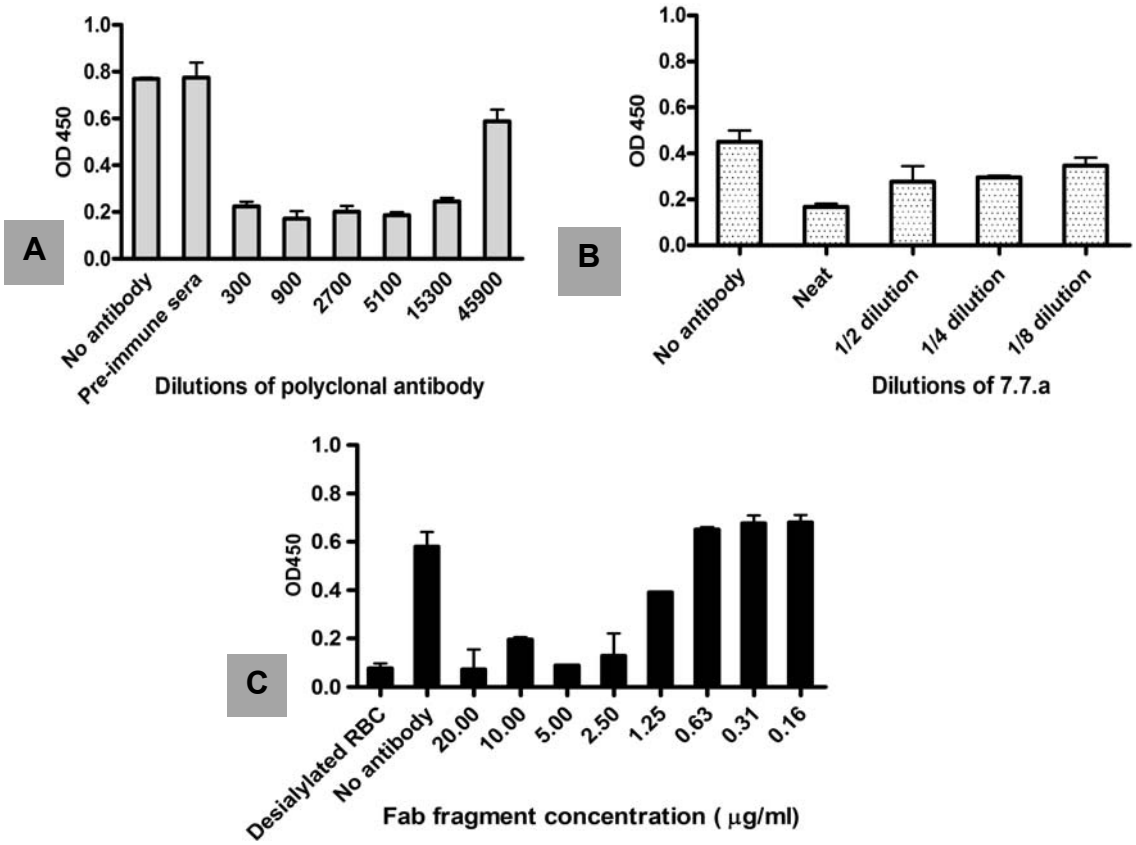

Figure 5.4: Siglec-7 antibodies block RBC adhesion: 96 well plates were coated with 100 µl of 12 µg/ml of goat anti-human IgG in bicarbonate buffer (p H 9.6). After overnight incubation, plates were blocked with 5% marvel in 1 X PBS. Following x3 washes in PBA, wells were coated with 100 µl of Siglec-7-Fc (@ 7 µg/ml) and incubated for 1 hour at 37^0C. Plates were then incubated with different dilutions of the Siglec-7 polyclonal antiserum (A), monoclonal antibody (B) or different concentrations of Fab fragments (C) and incubated at 37^0C for 30 minutes. 100 µl of prepared RBCs were added and incubated for 1 hour room temperature. Plates were washed using an orbital shaker to remove unbound RBC, cells fixed with methanol and 100 µl of TMB substrate added and incubated for 30 minutes at room temperature. The reaction was stopped using 100 µl of sulfuric acid and plates read at 450nm. Error bars represent standard deviations (n=3).

5.2.4 Antibodies do not block Siglec-7 mediated inhibition of cytotoxicity

The above tested antibodies were then used in cytotoxicity assays to determine if they block Siglec-7 mediated inhibition of cytotoxicity against GD3 expressing B16 target cells. IL-2 activated PBMCs were used as effectors in cytotoxicity

assays as described in section 5.2.1. Polyclonal antiserum (1/1000 dilution), undiluted monoclonal antibody supernatant or Fab fragments (10 µg/ml) were incubated with effectors for 15 minutes at room temperature prior to addition of target cells. Neither the polyclonal Siglec-7 antibody (figure 5.5, A) nor the monoclonal antibody (figure 5.5, B) could reverse the inhibition of Siglec-7 mediated cytotoxicity.

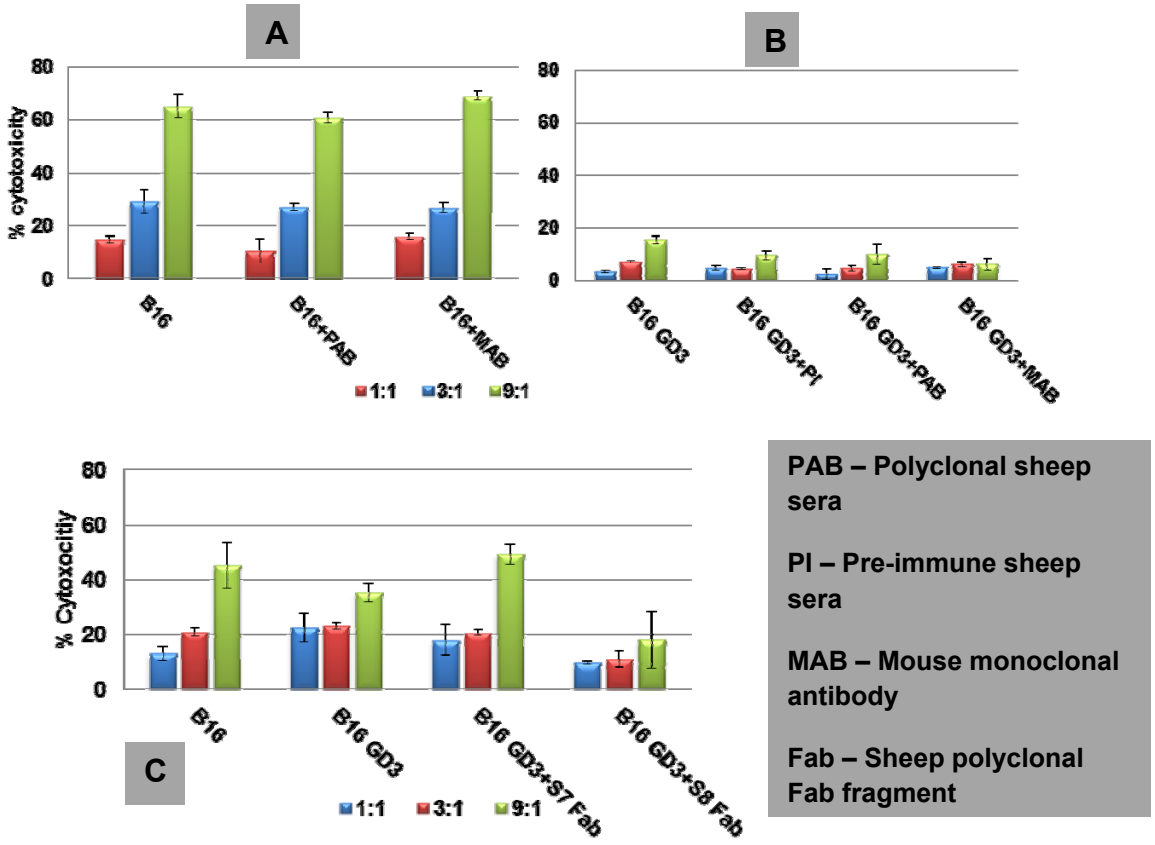

Figure 5.5: Antibodies do not block inhibition of NK cytotoxicity by Siglec-7: Cytotoxicity assay using IL-2 activated PBMCs and B16 (78) ± GD3 were carried out as described in figure 5.2 using (A) Siglec-7 polyclonal antibody @ 1/1000 dilution (B) Siglec-7 monoclonal antibody, clone 7.7A and (C) Siglec-7 Fab fragment @ 10 µg/ml. Fc receptors on PBMCs were blocked with human serum for 15 minutes prior to addition of antibodies. Error bars represent standard deviation (n=3) and experiment is representative of n=3.

The Fab fragment gave a very modest increase in lysis of B16 (78) GD3 cells at 9:1 effector : target ratio (figure 5.5, C). However, in this assay the B16 (78) GD3 cells were only slightly protected compared to the B16 (78) WT cells. The assays were repeated with the different antibodies and gave similar results.

5.2.5 Cytotoxicity of human melanoma cell line (SK-MEL-28)

Another approach adopted to investigate the inhibitory role of GD3 via ligand avidity for Siglec-7 was the use of a different target cell population, SK-MEL-28, with endogenously high expression of GD3.

IL-2 activated PBMC were incubated with either wild type or sialidase treated targets. Sialidase treatment of cells was confirmed by anti-GD3 antibody staining which showed a striking loss (figure 5.6, C). Upon removal of α 2,8 linkages by sialidase treatment, SK-MEL28 cells became more susceptible to PBMC mediated killing (figure 5.6, B).

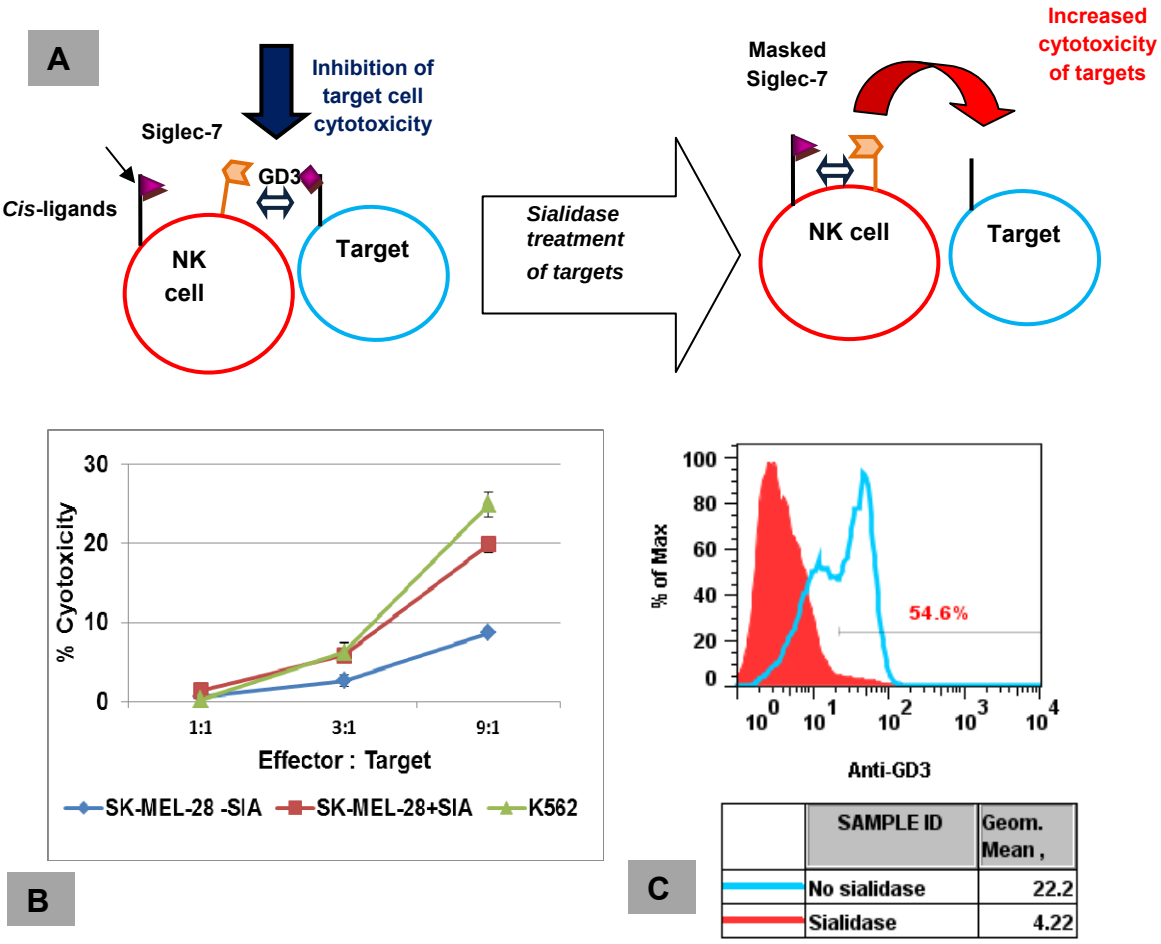

Figure 5.6: Sensitivity of SK-MEL-28 cells to NK cytotoxicity is decreased following sialidase treatment of cells. (A) Schematic shows Siglec-7 on effector NK cells recognize sialic acid ligands on target cells and inhibits cytotoxicity. However upon sialidase treatment of targets, the sialylated ligands are removed and Siglec-7 engages with *cis*-ligands, resulting in increased lysis of the targets (B) SK-MEL-28 cells +/- sialidase treatment were subject to lysis by IL-2 activated PBMCs as described in 5.2 (C) SK-MEL-28 cells used in the cytotoxicity assay were stained for GD3 using R24 antibody before and after sialidase treatment. Error bars represent standard deviation (n=3). Data represents experiment from n = 1.

5.3 Role of Siglec-7 in regulating cytotoxic functions of activating receptors via recognition of GD3

The above cytotoxicity data suggest the potential inhibitory role of Siglec-7 in inhibiting NK cytotoxicity of GD3 expressing B16 (78) and SK-MEL-28 cells.

To further establish these findings, an NK cell line, NK92, deficient in Siglec-7 expression was used as effector population. NK92 is known to express activating receptors such as – NKp46, NKp30, NKG2D, 2B4 and CD28 (Maki et al., 2001). This cell line has been characterized in Chapter 4 with regards to Siglec-7 expression.

5.3.1 Expression of GD3 on the K562 cell line

The prototype K562 target cell line, which is highly sensitive to killing by both primary NK cells and NK cells lines, was used.

K562 cells were analysed for expression of GD3 using the mouse anti-GD3 antibody (R24). The cell line was negative for the expression of GD3. Hence this cell line was transfected with cDNA for GD3S and overexpression of GD3 achieved as shown by flow cytometry staining in figure 5.7.

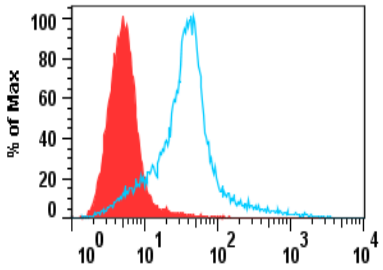

Figure 5.7: Flow cytometry staining of K562 cells for expression of GD3 : K562 cells were transfected with GD3S and expression of GD3 analysed using anti-GD3 antibody (R24). Histogram in red – wild type K562 cells ; Histogram in blue – K562 cells transfected with GD3S.

5.3.2 Siglec-7-Fc precomplex recognition of GD3 expressed on K562 ± GD3

Siglec-7 recognition of GD3 expressed on the K562 cells was analysed using Siglec-7-Fc precomplexes (figure 5.8). The pre-complexes bound strongly to both K562 wild type cells and GD3 expressing cells. Upon sialidase treatment of the cells, there was only a moderate decrease in the binding of these precomplexes. This is suggestive of the Siglec-7 precomplexes binding to the cells in a sialic acid independent manner. These results also suggest that this cell line, in contrast to the B16 (78) wild type cells, has a sialylation pattern that favours Siglec-7 recognition, independent of GD3.

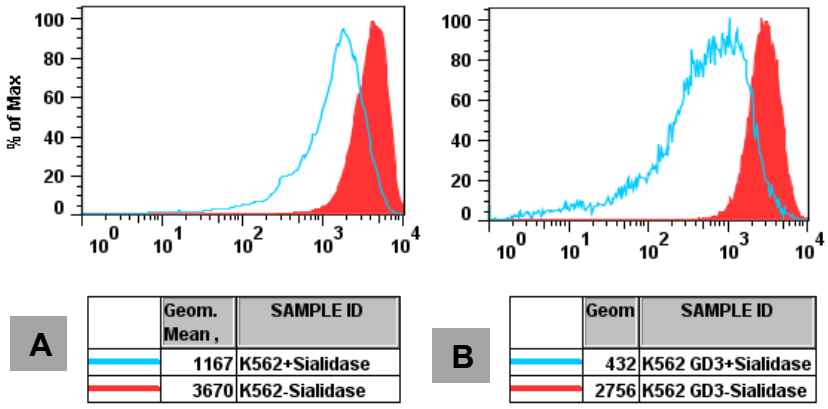

Figure 5.8 Siglec-7-Fc precomplexes bind K562 ± GD3 cells in a sialidase dependent manner. Precomplexes were prepared as described in chapter 4 and added to sialidase treated and non-treated K562 (A) and K562 GD3 (B) cells for 1 hour on ice. Cells were then analysed by flow cytometry. The mean fluoresence intensity of each sample is represented in the box below.

5.3.3 Siglec-7 modulates the cytotoxicity of K562 GD3 cells

K562 ± GD3 cells were then used as targets in cytotoxicity assays comparing killing mediated by NK92 ± Siglec-7. The expression of GD3 on K562 cells did not affect their sensitivity to killing by either the wild type NK92 cells (Figure

5.9,B) or the Siglec-7 expressing NK92 cells (figure 5.9, C). However sensitivity of both the wild type K562 and GD3 expressing K562 cells to Siglec-7 expressing NK92 clone was significantly lower than to the wild type NK92 cells (Figure 5.9, D and E).

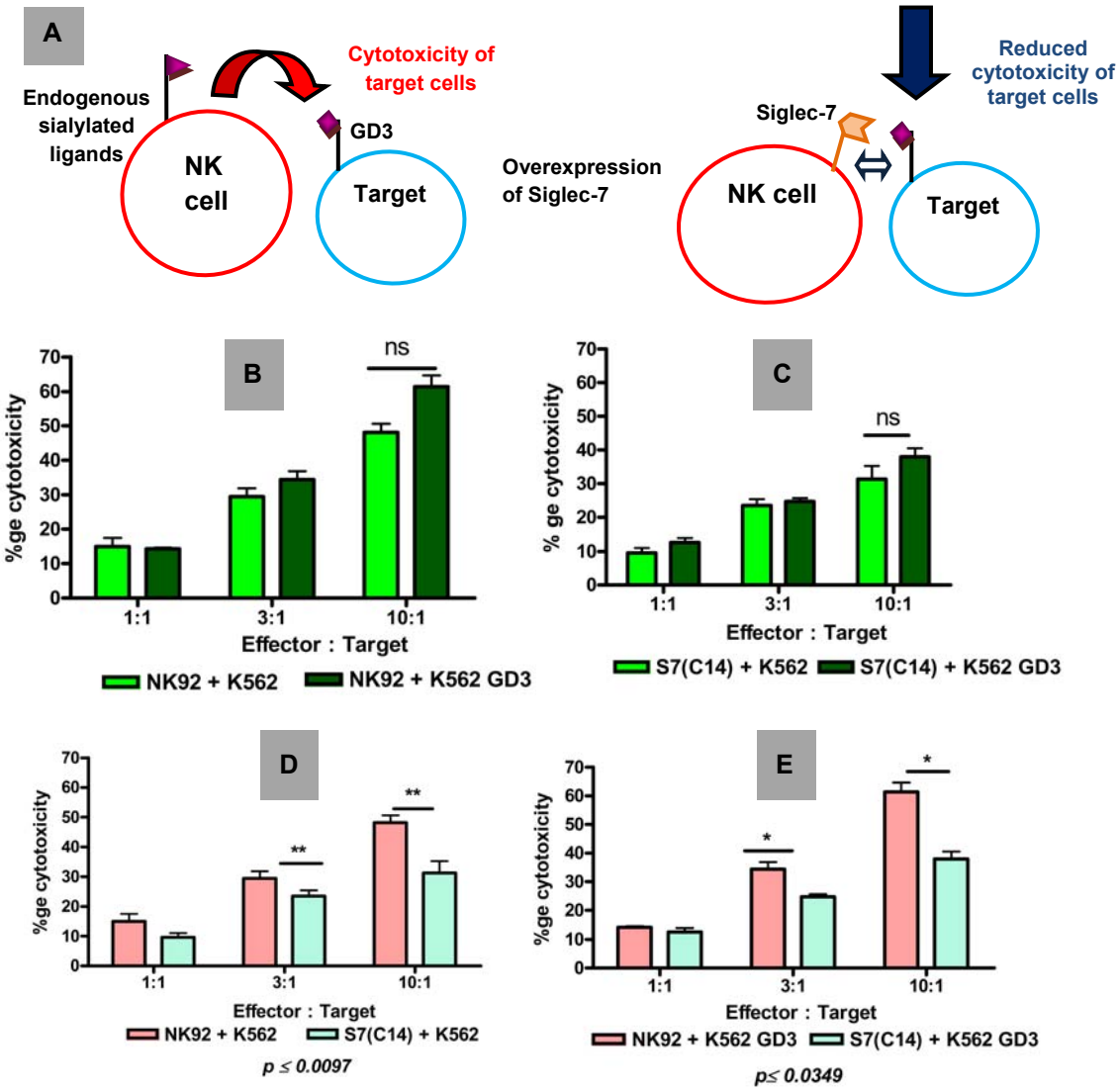

Figure 5.9: Siglec-7 modulates NK92 cytotoxicity of K562 GD3 expressing cells: Cytotoxicity assays were carried out as detailed in figure 1.2. (A) Schematic showing the expression of Siglec-7 favours *trans* interactions between glycans on target cells and reduces cytotoxicity of sensitive targets. (B) NK92 and (C) NK92 Siglec-7 cells (C14) were incubated with either K562 wild type cells or K562 GD3 cells. (D) K562 cells and (E) K562 GD3 cells were tested for their sensitivity to NK92 and NK92 S7 (C14) cells. Experiment is representative of n=2.

5.3.4 Sialidase treatment affects cytotoxicity of NK92 S7 expressing cells

In a separate experiment, sialidase treatment of effector cells, to unmask Siglec-7, was examined on K562 target cells, expressing GD3.

Sialidase treatment of the wild type cells reduces cytotoxicity of target cells (figure 5.10, B) however this effect is more significant (at all effector to target ratios) in Siglec -7 expressing NK92 cells (Figure .510, C). The cytotoxicity of Siglec-7 expressing NK92 cells (clone 14) was significantly lower at all effector to target concentrations, compared to sialidase non-treated and treated wild type cells (Figure 5.10, D and E).

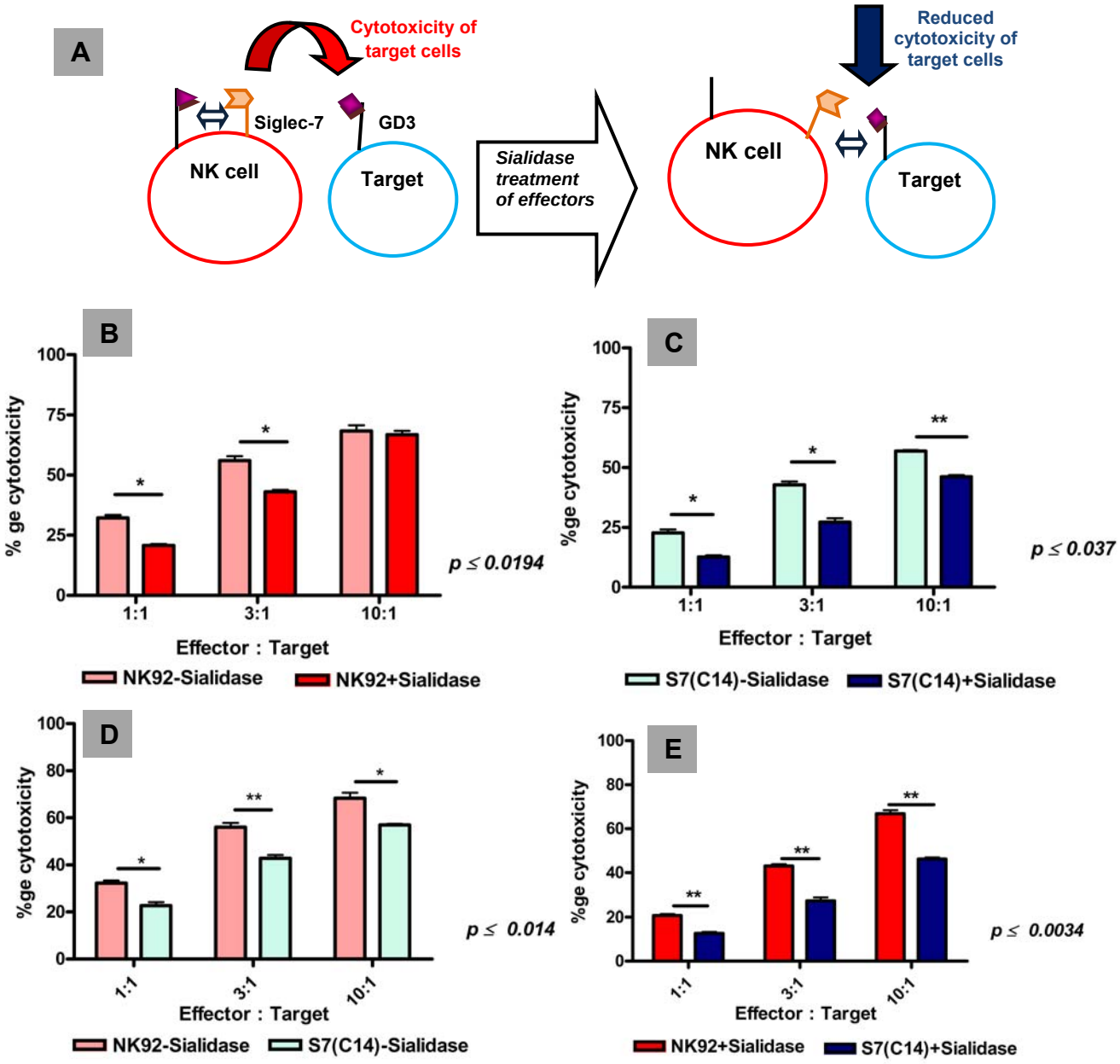

Figure 5.10 – Unmasked Siglec-7 show increased inhibition of cytotoxicity towards K562 GD3 cells – Cytotoxicity assays were carried out as described in figure 5.2 using K562 GD3 cells (A) Schematic showing how sialidase treatment affects Siglec-7 unmasking. Comparing cytotoxicity of sialidase untreated and treated (B) NK92 wild type cells (C) and Siglec 7 expressing NK92 cells – S7 (C14). Comparing cytotoxicity of NK92 and S7(C14) cells (D) before sialidase treatment (E) after sialidase treatment. Experiment is representative of n=1.

5.4 Siglec-7 affects LFA-1 mediated cytotoxicity

Unlike T cells and B cells, LFA-1 in NK cells has an important role in adhesion and provides for early cytotoxicity signals (Barber, Faure and Long, 2004). It also acts in concert with other activating receptors to bring about actin cytoskeletal re-organization and perforin granule polarization. Long et al., 2004 showed that LFA-1 is sufficient to cause lysis of insect cells in an ICAM-1 dependent manner by IL-2 activated cells and this is affected by KIR inhibitory signals.

Data described in chapter 4 using ICAM-1-Fc chimera showed that Siglec-7 plays a negative role in LFA-1 dependent adhesion of NK92 cells and that integrin dependent signalling was intercepted at the proximal stages of the signalling cascade. The biological significance of these findings can be examined by means of NK cytotoxicity assays where LFA-1 is known to play a role. Towards this, the NK92 effector cells were used as a model system to investigate the role of Siglec-7 in affecting LFA-1 cytotoxicity functions in a biological setting.

5.4.1 B16 cells lack ICAM-1 expression

Unlike human melanoma cells (Nakayama et al., 1997) the mouse B16 cell line is not known to express ICAM-1 under ordinary culture conditions. This was re-confirmed by flow cytometry staining, using an anti-mouse ICAM-1 antibody or isotype and mouse neutrophils as positive control (figure 5.11). Consistent with published reports, the B16 (78) cells had no expression of mouse ICAM-1 (Nakayama, J et al., 1997).

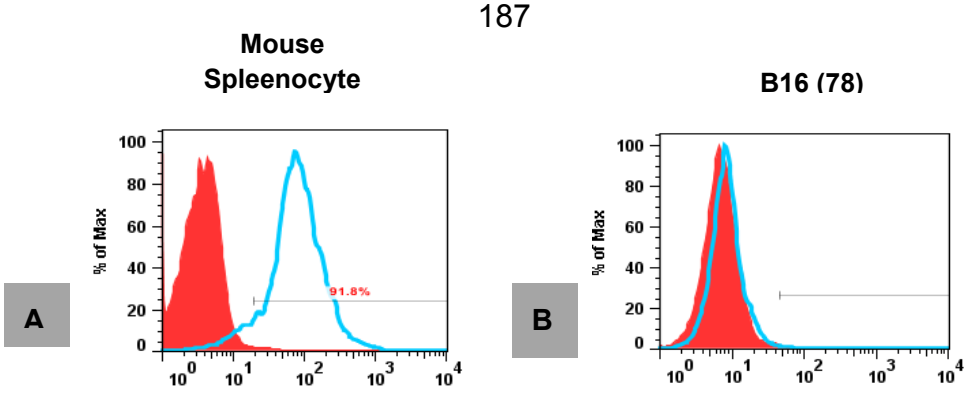

Figure 5.11: B16(78) cell line does not express ICAM-1 : Mouse splenocytes (A) and B16 mouse melanoma cells (B) were stained with 0.125 µg of anti-mouse ICAM-1 PE (blue histogram) antibody or isotype control (red filled histogram) in FACS buffer for 30 minutes on ice. Cells were then washed with FACS buffer, fixed with 1% PBA and analysed by flow cytometry.

5.4.2 Expression of human ICAM-1 on ± B16 GD3 cells

mRNA for human ICAM-1 was extracted from K562 cells and used to generate cDNA using suitable primers (described in materials and methods). ICAM-1 cDNA was then cloned into pcDNA 3.1 vector and purified plasmid DNA was transfected into B16 ± GD3 cells. After 2 weeks of culturing cells in selection media (hygromycin - @ 0.4 mg/ml), polyclonal cells stably expressing ICAM were analyzed by flow cytometry staining using antibodies to human ICAM-1. Cells were then subject to 1-2 rounds of MACS sorting to substantially enhance the percentage of ICAM-1 expressing cells.

Figure 5.12 shows the expression levels of both ICAM-1 (A) and GD3 (B) on the different populations of B16 (78) transfectants following MACS sorting. Wild type B16 (78) which do not express either GD3 or ICAM-1 was used as a negative control.

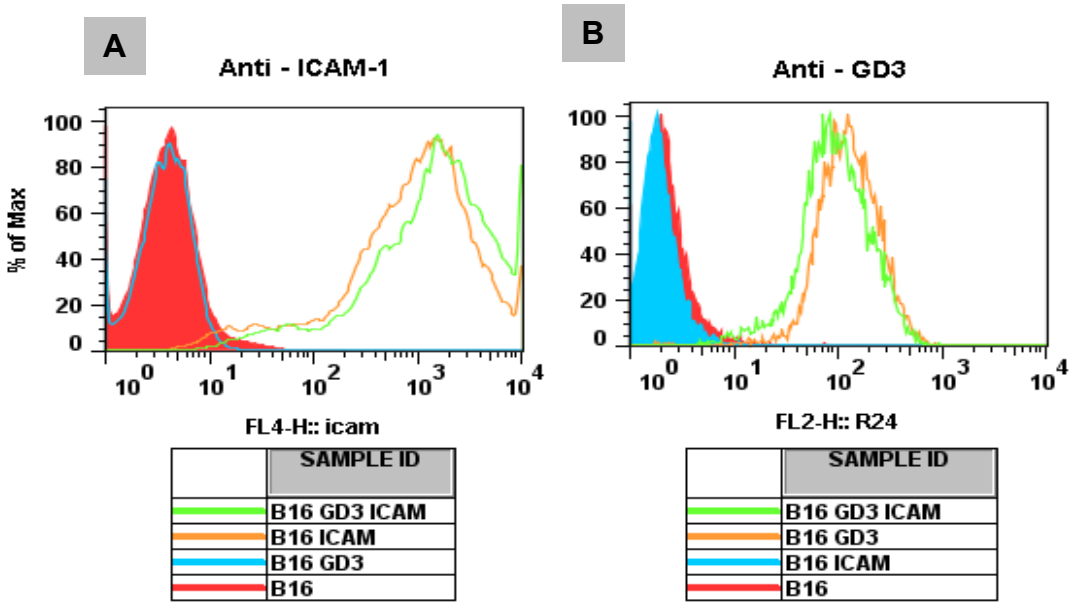

Figure 5.12: Expression of GD3 and ICAM-1 on B16 cell line: B16 wild type cell line and B16 GD3 expressing cell line were transfected with pCDNA3.1-ICAM-1. Cells were stained either with (A) anti-GD3 antibody (R24) or (B) with anti-ICAM-1 antibody for 30 minutes on ice. Following washes in FACS buffer, cells were stained with 1/200 dilution of anti-mouse PE or 1/500 dilution of streptavidin-APC. Cells were washed and fixed with 1% PFA and then analysed by flow cytometry.

5.4.3 SNA and Siglec-7-Fc precomplex binding to B16 ± ICAM cells

In chapter 3, Siglec-7-Fc precomplexes bound minimally to B16(78) wild type cells. Upon transfection of GD3 synthase, there was significantly stronger binding of the complexes in a sialic acid dependent manner. These results suggested that wild type B16 (78) cells express predominantly glycans with terminal sialic acids in mostly α 2,3 or α 2,6 linkages for example GM3 glycolipids that are the less preferred ligands for Siglec-7.

B16 cells overexpressing ICAM-1 were analysed using the lectin SNA and Siglec-7-Fc precomplexes. The binding of the lectin SNA would help reveal the

presence of sialic acids in α 2,6 linkages on cell surface glycoproteins and glycolipids that could act as putative Siglec-7 counter receptors .

Figure 5.13, A shows the binding of SNA lectin to B16 (78), B16 ICAM-1 and B16 GD3 ICAM cells with and without sialidase treatment. The lectin bound strongly to wild type cells and transfectants. Figure 5.13, B, shows the binding of Siglec-7-Fc precomplexes to these three populations of cells. Interestingly, there was no difference in the binding of these precomplexes to either the B16 (78) wild type or ICAM-1 positive cells. Stronger binding of the complexes to GD3 expressing cells was observed.

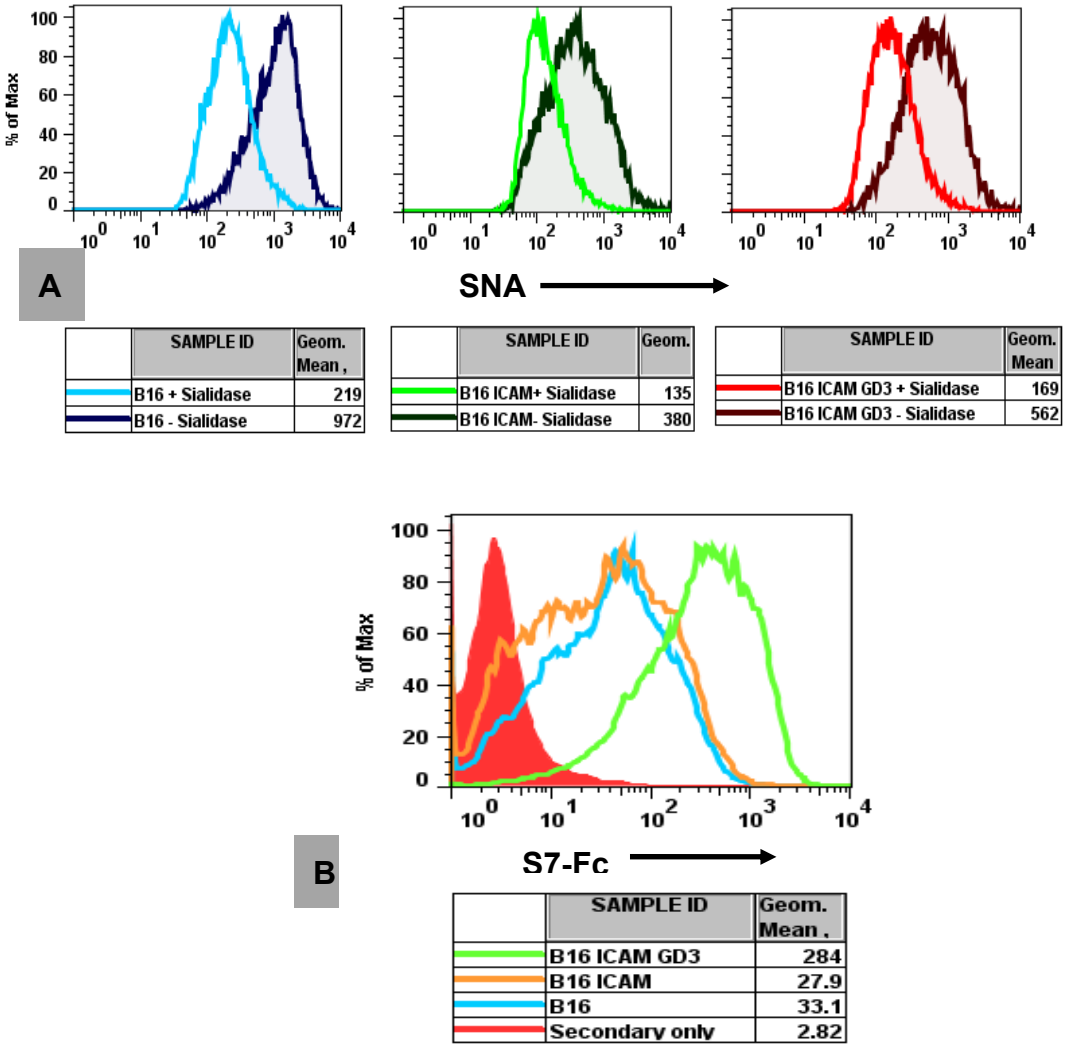

Figure 5.13 – Comparing binding of SNA and Siglec-7-Fc-precomplexes to B16, B16 GD3 and B16 GD3 ICAM cells. (A) Cells were harvested and treated with sialidase (0.17 IU/ml) in DMEM for 1 hour at 37^{0}C. Cells were then washed with DMEM + 10% FCS. Biotinylated SNA at 5 µg/ml was added to the samples for 30 minutes on ice. Following incubation, cells were washed in FACS buffer and then stained with 1/500 dilution of streptavidin-APC. Cells were washed and fixed with 1% PFA before analysing by flow cytometry. (B) Siglec-7-Fc (@ 1 µg/ml) precomplexes with anti-human Fc IgG (@3 µg/ml) was prepared in HBSS, for 1 hour on ice. 100 µl of complex was added to each cell sample and left to incubate for an hour on ice. Cells were then washed with FACS buffer and fixed with 1% PFA before analysing by flow cytometry

5.4.4 ICAM-1 expression increases sensitivity of B16 (78) targets to NK92 effectors

NK92 cells mediate cytotoxicity against a range of primary human target cells and cell lines. However the cytotoxic effect of these cells on the B16(78) cells has not been studied previously to the best of my knowledge. Initial 4 hour cytotoxicity assays using the NK92:B16(78) effector-target system showed that these target cells are highly resistant to the cytotoxic action of this effector cell line (data not shown).

Therefore it was decided to first test if the over-expression of ICAM-1 on these target cells would improve their sensitivity to NK92 killing by means of LFA-1/ICAM-1 interactions. To improve the signal to noise ratio, the assay time was extended to 5 hours. Figure 5.14 demonstrates a modest improvement in the senstivity of B16 (78) ICAM-1 and B16 (78) GD3 ICAM-1 cells to these effectors compared to wild type B16 (78) cells.

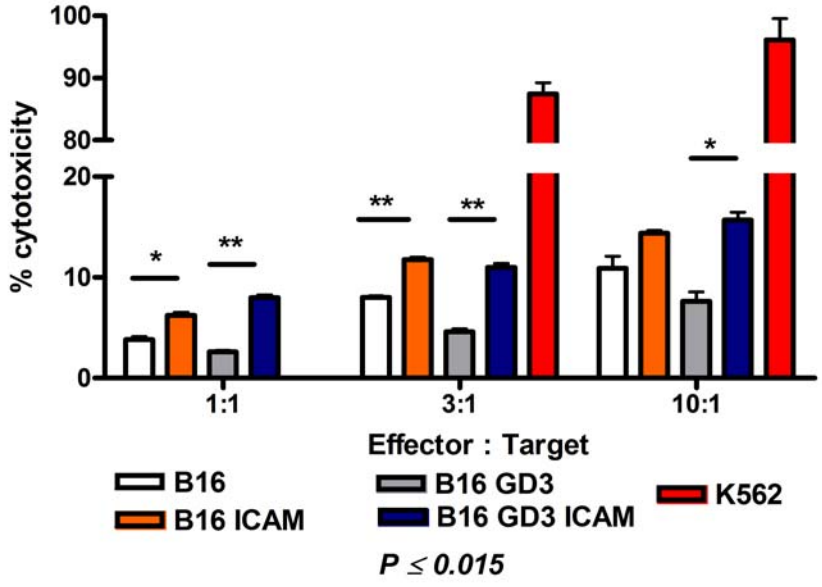

Figure 5.14: B16(78) ICAM-1 expressing cells are sensitive to NK cytotoxicity: B16 (+/-GD3) and B16 (+/-ICAM-1) were subject to cytotoxicity assay using NK92 effector cells as described in figure 4.17. K562 cells were used as a positive control in the experiment. Error bars represent standard deviation with n=4. Data represents experiment from n = 1.

5.4.5 Differential killing of B16 GD3 ICAM by NK92 and C14 cells

Using B16 (78) GD3 ICAM cells as targets, cytotoxic effects of wild type NK92 cells and Siglec-7 expressing NK92 (Clone 14) cells were examined. Sialidase treatment of both effector populations was carried out to unmask Siglec-7. Figure 5.15, A shows that both untreated effector populations were comparable in their cytotoxicity of these targets. However upon sialidase treatment, there was a significant reduction in target lysis by Siglec-7 expressing clone (C14) (Figure 5.15, B).

Siglec-7 expression was also tested by flow cytometry staining in both sialidase treated and untreated effectors (Figure 5.15, C). Sialidase treatment had no effect on the expression levels of Siglec-7 on these cells.

To confirm effectiveness of the sialidase treatment, effectors were incubated with biotinylated α 2,8 sialic acid PAA probes (Figure 5.15, D) and biotinylated LacCer PAA probes (Figure 5.15, E). While untreated and treated wild type NK92 cells were negative for binding of α 2,8 PAA probes, clone 14 (C14) cells bound strongly to the probe following sialidase treatment. All groups of cells were negative for binding to LacCer probes. Data represents experiment from n = 1.

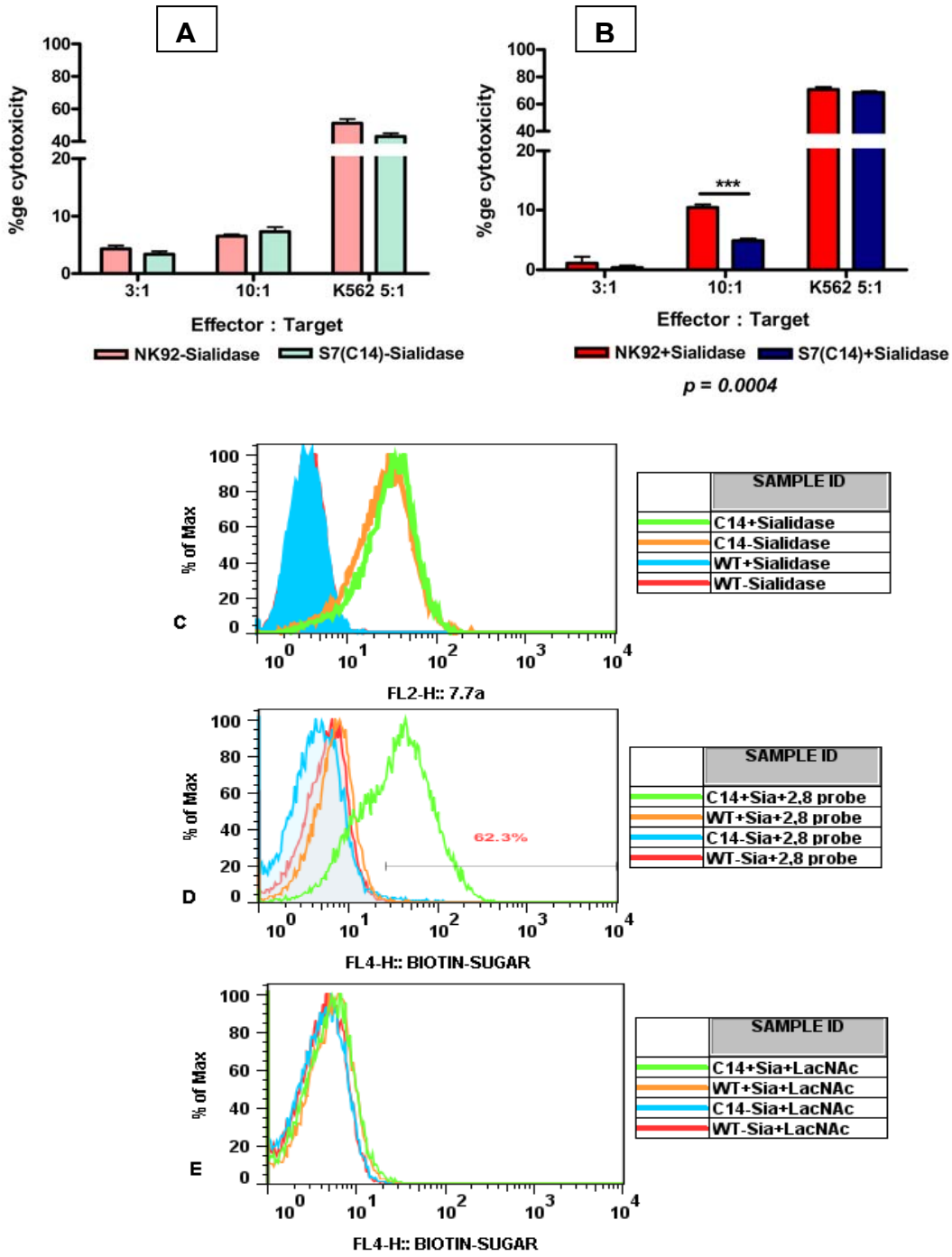

Figure 5.15: B16(78) GD3 ICAM target cells are less sensitive to the cytotoxic action of sialidase treated NK92 Siglec-7 cells : Assay was carried out as described in figure 4.17 using (A) non-sialidase treated effector cells and (B) sialidase treated effector cells. Targets and effectors were incubated for 5 hours and error bars represent standard deviation between samples (n=4). Effector cells using in the experiment were stained for Siglec-7 expression (C) and biotinylated sugar binding (D) as described in figures. Binding of effector cells to biotinylated LacCer PAA (E) was used as negative control.

5.5 Discussion

The data generated in the experiments described here point to the role of Siglec-7 in regulating NK cytotoxicity against tumour targets via 1) recognition of GD3 expressed on target cells and 2) dampening integrin mediated cytotoxicity signals.

GD3 in modulating the inhibitory functions of Siglec-7:

At the outset of this PhD project, the primary aim was to investigate the role of heteromeric complexes of GD3 and GM1 gangliosides in affecting Siglec-7 recognition and thereby modulation of NK cytotoxicity. The B16 (78) cell line was chosen for this purpose as it only expresses the precursor of all other ganglioside species ie GM3 and therefore could be genetically modified to overexpress glycosyltransferases leading to the synthesis of gangliosides GD3 and GM1. However, due to the lack of formation of GD3:GM1 complexes on the surface of these target cells, it was decided to shift focus on the role of GD3 expression on tumour cells in affecting NK cell functions , specifically cytotoxicity. The initial cytotoxicity assays were focused on reconfirming findings of Nicoll *et al.,* with respect to GD3 in the B16 (78) mouse melanoma cell line (discussed in introduction to this chapter). In the cytotoxicity assays conducted using B16 (78) vs. the B16 (78) GD3 target cells, there was a clear inhibition in the lysis of targets (Figure 5.2) by non-sialidase treated IL-2 activated PBMCS. These findings are interesting as they question the previous finding of the presence of a GD3 recognizing activating receptor on activated NK cells. Additionally if this is a Siglec-7 dependent effect, these results suggest that Siglec-7 is unmasked under the conditions used and is therefore capable of ligand recognition in *trans*. One possible explanation for this reduction in lysis

would be the over-coming of *cis*-interactions of Siglec-7 by endogenous sialylated ligands on the cell surface by high affinity ligands in *trans*. Strong inhibitory signals generated by Siglec-7 in the NK effector cells would increase the threshold required by activating receptors thereby reducing overall cytotoxicity of GD3 expressing targets. Indeed this phenomenon has been demonstrated for the B-cell expressing Siglec-2, CD22. In the presence of high affinity ligands, CD22 overcomes its threshold for *cis*-binding and is able to bind ligands in *trans* (Collins *et al*., 2006).

As shown in figure 5.2, sialidase treatment of PBMCs inhibited NK cell killing of B16 (78) GD3 targets but it also reduced the lysis of wild type B16 (78) cells. Sialidase treatment of effectors removes endogenous *cis* interactions and exposes the ligand binding site of Siglec-7. But it is also possible that this treatment affects glycosylation patterns of NK activating receptors and alters overall NK cytotoxicity (as has been shown for NKp44 (Hershkovitz et al., 2009)). Sialidases catalyze the cleavage of sialic acids from oligosaccharides presented by glycoproteins and glycolipids at the cell surface. For the cytotoxicity assays conducted here, sialidase from *Vibrio cholerae* (type III) was used. This sialidase has broad specificity and will catalyze cleavage of sialic acids in α 2,3- < α 2,6- < α 2,8- linkages (Chokawala et al., 2007).

The abundance of sialic acids on cell surfaces provides cells with their negative charge and contributes to many properties of cell-cell interactions (Varki and Gagneux, 2012). Therefore sialidase treatment of cells, to remove surface sialic acids, would decrease the overall negative charge on the cell, affect cell-cell interactions and possibly increase non-specific interactions (Zhang and Varki., 2004). Removal of sialic acids by sialidases was shown to expose the ligand binding site of β1-integrins and dramatically increased the adhesion of cells to

fibrinogen (Pretzlaff et al., 2000). Sialidase treatment of B cells has also been shown to play a role in modulating B cell : T cell interactions (Bagriacik and Miller., 1999).

The use of Siglec-7 antibodies in the cytotoxicity assays did not reverse the inhibitory effects of Siglec-7 (Figure 5.5). However these antibodies were able to block RBC adhesion to Siglec-7-Fc coated plates (Figure 5.4). The epitopes on Siglec-7 recognized by these antibodies have not been defined. Although the RBC adhesion assays suggests a blocking role for these antibodies, the possible effect of steric hindrance by the IgG molecules cannot be overlooked. In cellular assays, these antibodies could have little role in blocking the sugar binding site on Siglec-7. Ligation of anti-CD33 and cross-linking of Siglec-7 antibodies have been shown to inhibit the proliferation of acute myeloid leukemic cells (Balaian, Zhong and Ball, 2003;Vitale et al., 2001). Antibodies or glycan ligand-based cargo are also known to trigger receptor endocytosis in some members of the siglec family such as CD22 (B cell receptor), Siglec-F and Siglec-H (Shan and Press, 1995; Zhang et al., 2006; Tateno et al., 2007) (O'Reilly et al., 2011). Endocytosis leads to either recycling of the receptor back onto the surface (eg., CD22) or lysosomal degradation (eg., Siglec-F) (Stoddart et al., 2005). Polyclonal Siglec-7 antibody conjugated to nano-particles has also been reported to internalize Siglec-7 (Scott et al., 2008). A recycling pathway is not yet known for Siglec-7. But it is possible that the anti-Siglec-7 antibodies trigger rapid internalization and recycling of the receptor. This would result in the receptor being in a constant state of equilibrium on the cell surface and actively engaging in *trans* ligand interactions. This would partly explain why the antibodies were not able to reverse the inhibitory effects of Siglec-7 in the cytotoxicity assays conducted here.

To further define the inhibitory role of Siglec-7 in regulating NK cell mediated killing, CD107a release from CD3-CD56+ effectors following incubation with targets was measured as well as direct measure of killing using 7AAD staining as a marker for cell death was performed (data not shown). Data from both these assays demonstrated clear inhibition of NK mediated cytotoxicity when B16 (78) targets expressing GD3 was used.

Therefore it is reasonable to conclude that the availability of higher affinity Siglec-7 ligands such as disialylated GD3 on target cells is enough to over come *cis*-masking of Siglec-7 on NK cells and facilitate *trans* interactions in the absence of sialidase treatment. These interactions are sufficient to increase the threshold needed by NK activating receptors, resulting in decreased target cell lysis.

Another novel approach taken towards the goal of identifying the role of GD3 in modulating NK cell functions was the use of an NK cell line, deficient in Siglec-7. This cell line would help directly investigate the role played by this receptor in NK cell biology. The K562 leukemic cell line was chosen as a suitable target, as it is highly sensitive to both primary NK cells as well as the NK92 cell line. Interestingly it also lacked expression of the ganglioside GD3 (Figure 5.7). and was therefore manipulated to overexpress GD3. Binding of Siglec-7-Fc precomplexes on wild type K562 and GD3 expressing K562 cells gave very high shift in fluoresence intensities, implying presence of sialylated ligands on these cells. However these cells are known to express the Fc receptor, FcγRIIB, which could contribute to the high binding of these pre-complexes (Littaua et al., 1990). The nature of sialylated ligands on K562 cells or their linkages are not known and would require further investigation using either antibody or lectin

staining and analysis of messenger RNA levels of the different glycosyltransferases.

In cytotoxicity assays, NK92 Siglec-7 expressing cells showed a significant reduction in cytotoxicity of both K562 and K562 GD3 cells compared to wild type NK92 over a range of effector : target ratios (Figure 5.9). Unmasking Siglec-7 on these effectors by sialidase treatment enhanced the inhibition of lysis of K562 GD3 targets (Figure 5.10). These results are significant as they suggest that in the presence of targets that have expression of sialylated ligands in high density, Siglec-7 undergoes unmasking from *cis*-interactions and is able to bind ligands in *trans*. This results in generation of inhibitory signals which is capable of over-riding cytotoxicity signals initiated by activating receptors against this sensitive target. However sialidase treatment of wild type NK92 cells also led to decreased cytotoxicity of K562 GD3 cells. This is suggestive of the dual effects of sialidase treatment – a specific one which results in unmasking of Siglec-7 and a more non-specific effect resulting in decreased cytotoxicity.

These results are consistent with the data obtained using PBMCs on B16 (78) GD3 expressing targets but are different to results from the P185 model used previously in the lab. In the latter model, Siglec-7 on PBMCs had to be unmasked by sialidase treatment in order to recognize ligands in *trans* and exhibit inhibitory role. In the B16 (78) and K562 cell lines, unmasking the receptor was not a prerequisite for effective inhibitory responses. These differences could possibly arise from the differences in the cell line models used as well as density and presentation of ligands on the target cells.

As detailed in the introduction (Chapter 1), GD3 is aberrantly over expressed in tumours such as melanomas and acute lymphoblastic leukemias. Over-

expression of GD3 is known to facilitate various tumourigenic properties such as cell proliferation, invasion and metastasis (Cheresh et al., 1986;Zeng et al., 2000) (Hamamura et al., 2005). Breast cancer MDA-MB-231 cells over-expressing GD3 were shown to proliferate, independent of serum (Cazet et al., 2009). Constitutive activation of tyrosine kinases Erk1/2 and PI3K/Akt were shown to be responsible for this phenotype (Cazet et al., 2010). Recent reports from Furukawa's group have also tried to dissect the mechanisms relating to the altered phenotype of melanoma cell lines transfected with GD3S (discussed in introduction) (Hamamura et al., 2008;Ohkawa et al., 2010;Ohkawa et al., 2008). Put together these data underscores the role of GD3 in enhancing the malignant properties of tumours. GD3 has also been suggested as a possible inhibitor of NK cytotoxicity (Furukawa,K., 2008) (Bergelson et al., 1989). Based on these reports, the overexpression of GD3 on the K562 tumour cells could be expected to alter their susceptibility to NK cytotoxicity. However GD3 expression on K562 cells did not increase the resistance of these targets to NK cell lysis, in a Siglec-7 independent manner (Figure 5.9).

Integrin dependent modulation of NK cytotoxicity by Siglec-7:

LFA-1 is an important adhesion receptor for NK cells but also provide important signals required for natural cytotoxicity and ADCC. Initial studies on this receptor showed that LFA-1 contributed to early NK cytotoxicity signals (Barber et al., 2004). The cytotoxicity signals were shown to result in tyrosine phosphorylation of Vav-1, in a Src kinase dependent manner (Riteau et al., 2003). However, further studies revealed that LFA-1 signalling is important for NK cell granule polarization but not degranulation (March and Long., 2011)(Gross et al., 2010).

In chapter 4, results suggesting the regulatory role of Siglec-7 (expressed on NK92 cells) in affecting LFA-1 mediated functions such as adhesion, signalling and perforin polarization have been demonstrated. The data also showed a minimal role of sialic acid recognition in Siglec-7 activation. A model where constitutive *cis*-association of Siglec-7 with LFA-1 is sufficent to elicit its inhibitory roles was suggested as a mechanism (Figure 4.20,B).

The aim of this part of the project was to investigate if LFA-1 mediated cytotoxic action of IL-2 activated NK92 cells was affected by the over-expression of the inhibitory receptor Siglec-7 in these effector cells. The B16 (78) cell line was chosen as the target as they lack in ICAM-1 expression (Figure 5.11). Based on the model suggested in chapter 4, the B16(78) targets were modified to either express only ICAM-1 or co-express ICAM-1 and GD3 (figure 5.12). This approach would help examine if (1) Siglec-7 can affect cytotoxicity signals generated by LFA-1 by its constitutive association with the receptor (2) Siglec-7 requires the presence of a higher affinity glycan ligand such as GD3 in *trans* in order to regulate LFA-1 responses.

Siglec-7-Fc binding of ICAM-1 transfected B16 (78) cells showed no increased binding over wild type B16(78) cells. These cells were however bound the lectin SNA in a sialic acid dependent manner suggesting the expression of glycans carrying sialic acids in α 2,6 linkages (Figure 5.13). Expression of ICAM-1 on B16 (78) and B16 (78) GD3 cells caused a modest increase in their sensitivity to NK92 cytotoxicity compared to the wild type B16 (78) cells (Figure 5.14). Since wild type cells, lacking in ICAM-1 expression, were not sensitive to NK92 effectors, any increase in cytotoxicity of ICAM-1 positive targets was attributed

to a LFA-1/ICAM-1 mediated interactions. The use of anti-LFA-1 blocking antibodies to confirm the role of LFA-1 in this model system was not attempted.

In a preliminary experiment carried out, sensitivity of B16 (78) ICAM-1 GD3 expressing cells to both NK92 and NK92 Siglec-7 (S7(C14)) effectors was examined (Figure 5.15, A). The sensitivity of these targets was reduced significantly following the sialidase treatment of effector cells (Figure 5.15, B). The “masked” status of Siglec-7 on NK92 cells was confirmed with the help of suitable sialylated PAA probes, before and after sialidase treatment (Figure 5.15, C and D). These preliminary results are consistent with the notion that *trans* interactions of Siglec-7 with high affinity ligands such as GD3 or other disialylated glycolipids or glycoproteins can alter NK cytotoxicity responses.

The ganglioside disialosyl globopentaosylceramide (DSGb5), containing internally branched α 2,6 sialic acids, is a ligand for Siglec-7 (Kawasaki et al., 2010). Highly metastatic renal carcinoma cells, expressing DSGb5, was found to be resistant to NK cell cytotoxicity (Kawasakiet al., 2010).

However, using ICAM-1-Fc coated on to plates or beads, a constitutive *cis*-association between Siglec-7 and LFA-1, was demonstrated (Chapter 4). This *cis*- association was sufficient for Siglec-7 to mediate its inhibitory effects on LFA-1 signalling. Therefore the biological implication of these findings would require the use of ICAM-1 expressing target cells. Towards this experiments examining the sensitivity of B16 (78) ICAM-1 cells to NK92 cells, with and without Siglec-7 expression, will be needed.

Chapter 6

Discussion

The overall aim of this project was to dissect the role of the inhibitory receptor, Siglec-7, in NK cell recognition and killing of tumours via interactions with glycans. Healthy cells undergo aberrant changes in their ganglioside expression profiles during tumour transformation. They switch on the expression of complex gangliosides which are characteristically expressed during embryogenesis, for instance GD3 in cancers of neuroectodermal origin. These changes are known to support their survival and propagation.

The role of GD3 in enhancing tumour survival has been well demonstrated by using the human breast cancer cell line, MB-MDA-231, by Delannoy and group. Overexpression of GD3 on this cell line confers the cell with unusual growth properties (Cazet et al., 2009). Previous findings from our lab have shown that GD3 expression protects tumour cells from NK recognition (Nicoll et al., 2003). Thus it can be thought that the specific up-regulation of GD3 on tumours provide them with two main advantages – (1) survival (2) evasion of immune recognition. Recent evidence from glycolipid arrays consisting of combinations of gangliosides showed a clear modulation of Siglec-7 recognition of GD3 when present with structurally more complex gangliosides such as GM1 (Rinaldi et al., 2009). The implications of these findings in a biological setting would be the following:

(1) *cis*-interactions between GD3 and complex gangliosides such as GM1 on tumour surfaces could render the GD3 cryptic

(2) These interactions could alter Siglec-7 recognition and enhance NK cell killing

(3) These interactions can serve as potential novel mechanism of assessing tumour prognosis by screening for gangliosides

Although a previous study demonstrated that GD3 and GM1 do not exist on the same microdomains (Vyas et al., 2005), this was done using artificial monolayers and a single cell type, namely primary rat neuronal cells. Therefore in the present study it was felt important to perform an analysis of these gangliosides overexpressed in a tumour cell line

Flow cytometric analysis of the B16 (78) model cell line using Siglec-7-Fc proteins demonstrated decreased recognition of GD3 on cells with high expression of both GD3 and GM1. However, confocal microscopy analysis of these cells revealed that less than 3% of cells had patches of co-localization of GD3 and GM1. Lipid raft dissociation studies confirmed the absence of any cryptic GD3 on these cells. A breast cancer cell line was also genetically manipulated to over-express GD3. Confocal microscopy analysis of these cells confirmed that the two gangliosides existed on separate microdomains on the cell membrane. While my work was in progress, Dong et al reported similar findings in a breast cancer cell line (Dong et al., 2012). Their investigation into the molecular mechanism of this phenomenon showed that saturation levels and fatty acid composition of these gangliosides affected their accumulation in different microdomains. The inference from these findings is that *cis*-interactions between gangliosides are not favoured in model cell lines by means of genetic manipulation. However, it is possible that in primary tumours, such *cis*-interactions are formed and could contribute to tumour cell clearance by NK cells. The preferred segregation of gangliosides in membrane microdomains

could be a method of evasion adopted by tumour cells to escape NK cell surveillance. One of the main areas of research in the field of tumour cell biology is to understand the mechanisms involved in tumour cell escape from immunosurveillance. Therefore exploring such ganglioside cis-interactions in the context of primary tumours would be of potential benefit.

The second part of this project was to attempt to study the potential mechanisms by which Siglec-7 inhibits NK cell functions. We initiated the study by revisiting the role of the ganglioside ligand, GD3, in modulating the functions of this receptor. Here, we used two different effector systems and two different target models to confirm these findings. Indeed, Siglec-7 recognition of GD3 expressed on target cells resulted in the decrease of NK cell cytotoxic functions. These results were in line with the previous study from our lab (Nicoll et al., 2003). Most of the Siglecs are masked on cell surfaces and therefore require unmasking to interact with ligands in *trans*. Nicoll et al., also showed the same to be true for Siglec-7 in cytotoxicity assays involving GD3 expressing targets. Unmasking of the receptor expressed on the NK92 cell line was not a prerequisite for Siglec-7 recognition of ligand in *trans*. The receptor was able to overcome *cis* interactions with endogenous low affinity ligands and recognize ligands in *trans*. These results are interesting as they imply that NK responses can be effectively modulated by Siglec-7 recognition of high affinity ligands expressed on certain tumours, without the need for receptor unmasking. This may be a novel mechanism by which tumours affect immune cells. Therefore, Siglec-7 may be a potential target for antibody therapy in the treatment of certain classes of tumours with expression of high affinity ligands.

CD33 related Siglecs are broadly expressed on innate immune cells and their primary function is the tight regulation of immune responses. However sialylated pathogens seem to have evolved to take advantage of this function. The CD33 related Siglecs form a large gene cluster on the chromosome 19 and is thought to have originated by major inverse duplication of a small cluster of genes, over millions of years (Cao and Crocker, 2011). This cluster is well conserved in mammals. During the course of evolution, large scale gene deletion formed the rodent CD33r Siglec cluster from which the primate cluster is thought to have evolved (Cao et al., 2009). The latter cluster expanded as a result of gene duplication and is continually evolving (Varki and Angata, 2006). This expansion also led the formation of receptors with activating roles such as Siglec-14 and Siglec-16. However, specific de-selective pressure has led these receptors to become non-functional pseudogenes. Unlike primates, the rodent CD33r Siglec cluster is not evolving. This rapidly expanding repertoire of CD33r Siglecs in primates could be thought of as an evolutionary process to keep up with the different pathogens. Rodent NK cells do not have an equivalent of primate Siglec-7 that specifically recognizes disialic acids. This would imply that Siglec-7 on primate NK cells must have clear functional roles as an inhibitory receptor that justify its expression on NK cells, for example in the self-recognition of the cells of the nervous system. Neuronal cells lack MHC-I molecules and have been shown to be sensitive to direct killing by NK cells. (Backstrom et al., 2000). The recognition of disialylated gangliosides, expressed in abundance on neuronal cells, by Siglec-7, could protect them from NK mediated lysis (Nicoll et al., 2003).

During the course of this project, new evidence on the regulatory role of Siglec-E in controlling neutrophil responses via integrin signaling was published by our

laboratory (McMillan et al, 2013). Siglec-7 and Siglec-9 in primates are evolutionarily highly related to the rodent Siglec-E and are considered ‘functional orthologues’. It was thought possible that the regulatory role of Siglec-E in integrin signaling could be a conserved feature of these highly related siglecs. To investigate this for Siglec-7, an NK cell line deficient in the expression of Siglec-7 was used. Results showed that Siglec-7 expressing NK effector cells have the reduced ability to adhere to ICAM-1-Fc as well as to bring about polarization of perforin granules upon contact with ICAM-1-Fc coated beads. In an attempt to dissect the signaling mechanisms involved in this regulation, biochemical studies were able to identify Src kinase as a potential substrate of this inhibitory signalling pathway. Similar experiments, using target cells expressing ligands for LFA-1, would be needed to reconfirm these findings.

Vav-1, an important regulator of NK cytotoxicity, has been identified as one of the substrates of SHP-1 phosphatase activity. However these reports have made use of immunoprecipitation and a pan antibody against tryrosine phosphorylation. In this project, Vav-1 phosphorylation status in western blotting experiments was examined using an anti-phospho-Vav-1 antibody. Although blots are suggestive of the decreased phosphorylation of this guanine nucleotide exchange factor, further optimization of the antibody will be needed to confirm findings. Due to time constraints, it was not possible to investigate the previously described recruitment of SHP-1 with Siglec-7.

A few preliminary experiments looking at NK cytotoxicity of targets expressing the LFA-1 ligand, ICAM-1, also suggested that cytotoxicity responses were dampened in a Siglec-7 dependent manner. However, repeat experiments will

be needed to validate these findings and to clearly elucidate the mechanisms by which Siglec-7 recognition of ligands occurs.

The results obtained here may help define some of the factors involved in the modulation of NK cell function via the inhibitory receptor, Siglec-7. Upregulation of gangliosides and changes in glycosylation patterns on tumour targets may trigger strong inhibitory signals by Siglec-7 and increase the threshold needed by activatory signals to act on these targets. Effective strategies at blocking this receptor may enhance NK effector actions and thereby a stronger innate immune response against tumours.

References

Abram, C. L., and Lowell, C. A. (2009). The ins and outs of leukocyte integrin signaling. Annu Rev Immunol 27, 339.

Adamczyk, B., Tharmalingam, T., and Rudd, P. M. (2012). Glycans as cancer biomarkers. Biochim Biophys Acta 1820, 1347.

Akira, S., Uematsu, S., and Takeuchi, O. (2006). Pathogen recognition and innate immunity. Cell 124, 783.

Al Omar, S. Y., Marshall, E., Middleton, D., and Christmas, S. E. (2011). Increased killer immunoglobulin-like receptor expression and functional defects in natural killer cells in lung cancer. Immunology 133, 94.

Alphey, M. S., Attrill, H., Crocker, P. R., and van Aalten, D. M. (2003). High resolution crystal structures of Siglec-7. Insights into ligand specificity in the Siglec family. J Biol Chem 278, 3372.

Ando, M., Tu, W., Nishijima, K., and Iijima, S. (2008). Siglec-9 enhances IL-10 production in macrophages via tyrosine-based motifs. Biochemical and biophysical research communications 369, 878.

Angata, T., Hayakawa, T., Yamanaka, M., Varki, A., and Nakamura, M. (2006). Discovery of Siglec-14, a novel sialic acid receptor undergoing concerted evolution with Siglec-5 in primates. FASEB J 20, 1964.

Angata, T., Hingorani, R., Varki, N. M., and Varki, A. (2001). Cloning and characterization of a novel mouse Siglec, mSiglec-F: differential evolution of the mouse and human (CD33) Siglec-3-related gene clusters. The Journal of biological chemistry 276, 45128.

Angata, T., Ishii, T., Motegi, T., Oka, R., Taylor, R. E., Soto, P. C., Chang, Y. C., Secundino, I., Gao, C. X., Ohtsubo, K., Kitazume, S., Nizet, V., Varki, A., Gemma, A., Kida, K., and Taniguchi, N. (2013). Loss of Siglec-14 reduces the risk of chronic obstructive pulmonary disease exacerbation. Cell Mol Life Sci 70, 3199.

Angata, T., and Varki, A. (2000). Siglec-7: a sialic acid-binding lectin of the immunoglobulin superfamily. Glycobiology 10, 431.

Attrill, H., Imamura, A., Sharma, R. S., Kiso, M., Crocker, P. R., and van Aalten, D. M. (2006a). Siglec-7 undergoes a major conformational change when complexed with the alpha(2,8)-disialylganglioside GT1b. J Biol Chem 281, 32774.

Attrill, H., Takazawa, H., Witt, S., Kelm, S., Isecke, R., Brossmer, R., Ando, T., Ishida, H., Kiso, M., Crocker, P. R., and van Aalten, D. M. (2006b). The structure of siglec-7 in complex with sialosides: leads for rational structure-based inhibitor design. Biochem J 397, 271.

Avril, T., Floyd, H., Lopez, F., Vivier, E., and Crocker, P. R. (2004). The membrane-proximal immunoreceptor tyrosine-based inhibitory motif is critical for the inhibitory signaling mediated by Siglecs-7 and -9, CD33-related Siglecs expressed on human monocytes and NK cells. J Immunol 173, 6841.

Avril, T., North, S. J., Haslam, S. M., Willison, H. J., and Crocker, P. R. (2006a). Probing the cis interactions of the inhibitory receptor Siglec-7 with alpha2,8-disialylated ligands on natural killer cells and other leukocytes using glycan-specific antibodies and by analysis of alpha2,8-sialyltransferase gene expression. J Leukoc Biol 80, 787.

Avril, T., Wagner, E. R., Willison, H. J., and Crocker, P. R. (2006b). Sialic acid-binding immunoglobulin-like lectin 7 mediates selective recognition of sialylated glycans expressed on Campylobacter jejuni lipooligosaccharides. Infect Immun 74, 4133.

Backstrom, E., Chambers, B. J., Kristensson, K., and Ljunggren, H. G. (2000). Direct NK cell-mediated lysis of syngenic dorsal root ganglia neurons in vitro. J Immunol 165, 4895.

Bagriacik, E.U., Miller, K.S. (1999). Cell surface sialic acid and the regulation of immune cell interactions: the neuraminidase effect reconsidered. Glycobiology 9, 267.

Bakker, G. J., Eich, C., Torreno-Pina, J. A., Diez-Ahedo, R., Perez-Samper, G., van Zanten, T. S., Figdor, C. G., Cambi, A., and Garcia-Parajo, M. F. (2012). Lateral mobility of individual integrin nanoclusters orchestrates the onset for leukocyte adhesion. Proc Natl Acad Sci U S A 109, 4869.

Balaian, L., Zhong, R. K., and Ball, E. D. (2003). The inhibitory effect of anti-CD33 monoclonal antibodies on AML cell growth correlates with Syk and/or ZAP-70 expression. Exp Hematol 31, 363.

Balsamo, M., Manzini, C., Pietra, G., Raggi, F., Blengio, F., Mingari, M. C., Varesio, L., Moretta, L., Bosco, M. C., and Vitale, M. (2013). Hypoxia downregulates the expression of activating receptors involved in NK-cell-mediated target cell killing without affecting ADCC. Eur J Immunol.

Barber, D. F., Faure, M., and Long, E. O. (2004). LFA-1 contributes an early signal for NK cell cytotoxicity. J Immunol 173, 3653.

Barber, D. F., and Long, E. O. (2003). Coexpression of CD58 or CD48 with intercellular adhesion molecule 1 on target cells enhances adhesion of resting NK cells. J Immunol 170, 294.

Bennett, N. J., Ashiru, O., Morgan, F. J., Pang, Y., Okecha, G., Eagle, R. A., Trowsdale, J., Sissons, J. G., and Wills, M. R. (2010). Intracellular sequestration of the NKG2D ligand ULBP3 by human cytomegalovirus. J Immunol 185, 1093.

Billadeau, D. D., Upshaw, J. L., Schoon, R. A., Dick, C. J., and Leibson, P. J. (2003). NKG2D-DAP10 triggers human NK cell-mediated killing via a Syk-independent regulatory pathway. Nat Immunol 4, 557.

Birkle, S., Zeng, G., Gao, L., Yu, R. K., and Aubry, J. (2003). Role of tumor-associated gangliosides in cancer progression. Biochimie 85, 455.

Biswas, S., Biswas, K., Richmond, A., Ko, J., Ghosh, S., Simmons, M., Rayman, P., Rini, B., Gill, I., Tannenbaum, C. S., and Finke, J. H. (2009). Elevated levels of select gangliosides in T cells from renal cell carcinoma patients is associated with T cell dysfunction. J Immunol 183, 5050.

Blasius, A. L., Cella, M., Maldonado, J., Takai, T., and Colonna, M. (2006). Siglec-H is an IPC-specific receptor that modulates type I IFN secretion through DAP12. Blood 107, 2474.

Blixt, O., Collins, B. E., van den Nieuwenhof, I. M., Crocker, P. R., and Paulson, J. C. (2003). Sialoside specificity of the siglec family assessed using novel multivalent probes: identification of potent inhibitors of myelin-associated glycoprotein. J Biol Chem 278, 31007.

Bonilla, F. A., and Oettgen, H. C. (2010). Adaptive immunity. The Journal of allergy and clinical immunology 125, S33.

Borhis, G., Ahmed, P. S., Mbiribindi, B., Naiyer, M. M., Davis, D. M., Purbhoo, M. A., and Khakoo, S. I. (2013). A peptide antagonist disrupts NK cell inhibitory synapse formation. J Immunol 190, 2924.

Boyd, C. R., Orr, S. J., Spence, S., Burrows, J. F., Elliott, J., Carroll, H. P., Brennan, K., Ni Gabhann, J., Coulter, W. A., Jones, C., Crocker, P. R., Johnston, J. A., and Jefferies, C. A. (2009). Siglec-E is up-regulated and phosphorylated following lipopolysaccharide stimulation in order to limit TLR-driven cytokine production. J Immunol 183, 7703.

Brandt, C. S., Baratin, M., Yi, E. C., Kennedy, J., Gao, Z., Fox, B., Haldeman, B., Ostrander, C. D., Kaifu, T., Chabannon, C., Moretta, A., West, R., Xu, W., Vivier, E., and Levin, S. D. (2009). The B7 family member B7-H6 is a tumor cell ligand for the activating natural killer cell receptor NKp30 in humans. J Exp Med 206, 1495.

Braud, V. M., Allan, D. S., O'Callaghan, C. A., Soderstrom, K., D'Andrea, A., Ogg, G. S., Lazetic, S., Young, N. T., Bell, J. I., Phillips, J. H., Lanier, L. L., and McMichael, A. J. (1998). HLA-E binds to natural killer cell receptors CD94/NKG2A, B and C. Nature 391, 795.

Brodin, P., Lakshmikanth, T., Johansson, S., Karre, K., and Hoglund, P. (2009). The strength of inhibitory input during education quantitatively tunes the functional responsiveness of individual natural killer cells. Blood 113, 2434.

Bruhns, P., Marchetti, P., Fridman, W. H., Vivier, E., and Daeron, M. (1999). Differential roles of N- and C-terminal immunoreceptor tyrosine-based

inhibition motifs during inhibition of cell activation by killer cell inhibitory receptors. J Immunol 162, 3168.

Brunetta, E., Fogli, M., Varchetta, S., Bozzo, L., Hudspeth, K. L., Marcenaro, E., Moretta, A., and Mavilio, D. (2009). The decreased expression of Siglec-7 represents an early marker of dysfunctional natural killer-cell subsets associated with high levels of HIV-1 viremia. Blood 114, 3822.

Bryceson, Y. T., Ljunggren, H. G., and Long, E. O. (2009). Minimal requirement for induction of natural cytotoxicity and intersection of activation signals by inhibitory receptors. Blood 114, 2657.

Bryceson, Y. T., and Long, E. O. (2008). Line of attack: NK cell specificity and integration of signals. Curr Opin Immunol 20, 344.

Bryceson, Y. T., March, M. E., Barber, D. F., Ljunggren, H. G., and Long, E. O. (2005). Cytolytic granule polarization and degranulation controlled by different receptors in resting NK cells. J Exp Med 202, 1001.

Bryceson, Y. T., March, M. E., Ljunggren, H. G., and Long, E. O. (2006). Activation, coactivation, and costimulation of resting human natural killer cells. Immunol Rev 214, 73.

Burshtyn, D. N., Shin, J., Stebbins, C., and Long, E. O. (2000). Adhesion to target cells is disrupted by the killer cell inhibitory receptor. Curr Biol 10, 777.

Burshtyn, D. N., Yang, W., Yi, T., and Long, E. O. (1997). A novel phosphotyrosine motif with a critical amino acid at position -2 for the SH2 domain-mediated activation of the tyrosine phosphatase SHP-1. J Biol Chem 272, 13066.

Byrd, A., Hoffmann, S. C., Jarahian, M., Momburg, F., and Watzl, C. (2007). Expression analysis of the ligands for the Natural Killer cell receptors NKp30 and NKp44. PLoS One 2, e1339.

Cabanas, C., and Hogg, N. (1993). Ligand intercellular adhesion molecule 1 has a necessary role in activation of integrin lymphocyte function-associated molecule 1. Proc Natl Acad Sci U S A 90, 5838.

Calderwood, D. A., Yan, B., de Pereda, J. M., Alvarez, B. G., Fujioka, Y., Liddington, R. C., and Ginsberg, M. H. (2002). The phosphotyrosine binding-like domain of talin activates integrins. J Biol Chem 277, 21749.

Cao, H., and Crocker, P. R. (2011). Evolution of CD33-related siglecs: regulating host immune functions and escaping pathogen exploitation? Immunology 132, 18.

Cao, H., de Bono, B., Belov, K., Wong, E. S., Trowsdale, J., and Barrow, A. D. (2009). Comparative genomics indicates the mammalian CD33rSiglec locus evolved by an ancient large-scale inverse duplication and suggests all Siglecs share a common ancestral region. Immunogenetics 61, 401.

Cairo, C. W., Mirchev, R., and Golan, D. E. (2006). Cytoskeletal regulation couples LFA-1 conformational changes to receptor lateral mobility and clustering. Immunity 25, 297.

Carlin, A. F., Chang, Y. C., Areschoug, T., Lindahl, G., Hurtado-Ziola, N., King, C. C., Varki, A., and Nizet, V. (2009a). Group B Streptococcus suppression of phagocyte functions by protein-mediated engagement of human Siglec-5. J Exp Med 206, 1691.

Carlin, A. F., Uchiyama, S., Chang, Y. C., Lewis, A. L., Nizet, V., and Varki, A. (2009b). Molecular mimicry of host sialylated glycans allows a bacterial pathogen to engage neutrophil Siglec-9 and dampen the innate immune response. Blood 113, 3333.

Cazet, A., Bobowski, M., Rombouts, Y., Lefebvre, J., Steenackers, A., Popa, I., Guerardel, Y., Le Bourhis, X., Tulasne, D., and Delannoy, P. (2012). The ganglioside G(D2) induces the constitutive activation of c-Met in MDA-MB-231 breast cancer cells expressing the G(D3) synthase. Glycobiology 22, 806.

Cazet, A., Groux-Degroote, S., Teylaert, B., Kwon, K. M., Lehoux, S., Slomianny, C., Kim, C. H., Le Bourhis, X., and Delannoy, P. (2009). GD3 synthase overexpression enhances proliferation and migration of MDA-MB-231 breast cancer cells. Biol Chem 390, 601.

Cazet, A., Julien, S., Bobowski, M., Burchell, J., and Delannoy, P. (2010). Tumour-associated carbohydrate antigens in breast cancer. Breast Cancer Res 12, 204.

Cazet, A., Lefebvre, J., Adriaenssens, E., Julien, S., Bobowski, M., Grigoriadis, A., Tutt, A., Tulasne, D., Le Bourhis, X., and Delannoy, P. (2010). GD(3) synthase expression enhances proliferation and tumor growth of MDA-MB-231 breast cancer cells through c-Met activation. Mol Cancer Res 8, 1526.

Chalifour, A., Scarpellino, L., Back, J., Brodin, P., Devevre, E., Gros, F., Levy, F., Leclercq, G., Hoglund, P., Beermann, F., and Held, W. (2009). A Role for cis Interaction between the Inhibitory Ly49A receptor and MHC class I for natural killer cell education. Immunity 30, 337.

Chaplin, D. D. (2003). 1. Overview of the immune response. The Journal of allergy and clinical immunology 111, S442.

Chen, G. Y., Chen, X., King, S., Cavassani, K. A., Cheng, J., Zheng, X., Cao, H., Yu, H., Qu, J., Fang, D., Wu, W., Bai, X. F., Liu, J. Q., Woodiga, S. A., Chen, C., Sun, L., Hogaboam, C. M., Kunkel, S. L., Zheng, P., and Liu, Y. (2011). Amelioration of sepsis by inhibiting sialidase-mediated disruption of the CD24-SiglecG interaction. Nat Biotechnol 29, 428.

Chen, W., Han, C., Xie, B., Hu, X., Yu, Q., Shi, L., Wang, Q., Li, D., Wang, J., Zheng, P., Liu, Y., and Cao, X. (2013). Induction of Siglec-G by RNA viruses inhibits the innate immune response by promoting RIG-I degradation. Cell 152, 467.

Cheresh, D. A., Pierschbacher, M. D., Herzig, M. A., and Mujoo, K. (1986). Disialogangliosides GD2 and GD3 are involved in the attachment of human melanoma and neuroblastoma cells to extracellular matrix proteins. J Cell Biol 102, 688.

Cho, D., Shook, D. R., Shimasaki, N., Chang, Y. H., Fujisaki, H., and Campana, D. (2010). Cytotoxicity of activated natural killer cells against pediatric solid tumors. Clin Cancer Res 16, 3901.

Chokhawala, H.A., Yu, H., Chen, X. (2007). High-throughput substrate specificity studies of sialidases by using chemoenzymatically synthesized sialoside libraries. Chembiochem 8, 194.

Chua, H. L., Serov, Y., and Brahmi, Z. (2004). Regulation of FasL expression in natural killer cells. Human immunology 65, 317.

Collins, B. E., Blixt, O., DeSieno, A. R., Bovin, N., Marth, J. D., and Paulson, J. C. (2004). Masking of CD22 by cis ligands does not prevent redistribution of CD22 to sites of cell contact. Proc Natl Acad Sci U S A 101, 6104.

Collins, B.E., Blixt, O., Han, S., Duong, B., Li, H., Nathan, J.K., Bovin, N., Paulson, J.C. (2006). High-affinity ligand probes of CD22 overcome the threshold set by cis ligands to allow for binding, endocytosis, and killing of B cells. J Immunol 177, 2994.

Costantini, C., Cassatella, M.A. (2011). The defensive alliance between neutrophils and NK cells as a novel arm of innate immunity. J Leukoc Biol 89, 221.

Coudert, J. D., Scarpellino, L., Gros, F., Vivier, E., and Held, W. (2008). Sustained NKG2D engagement induces cross-tolerance of multiple distinct NK cell activation pathways. Blood 111, 3571.

Crocker, P. R. (2005). Siglecs in innate immunity. Curr Opin Pharmacol 5, 431.

Cruz-Munoz, M. E., and Veillette, A. (2010). Do NK cells always need a license to kill? Nature immunology 11, 279.

de Kruijf, E. M., Sajet, A., van Nes, J. G., Putter, H., Smit, V. T., Eagle, R. A., Jafferji, I., Trowsdale, J., Liefers, G. J., van de Velde, C. J., and Kuppen, P. J. (2012). NKG2D ligand tumor expression and association with clinical outcome in early breast cancer patients: an observational study. BMC Cancer 12, 24.

De Maria, A., Fogli, M., Costa, P., Murdaca, G., Puppo, F., Mavilio, D., Moretta, A., and Moretta, L. (2003). The impaired NK cell cytolytic function in viremic HIV-1 infection is associated with a reduced surface expression of natural cytotoxicity receptors (NKp46, NKp30 and NKp44). Eur J Immunol 33, 2410.

Decot, V., Voillard, L., Latger-Cannard, V., Aissi-Rothe, L., Perrier, P., Stoltz, J. F., and Bensoussan, D. (2010). Natural-killer cell amplification for adoptive leukemia relapse immunotherapy: comparison of three cytokines, IL-2, IL-

15, or IL-7 and impact on NKG2D, KIR2DL1, and KIR2DL2 expression. Exp Hematol 38, 351.

Dennehy, K. M., Klimosch, S. N., and Steinle, A. (2011). Cutting edge: NKp80 uses an atypical hemi-ITAM to trigger NK cytotoxicity. Journal of immunology 186, 657.

Diefenbach, A., Tomasello, E., Lucas, M., Jamieson, A. M., Hsia, J. K., Vivier, E., and Raulet, D. H. (2002). Selective associations with signaling proteins determine stimulatory versus costimulatory activity of NKG2D. Nat Immunol 3, 1142.

Dong, Z., Cruz-Munoz, M. E., Zhong, M. C., Chen, R., Latour, S., and Veillette, A. (2009). Essential function for SAP family adaptors in the surveillance of hematopoietic cells by natural killer cells. Nat Immunol 10, 973.

Dransfield, I., Cabanas, C., Craig, A., and Hogg, N. (1992). Divalent cation regulation of the function of the leukocyte integrin LFA-1. J Cell Biol 116, 219.

Dustin, M. L. (2010). Insights into function of the immunological synapse from studies with supported planar bilayers. Curr Top Microbiol Immunol 340, 1.

Eisele, G., Wischhusen, J., Mittelbronn, M., Meyermann, R., Waldhauer, I., Steinle, A., Weller, M., and Friese, M. A. (2006). TGF-beta and metalloproteinases differentially suppress NKG2D ligand surface expression on malignant glioma cells. Brain 129, 2416.

Erkeller-Yuksel, F. M., Lydyard, P. M., and Isenberg, D. A. (1997). Lack of NK cells in lupus patients with renal involvement. Lupus 6, 708.

Evans, R., Patzak, I., Svensson, L., De Filippo, K., Jones, K., McDowall, A., and Hogg, N. (2009). Integrins in immunity. J Cell Sci 122, 215.

Falco, M., Biassoni, R., Bottino, C., Vitale, M., Sivori, S., Augugliaro, R., Moretta, L., and Moretta, A. (1999). Identification and molecular cloning of p75/AIRM1, a novel member of the sialoadhesin family that functions as an inhibitory receptor in human natural killer cells. J Exp Med 190, 793.

Fauci, A. S., Mavilio, D., and Kottilil, S. (2005). NK cells in HIV infection: paradigm for protection or targets for ambush. Nat Rev Immunol 5, 835.

Faure, M., Barber, D. F., Takahashi, S. M., Jin, T., and Long, E. O. (2003). Spontaneous clustering and tyrosine phosphorylation of NK cell inhibitory receptor induced by ligand binding. J Immunol 170, 6107.

Ferlazzo, G., Pack, M., Thomas, D., Paludan, C., Schmid, D., Strowig, T., Bougras, G., Muller, W. A., Moretta, L., and Munz, C. (2004). Distinct roles of IL-12 and IL-15 in human natural killer cell activation by dendritic cells from secondary lymphoid organs. Proc Natl Acad Sci U S A 101, 16606.

Freeman, S. D., Kelm, S., Barber, E. K., and Crocker, P. R. (1995). Characterization of CD33 as a new member of the sialoadhesin family of cellular interaction molecules. Blood 85, 2005.

Furukawa, K., Hamamura, K., Ohkawa, Y., and Ohmi, Y. (2012). Disialyl gangliosides enhance tumor phenotypes with differential modalities. Glycoconj J 29, 579.

Furukawa, K., Hamamura, K., Nakashima, H., Furukawa, K. (2008). Molecules in the signaling pathway activated by gangliosides can be targets of therapeutics for malignant melanomas. Proteomics 8, 3312.

Gabri, M.R., Otero, L.L., Gomez, D.E., Alonso, D.F. (2009). Exogenous incorporation of neugc-rich mucin augments n-glycolyl sialic acid content and promotes malignant phenotype in mouse tumor cell lines. J Exp C Cancer Res 28, 146.

Galandrini, R., Palmieri, G., Piccoli, M., Frati, L., and Santoni, A. (1999). Role for the Rac1 exchange factor Vav in the signaling pathways leading to NK cell cytotoxicity. J Immunol 162, 3148.

Gasser, S., Orsulic, S., Brown, E. J., and Raulet, D. H. (2005). The DNA damage pathway regulates innate immune system ligands of the NKG2D receptor. Nature 436, 1186.

Gauld, S.B., Cambier, J.C. (2004). Src-family kinases in B-cell development and signaling. Oncogene 23, 8001.

Gazit, R., Gruda, R., Elboim, M., Arnon, T. I., Katz, G., Achdout, H., Hanna, J., Qimron, U., Landau, G., Greenbaum, E., Zakay-Rones, Z., Porgador, A., and Mandelboim, O. (2006). Lethal influenza infection in the absence of the natural killer cell receptor gene Ncr1. Nat Immunol 7, 517.

Geissmann, F., Manz, M. G., Jung, S., Sieweke, M. H., Merad, M., and Ley, K. (2010). Development of monocytes, macrophages, and dendritic cells. Science 327, 656.

Gerosa, F., Gobbi, A., Zorzi, P., Burg, S., Briere, F., Carra, G., and Trinchieri, G. (2005). The reciprocal interaction of NK cells with plasmacytoid or myeloid dendritic cells profoundly affects innate resistance functions. J Immunol 174, 727.

Gilfillan, S., Ho, E. L., Cella, M., Yokoyama, W. M., and Colonna, M. (2002). NKG2D recruits two distinct adapters to trigger NK cell activation and costimulation. Nat Immunol 3, 1150.

Gismondi, A., Jacobelli, J., Mainiero, F., Paolini, R., Piccoli, M., Frati, L., and Santoni, A. (2000). Cutting edge: functional role for proline-rich tyrosine kinase 2 in NK cell-mediated natural cytotoxicity. J Immunol 164, 2272.

Glasner, A., Ghadially, H., Gur, C., Stanietsky, N., Tsukerman, P., Enk, J., and Mandelboim, O. (2012). Recognition and prevention of tumor metastasis by the NK receptor NKp46/NCR1. J Immunol 188, 2509.

Gong, J. H., Maki, G., and Klingemann, H. G. (1994). Characterization of a human cell line (NK-92) with phenotypical and functional characteristics of activated natural killer cells. Leukemia 8, 652.

Graham, D. B., Cella, M., Giurisato, E., Fujikawa, K., Miletic, A. V., Kloeppel, T., Brim, K., Takai, T., Shaw, A. S., Colonna, M., and Swat, W. (2006). Vav1 controls DAP10-mediated natural cytotoxicity by regulating actin and microtubule dynamics. Journal of immunology 177, 2349.

Greenshields KN, Halstead SK, Zitman FM, Rinaldi S, Brennan KM, O'Leary C, et al. The neuropathic potential of anti-GM1 autoantibodies is regulated by the local glycolipid environment in mice. J Clin Invest 2009; 119:595-610.

Gross, C. C., Brzostowski, J. A., Liu, D., and Long, E. O. (2010). Tethering of intercellular adhesion molecule on target cells is required for LFA-1-dependent NK cell adhesion and granule polarization. J Immunol 185, 2918.

Guo, H. B., Lee, I., Kamar, M., Akiyama, S. K., and Pierce, M. (2002). Aberrant N-glycosylation of beta1 integrin causes reduced alpha5beta1 integrin clustering and stimulates cell migration. Cancer Res 62, 6837.

Gur, C., Enk, J., Weitman, E., Bachar, E., Suissa, Y., Cohen, G., Schyr, R. B., Sabanay, H., Horwitz, E., Glaser, B., Dor, Y., Pribluda, A., Hanna, J. H., Leibowitz, G., and Mandelboim, O. (2013). The expression of the Beta cell-derived autoimmune ligand for the killer receptor nkp46 is attenuated in type 2 diabetes. PLoS One 8, e74033.

Hakomori, S. (2003). Structure, organization, and function of glycosphingolipids in membrane. Curr Opin Hematol 10, 16.

Hamamura, K., Tsuji, M., Hotta, H., Ohkawa, Y., Takahashi, M., Shibuya, H., Nakashima, H., Yamauchi, Y., Hashimoto, N., Hattori, H., Ueda, M., and Furukawa, K. (2011). Functional activation of Src family kinase yes protein is essential for the enhanced malignant properties of human melanoma cells expressing ganglioside GD3. J Biol Chem 286, 18526.

Hamamura, K., Tsuji, M., Ohkawa, Y., Nakashima, H., Miyazaki, S., Urano, T., Yamamoto, N., Ueda, M., and Furukawa, K. (2008). Focal adhesion kinase as well as p130Cas and paxillin is crucially involved in the enhanced malignant properties under expression of ganglioside GD3 in melanoma cells. Biochim Biophys Acta 1780, 513.

Harburger, D. S., and Calderwood, D. A. (2009). Integrin signalling at a glance. J Cell Sci 122, 159.

Harris, E. S., McIntyre, T. M., Prescott, S. M., and Zimmerman, G. A. (2000). The leukocyte integrins. J Biol Chem 275, 23409.

Hecht, M. L., Rosental, B., Horlacher, T., Hershkovitz, O., De Paz, J. L., Noti, C., Schauer, S., Porgador, A., and Seeberger, P. H. (2009). Natural cytotoxicity

receptors NKp30, NKp44 and NKp46 bind to different heparan sulfate/heparin sequences. J Proteome Res 8, 712.

Heikema, A. P., Jacobs, B. C., Horst-Kreft, D., Huizinga, R., Kuijf, M. L., Endtz, H. P., Samsom, J. N., and van Wamel, W. J. (2013). Siglec-7 specifically recognizes Campylobacter jejuni strains associated with oculomotor weakness in Guillain-Barre syndrome and Miller Fisher syndrome. Clin Microbiol Infect 19, E106.

Helander, T. S., and Timonen, T. (1998). Adhesion in NK cell function. Curr Top Microbiol Immunol 230, 89.

Hershkovitz, O., Rosental, B., Rosenberg, L. A., Navarro-Sanchez, M. E., Jivov, S., Zilka, A., Gershoni-Yahalom, O., Brient-Litzler, E., Bedouelle, H., Ho, J. W., Campbell, K. S., Rager-Zisman, B., Despres, P., and Porgador, A. (2009). NKp44 receptor mediates interaction of the envelope glycoproteins from the West Nile and dengue viruses with NK cells. J Immunol 183, 2610.

Hirabayashi Y, Hamaoka A, Matsumoto M, Matsubara T, Tagawa M, Wakabayashi S, et al.(1985). Syngeneic monoclonal antibody against melanoma antigen with interspecies cross-reactivity recognizes GM3, a prominent ganglioside of B16 melanoma. J Biol Chem ; 260:13328-33.

Hogg, N., Henderson, R., Leitinger, B., McDowall, A., Porter, J., and Stanley, P. (2002). Mechanisms contributing to the activity of integrins on leukocytes. Immunol Rev 186, 164.

Hogg, N., Laschinger, M., Giles, K., and McDowall, A. (2003). T-cell integrins: more than just sticking points. J Cell Sci 116, 4695.

Hogg, N., Patzak, I., and Willenbrock, F. (2011). The insider's guide to leukocyte integrin signalling and function. Nat Rev Immunol 11, 416.

Hoglund, P., and Brodin, P. (2010). Current perspectives of natural killer cell education by MHC class I molecules. Nat Rev Immunol 10, 724.

Hossler, P., Khattak, S. F., and Li, Z. J. (2009). Optimal and consistent protein glycosylation in mammalian cell culture. Glycobiology 19, 936.

Hubbard, A.K., Rothlein, R. (2000). Intercellular adhesion molecule-1 (ICAM-1) expression and cell signaling cascades. Free Radic Biol Med 28, 1379.

Hudspeth, K., Silva-Santos, B., and Mavilio, D. (2013). Natural cytotoxicity receptors: broader expression patterns and functions in innate and adaptive immune cells. Front Immunol 4, 69.

Husain, Z., Huang, Y., Seth, P., and Sukhatme, V. P. (2013). Tumor-derived lactate modifies antitumor immune response: effect on myeloid-derived suppressor cells and NK cells. J Immunol 191, 1486.

Ikehara, Y., Ikehara, S. K., and Paulson, J. C. (2004). Negative regulation of T cell receptor signaling by Siglec-7 (p70/AIRM) and Siglec-9. J Biol Chem 279, 43117.

Ingley, E. (2012). Functions of the Lyn tyrosine kinase in health and disease. Cell Commun Signal 10, 21.

Ishida-Kitagawa, N., Tanaka, K., Bao, X., Kimura, T., Miura, T., Kitaoka, Y., Hayashi, K., Sato, M., Maruoka, M., Ogawa, T., Miyoshi, J., and Takeya, T. (2012). Siglec-15 protein regulates formation of functional osteoclasts in concert with DNAX-activating protein of 12 kDa (DAP12). The Journal of biological chemistry 287, 17493.

Ito, K., Higai, K., Sakurai, M., Shinoda, C., Yanai, K., Azuma, Y., and Matsumoto, K. (2011). Binding of natural cytotoxicity receptor NKp46 to sulfate- and alpha2,3-NeuAc-containing glycans and its mutagenesis. Biochem Biophys Res Commun 406, 377.

Ito, K., Higai, K., Shinoda, C., Sakurai, M., Yanai, K., Azuma, Y., and Matsumoto, K. (2012). Unlike natural killer (NK) p30, natural cytotoxicity receptor NKp44 binds to multimeric alpha2,3-NeuNAc-containing N-glycans. Biol Pharm Bull 35, 594.

Izawa, M., Kumamoto, K., Mitsuoka, C., Kanamori, C., Kanamori, A., Ohmori, K., Ishida, H., Nakamura, S., Kurata-Miura, K., Sasaki, K., Nishi, T., and Kannagi, R. (2000). Expression of sialyl 6-sulfo Lewis X is inversely correlated with conventional sialyl Lewis X expression in human colorectal cancer. Cancer Res 60, 1410.

Janeway CA Jr, Travers P, Walport M, et al. Immunobiology: The Immune System in Health and Disease. 5th edition. New York: Garland Science; 2001. B-cell activation by armed helper T cells. Available from:

Jellusova, J., Wellmann, U., Amann, K., Winkler, T. H., and Nitschke, L. (2010). CD22 x Siglec-G double-deficient mice have massively increased B1 cell numbers and develop systemic autoimmunity. J Immunol 184, 3618.

Jensen, H., Andresen, L., Nielsen, J., Christensen, J. P., and Skov, S. (2011). Vesicular stomatitis virus infection promotes immune evasion by preventing NKG2D-ligand surface expression. PLoS One 6, e23023.

Jiang, K., Zhong, B., Gilvary, D. L., Corliss, B. C., Vivier, E., Hong-Geller, E., Wei, S., and Djeu, J. Y. (2002). Syk regulation of phosphoinositide 3-kinase-dependent NK cell function. J Immunol 168, 3155.

Johansson, S., Johansson, M., Rosmaraki, E., Vahlne, G., Mehr, R., Salmon-Divon, M., Lemonnier, F., Karre, K., and Hoglund, P. (2005). Natural killer cell education in mice with single or multiple major histocompatibility complex class I molecules. J Exp Med 201, 1145.

Jonsson, A. H., and Yokoyama, W. M. (2009). Natural killer cell tolerance licensing and other mechanisms. Advances in immunology 101, 27.

Joyce, M. G., and Sun, P. D. (2011). The structural basis of ligand recognition by natural killer cell receptors. J Biomed Biotechnol 2011, 203628.

Jun, C. D., Shimaoka, M., Carman, C. V., Takagi, J., and Springer, T. A. (2001). Dimerization and the effectiveness of ICAM-1 in mediating LFA-1-dependent adhesion. Proc Natl Acad Sci U S A 98, 6830.

Kabat, J., Borrego, F., Brooks, A., and Coligan, J. E. (2002). Role that each NKG2A immunoreceptor tyrosine-based inhibitory motif plays in mediating the human CD94/NKG2A inhibitory signal. J Immunol 169, 1948.

Kaida, K., Morita, D., Kanzaki, M., Kamakura, K., Motoyoshi, K., Hirakawa, M., and Kusunoki, S. (2004). Ganglioside complexes as new target antigens in Guillain-Barre syndrome. Ann Neurol 56, 567.

Kane, L. P., Lin, J., and Weiss, A. (2000). Signal transduction by the TCR for antigen. Current opinion in immunology 12, 242.

Kardava, L., Moir, S., Wang, W., Ho, J., Buckner, C. M., Posada, J. G., O'Shea, M. A., Roby, G., Chen, J., Sohn, H. W., Chun, T. W., Pierce, S. K., and Fauci, A. S. (2011). Attenuation of HIV-associated human B cell exhaustion by siRNA downregulation of inhibitory receptors. J Clin Invest 121, 2614.

Karre, K. (2008). Natural killer cell recognition of missing self. Nature immunology 9, 477.

Karre, K., Ljunggren, H. G., Piontek, G., and Kiessling, R. (1986). Selective rejection of H-2-deficient lymphoma variants suggests alternative immune defence strategy. Nature 319, 675.

Katagiri, K., Imamura, M., and Kinashi, T. (2006). Spatiotemporal regulation of the kinase Mst1 by binding protein RAPL is critical for lymphocyte polarity and adhesion. Nat Immunol 7, 919.

Kawai, T., and Akira, S. (2010). The role of pattern-recognition receptors in innate immunity: update on Toll-like receptors. Nat Immunol 11, 373.

Kawasaki, N., Rademacher, C., and Paulson, J. C. (2011). CD22 regulates adaptive and innate immune responses of B cells. J Innate Immun 3, 411.

Kawasaki, Y., Ito, A., Withers, D. A., Taima, T., Kakoi, N., Saito, S., and Arai, Y. (2010). Ganglioside DSGb5, preferred ligand for Siglec-7, inhibits NK cell cytotoxicity against renal cell carcinoma cells. Glycobiology 20, 1373.

Kazarian, T., Jabbar, A. A., Wen, F. Q., Patel, D. A., and Valentino, L. A. (2003). Gangliosides regulate tumor cell adhesion to collagen. Clin Exp Metastasis 20, 311.

Kelm, S., Pelz, A., Schauer, R., Filbin, M. T., Tang, S., de Bellard, M. E., Schnaar, R. L., Mahoney, J. A., Hartnell, A., Bradfield, P., and et al. (1994). Sialoadhesin, myelin-associated glycoprotein and CD22 define a new family of sialic acid-dependent adhesion molecules of the immunoglobulin superfamily. Curr Biol 4, 965.

Kikuchi-Maki, A., Catina, T. L., and Campbell, K. S. (2005). Cutting edge: KIR2DL4 transduces signals into human NK cells through association with the Fc receptor gamma protein. J Immunol 174, 3859.

Kim, H. S., Das, A., Gross, C. C., Bryceson, Y. T., and Long, E. O. (2010). Synergistic signals for natural cytotoxicity are required to overcome inhibition by c-Cbl ubiquitin ligase. Immunity 32, 175.

Kim, H. S., and Long, E. O. (2012). Complementary phosphorylation sites in the adaptor protein SLP-76 promote synergistic activation of natural killer cells. Science signaling 5, ra49.

Kim, Y. H., Park, C. S., Lim, D. H., Son, B. K., Kim, J. H., Ahn, S. H., Bochner, B. S., Na, K., and Jang, T. Y. (2013). Antiallergic effect of anti-Siglec-F through reduction of eosinophilic inflammation in murine allergic rhinitis. Am J Rhinol Allergy 27, 187.

Kivi, E., Elima, K., Aalto, K., Nymalm, Y., Auvinen, K., Koivunen, E., Otto, D. M., Crocker, P. R., Salminen, T. A., Salmi, M., and Jalkanen, S. (2009). Human Siglec-10 can bind to vascular adhesion protein-1 and serves as its substrate. Blood 114, 5385.

Klaas, M., Oetke, C., Lewis, L. E., Erwig, L. P., Heikema, A. P., Easton, A., Willison, H. J., and Crocker, P. R. (2012). Sialoadhesin promotes rapid proinflammatory and type I IFN responses to a sialylated pathogen, Campylobacter jejuni. J Immunol 189, 2414.

Knibbs, R. N., Goldstein, I. J., Ratcliffe, R. M., and Shibuya, N. (1991). Characterization of the carbohydrate binding specificity of the leukoagglutinating lectin from Maackia amurensis. Comparison with other sialic acid-specific lectins. J Biol Chem 266, 83.

Kornbluth, J., Flomenberg, N., Dupont, B. (1982). Cell surface phenotype of a cloned line of human natural killer cells. J Immunol 129, 2831.

Kurzinger, K., Reynolds, T., Germain, R. N., Davignon, D., Martz, E., and Springer, T. A. (1981). A novel lymphocyte function-associated antigen (LFA-1): cellular distribution, quantitative expression, and structure. J Immunol 127, 596.

Kohl, S., Springer, T. A., Schmalstieg, F. C., Loo, L. S., and Anderson, D. C. (1984). Defective natural killer cytotoxicity and polymorphonuclear leukocyte antibody-dependent cellular cytotoxicity in patients with LFA-1/OKM-1 deficiency. J Immunol 133, 2972.

Kojima, M., Cease, K.B., Buckenmeyer, G.K., Berzofsky, J.A. (1988). Limiting dilution comparison of the repertoires of high and low responder MHC-restricted T cells. J Exp Med 167, 1100.

Kraft, M. L. (2013). Plasma membrane organization and function: moving past lipid rafts. Mol Biol Cell 24, 2765.

Kudo, D., Rayman, P., Horton, C., Cathcart, M. K., Bukowski, R. M., Thornton, M., Tannenbaum, C., and Finke, J. H. (2003). Gangliosides expressed by the renal cell carcinoma cell line SK-RC-45 are involved in tumor-induced apoptosis of T cells. Cancer Res 63, 1676.

Kurosaki, T., Shinohara, H., and Baba, Y. (2010). B cell signaling and fate decision. Annual review of immunology 28, 21.

Kwak-Kim, J., and Gilman-Sachs, A. (2008). Clinical implication of natural killer cells and reproduction. Am J Reprod Immunol 59, 388.

Labadia, M. E., Jeanfavre, D. D., Caviness, G. O., and Morelock, M. M. (1998). Molecular regulation of the interaction between leukocyte function-associated antigen-1 and soluble ICAM-1 by divalent metal cations. J Immunol 161, 836.

Lakshmikanth, T., Burke, S., Ali, T. H., Kimpfler, S., Ursini, F., Ruggeri, L., Capanni, M., Umansky, V., Paschen, A., Sucker, A., Pende, D., Groh, V., Biassoni, R., Hoglund, P., Kato, M., Shibuya, K., Schadendorf, D., Anichini, A., Ferrone, S., Velardi, A., Karre, K., Shibuya, A., Carbone, E., and Colucci, F. (2009). NCRs and DNAM-1 mediate NK cell recognition and lysis of human and mouse melanoma cell lines in vitro and in vivo. J Clin Invest 119, 1251.

Lam, K. K., Chiu, P. C., Lee, C. L., Pang, R. T., Leung, C. O., Koistinen, H., Seppala, M., Ho, P. C., and Yeung, W. S. (2011). Glycodelin-A protein interacts with Siglec-6 protein to suppress trophoblast invasiveness by down-regulating extracellular signal-regulated kinase (ERK)/c-Jun signaling pathway. J Biol Chem 286, 37118.

Landis, R. C., McDowall, A., Holness, C. L., Littler, A. J., Simmons, D. L., and Hogg, N. (1994). Involvement of the "I" domain of LFA-1 in selective binding to ligands ICAM-1 and ICAM-3. J Cell Biol 126, 529

Lanier, L.L. (2003). Natural killer cell receptor signaling. Curr Opin Immunol 15, 308.

Lanier, L.L. (2005). NK cell recognition. Annu Rev Immunol 23, 225.

Lanoue, A., Batista, F. D., Stewart, M., and Neuberger, M. S. (2002). Interaction of CD22 with alpha2,6-linked sialoglycoconjugates: innate recognition of self to dampen B cell autoreactivity? Eur J Immunol 32, 348.

Lawson, C., Wolf, S. (2009). ICAM-1 signaling in endothelial cells. Pharmacol Rep 61, 22.

Lee, E. U., Roth, J., and Paulson, J. C. (1989). Alteration of terminal glycosylation sequences on N-linked oligosaccharides of Chinese hamster ovary cells by expression of beta-galactoside alpha 2,6-sialyltransferase. J Biol Chem 264, 13848.

Li, F., Wei, H., Gao, Y., Xu, L., Yin, W., Sun, R., and Tian, Z. (2013). Blocking the natural killer cell inhibitory receptor NKG2A increases activity of human natural killer cells and clears hepatitis B virus infection in mice. Gastroenterology 144, 392.

Liu, G., Atteridge, C. L., Wang, X., Lundgren, A. D., and Wu, J. D. (2010). The membrane type matrix metalloproteinase MMP14 mediates constitutive shedding of MHC class I chain-related molecule A independent of A disintegrin and metalloproteinases. J Immunol 184, 3346.

Liu, J. H., Wei, S., Blanchard, D. K., and Djeu, J. Y. (1994). Restoration of lytic function in a human natural killer cell line by gene transfection. Cell Immunol 156, 24.

Littaua, R., Kurane, I., Ennis, F.A. (1990). Human IgG Fc receptor II mediates antibody-dependent enhancement of dengue virus infection. J Immunol 144, 3183.

Ljutic, B., Carlyle, J. R., Filipp, D., Nakagawa, R., Julius, M., and Zuniga-Pflucker, J. C. (2005). Functional requirements for signaling through the stimulatory and inhibitory mouse NKR-P1 (CD161) NK cell receptors. J Immunol 174, 4789.

Lloyd, K.O., Gordon, C.M., Thampoe, I.J., DiBenedetto, C. (1992). Cell surface accessibility of individual gangliosides in malignant melanoma cells to antibodies is influenced by the total ganglioside composition of the cells. Cancer Res 52, 4948.

Long, E. O. (2008). Negative signaling by inhibitory receptors: the NK cell paradigm. Immunol Rev 224, 70.

Long, E. O., Kim, H. S., Liu, D., Peterson, M. E., and Rajagopalan, S. (2013). Controlling natural killer cell responses: integration of signals for activation and inhibition. Annual review of immunology 31, 227.

Lopez, P. H., and Schnaar, R. L. (2009). Gangliosides in cell recognition and membrane protein regulation. Curr Opin Struct Biol 19, 549.

Lorenz, U. (2009). SHP-1 and SHP-2 in T cells: two phosphatases functioning at many levels. Immunol Rev 228, 342.

Lou, Z., Jevremovic, D., Billadeau, D. D., and Leibson, P. J. (2000). A balance between positive and negative signals in cytotoxic lymphocytes regulates the polarization of lipid rafts during the development of cell-mediated killing. J Exp Med 191, 347.

Love, P. E., and Hayes, S. M. (2010). ITAM-mediated signaling by the T-cell antigen receptor. Cold Spring Harbor perspectives in biology 2, a002485.

Lowell, C.A. (2011). Src-family and Syk kinases in activating and inhibitory pathways in innate immune cells: signaling cross talk. Cold Spring Harb Perspect Biol 3.

Lutz, C. T., and Kurago, Z. B. (1999). Human leukocyte antigen class I expression on squamous cell carcinoma cells regulates natural killer cell activity. Cancer Res 59, 5793.

Mace, E. M., Zhang, J., Siminovitch, K. A., and Takei, F. (2010). Elucidation of the integrin LFA-1-mediated signaling pathway of actin polarization in natural killer cells. Blood 116, 1272.

Magri, G., Muntasell, A., Romo, N., Saez-Borderias, A., Pende, D., Geraghty, D. E., Hengel, H., Angulo, A., Moretta, A., and Lopez-Botet, M. (2011). NKp46 and DNAM-1 NK-cell receptors drive the response to human cytomegalovirus-infected myeloid dendritic cells overcoming viral immune evasion strategies. Blood 117, 848.

Malinin, N. L., Plow, E. F., and Byzova, T. V. (2010). Kindlins in FERM adhesion. Blood 115, 4011.

Malpass, K. (2013). Alzheimer disease: functional dissection of CD33 locus implicates innate immune response in Alzheimer disease pathology. Nat Rev Neurol 9, 360.

Mainiero, F., Soriani, A., Strippoli, R., Jacobelli, J., Gismondi, A., Piccoli, M., Frati, L., and Santoni, A. (2000). RAC1/P38 MAPK signaling pathway controls beta1 integrin-induced interleukin-8 production in human natural killer cells. Immunity 12, 7.

Maki, G., Klingemann, H. G., Martinson, J. A., and Tam, Y. K. (2001). Factors regulating the cytotoxic activity of the human natural killer cell line, NK-92. J Hematother Stem Cell Res 10, 369.

lboim, O., Lieberman, N., Lev, M., Paul, L., Arnon, T. I., Bushkin, Y., Davis, D. M., Strominger, J. L., Yewdell, J. W., and Porgador, A. (2001). Recognition of haemagglutinins on virus-infected cells by NKp46 activates lysis by human NK cells. Nature 409, 1055.

Mantovani, A., Cassatella, M. A., Costantini, C., and Jaillon, S. (2011). Neutrophils in the activation and regulation of innate and adaptive immunity. Nature reviews. Immunology 11, 519.

March, M. E., and Long, E. O. (2011). beta2 integrin induces TCRzeta-Syk-phospholipase C-gamma phosphorylation and paxillin-dependent granule polarization in human NK cells. J Immunol 186, 2998.

Marlin, S.D., Springer, T.A. (1987). Purified intercellular adhesion molecule-1 (ICAM-1) is a ligand for lymphocyte function-associated antigen 1 (LFA-1). Cell 51, 813.

Martner, A., Thoren, F. B., Aurelius, J., and Hellstrand, K. (2013). Immunotherapeutic strategies for relapse control in acute myeloid leukemia. Blood Rev 27, 209.

Marwali, M. R., Rey-Ladino, J., Dreolini, L., Shaw, D., and Takei, F. (2003). Membrane cholesterol regulates LFA-1 function and lipid raft heterogeneity. Blood 102, 215.

McGilvray, R. W., Eagle, R. A., Rolland, P., Jafferji, I., Trowsdale, J., and Durrant, L. G. (2010). ULBP2 and RAET1E NKG2D ligands are independent predictors of poor prognosis in ovarian cancer patients. Int J Cancer 127, 1412.

McGilvray, R. W., Eagle, R. A., Watson, N. F., Al-Attar, A., Ball, G., Jafferji, I., Trowsdale, J., and Durrant, L. G. (2009). NKG2D ligand expression in human colorectal cancer reveals associations with prognosis and evidence for immunoediting. Clin Cancer Res 15, 6993.

McMillan, S. J., and Crocker, P. R. (2008). CD33-related sialic-acid-binding immunoglobulin-like lectins in health and disease. Carbohydr Res 343, 2050.

McMillan, S. J., Sharma, R. S., McKenzie, E. J., Richards, H. E., Zhang, J., Prescott, A., and Crocker, P. R. (2013). Siglec-E is a negative regulator of acute pulmonary neutrophil inflammation and suppresses CD11b beta2-integrin-dependent signaling. Blood 121, 2084.

Mendelson, M., Tekoah, Y., Zilka, A., Gershoni-Yahalom, O., Gazit, R., Achdout, H., Bovin, N. V., Meningher, T., Mandelboim, M., Mandelboim, O., David, A., and Porgador, A. (2010). NKp46 O-glycan sequences that are involved in the interaction with hemagglutinin type 1 of influenza virus. J Virol 84, 3789.

Milani, S., Sottocornola, E., Zava, S., Galbiati, M., Berra, B., and Colombo, I. (2010). Gangliosides influence EGFR/ErbB2 heterodimer stability but they do not modify EGF-dependent ErbB2 phosphorylation. Biochim Biophys Acta 1801, 617.

Miljan, E. A., Meuillet, E. J., Mania-Farnell, B., George, D., Yamamoto, H., Simon, H. G., and Bremer, E. G. (2002). Interaction of the extracellular domain of the epidermal growth factor receptor with gangliosides. J Biol Chem 277, 10108.

Miyazaki, K., Ohmori, K., Izawa, M., Koike, T., Kumamoto, K., Furukawa, K., Ando, T., Kiso, M., Yamaji, T., Hashimoto, Y., Suzuki, A., Yoshida, A., Takeuchi, M., and Kannagi, R. (2004). Loss of disialyl Lewis(a), the ligand for lymphocyte inhibitory receptor sialic acid-binding immunoglobulin-like lectin-7 (Siglec-7) associated with increased sialyl Lewis(a) expression on human colon cancers. Cancer Res 64, 4498.

Miyazaki, K., Sakuma, K., Kawamura, Y. I., Izawa, M., Ohmori, K., Mitsuki, M., Yamaji, T., Hashimoto, Y., Suzuki, A., Saito, Y., Dohi, T., and Kannagi, R. (2012). Colonic epithelial cells express specific ligands for mucosal macrophage immunosuppressive receptors siglec-7 and -9. J Immunol 188, 4690.

Mocsai, A. (2013). Diverse novel functions of neutrophils in immunity, inflammation, and beyond. J Exp Med 210, 1283.

Mocsai, A., Abram, C. L., Jakus, Z., Hu, Y., Lanier, L. L., and Lowell, C. A. (2006). Integrin signaling in neutrophils and macrophages uses adaptors containing immunoreceptor tyrosine-based activation motifs. Nat Immunol 7, 1326.

Mocsai, A., Ruland, J., and Tybulewicz, V. L. (2010). The SYK tyrosine kinase: a crucial player in diverse biological functions. Nat Rev Immunol 10, 387.

Mocsai, A., Zhou, M., Meng, F., Tybulewicz, V. L., and Lowell, C. A. (2002). Syk is required for integrin signaling in neutrophils. Immunity 16, 547.

Monteiro de Castro, G., Eduarda Zanin, M., Ventura-Oliveira, D., Aparecida Vilella, C., Ashimine, R., and de Lima Zollner, R. (2004). Th1 and Th2 cytokine immunomodulation by gangliosides in experimental autoimmune encephalomyelitis. Cytokine 26, 155.

Montel, A. H., Bochan, M. R., Hobbs, J. A., Lynch, D. H., and Brahmi, Z. (1995). Fas involvement in cytotoxicity mediated by human NK cells. Cellular immunology 166, 236.

Morandi, B., Mortara, L., Chiossone, L., Accolla, R. S., Mingari, M. C., Moretta, L., Moretta, A., and Ferlazzo, G. (2012). Dendritic cell editing by activated natural killer cells results in a more protective cancer-specific immune response. PLoS One 7, e39170.

Moretta, A., Pende, D., Locatelli, F., and Moretta, L. (2009). Activating and inhibitory killer immunoglobulin-like receptors (KIR) in haploidentical haemopoietic stem cell transplantation to cure high-risk leukaemias. Clin Exp Immunol 157, 325.

Moretta, L., and Moretta, A. (2004). Unravelling natural killer cell function: triggering and inhibitory human NK receptors. EMBO J 23, 255.

Muller, J., Obermeier, I., Wohner, M., Brandl, C., Mrotzek, S., Angermuller, S., Maity, P. C., Reth, M., and Nitschke, L. (2013). CD22 ligand-binding and signaling domains reciprocally regulate B-cell Ca2+ signaling. Proc Natl Acad Sci U S A 110, 12402.

Mutoh, T., Tokuda, A., Miyadai, T., Hamaguchi, M., and Fujiki, N. (1995). Ganglioside GM1 binds to the Trk protein and regulates receptor function. Proc Natl Acad Sci U S A 92, 5087.

Nakakuma, H., Horikawa, K., Kawaguchi, T., Hidaka, M., kura, S., Hirai, S., Kageshita, T., Ono, T., Kagimoto, T., Iwamori, M., and et al. (1992). Common phenotypic

expression of gangliosides GM3 and GD3 in normal human tissues and neoplastic skin lesions. Jpn J Clin Oncol 22, 308.

Nakayama, J., Guan, X. C., Nakashima, M., Mashino, T., and Hori, Y. (1997). In vitro comparison between mouse B16 and human melanoma cell lines of the expression of ICAM-1 induced by cytokines and/or hyperthermia. J Dermatol 24, 351.

Nicoll, G., Avril, T., Lock, K., Furukawa, K., Bovin, N., and Crocker, P. R. (2003). Ganglioside GD3 expression on target cells can modulate NK cell cytotoxicity via siglec-7-dependent and -independent mechanisms. Eur J Immunol 33, 1642.

Nicoll, G., Ni, J., Liu, D., Klenerman, P., Munday, J., Dubock, S., Mattei, M. G., and Crocker, P. R. (1999). Identification and characterization of a novel siglec, siglec-7, expressed by human natural killer cells and monocytes. J Biol Chem 274, 34089.

O'Keefe, T. L., Williams, G. T., Davies, S. L., and Neuberger, M. S. (1996). Hyperresponsive B cells in CD22-deficient mice. Science 274, 798.

Ohkawa, Y., Miyazaki, S., Hamamura, K., Kambe, M., Miyata, M., Tajima, O., Ohmi, Y., Yamauchi, Y., and Furukawa, K. (2010). Ganglioside GD3 enhances adhesion signals and augments malignant properties of melanoma cells by recruiting integrins to glycolipid-enriched microdomains. J Biol Chem 285, 27213.

Ohkawa, Y., Miyazaki, S., Miyata, M., Hamamura, K., and Furukawa, K. (2008). Essential roles of integrin-mediated signaling for the enhancement of malignant properties of melanomas based on the expression of GD3. Biochem Biophys Res Commun 373, 14.

Ohmi, Y., Tajima, O., Ohkawa, Y., Yamauchi, Y., Sugiura, Y., and Furukawa, K. (2011). Gangliosides are essential in the protection of inflammation and neurodegeneration via maintenance of lipid rafts: elucidation by a series of ganglioside-deficient mutant mice. J Neurochem 116, 926.

Ohta, M., Ishida, A., Toda, M., Akita, K., Inoue, M., Yamashita, K., Watanabe, M., Murata, T., Usui, T., and Nakada, H. (2010). Immunomodulation of monocyte-derived dendritic cells through ligation of tumor-produced mucins to Siglec-9. Biochem Biophys Res Commun 402, 663.

Orange, J. S. (2008). Formation and function of the lytic NK-cell immunological synapse. Nat Rev Immunol 8, 713.

Park, Y. P., Choi, S. C., Kiesler, P., Gil-Krzewska, A., Borrego, F., Weck, J., Krzewski, K., and Coligan, J. E. (2011). Complex regulation of human NKG2D-DAP10 cell surface expression: opposing roles of the gammac cytokines and TGF-beta1. Blood 118, 3019.

Parsons, S.J., Parsons, J.T. (2004). Src family kinases, key regulators of signal transduction. Oncogene 23, 7906.

Paulson, J. C., Macauley, M. S., and Kawasaki, N. (2012). Siglecs as sensors of self in innate and adaptive immune responses. Ann N Y Acad Sci 1253, 37.

Pereira, S., Zhou, M., Mocsai, A., and Lowell, C. (2001). Resting murine neutrophils express functional alpha 4 integrins that signal through Src family kinases. J Immunol 166, 4115.

Perez, O.D., Mitchell, D., Jager, G.C., Nolan, G.P. (2004). LFA-1 signaling through p44/42 is coupled to perforin degranulation in CD56+CD8+ natural killer cells. Blood 104, 1083.

Peterson, M. E., and Long, E. O. (2008). Inhibitory receptor signaling via tyrosine phosphorylation of the adaptor Crk. Immunity 29, 578.

Poe, J. C., and Tedder, T. F. (2012). CD22 and Siglec-G in B cell function and tolerance. Trends Immunol 33, 413.

Porter, J. C., Bracke, M., Smith, A., Davies, D., and Hogg, N. (2002). Signaling through integrin LFA-1 leads to filamentous actin polymerization and remodeling, resulting in enhanced T cell adhesion. J Immunol 168, 6330.

Pretzlaff, R.K., Xue, V.W., Rowin, M.E. (2000). Sialidase treatment exposes the beta1-integrin active ligand binding site on HL60 cells and increases binding to fibronectin. Cell Adhes Commun 7, 491.

Purdy, A. K., and Campbell, K. S. (2009). Natural killer cells and cancer: regulation by the killer cell Ig-like receptors (KIR). Cancer Biol Ther 8, 2211.

Raulet, D. H., Gasser, S., Gowen, B. G., Deng, W., and Jung, H. (2013). Regulation of ligands for the NKG2D activating receptor. Annu Rev Immunol 31, 413.

Raulet, D. H., and Vance, R. E. (2006). Self-tolerance of natural killer cells. Nature reviews. Immunology 6, 520.

Razi, N., and Varki, A. (1998). Masking and unmasking of the sialic acid-binding lectin activity of CD22 (Siglec-2) on B lymphocytes. Proc Natl Acad Sci U S A 95, 7469.

Razi, N., and Varki, A. (1999). Cryptic sialic acid binding lectins on human blood leukocytes can be unmasked by sialidase treatment or cellular activation. Glycobiology 9, 1225.

Rinaldi, S., Brennan, K. M., Goodyear, C. S., O'Leary, C., Schiavo, G., Crocker, P. R., and Willison, H. J. (2009). Analysis of lectin binding to glycolipid complexes using combinatorial glycoarrays. Glycobiology 19, 789.

Rinaldi, S., Brennan, K. M., and Willison, H. J. (2010). Heteromeric glycolipid complexes as modulators of autoantibody and lectin binding. Progress in lipid research 49, 87.

Riteau, B., Barber, D. F., and Long, E. O. (2003). Vav1 phosphorylation is induced by beta2 integrin engagement on natural killer cells upstream of actin cytoskeleton and lipid raft reorganization. J Exp Med 198, 469.

Rodacki, M., Svoren, B., Butty, V., Besse, W., Laffel, L., Benoist, C., and Mathis, D. (2007). Altered natural killer cells in type 1 diabetic patients. Diabetes 56, 177.

Roland, C.L., Harken, A.H., Sarr, M.G., Barnett, C.C., Jr. (2007). ICAM-1 expression determines malignant potential of cancer. Surgery 141, 705.

Ruan S, Lloyd KO. (1992) Glycosylation pathways in the biosynthesis of gangliosides in melanoma and neuroblastoma cells: relative glycosyltransferase levels determine ganglioside patterns. Cancer Res; 52:5725-31.

Ruan, S., Raj, B.K., Lloyd, K.O. (1999). Relationship of glycosyltransferases and mRNA levels to ganglioside expression in neuroblastoma and melanoma cells. J Neurochem 72, 514.

Ruckhaberle, E., Karn, T., Rody, A., Hanker, L., Gatje, R., Metzler, D., Holtrich, U., and Kaufmann, M. (2009). Gene expression of ceramide kinase, galactosyl ceramide synthase and ganglioside GD3 synthase is associated with prognosis in breast cancer. J Cancer Res Clin Oncol 135, 1005.

Salih, H. R., Rammensee, H. G., and Steinle, A. (2002). Cutting edge: down-regulation of MICA on human tumors by proteolytic shedding. J Immunol 169, 4098.

Santana, M. A., and Rosenstein, Y. (2003). What it takes to become an effector T cell: the process, the cells involved, and the mechanisms. Journal of cellular physiology 195, 392.

Saulquin, X., Gastinel, L. N., and Vivier, E. (2003). Crystal structure of the human natural killer cell activating receptor KIR2DS2 (CD158j). J Exp Med 197, 933.

Savan, R., Chan, T., Young, H.A. (2010). Lentiviral gene transduction in human and mouse NK cell lines. Methods Mol Biol 612, 209.

Schnaar RL, Suzuki A, Stanley P. Glycosphingolipids. In: Varki A, Cummings RD, Esko JD, et al., editors. 2009. Essentials of Glycobiology. 2nd edition. Cold Spring Harbor (NY): Cold Spring Harbor Laboratory Press; Chapter 10.

Schleinitz, N., March, M. E., and Long, E. O. (2008). Recruitment of activation receptors at inhibitory NK cell immune synapses. PLoS One 3, e3278.

Schleinitz, N., Vely, F., Harle, J. R., and Vivier, E. (2010). Natural killer cells in human autoimmune diseases. Immunology 131, 451.

Scott, C.J., Marouf, W.M., Quinn, D.J., Buick, R.J., Orr, S.J., Donnelly, R.F., McCarron, P.A. (2008). Immunocolloidal targeting of the endocytotic siglec-7 receptor using peripheral attachment of siglec-7 antibodies to poly(lactide-co-glycolide) nanoparticles. Pharm Res 25, 135.

Segovis, C. M., Schoon, R. A., Dick, C. J., Nacusi, L. P., Leibson, P. J., and Billadeau, D. D. (2009). PI3K links NKG2D signaling to a CrkL pathway involved in natural killer cell adhesion, polarity, and granule secretion. J Immunol 182, 6933.

Shibuya, K., Lanier, L. L., Phillips, J. H., Ochs, H. D., Shimizu, K., Nakayama, E., Nakauchi, H., and Shibuya, A. (1999). Physical and functional association of LFA-1 with DNAM-1 adhesion molecule. Immunity 11, 615.

Shimizu, Y., and Mobley, J. L. (1993). Distinct divalent cation requirements for integrin-mediated CD4+ T lymphocyte adhesion to ICAM-1, fibronectin, VCAM-1, and invasin. J Immunol 151, 4106.

Simons, K., and Sampaio, J. L. (2011). Membrane organization and lipid rafts. Cold Spring Harb Perspect Biol 3, a004697.

Sivori, S., Parolini, S., Marcenaro, E., Castriconi, R., Pende, D., Millo, R., Moretta, A. (2000). Involvement of natural cytotoxicity receptors in human natural killer cell-mediated lysis of neuroblastoma and glioblastoma cell lines. J Neuroimmunol 107, 220.

Smith, A., Carrasco, Y. R., Stanley, P., Kieffer, N., Batista, F. D., and Hogg, N. (2005). A talin-dependent LFA-1 focal zone is formed by rapidly migrating T lymphocytes. J Cell Biol 170, 141.

Smith-Garvin, J. E., Koretzky, G. A., and Jordan, M. S. (2009). T cell activation. Annual review of immunology 27, 591.

Sonnino, S., Mauri, L., Chigorno, V., and Prinetti, A. (2007). Gangliosides as components of lipid membrane domains. Glycobiology 17, 1R.

Sonnino, S., and Prinetti, A. (2013). Membrane domains and the "lipid raft" concept. Curr Med Chem 20, 4.

Standeven, L. J., Carlin, L. M., Borszcz, P., Davis, D. M., and Burshtyn, D. N. (2004). The actin cytoskeleton controls the efficiency of killer Ig-like receptor accumulation at inhibitory NK cell immune synapses. J Immunol 173, 5617.

Stebbins, C. C., Watzl, C., Billadeau, D. D., Leibson, P. J., Burshtyn, D. N., and Long, E. O. (2003). Vav1 dephosphorylation by the tyrosine phosphatase SHP-1 as a mechanism for inhibition of cellular cytotoxicity. Mol Cell Biol 23, 6291.

Sun, C., Fu, B., Gao, Y., Liao, X., Sun, R., Tian, Z., and Wei, H. (2012). TGF-beta1 down-regulation of NKG2D/DAP10 and 2B4/SAP expression on human NK cells contributes to HBV persistence. PLoS Pathog 8, e1002594.

Tai T, Kawashima I, Furukawa K, Lloyd KO. (1988). Monoclonal antibody R24 distinguishes between different N-acetyl- and N-glycolylneuraminic acid derivatives of ganglioside GD3. Arch Biochem Biophys ; 260:51-5

Takeuchi, O., and Akira, S. (2010). Pattern recognition receptors and inflammation. Cell 140, 805.

Tam, Y. K., Maki, G., Miyagawa, B., Hennemann, B., Tonn, T., and Klingemann, H. G. (1999). Characterization of genetically altered, interleukin 2-independent natural killer cell lines suitable for adoptive cellular immunotherapy. Hum Gene Ther 10, 1359.

Tateno, H., Li, H., Schur, M.J., Bovin, N., Crocker, P.R., Wakarchuk, W.W., Paulson, J.C. (2007). Distinct endocytic mechanisms of CD22 (Siglec-2) and Siglec-F reflect roles in cell signaling and innate immunity. Mol Cell Biol 27, 5699

Torres Demichelis, V., Vilcaes, A. A., Iglesias-Bartolome, R., Ruggiero, F. M., and Daniotti, J. L. (2013). Targeted delivery of immunotoxin by antibody to ganglioside GD3: a novel drug delivery route for tumor cells. PLoS One 8, e55304.

Totani, L., Piccoli, A., Manarini, S., Federico, L., Pecce, R., Martelli, N., Cerletti, C., Piccardoni, P., Lowell, C.A., Smyth, S.S., Berton, G., Evangelista, V. (2006). Src-family kinases mediate an outside-in signal necessary for beta2 integrins to achieve full activation and sustain firm adhesion of polymorphonuclear leucocytes tethered on E-selectin. Biochem J 396, 89.

Trapani, J. A., and Smyth, M. J. (2002). Functional significance of the perforin/granzyme cell death pathway. Nature reviews. Immunology 2, 735.

Tsukerman, P., Stern-Ginossar, N., Gur, C., Glasner, A., Nachmani, D., Bauman, Y., Yamin, R., Vitenshtein, A., Stanietsky, N., Bar-Mag, T., Lankry, D., and Mandelboim, O. (2012). MiR-10b downregulates the stress-induced cell surface molecule MICB, a critical ligand for cancer cell recognition by natural killer cells. Cancer Res 72, 5463.

Uhrberg, M., Valiante, N. M., Shum, B. P., Shilling, H. G., Lienert-Weidenbach, K., Corliss, B., Tyan, D., Lanier, L. L., and Parham, P. (1997). Human diversity in killer cell inhibitory receptor genes. Immunity 7, 753.

Upshaw, J. L., Arneson, L. N., Schoon, R. A., Dick, C. J., Billadeau, D. D., and Leibson, P. J. (2006). NKG2D-mediated signaling requires a DAP10-bound Grb2-Vav1 intermediate and phosphatidylinositol-3-kinase in human natural killer cells. Nature immunology 7, 524.

Vacca, P., Mingari, M. C., and Moretta, L. (2013). Natural killer cells in human pregnancy. J Reprod Immunol 97, 14.

Varki, A., and Angata, T. (2006). Siglecs--the major subfamily of I-type lectins. Glycobiology 16, 1R.

Varki A, Cummings R, Esko J, et al., editors. (1999) Essentials of Glycobiology. Cold Spring Harbor (NY): Cold Spring Harbor Laboratory Press; Chapter 4, Protein-Glycan Interactions.

Varki, A., and Gagneux, P. (2012). Multifarious roles of sialic acids in immunity. Ann N Y Acad Sci 1253, 16.

Varki A, Schauer R. Sialic Acids. (20090 In: Varki A, Cummings RD, Esko JD, et al., editors. Essentials of Glycobiology. 2nd edition. Cold Spring Harbor (NY): Cold Spring Harbor Laboratory Press; Chapter 14.

Veillette, A. (2010). SLAM-family receptors: immune regulators with or without SAP-family adaptors. Cold Spring Harb Perspect Biol 2, a002469.

Vely, F., Olivero, S., Olcese, L., Moretta, A., Damen, J. E., Liu, L., Krystal, G., Cambier, J. C., Daeron, M., and Vivier, E. (1997). Differential association of phosphatases with hematopoietic co-receptors bearing immunoreceptor tyrosine-based inhibition motifs. Eur J Immunol 27, 1994.

Vitale, C., Romagnani, C., Puccetti, A., Olive, D., Costello, R., Chiossone, L., Pitto, A., Bacigalupo, A., Moretta, L., and Mingari, M. C. (2001). Surface expression and function of p75/AIRM-1 or CD33 in acute myeloid leukemias: engagement of CD33 induces apoptosis of leukemic cells. Proc Natl Acad Sci U S A 98, 5764.

Vivier, E., Nunes, J. A., and Vely, F. (2004). Natural killer cell signaling pathways. Science 306, 1517.

Vivier, E., Tomasello, E., Baratin, M., Walzer, T., and Ugolini, S. (2008). Functions of natural killer cells. Nature immunology 9, 503.

Vyas, Y. M., Mehta, K. M., Morgan, M., Maniar, H., Butros, L., Jung, S., Burkhardt, J. K., and Dupont, B. (2001). Spatial organization of signal transduction molecules in the NK cell immune synapses during MHC class I-regulated noncytolytic and cytolytic interactions. J Immunol 167, 4358.

Walzer, T., Dalod, M., Robbins, S. H., Zitvogel, L., and Vivier, E. (2005). Natural-killer cells and dendritic cells: "l'union fait la force". Blood 106, 2252.

Wang, X. Q., Sun, P., and Paller, A. S. (2002). Ganglioside modulation regulates epithelial cell adhesion and spreading via ganglioside-specific effects on signaling. J Biol Chem 277, 40410.

Wang, H., Zheng, X., Wei, H., Tian, Z., Sun, R.(2012). Important role for NKp30 in synapse formation and activation of NK cells. Immunol Invest 41, 367.

Watzl, C., and Urlaub, D. (2012). Molecular mechanisms of natural killer cell regulation. Frontiers in bioscience 17, 1418.

Wu, C., Rauch, U., Korpos, E., Song, J., Loser, K., Crocker, P. R., and Sorokin, L. M. (2009). Sialoadhesin-positive macrophages bind regulatory T cells,

negatively controlling their expansion and autoimmune disease progression. J Immunol 182, 6508.

(Yagita, et al., 2000)Yagita, M., Huang, C.L., Umehara, H., Matsuo, Y., Tabata, R., Miyake, M., Konaka, Y., Takatsuki, K. (2000). A novel natural killer cell line (KHYG-1) from a patient with aggressive natural killer cell leukemia carrying a p53 point mutation. Leukemia 14, 922.

Yamaji, T., Mitsuki, M., Teranishi, T., and Hashimoto, Y. (2005). Characterization of inhibitory signaling motifs of the natural killer cell receptor Siglec-7: attenuated recruitment of phosphatases by the receptor is attributed to two amino acids in the motifs. Glycobiology 15, 667.

Yamanaka, M., Kato, Y., Angata, T., and Narimatsu, H. (2009). Deletion polymorphism of SIGLEC14 and its functional implications. Glycobiology 19, 841.

Yan, S. R., Fumagalli, L., and Berton, G. (1995). Activation of p58c-fgr and p53/56lyn in adherent human neutrophils: evidence for a role of divalent cations in regulating neutrophil adhesion and protein tyrosine kinase activities. J Inflamm 45, 297.

Yasamura, Y., Tashijan, A.H Jr., Sato, G.H. (1966). Establishment of four functional, clonal strains of animal cells in culture. Science 154, 1186-9.

Yokoyama, W. M., and Kim, S. (2006). Licensing of natural killer cells by self-major histocompatibility complex class I. Immunol Rev 214, 143.

Yu, R. K., Tsai, Y. T., Ariga, T., and Yanagisawa, M. (2011). Structures, biosynthesis, and functions of gangliosides--an overview. J Oleo Sci 60, 537.

Yu, T. K., Caudell, E. G., Smid, C., and Grimm, E. A. (2000). IL-2 activation of NK cells: involvement of MKK1/2/ERK but not p38 kinase pathway. J Immunol 164, 6244

Yusa, S., Campbell, K.S. (2003). Src homology region 2-containing protein tyrosine phosphatase-2 (SHP-2) can play a direct role in the inhibitory function of killer cell Ig-like receptors in human NK cells. J Immunol 170, 4539.

Zafirova, B., Wensveen, F. M., Gulin, M., and Polic, B. (2011). Regulation of immune cell function and differentiation by the NKG2D receptor. Cell Mol Life Sci 68, 3519

Zeng, G., Gao, L., Birkle, S., and Yu, R. K. (2000). Suppression of ganglioside GD3 expression in a rat F-11 tumor cell line reduces tumor growth, angiogenesis, and vascular endothelial growth factor production. Cancer Res 60, 6670

Zhang, M., Bai, C.X., Zhang, X., Chen, J., Mao, L., Gao, L. (2004). Downregulation enhanced green fluorescence protein gene expression by RNA interference in mammalian cells. RNA Biol 1, 74.

Zhang, J., Raper, A., Sugita, N., Hingorani, R., Salio, M., Palmowski, M.J., Cerundolo, V., Crocker, P.R. (2006). Characterization of Siglec-H as a novel endocytic receptor expressed on murine plasmacytoid dendritic cell precursors. Blood 107, 3600.

Zhang, M., Varki, A. (2004). Cell surface sialic acids do not affect primary CD22 interactions with CD45 and surface IgM nor the rate of constitutive CD22 endocytosis. Glycobiology 14, 939.

Zheng, X., Wang, Y., Wei, H., Sun, R., and Tian, Z. (2009). LFA-1 and CD2 synergize for the Erk1/2 activation in the Natural Killer (NK) cell immunological synapse. J Biol Chem 284, 21280.

Zindl, C.L., Chaplin, D.D.(2010). Immunology. Tumor immune evasion. Science 328, 697.

.

Appendix

1. Optimizing detection of liposome incorporated GD3 and GM1 with anti-GD3 antibody and cholera toxin subunit B (CTB), respectively

In order to confirm the presence of GM1 and GD3 incorporated in liposomes, an anti-GD3 monoclonal antibody (R24 mAb) and biotinylated cholera toxin subunit B (CTB) was used to detect these gangliosides. Detection with antibody and toxin was optimized with respect to the secondary antibody dilution, as shown in figure A1.

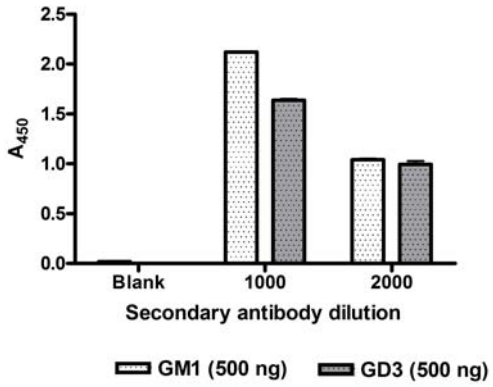

Figure A1: Optimizing R24 and CTB for the detection of GD3 and GM1 respectively. Liposomes carrying GD3 and GM1 were plated onto microtitre plates. Plates were incubated with either 10 µg/ml of R24 mAb or 1 µg/ml of CTB, for 1 hour at room temperature. Plates were washed and then incubated with anti-mouse HRP or Streptavidin HRP for 1 hour at room temperature. Plates were washed and then TMB substrate added for detection. Plates were read at 450nm. Error bars represent standard deviation (n=3).

2. Titration of anti-GD1a antibody (MOG35) antibody

Expression of GD1a on B16 (78) cells was tested using the mouse anti-GD1a antibody, MOG35. This antibody and 2 other non-specific antibodies (MOG1

and MOG16) was a kind gift from Dr. Hugh Willison(Greenshields et al., 2009). GD1a, coated onto 96-well titre plates were detected using various concentrations of the antibody by ELISA (Figure A2). The results obtained, suggests that the working range of this antibody is between 20 µg/ml and 2.5 µg/ml.

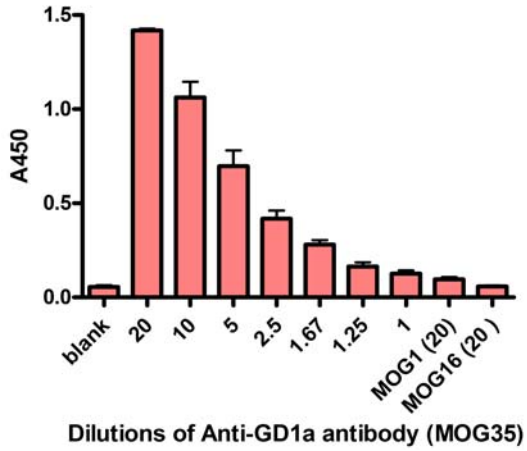

Figure A2: Optimization of GD1a detection using anti-GD1a antibody (MOG35): 96-well microtitre plates were coated with 100 µl of GD1a at 2 µg/ml (dissolved in methanol). Methanol alone was used as the blank in the assay. The plate was left to dry overnight at 40C. The plate was then blocked with 5% marvel in PBA, for one hour at room temperature. Different dilutions of the anti-GD1a antibody and non-specific antibodies (MOG1 and MOG16 @ 20 µg/ml) were diluted in blocking buffer and left to incubate for one hour at room temperature (RT). Plate was washed with 1%PBA (x3). Anti-mouse HRP (1/5000 dilution in TBA) was added to the plate and left to incubate for 1 hour at RT. Plate was washed again before carrying out detection with TMB substrate. Error bars represent standard deviation between samples (n=3).

3. Expression of GD1a in B16 (78) GM1 positive cells

MOG35 antibody was then used to check for expression of GD1a on B16 (78) transfected with GM2s and expressing GM1 (Figure A3). The human neuroblastoma cell line, SH-SY5Y, was used as a positive control (data not shown). Only < 1% of GM1 positive cells expressed GD1a.

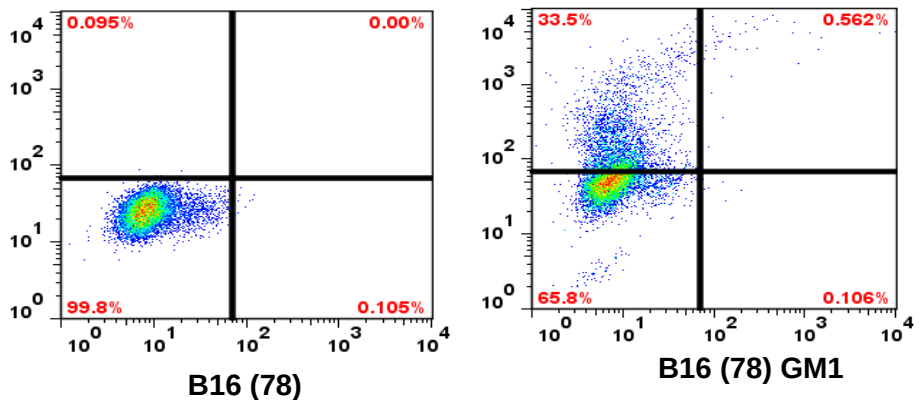

Figure A3: Expression of GD1a on B16 (78) GM1 cells: B16 (78) wild type and GM1 expressing cells were harvested and stained for GM1 and GD1a using CTB and anti-GD1a antibody respectively, as described in section 3.5.3 .

4. Phosphorylation of Akt following LFA-1 recognition of ICAM-1

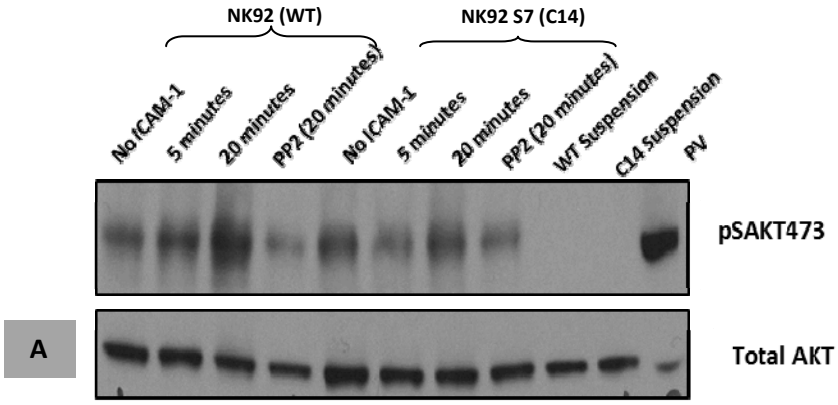

Figure A4: Comparing LFA-1 mediated AKT phosphorylation between wild type NK92 cells and Siglec-7 expressing NK92 (C14): Whole cell lysates were blotted for Ser473Akt and total Akt. Experiments were conducted as described in figure 4.16. Densitometry not done since only one experiment conducted.

5. Sialic acid independent adhesion of NK92 Siglec-7 cells to ICAM-1-Fc

As discussed in section 4.5.2, repeat experiments analysing the effect of sialic acid on the adhesion of Siglec-7 expressing NK92 cells to ICAM-1-Fc. In this experiment the Siglec-7 R124A mutant was also tested (polyclonal cells and clone A). Sialidase untreated and treated ICAM-1-Fc was used in the experiment. As shown in figure 4.14, the adhesion of Siglec-7 expressing cells and the mutant was reduced and this was independent of sialic acid.

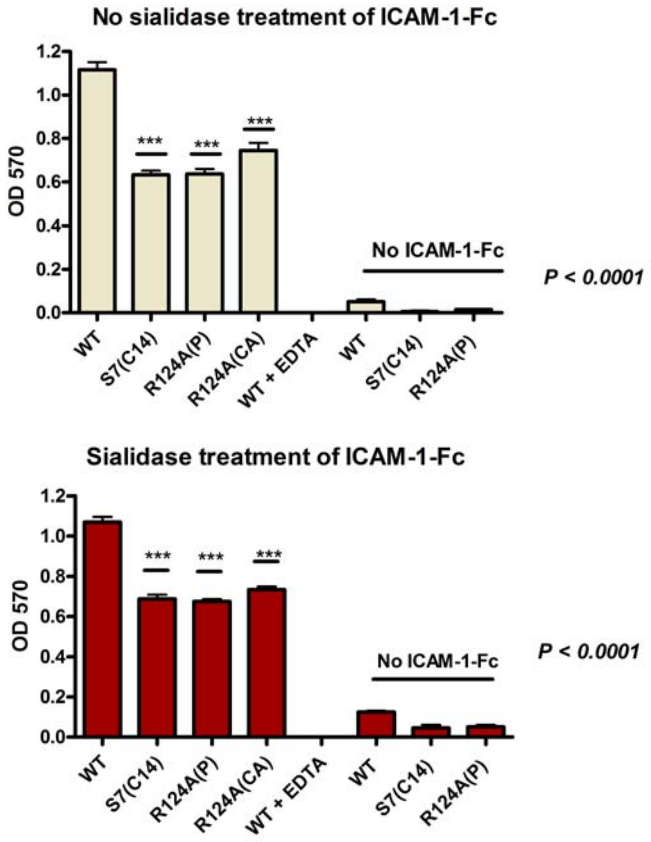

Figure A5: Sialic acid independent adhesion of NK92 WT or NK92 Siglec-7 (C14) cells to ICAM-1-Fc : 96 well tissue culture plates with protein A or PLL, followed by ICAM-1-Fc. ICAM-1-Fc coated plates were treated (A) without sialidase or (B) with 0.17 IU/ml of sialidase for 1 hour at 37 ^{0}C. Sialidase treatment was quenched using 10%FCS. 2 x 10 E5 cells are washed and resuspended in 1XHBSS (-Ca^{2+}, +Mg^{2+}). EDTA treated cells were used as negative control. Cells were added to wells, spun down and incubated for 30 minutes at 37^{0}C. Unbound cells were then removed from the plate by gravity wash and bound cells were fixed, stained and plates read at 570 nm. Cells added to PLL coated plate was used as control to obtain maximal binding of cells (data not shown). Error bars represent standard deviation between samples , n = 5.

6. Adhesion of Siglec-7 expressing NK92 cells to different preparations of ICAM-1-Fc

The adhesion of NK92 wild type cells and Siglec-7 expressing cells to different preparations of ICAM-1-Fc (from CHO cell clone 54 and clone 17) was analysed. The sugar binding mutant of Siglec-7 (polyclonal cells and Clone A) was also included in this experiment. Treatment of each group of cells with EDTA was used as a negative control in this experiment. The results reconfirm findings described in section 4.5.1(Chapter 4). Siglec-7 expression on NK92 cells negatively regulates the adhesion of cells to ICAM-1-Fc. The reduced adhesion of Siglec-7 sugar binding mutant (R124A) to ICAM-1-Fc also confirms the sialic acid independent nature of ligand recognition by Siglec-7.

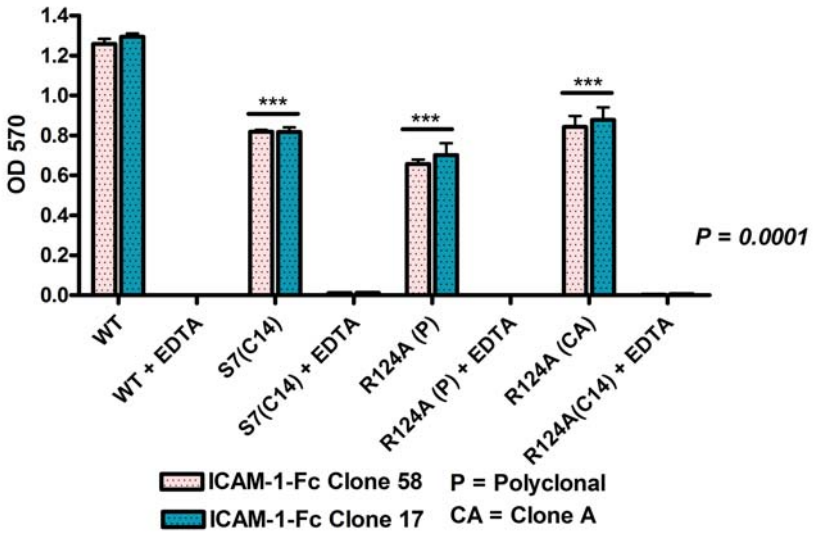

Figure A5: Siglec-7 negatively affects adhesion of NK92 Siglec-7 (C14) cells to ICAM-1-Fc : Experiment was carried out as explained in figure A5. EDTA treated cells were used as negative control. Cells added to PLL coated plate was used as control to obtain maximal binding of cells (data not shown). Error bars represent standard deviation between samples , n = 5.